Study of Novel NNRTIs as Potential Agents Against HIV-1 and Opportunistic Infections

THESIS

Submitted in partial fulfillment

of the requirements for the degree of

DOCTOR OF PHILOSOPHY

by

Subhash Chander

ID. No. 2012PHXF404P

Under the Supervision of

Dr. S. Murugesan

BIRLA INSTITUTE OF TECHNOLOGY AND SCIENCE, PILANI

(RAJASTHAN) INDIA

2017

BIRLA INSTITUTE OF TECHNOLOGY & SCIENCE
PILANI (RAJASTHAN-333031) INDIA

CERTIFICATE

This is to certify that the thesis entitled "**Study of Novel NNRTIs as Potential Agents Against HIV-1 and Opportunistic Infections"** submitted by **Subhash Chander, ID No. 2012PHXF404P** for the award of Ph. D. degree of the institute embodies the original work done by him under my supervision.

Signature in full of the supervisor: _____

Name in capital block Letters: **Dr. S. MURUGESAN**

Designation: **Assistant Professor,**
Department of Pharmacy,
Birla Institute of Technology & Science
Pilani, Pilani Campus, Pilani-333031

Date:

Place:

Contents

Acknowledgments

First and foremost, I would like to extend my sincere gratitude to my research guide **Dr. S. Murugesan** for his dedicated help, advice, encouragement, inspiration and continuous support throughout my Ph. D. I have been very lucky to have a supervisor who cared so much about my work and who responded to my questions and queries so promptly. His enthusiasm and integral view on research has made a deep impression on me. **Dr. S. Murugesan** has given me full liberty to pursue my research work but in parallel he also provide full support by virtue of which I successfully overcame all difficulties faced during my Ph. D work. Main positive thing I felt is that, every time I found myself full of energy and enthusiasm after interaction or discussion with him.

I am immensely thankful to **Prof. Souvik Bhattacharyya,** Vice-Chancellor, BITS-Pilani, **Prof. V. S. Rao, Prof. B. N. Jain** (ex Vice-Chancellors, BITS-Pilani), **Prof. A. K. Sarkar,** Director, BITS-Pilani, Pilani Campus and **Prof. G. Raghurama** (ex Director, BITS-Pilani, Pilani Campus), for permitting me to carry out this research work in BITS-Pilani.

I would like to express my gratitude to **Prof. R. N. Saha**, Director, BITS-Pilani, Dubai Campus and **Prof. R. Mahesh**, Dean Faculty Affairs, BITS Pilani for their suggestions and impetus during my research work. I am grateful to **Prof. S. C. Sivasubramanian,** Dean Administration BITS Pilani**, Prof. S. K. Verma**, Dean, Academic Research Division BITS-Pilani, and **Dr. Anshuman**, Unit Chief, Estate Management, BITS Pilani for their support during the period of stay in BITS-Pilani.

I am thankful to my thesis Doctoral Advisory Committee members, **Prof. Hemant R Jadhav**, Associate Dean, Academic Research Division and **Dr. Atish T. Paul,** DRC convener, Department of Pharmacy for their valuable suggestions as well as evaluation of my work in constructive way.

I owe my gratitude to **Dr. Anil Gaikwad,** Head, Department of Pharmacy for his constant support and guidance to pursue my doctoral thesis. I would like to express my thanks to **Dr. Srikant Charde,** Associate Professor, Department of Pharmacy BITS Pilani-Hyderabad Campus for the timely guidance during my work.

I would also like to acknowledge **Dr. R.P. Pareek**, **Dr. Rajeev Taliyan, Dr. Sunil Dubey**, **Dr. Deepak Chitkara, Dr. Anupama Mittal, Dr. Anil Jindal, Dr. M.M. Pandey**, **Dr. Gautam**

Singhvi, Dr. Aniruddha Roy, **Dr. Shvetank Bhatt, Mr. Mahaveer, Dr. Priti Jain** and **Mrs. Archana** for sharing their knowledge which made a remarkable influence on my entire work in the field.

I sincerely express my gratitude to all our collaborators; **Dr. Yong-Tang Zheng**, (Professor, Kunming Institute of Zoology, China), **Dr. Davie Cappoen,** (Universiteit Antwerpen, Wilrijk, België), **Dr. Paul Horrocks** (Professor, Huxley Building, Keele University, Staffordshire, United Kingdom), **Dr. Inshad Ali Khan** (Principal scientist, Indian Institute of Integrative Medicine, Jammu, India), **Professor Tanya Parish** (Vice President, Drug Discovery, University of Washington, USA), **Dr. Manormoney Pillay** (Scientist, Medical Research Institute, University of KwaZulu-Natal, Durban, South Africa), **Dr. Rafael Balana Fouce** (Professor of Biomedical Sciences, University of Leon), and **Dr. Prabhat Nath Jha**, (Associate Professor, Department of Biological Sciences, BITS Pilani, India) for their untiring support during my research work.
My special thanks to **Dr. Penta Ashok, Dr. Arpit Bhargava, Dr. Ajay Bisnoi** and **Mr. Naveen Bokolia** for their valuable help during my research work.

My heartfelt thanks to my seniors **Dr. Vadiraj, Dr. Ankur, Dr. Emil, Dr. Prashant, Dr. Muthu, Dr. Arghya, Mr. Sourabh Mundra, Dr. Sushil, Dr. Garima Balwani, Dr. Vibhu Nagpal, Mr. Yeshwant**, **Mr. Satish Reddy, Ms Deepali** and **Mr. Mukund.** I will always cherish the warmth shown by them.

A special mention of thanks to my friends **Mr. Sridhar, Mr. Sorabh Sharma, Mr. Santosh Goru, Ms Anuradha, Mrs. Shruti**, **Ms Nisha**, **Mr. Vajir**, **Mr. Kishan, Mr. Saurabh Sharma Mr. Ginson, Mr. Krishna, Ms. Parcheta, Mr. S.K. Dass, Mr. Dinesh Kumar, Mr. Shiv Dhiman, Mr. Hitesh Saini, Mr. Sachin, Mr. Anoop Singh, Mr. Nitesh, Mr. Ashok Sharma, Mr. Saleem Pasha, Mr. Faiyaz Baig, Mr. Manish Mehra, Mr. Abdul Shakoor, Mr. Venkata Reddy, Mr. Santosh Khandagale, Mr. Vimal Kumar, Mr. Vishal Kachwal, Mr. Rajnish Singh, Mr. Vikram** and **Mr. M. A. Khan.**

I extend my special thanks to my friends **Mr. Pankaj Wadhwa** and **Mr. Almesh Kadakol** for always being there for me, their presence made this journey memorable.

I would also like to acknowledge **SAIF, CSIR-CDRI, Lucknow**, and **Guru Jambheshwar University of Science & Technology, Hisar** for providing analytical facilities related to my research work.

I thank the non-teaching staff, **Mr. Rampratap, Sajjan Ji, Mr. Puran, Mr. Tara Chand, Mr. Mahendra, Mr. Laxman, Mr. Mahipal, Mr. Naveen, Mr. Mukesh**, **Mr. Shivkumar** and **Mr. Vishal** for their help.

I owe my deepest gratitude towards my better half **Pragati** for her eternal support and understanding of my goals and aspirations. Her infallible love and support has always been my strength. Her patience and sacrifice will remain my inspiration throughout my life. I am thankful to my little angel and happiness booster **Ms. Hezal Saini**, her presence has filled our life with full of joy.

My warmest thanks belong to my family members and my in-laws for their never ending love, encouragement and support. I owe a lot to my mother and father, who encouraged and helped me at every stage of my personal and academic life.

I would like to thank **Department of Science & Technology, Science and Engineering Research Board,** New Delhi for providing the fellowship and funding for the research.

I gratefully acknowledge **Department of Pharmacy** and **BITS Pilani University** for providing me an opportunity to carry out my research as well as for providing institute fellowship.

My sincere thanks and regrets to all friends and people I missed to acknowledge who had directly or indirectly helped me to accomplish this task.

Last but not the least; I pay my obeisance to GOD, the almighty to have bestowed upon me good health, courage, inspiration, zeal and grace due to which I became able to finish this task

Subhash Chander

List of Abbreviations / Symbols

^{1}H NMR	Proton Nuclear Magnetic Resonance
5-HT	5-Hydroxytryptamine
3TC	Lamivudine
Å	Angstrom
β	Beta
δ	Delta
AIDS	Acquired Immune Deficiency Syndrome
ART	Anti-Retroviral Treatment
AcOH	Acetic Acid
A. niger	*Aspergillus niger*
A. flavus	*Aspergillus flavus*
A. fumigates	*Aspergillus fumigatus*
A. solani	*Alternaria solani*
ACN	Acetonitrile
Asn or N	Asparagine
Asp or D	Aspartic Acid
ATCC	American Type Culture Collection
AZT	Zidovudine
B. cereus	*Bacillus cereus*
B. sphaericus	*Bacillus sphaericus*
B. subtilis	*Bacillus subtilis*
BZDs	Benzodiazepines
brs	Broad singlet
C. albicans	*Candida albicans*
C. cladosporoide	*Cladosporium cladosporioides*
CFU	Colony Forming Units
C. Krusei	*Candida krusei*
C. glabrata	*Candida glabrata*
C. parapsilosis	*Candida parapsilosis*
CPE	Cytopathic Effect
C. neoformans	*Cryptococcus neoformans*
C. tropicalis	*Candida tropicalis*

C. violaceum	*Chromobacterium violaceum*
Cys or C	Cysteine
CD4	Cluster of differentiation 4
cDNA	Complementary DNA
CNS	Central Nervous System
d	Doublet
D4T	Stavudine
dd	Doublet of doublet
ddC	Zalcitabine
DDI	Didanosine
DA	Dopamine
DCM	Dichloromethane
DLV	Delavirdine
DIG	Digoxigenin
DNA	Deoxyribonucleic acid
dNTP	Deoxynucleoside triphosphate
DMF	*N,N*-Dimethylformamide
DMSO	Dimethylsulfoxide
ds	Double stranded
E. coli	*Escherichia coli*
E. faecalis	*Enterococcus faecalis*
E. floccosum	*Epidermophyton floccosum*
EDC	1-(3-dimethylaminopropyl)-3-ethylcarbodiimide
EFZ	Efavirenz
eqv.	Equivalent
ELISA	Enzyme-linked immunosorbent assay
ESI-MS	Electrospray ionization mass spectrometry
EtOAc	Ethyl acetate
EtOH	Ethanol / Ethyl alcohol
Et_3N	Triethylamine
FDA	Food and Drug Administration
F. graminearum	*Fusarium graminearum*
F. semitectum	*Fusarium semitectum*
FTC	Emtricitabine

FT-IR	Fourier Transform-Infra Red
gp120	Glycoprotein 120
Glu or E	Glutamate
G. zeae	Gibberella zeae
G(+)ve	Gram Positive
G(-)ve	Gram Negative
h	Hour (s)
HAART	Highly Active Anti Retroviral Therapy
H. burtonii	*Hyphopichia burtonii*
His or H	Histidine
HIV	Human Immunodeficiency Virus
HOBt	1-Hydroxybenzotriazole
HSV	Herpes Simplex Virus
Hz	Hertz
IC_{50}	Half maximal inhibitory concentration
i.p.	Intra-peritoneal
i.v.	Intravenous
IBS	Irritable Bowel Syndrome
IR	Infra-Red
µg/mL	Microgram per Milliliter
µL	Microliter
µM	Micromolar
K. aerogenes	*Klebsiella aerogenes*
Leu or L	Leucine
L. monocytogenes	*Listeria monocytogenes*
Lys or K	Lysine
m	Multiplet
M. canis	*Microsporum canis*
M. fortuitum	*Mycobacterium fortuitum*
M. gypseum	*Microsporum gypseum*
M. luteus	*Micrococcus luteus*
M. purpureus	*Monascus purpureus*
M. smegmatis	*Mycobacterium smegmatis*
mmol	Millimole

mL	Milliliter
m.p.	Melting point
Mtb	Mycobacterium tuberculosis
m/z	Mass/charge
MAOIs	Monoamine Oxidase Inhibitors
mg	Milligram
MIC	Minimum Inhibitory Concentration
min	Minute(s)
MS	Mass Spectra
MTP	Microtiter Plate
MTCC	Microbial Type Culture Collection
MW	Molecular Weight
nM	Nanomolar
$NaBH_4$	Sodium borohydride
NMDA	*N*-methyl-D-aspartase
NNIBP	Non-Nucleoside Inhibitory Binding Pocket
NNRTIs	Non-Nucleoside Reverse Transcriptase Inhibitors
NRTIs	Nucleoside Reverse Transcriptase Inhibitors
NtRTIs	Nucleotide Reverse Transcriptase Inhibitors
NVP	Nevirapine
OIs	Opportunistic Infection
P. citrinum	*Penicillium citrinum*
P. cubensis	*Psilocybe cubensis*
Phe or F	Phenylalanine
P. marneffei	*Penicillium marneffei*
P. putida	*Pseudomonas putida*
Pro or P	Proline
P. sasakii	Paralepetopsis sasakii
PDE5	Phosphodiesterase-5
POD	Peroxidase
ppm	Parts per million
q	Quartet
quin	Quintet
RNA	Ribonucleic acid

R. bogoriensis	*Rhodotorula bogoriensis*
R. solani	*Rhizoctonia solani*
RT	Reverse Transcriptase
rt	Room Temperature
s	Singlet
Ser or S	Serine
S. aureus	*Staphylococcus aureus*
S. cerevisiae	*Saccharomyces cerevisiae*
S. epidermidis	*Staphylococcus epidermidis*
S. pneumoniae	*Streptococcus pneumoniae*
S. pyrogenes	*Streptococcus pyogenes*
S. typhi	*Salmonella typhi*
ss	Single Stranded
t	Triplet
TB	Tuberculosis
TDF	Tenofovir
THF	Tetrahydrofuran
THIQ	Tetrahydroisoquinoline
TLC	Thin Layer Chromatography
TMS	Tetramethylsilane
TMV	Tobacco Mosaic Virus
T. brucei	*Trypanosoma brucei*
T. cruzi	*Trypanosoma cruzi*
T. mentagrophytes	*Trichophyton mentagrophytes*
Trp or W	Tryptophan
T. rubrum	*Trichophyton rubrum*
Tyr or Y	Tyrosine
*t*RNA	Transfer Ribonucleic Acid
UNAIDS	United Nations Programme on HIV and AIDS
USP	United State Pharmacopoeia
Val or V	Valine
V. cholera	*Vibrio cholerae*
V. mali	*Valsa mali*
WHO	World Health Organization

X. oryzae	*Xanthomonas oryzae*
ZOI	Zone of Inhibition

List of Tables

List of Figures

Abstract

Acquired Immune Deficiency Syndrome (AIDS) is a chronic and life-threatening disease caused by Human Immunodeficiency Virus (HIV). According to UNAIDS 2016 report, around 36.7 million people are living with HIV globally and in the same year AIDS claimed around 1.1 million deaths. Reverse Transcriptase (RT) inhibitors are the key components of antiretroviral therapy and more than half of the drugs available in the market belong to this class. Currently, two different sub-classes of drugs acting on HIV-1 RT are Nucleoside/Nucleotide Reverse Transcriptase Inhibitors (NRTIs) and Non-Nucleoside Reverse Transcriptase Inhibitors (NNRTIs). Among these, NNRTIs are playing vital role in drug combination therapy called "Highly Active Antiretroviral Therapy" (HAART) which is currently used for HIV/AIDS treatment due to their high specificity and low toxicity. Although, after the advent of HAART, the mortality rate due to AIDS has reduced from 60 to 80% in last one decade and highly fatal AIDS is now become a chronic manageable disease. But, management of this disease is still complex and worrisome due to problems such as persistently development of drug resistance and poor drug tolerability. Above factors drive the need for new anti-HIV drugs having good potency against the wild as well as mutant strains of HIV with improved safety and pharmacokinetic profile.

In the present dissertation work, using the information of the crystal structure of HIV-1 RT, structure of potent NNRTIs and mutations responsible for drug resistance, attempts are made for the discovery of novel RT inhibitors. In this direction, twenty six nitrogen containing heterocyclic scaffolds (having nucleus like tetrahydroisoquinoline, tetrahydroquinoline, quinoline and piperazine) were designed as NNRTIs while considering required pharmacophoric features established from the structure of literature reported potential hits. Further, five scaffolds containing oxindole as nucleus were designed based upon the outcome of virtual screening studies. All designed thirty one scaffolds were *in-silico* screened (via docking studies) against three strains of HIV-1 RT (one wild and two mutant strains) and eleven scaffolds were selected which exhibited significant *in-silico* inhibitory activity against all three selected strains. Finally, using the selected eleven scaffolds series of compounds (**5a-o, 9a-o, 14a-k, 17a-o, 23a-o, 28a-l, 32a-n, 38a-o, 43a-p, 51a-n** and **54a-k**) were generated by making the different substitutions

The drug-likeness behavior of the designed compounds was assessed by the *in-silico* prediction of drug likeness parameters using three tools (Qik-prop, admetSAR and FAF-*Drugs*[3]). Further, designed compounds were synthesized by conventional as well as non-conventional (microwave assisted) approaches. Synthesized compounds were purified and preliminarily characterized by physicochemical methods like melting point and thin layer chromatography,

while final structure of the compounds was further confirmed by spectral techniques like IR, ^{1}H NMR, ESI-MS. Synthesized compounds **5a-o, 9a-o, 14a-k, 17a-o, 23a-o, 28a-l, 32a-n, 38a-o, 43a-p, 51a-n** and **54a-k** were screened for HIV-RT inhibitory activity using ELISA based *in-vitro* assay. During the preliminary screening studies (at 100 µM concentration), none of the compounds of series **14a-k** and **23a-o** displayed significant activity (% inhibition of RT remained <50)**,** while only one compound of series **32a-n** found to be significantly active. From the series **5a-o, 9a-o, 17a-o,** and **43a-p,** five, five, thirteen and nine compounds, respectively displayed significant inhibition but none of the compounds exhibited much encouraging results compared to the reference drugs, moreover their RT inhibitory ability remained <75 %.

Several compounds of series **28a-l, 38a-o, 51a-n** and **54a-k** displayed overall superior inhibition (>75% inhibition) of HIV-1 RT during the preliminarily screening. Therefore, IC_{50} was calculated for all the compounds of above four series, which revealed that twenty compounds (**28b, 28h, 28i, 28j, 28l, 38a, 38b, 38j, 38k 38o, 51a, 51b, 51d, 51k, 51l**, **51m, 54b, 54d, 54e** and **54k**) collectively displayed IC_{50} ≤25 µM. Further, two compounds (**28b** and **28j**) of series **28a-l** and four compounds (**54b, 54d, 54e, 54k**) of series **54a-k** displayed good to excellent potency against RT with IC_{50} ≤10 µM. Moreover, two compounds (**54b** and **54e**) of series **54a-k,** showed sub-micromolar potency (IC_{50} 0.27 and 0.76 µM, respectively) against HIV-1 RT. Reference drug efavirenz displayed promising activity with 98.87% inhibition of HIV-RT and IC_{50} of 0.057 µM.

In order to study the putative binding mode as well as interaction pattern, docking studies were performed against the wild HIV-1 RT using the best and least active compounds (in-vitro RT assay) from each series.

Selected fifteen compounds (**28b, 28j, 28l, 38a, 38b, 38j, 38o, 51a, 51d, 51k, 51m, 54b, 54d, 54e** and **54k**) of series **28a-l, 38a-o, 51a-n** and **54a-k,** which possessed good/excellent inhibition potency against HIV-1 RT were selected for anti-HIV-1 activity and cytotoxicity, using zidovudine as reference compound. The result of the study revealed that out of fifteen compounds, eight compounds (**28j, 38b, 51a, 51k, 51m, 54b, 54e** and **54k**) displayed good to excellent potency (EC_{50} <10 µg/mL) against HIV-1 cells, further except compound **51d** rest of the compounds (**28b**, **28l**, **38a**, **38j**, **38o** and **54d**) can be considered as moderately active against HIV-1 (EC_{50} ≥10 to <20 µg/mL).

Interestingly, best potent hits (**54b** and **54e**) of HIV-1 RT assay also found to be active against HIV-1 with EC_{50} 0.030 µg/mL and EC_{50} 0.59 µg/mL, respectively, Furthermore, both of the compounds **54b** and **54e** displayed admirable safety index (6200 and >338.9, respectively).

Reference compounds zidovudine displayed promising potency (0.0034µg/mL) against HIV-1 with remarkable safety index (460505.88). So, overall RT inhibitory, anti-HIV-1 and cytotoxicity studies afforded two potential hit (**54b** and **54e**) which possessed potent RT inhibitory as well as anti-HIV-1 activity with good safety index.

Opportunistic infections (OIs) are the most common cause of death among HIV/AIDS patients due to their weak immune system, most of OIs are caused by microorganisms such as bacteria, fungi, virus, protozoa etc, also some specific forms of cancers are frequently reported in the AIDS patients. For the sake of concision, we selected few microbial strains which are frequently encountered as co-infective agents among the AIDS patients. Subsequently, all synthesized compounds were screened against these strains which included, *Mycobacterium tuberculosis*, four other bacterial strains (*Staphylococcus aureus*, *Bacillus cereus*, *Escherichia coli* and *Pseudomonas putida*) and two fungal strains (*Candida albicans* and *Aspergillus niger*).

In-vitro screening of tested compounds against the four bacterial strains revealed that out of all tested compounds, forty, thirty five, thirty seven and twenty five compounds possessed significant antibacterial activity (ZOI ≥15) against the *E. coli, S. aureus, P. putida,* and *B. cereus,* respectively. Among the tested compounds, twelve compounds (**5f, 5j, 5k**, **9f, 17d, 17f, 17j**, **28j, 28k, 28l, 38n** and **54j**) showed significant antibacterial activity with ZOI ≥15 mm against the all four tested bacterial strains, in which majority of compounds belongs to three series **5a-o, 17a-o** and **28a-l**. Structurally, scaffolds **5a-o** and **17a-o** are based on 6,7-dimethoxy tetrahydroisoquinoline connected via glycinamide liker to substituted phenyl ring, while series **28a-l** is basically tetrahydroquinoline based scaffold containing carbamate linker. Overall, all three scaffolds can be considered of interest regarding their antibacterial potency. Reference compound chloramphenicol displayed potent activity against the all tested bacterial strains with ZOI ranges from 21-23 mm and MIC 16 µg/mL.

In-vitro screening result of the synthesized compounds against two fungal strains revealed that out of all tested compounds, thirty and thirty nine compounds significantly inhibited (ZOI ≥15 mm) the growth of *C. albicans* and *A. niger,* respectively. Collectively, fifteen compounds (**9m, 17j, 17k, 23i, 23j, 28e, 28f, 28g, 28h, 28l, 38f, 38l, 38n, 54g** and **54h**) exhibited significant growth inhibition (ZOI ≥15 mm) of both the tested fungal strains. Moreover, scaffolds containing tetrahydroquinoline moiety with carbamate linker **(28a-l)** and tetrahydroquinoline based compounds attached with phenylpiperazine entity (**38a-o**) possessed potential antifungal activity. Reference compound fluconazole displayed potent activity against *C. albicans* and *A. niger* strains with ZOI 21, 22 mm, respectively and MIC 16 µg/mL against each strain.

Furthermore, compounds **9m**, **17k**, **38n** exhibited potent activity against *A. niger* with ZOI 18-20 mm and MIC 16 µg/mL. Whereas, against *C. albicans* compounds **28g, 28h, 28l, 54g, 54h** showed potent antifungal activity with ZOI 17-20 mm and MIC 8-16 µg/mL.

Overall, majority of tested compounds not displayed encouraging potency against the growth of *Mtb*. Among all the tested compounds, seven compounds (**14j, 23h**, **23o, 43h**, **43j**, **43l** and **43m**) exhibited significant potency (MIC ≤25 µg/mL), also seven compounds (**14i, 23a, 23l**, **28j, 43d, 43k** and **43n**) showed moderate potency (MIC between >25 to ≤50 µg/mL), while rest of the compounds possessed weak or no activity against *Mtb*. Compounds of series **43a-p** exhibited relatively better anti-*Mtb* activity among the all tested series. Four compounds of series **43a-p** showed significant potency (MIC ≤25 µg/mL), in which compounds **43j** and **43m** showed MIC <10 µg/mL with safety index of more than twenty six. So, anti-*Mtb* evaluation studies afforded two hits **43j** and **43m** with good anti-*Mtb* potency and safety index which can be used for further lead optimization studies or in designing of novel anti-*Mtb* agents.

1. INTRODUCTION

Acquired Immune Deficiency Syndrome (AIDS) is a chronic and life-threatening disease, first reported in the United States in 1981, since then AIDS has been spread throughout the world [1]. AIDS is caused by the virus called Human Immunodeficiency Virus (HIV), a pathogenic retrovirus, belongs to the family Retroviridae. HIV has two major categories; HIV-1 and HIV-2, in which HIV-1 has about 10 subtypes and they are most common worldwide, while HIV-2 is less virulent and currently restricted to West Africa [2]. United Nations Programme on HIV and AIDS (UNAIDS) 2016 report revealed that currently, around 36.7 million people are living with HIV across the world, among them only 17 million people are receiving anti-retroviral therapy, in the same year AIDS claimed around 1.1 million deaths [3].

According to National AIDS Control Organisation (NACO), 2015-2016 report, the total number of people living with HIV in India were estimated around 2.11 million, slightly less than compared to 2007 (2.22 million). Around 86 thousand new HIV infections were reported in 2015 nationally, showing 66% decline in new infections from 2000 and 32% decline from 2007. In spite of this, in the year 2015, it was estimated that around 67.6 thousand people died of AIDS related diseases in India. Although, the number of AIDS Related Deaths (ARD) started to show a declining trend since 2007, it has declined by 54% from 2007 to 2015 [4]. But, still India has the third largest HIV epidemic in the world, HIV prevalence in India was an estimated 0.3%. This figure is small when compared to the most of other middle-income countries but because of India's huge population (more than 1.2 billion), this equates to 2.1 million HIV-positive population [5].

HIV specifically attacks and destroys $CD4^+$ lymphocytes (also called T-helper cells), which play an important role in cell-mediated immunity. This intern decreases in the number of T-cells weaken the immune system; consequently host becomes susceptible to other opportunistic infections, which finally leads to death [6].

1.1 HIV Life Cycle

HIV life cycle (Fig. **1.1**) encompasses various crucial events that are exploited as potential targets for chemotherapy against HIV [7]. The various events are as follows;

1.1.1 HIV Entry

HIV can undergo replication only inside the living cell. After entering into the body, HIV attacks T-cells in a short period of time, it attaches to the CD4 receptors of the T-cell with surface protein gp-120 and fuses with the cell membrane. Next, it injects genetic material into the cell, leaving the envelope behind plasma membrane [8].

1.1.2 Reverse Transcription and Integration

HIV's single stranded Ribonucleic Acid (ssRNA) is converted into viral double-stranded Deoxyribonucleic Acid (dsDNA) by the enzyme called Reverse Transcriptase (RT). Newly formed dsDNA moves into the cell nucleus and integrate with the host DNA. The viral enzyme called integrase is responsible for movement and integration of viral genetic material with host DNA, now it is known as provirus [9].

1.1.3 Transcription and Translation

HIV provirus remains in the dormant stage and waits for the activation of the cell. Once the cell is activated, proviral DNA is transcribed into messenger RNA via the enzymes of the host cell. Messenger RNA is transported into cytosol, where it produces large number of viral proteins and enzymes [10].

1.1.4 Assembly, Budding and Maturation

The newly formed proteins, enzymes and other components assemble together to produce complete virion at the plasma membrane. The enzyme protease plays a vital role at this stage of HIV life cycle to produce mature viral cores. Matured HIV particles released from infected T-cell and ready to infect another healthy cell to begin replication process again [11].

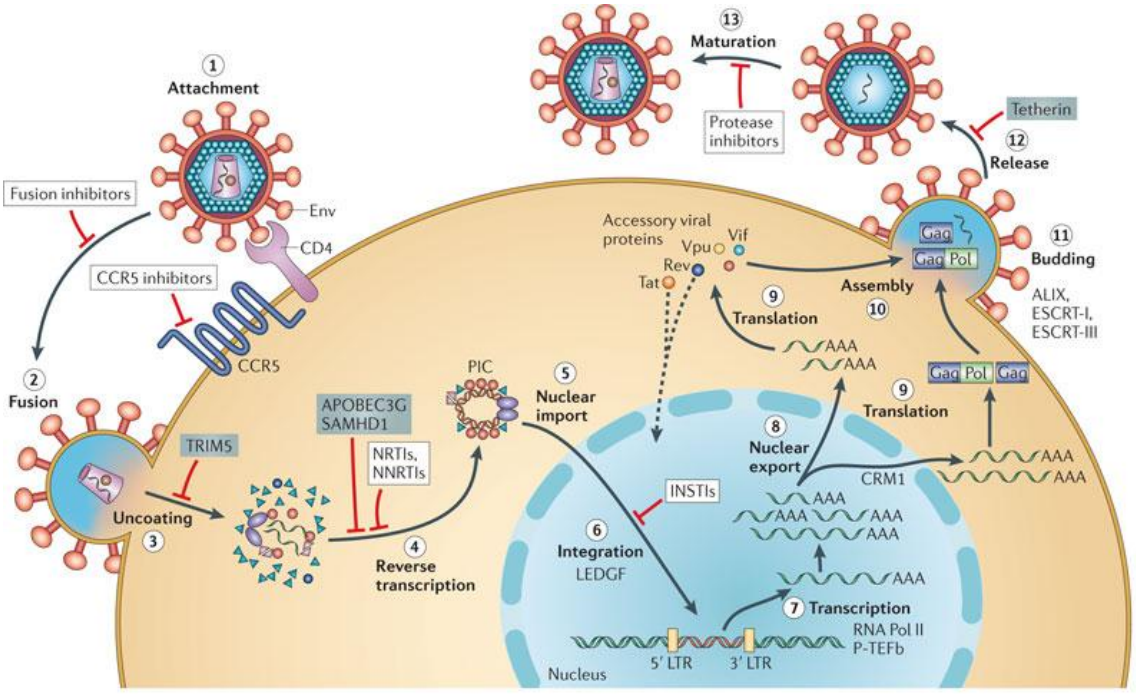

Fig. 1.1 Life cycle of HIV virus [6]

1.2 Anti-retroviral Therapy

There are five major types of drugs used to treat HIV/AIDS called anti-retrovirals because they act against the retrovirus HIV. Drugs are grouped depending upon the mechanism of action; these are entry inhibitors, fusion inhibitors, reverse transcriptase inhibitors, integrase inhibitors and protease inhibitors. RT inhibitors are the key components of anti-retroviral therapy and more than half of the drugs available in the market belong to this class. Currently, two different sub-classes of drugs acting on HIV-1 RT are Nucleoside/Nucleotide Reverse Transcriptase Inhibitors (NRTIs) and Non-Nucleoside Reverse Transcriptase Inhibitors (NNRTIs). Among these, NNRTIs are playing vital role in drug combination therapy called "Highly Active Anti-retroviral Therapy" (HAART) which is currently used for HIV/AIDS treatment due to their high specificity and low toxicity [12, 13].

HAART is often called as “drug cocktail” or "triple-therapy" was started in 1996. HAART involves the combination of three or more anti-HIV drugs which generally include two Nucleoside/Nucleotide Reverse Transcriptase Inhibitors and one Protease Inhibitor, alternately two Nucleoside/Nucleotide Reverse Transcriptase Inhibitors and one Non-Nucleoside Reverse Transcriptase Inhibitor. Combination therapy is given in order to reduce the emergence of viral resistance [14, 15]. With the advent of HAART, the mortality rate due to AIDS has reduced from 60 to 80% in last one decade and highly fatal AIDS is now become a chronic manageable disease. However, management of this disease is still complex and worrisome due to problems such as development of drug resistance persistently, monitoring of therapy efficacy and poor drug tolerability. Therefore, there is a compelling need for the search of novel NNRTIs that possess an improved safety profile, better potency and active against both wild as well as mutant strains of HIV [16].

1.3 Drug Targets

Three viral enzymes named, Reverse Transcriptase (RT), Protease and Integrase play the central role in the virus life cycle. Among these, Reverse Transcriptase is an asymmetric, heterodimeric multifunctional enzyme. It catalyzes the conversion of single-stranded viral RNA (ssRNA) into double-stranded proviral DNA (dsDNA) which is then integrated with the host genome. The crucial role of RT enzyme in viral replication makes it a prime target for anti-HIV therapy. Enzyme protease plays an important role in the formation and release of viral particles from infected T-cell. Viral integrase enzyme performs integration of the viral dsDNA with human DNA [17].

1.3.1 Reverse Transcriptase (RT)

HIV-1 reverse transcriptase (HIV-1 RT) is an asymmetric heterodimer, comprising a p66 subunit (560 amino acids) and a p51 subunit (440 amino acids). Subunit p66 is an open and flexible structure consists of catalytic domain (active site) at amino terminal and RNase H domain at carboxyl terminal. The three-dimensional structure of p66 subunit is often compared to a right hand (Fig. **1.2**), with fingers (amino acids 1-85 and 118-155), a palm (amino acids 86-117 and 156-237) and a thumb (amino acids 238-318). The palm domain contains polymerase active site with its three aspartic acid (110, 185 and 186) residues. RNase H domain, linked to the active site by connection domain (amino acids 319-426). The connection domain is also involved in interactions with nucleic acid and p51 subunit.

Furthermore, p66 subunit also contains a hydrophobic Non-Nucleoside Inhibitory Binding Pocket (NNIBP) at a distance of approximately 10 Å away from the catalytic site of the enzyme. This hydrophobic pocket constituted by the aromatic (Tyrosine 181, Tyrosine 188, Phenylalanine 227, Tryptophan 229 and Tyrosine 232), hydrophobic (Proline 59, Leucine 100, Valine 106, Valine 179, Leucine 234 and Proline 236) and hydrophilic residues (Lysine 101, Lysine 103, Serine 105, Aspartic acid 132 and Glutamic acid 224). The NNIBP is dynamic and does not exist unless an NNRTI is bound to RT. In fact, HIV-1 RT changes its conformation to create an NNIBP which can accommodate an NNRTI as soon as it enters the RT. The NNIBP is elastic and its conformation depends on the size, shape, specific chemical composition and the binding mode of a particular NNRTI. Binding of an NNRTI inhibits the catalytic steps of polymerization possibly by inducing conformational changes in the actual polymerase site. P51 subunit lacks RNase H domain and due to its compact nature, it plays an important role in structural rigidity of the enzyme and it also provides a binding site for the lysine-tRNA primer to initiate DNA synthesis [18-20].

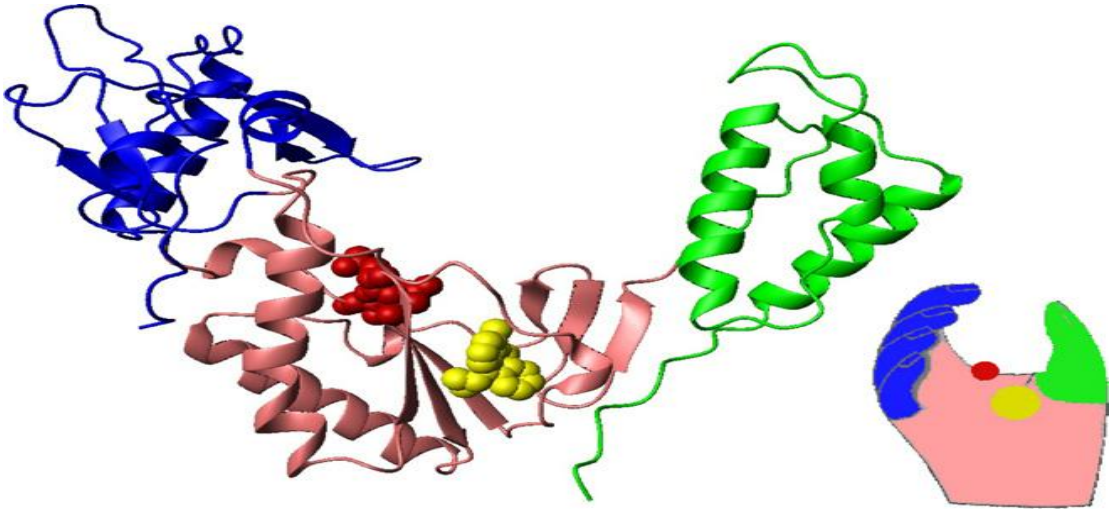

Fig. 1.2 p66 subunit in hand-like structure, showing fingers (blue), palm (pink), thumb (green), active site (red) and NNRTIs binding pocket (yellow) [20]

1.3.1.1 Nucleoside/Nucleotide Reverse Transcriptase Inhibitors (NRTIs/ NtRTIs)

Nucleoside reverse transcriptase inhibitors (NRTIs) comprise the first class of drugs discovered against HIV, structurally these mimics to the endogenous nucleosides which lack hydroxyl group at the 3rd position of ribose sugar [21]. NRTIs get convert into their active triphosphate (dNTP) form by the successive phosphorylation, catalyzed by the host cellular enzyme. Further, phosphorylated NRTIs get incorporated into the viral DNA during reverse transcription process by RT and due to lack of hydroxyl group at the 3rd position these fails to form the phosphodiester bond with the incoming nucleotide leading to the termination of DNA chain elongation [22]. Till now, seven NRTIs (Fig.**1.3**) got US-FDA approval as anti-HIV drugs for the treatment of patients, these include, zidovudine (AZT), stavudine (D4T), lamivudine (3TC), didanosine, abacavir (ABC), zalcitabine (ddC), emtricitabine (FTC) [23, 24].

In contrast to NRTIs, Nucleotide Reverse Transcriptase Inhibitors (NtRTIs) are already equipped with a phosphonate group which remains stable against the hydrolyzing esterases. Mechanistically, NtRTIs also act in the same way as NRTIs and ultimately disrupt the formation of a new proviral DNA [25]. The only US-FDA approved NtRTI for the treatment of HIV and hepatitis B is tenofovir disoproxil fumarate (Fig.**1.3**), which was developed by Gilead Sciences Inc USA) [26].

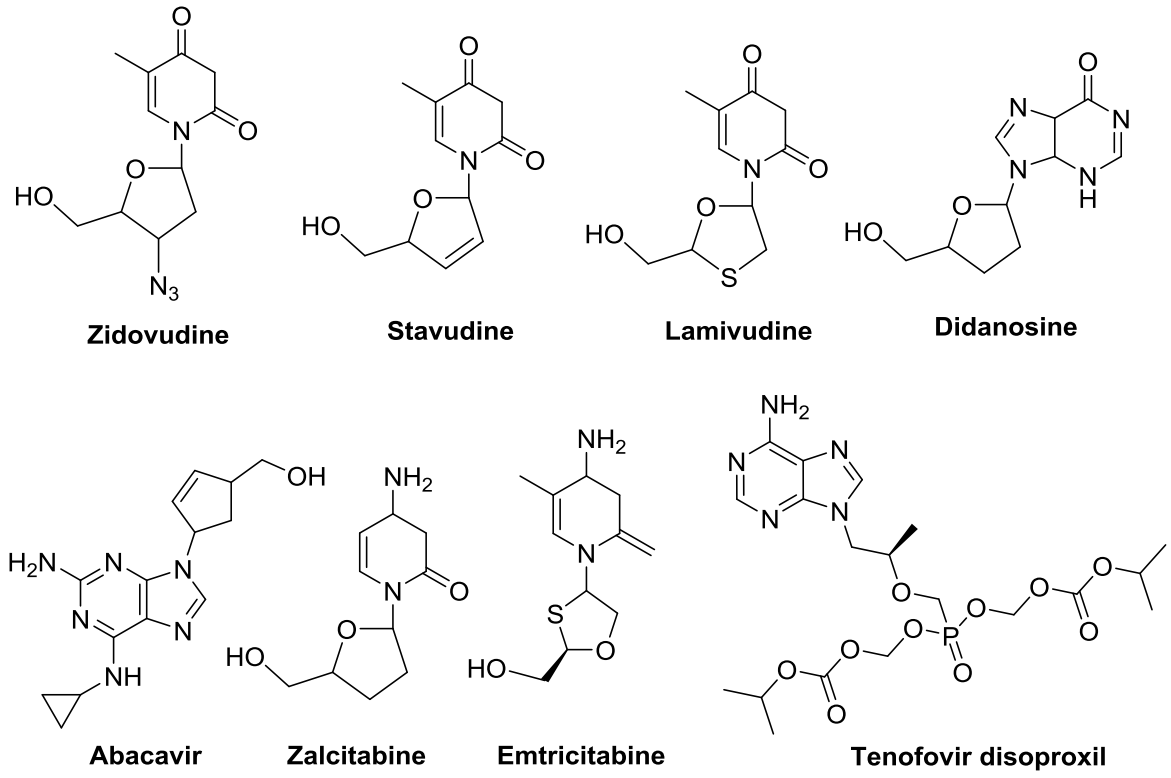

Fig. 1.3 Structure of approved Nucleoside/Nucleotide Reverse Transcriptase Inhibitors

Limitations of NRTIs/ NtRTIs

Generally, patients taking one or more nucleoside/nucleotide analogs faced different toxicities like peripheral neuropathy, cardiac and skeletal muscle myopathy, pancreatitis and bone marrow suppression [27]. The molecular basis for most of these side effects appears linked with the inhibition of mitochondrial DNA replication catalyzed by polymerase gamma (pol γ) [28]. Despite their widespread use, the therapeutic utility of this class of drugs is often restricted predominately due to the development of drug resistance. Although, resistance to nucleoside/nucleotide analogs may develop due to certain mechanism, but selective point mutations in RT that hinder the incorporation of nucleoside/nucleotide based drug is considered the prime cause of resistance [29].

Furthermore, three consecutive intracellular phosphorylation reactions required for the activation of NRTIs represent a problematic step for many nucleoside analogs. In particular, the first phosphorylation step, which results in the formation of the nucleoside monophosphate is considered to be the most difficult and rate limiting [30]. On the other hand, nucleotide reverse transcriptase inhibitors like tenofovir bear two negative charges which also limit their transport into cells [31].

1.3.1.2 Non-Nucleoside Reverse Transcriptase Inhibitors (NNRTIs)

NNRTIs bind to reverse transcriptase at a site adjacent (allosteric site) to the active site which results the conformational changes in active site and consequently leads to the inhibition of enzyme's catalytic function. The major advantage of NNRTIs is that they specifically inhibit the viral reverse transcriptase without showing any effects on host polymerases and moreover these do not show cross resistance with NRTIs [32].

NNRTIs approved by US FDA

The NNRTIs are active specifically against HIV-1 and these do not show activity against HIV-2 or other retroviruses. The first NNRTI drug was nevirapine, discovered by researchers at Boehringer Ingelheim and it was approved in 1996 by US Food and Drug Administration (FDA). Next to this, within two years, two more NNRTIs delavirdine and efavirenz were also approved by FDA [33]. Above mentioned three drugs are called as first generation NNRTIs and further need for NNRTIs with better efficacy against the resistance strains led to the discovery of the next generation NNRTIs. The research group at Janssens Foundation and Tibotec discovered the first drug of this class, etravirine, which was approved in 2008 by FDA. The second drug in this class was rilpivirine, also discovered by Tibotec and approved by FDA in the year 2011. Structures of the approved NNRTIs for the treatment of HIV/AIDS are shown in the Fig. **1.4** [34, 35].

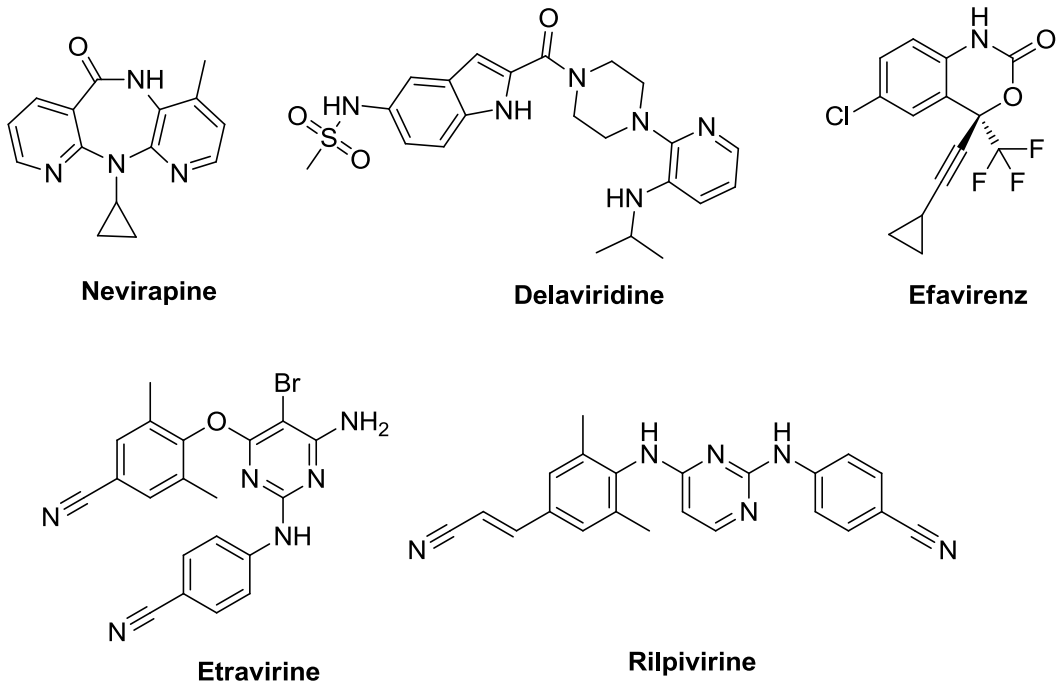

Fig. 1.4 Structure of approved Non-Nucleoside Reverse Transcriptase Inhibitors (NNRTIs)

New clinically investigated NNRTIs

RDEA806 is NNRTI of triazole class (Fig. **1.5**), presented by researchers from the Ardea Biosciences pharmaceutical company showed positive results in phase IIa for the treatment of HIV. It exhibited potent anti-retroviral activity in short-term monotherapy with HIV-infected subjects. Available reports revealed the good tolerance of RDEA806 and there are no discontinuation reports due to adverse events [36].

Fosdevirine also known as IDX899 or GSK-2248761 is another next generation NNRTI developed by Idenix Pharmaceuticals and ViiV Healthcare (Fig. **1.5**). It belongs to the family of 3-phosphoindoles and its *in-vitro* studies showed potent HIV-1 RT inhibitory activity as well anti-HIV-1 activity. The study of fosdevirine as NNRTI has been discontinued by US FDA because of seizures occurred among five participants in a Phase IIb study [37].

Lersivirine, another molecule developed by ViiV Healthcare belongs to the pyrazole family (Fig. **1.5**), also explored as next generation NNRTI and reached up to clinical trials. The study of lersivirine as an NNRTI was discontinued in the year 2013 because the inventor company has declared that the proposed lersivirine would not provide any extra benefit over currently approved NNRITIs which are already in clinical practice [38].

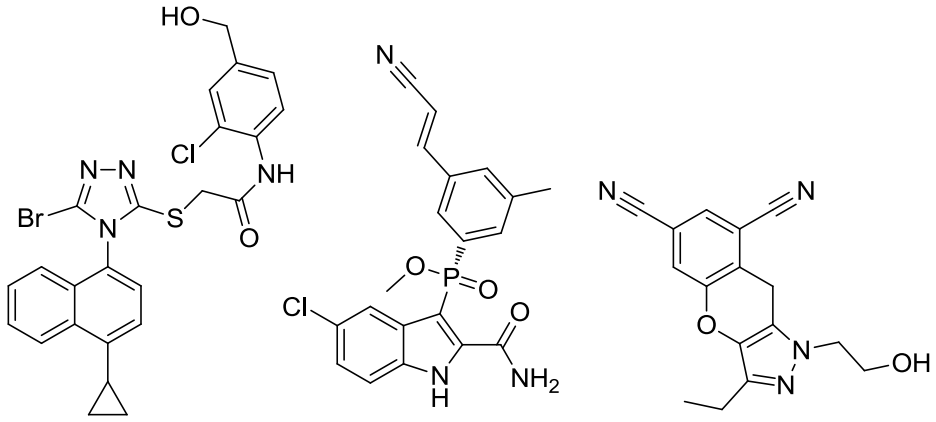

RDEA806 **Fosdevirine** **Lersivirine**

Fig.1.5 Structure of new clinically investigated NNRTIs

Limitations and current status of NNRTIs

NNRTIs such as efavirenz, nevirapine and delavirdine (first generation NNRTIs) show reduced or no efficacy against certain mutant strain of HIV. Diaryl Pyrimidine derivatives (DAPY) such as etravirine and rilpivirine (second generation NNRTIs), retain potency against many of the mutant strains, since they can adopt different conformational modes while binding with the RT enzyme. These compounds (etravirine and rilpivirine) showed remarkable torsional flexibility (‘‘wiggling’’) and ability to reposition (‘‘jiggling’’) within the

NNRTI binding pocket, thereby optimizing their interactions with the enzyme. Although, second generation NNRTIs are clinically effective against wide range of HIV-1 RT strains, but recently some strains of HIV-1 RT have shown less susceptibility against these second generation drugs also [39, 40].

1.4 Need of new anti-HIV Drugs

Although, after the advent of HAART, the mortality rate due to AIDS has reduced up to 60-80%, which made the AIDS a chronic manageable disease from its fatal nature. However, management of HIV/AIDS is still worrisome and complex due to certain problems associated with current therapy, like development of drug resistance, poor drug tolerability, monitoring of therapy and efficacy. So, all these factors drive the need for the search of new inhibitors with potent antiviral activity against wild as well as resistance strains, improved safety and better pharmacokinetic profile [41].

1.5 Opportunistic infections associated with AIDS

Opportunistic infections (OIs) are the most common cause of death among the HIV/AIDS patients due to their weak immune system [42]. Destruction of immune cells resulting in immuno-suppression is continually ongoing during HIV infection, which allows the onset of another infection in an already weakened host. Complicating agents that take hold during HIV infection are often opportunistic; means under normal or immuno-competent conditions, these agents would not be infective. As, most of these infections are caused by microorganisms such as bacteria, fungi, virus, protozoa etc, also some specific forms of cancers are frequently reported in AIDS patients [43]. OIs such as candidiasis, invasive cervical cancer, coccidioidomycosis, cryptococcosis, cytomegalovirus disease, herpes simplex, histoplasmosis, Kaposi's sarcoma, lymphoma, multiple forms, mycobacterium avium complex, tuberculosis, pneumocystis, leukoencephalopathy and toxoplasmosis of brain are most frequently appears in immune-compromised patients. Above mentioned OIs along with some other microbial infections are generally accounted for the major cause of morbidity and mortality of HIV infected patients [44].

For the sake of concision, we focus on *Mycobacterium tuberculosis* (Mtb) and four other bacterial strains for study, which include two G (+)ve (Gram positive) strains (*Staphylococcus aureus* and *Bacillus cereus*) and two G (-)ve (Gram negative) strains (*Escherichia coli* and *Pseudomonas putida*). Furthermore, we also included two fungal strains (*Candida albicans* and *Aspergillus niger*) in the study. Rationality for the selection of aforementioned pathogenic strains as well as their co-relation with HIV is briefly discussed in the below section:

1.5.1 Tuberculosis as opportunistic infection associated with AIDS

Tuberculosis (TB) is a pulmonary infectious disease with pandemic proportions. TB is caused by different members of *Mycobacterium tuberculosis* complex, predominantly by *Mycobacterium tuberculosis* (Mtb). According to the WHO global tuberculosis report of 2015, over 9.6 million people fell ill and more than 1.5 million people died due to TB-related complications in 2014. Although, a highly effective treatment with the first-line drugs (isoniazid, rifampicin, pyrazinamide, ethambutol and streptomycin) is available, but above chemotherapeutics are effective mainly against non drug resistant strains of Mtb [45, 46].

The increasing incidence of bacillary resistance towards the conventional drugs fuelled by the co-incidence of HIV has led to an increasing occurrence of treatment failure [47, 48]. Generally, HIV infection speed up the progression of TB from latent to active, moreover few reports revealed that TB and HIV co-infection speeds up the progress of each other [49]. In the year 2013, around 9 million people developed TB, in which nearby 1.1 million (13%) were found to be HIV-positive [50]. The natural history of TB is generally altered in the immune-compromised patients, in such patients, a long latency phase between infection and development of active disease generally reduced to few weeks to months while in normal patients this period remains from years to decades. The average progression time from latent to active TB is estimated much faster in people living with HIV compared to the HIV-negative patients [51].

Challenges in the treatment of tuberculosis

Standard anti-TB drugs have been used for decades and resistance to these medicines is widespread. Disease strains that are resistant to a single anti-TB drug have been documented in every surveyed country. Multidrug-resistant tuberculosis (MDR-TB) is now prevailing in a faster way, this form of TB does not respond to the two standard anti-TB drugs (isoniazid and rifampicin). Generally, non-adherence to the proper anti-TB therapy, incorrect use of anti-TB drugs or use of poor quality medicines are the prime cause of MDR-TB. Although, MDR-TB possessed less susceptibility towards the conventional first-line treatment, but it can be cured by the second-line drugs. However, drugs used in second-line therapy are also associated with certain problems like non-availability, high price, drug-drug interaction and toxicity. Apart from MDR-TB, in some cases, more severe drug resistance form of TB is also observed, known as extensively drug-resistant TB (XDR-TB), this responds to even fewer available medicines, including the most effective second-line anti-TB drugs [52, 53].

One more worst form of TB, reported since last few years is totally drug resistant TB, (TDR-TB), bacteria of these strains are resistant to all the first as well as second line TB drugs like

Isoniazid (INH), Rifampicin (RIF), Streptomycin (STM), ethambutol, pyrazinamide, ethionamide, para-aminosalicylic acid (PAS), ofloxacin, amikacin, ciprofloxacin, capreomycin and kanamycin. The presence of TDR-TB was first observed in two patients in Italy in the year 2003 and subsequently reported by Migliori *et al*. in 2007 [54]. In 2012, four cases of TDR-TB were reported in India, one of the countries with the highest burden of drug-resistant TB [55].

The provision of anti-retroviral therapy and anti-TB drug treatment at the same time involves a number of potential difficulties including drug-drug interactions, cumulative drug toxicities, high pill burden and Immune re-constitution inflammatory syndrome (IRIS). IRIS is an exaggerated inflammatory response against any concurrent opportunistic infection, which generally appears when a person put on anti-retroviral therapy. TB IRIS was estimated to occur in 28-36% of patients co-infected with TB and HIV [56]. US-FDA and European Medicines Agency have approved two new drugs, bedaquiline and delamanid, respectively, that may offer a therapeutic solution for TDR-TB [57]. But still due to increasing incidence of TB bacterial resistance towards the conventional drugs, fuelled by the co-incidence of HIV have led to an increasing occurrence of treatment failure [58, 59]. As a result, there is compiling need for the search of newer drugs active against both drug sensitive and resistant strains of Mtb, which can also act as a companion drug for existing treatment regimen of TB.

1.5.2 Bacterial infections associated with AIDS

HIV-positive patients, especially those has progressed to AIDS are found more susceptible to other bacterial born infections also apart from TB. In the current work, some representative bacterial strains such as *S. aureus*, *B. cereus*, *E. coli* and *P. putida* which occurs with HIV as co-infective agents have been selected for the study. Among this, *S. aureus* is a Gram (+)ve coccal bacterium, which is re-surged as one of the nosocomial pathogen, commonly found among HIV-positive particularly in hospitalized patients [60]. A study conducted by Kumar and group on 1000 HIV-positive hospitalized patients revealed that, around 13.2% patients were found infected with *S. aureus* as compared to 0.8% incidence among HIV-negative, yielding a 16.5 fold increase in the odds ratio [61]. Since, last decade methicillin-resistant *S. aureus* (MRSA) has emerged as the major cause of health problem particularly among the immune compromised or HIV-1 positive patients [62]. Further, *B. cereus* is also a Gram (+)ve, motile, spore-forming rod, that is found in wound infection, gastrointestinal infection, pneumonia, meningitis and septicaemia etc. Some studies have illustrated the increased incidence of *B. cereus* infections among the immune-compromised or HIV-positive patients [63].

Gram (-)ve bacterium, *E. coli* is commonly found inside the lower intestine of higher organisms, most of them are harmless except few strains. However, in immune-compromised or AIDS patients, the high prevalence of urinary tract infections and severe diarrhoea cases associated with *E. coli* are reported. The incidence of diarrhoea among HIV patients has been estimated to be 30 to 70% throughout their lifetime [64]. In a study conducted on 70 HIV-positive children suffering from diarrhoea, around 19% children were isolated with diarrheagenic *E. coli* as pathogen [65]. Another, Gram (-)ve bacterium *P. putida* is a rod-shaped, saprotrophic soil bacterium which is non-pathogenic for human and only rare cases are reported, where it act as pathogen in a healthy individual. However, it primarily causes infection in immunosuppressed hosts and in patients with invasive medical devices [66, 67].

Challenges in the treatment of bacterial borne infection

The rapid emergence of drug resistance bacterial strains is occurring worldwide, endangering the efficacy of currently available antibiotics. The antibiotic resistance crisis has been attributed due to over the counter and irrational use of these medications. The process of new drug development by the pharmaceutical industry has become tough due to reduced economic incentives and challenging regulatory requirements. Recent studies revealed that among Gram (+)ve pathogens, a global pandemic of resistant *S. aureus* and Enterococcus species currently poses the biggest threat [68]. Furthermore, as HAART involves the combination of several drugs and many scientific reports demonstrated the unfavourable interactions between anti-HIV and anti-bacterial drugs [69]. So, all these factors drive the need for the search of new anti-bacterial drugs with better potency against the resistant strains, less toxicity and better compatibility with other anti-HIV drugs.

1.5.3 Fungal infections associated with AIDS

Although, the number of fungal species have been reported as co-infective along with HIV, however, in the current research work, two representative species; *C. albicans* and *A. niger* that are commonly encountered pathogens in immune compromised patients [70] have been selected for study. Candidiasis is a common opportunistic fungal infection in HIV-infected patients, which mainly affects mucocutaneous system but other invasive forms are also common. *Candida albicans* is the most common cause of candidiasis, although some other species of Candida are also known for the same [71]. In a study conducted in Nigeria by Nweze*et al.,* demonstrated that out of 200 HIV-positive patients screened, around 120 (60%) were found to be colonized by yeasts and *C. albicans* as dominating species. The low count of $CD4^+$ T-lymphocyte has conventionally been cited as the main risk factor for the development of oropharyngeal candidiasis. In some patients particularly with advanced

immune suppression, the gradual emergence of non-albicans candida species as a cause of refractory mucosal and invasive has been reported [72, 73].

Aspergillus species are ubiquitous throughout the world, which commonly grows in decaying soil and vegetation. Although, more than 300 species of Aspergillus are known, but the literature implicates only a few species like *A. fumigatus*, *A. niger* and *A. flavus* causes disease in human beings [74, 75]. Aspergillosis is an infection caused by members of Aspergillus species, generally, most people breathe Aspergillus spores every day without getting the infection. However, people with weakened immune systems or having lung diseases are at higher risk of developing health problems. Health complications caused by Aspergillus include allergic reactions, lung infections; moreover, invasive aspergillosis also occurs in patients with advanced HIV infection or those who are not getting anti-retroviral therapy (ART). In general, patients who possess HIV-associated aspergillosis typically have CD4 cell counts <100 cells/mm^3 [76, 77].

Challenges in the treatment of fungal borne infections

Despite improvement of anti-fungal therapies over the last 30 years, the phenomenon of anti-fungal resistance is still of major concern in clinical practice [78]. For example, *Candida albicans* is the most important fungal opportunistic pathogen; drugs like fluconazole and itraconazole have been used extensively for the treatment of its systemic infections. Afterwards, fluconazole resistance has been described in a high percentage of patients. Moreover, azole-resistant *C. albicans* is frequently encountered in HIV-infected patients with oropharyngeal candidiasis [79].

Resistance has been described for virtually all anti-fungal agents in diverse pathogens including *Candida* and *Aspergillus* species, moreover, frequency of resistance strains increases in co-infection with HIV. Therefore, therapeutic choices are limited for the control of fungal diseases, and it is tempting to combine different class of drugs to achieve better therapeutic efficacy. In the recent years, several novel resistance patterns have been observed, including resistance originating from environmental sources in some species of Aspergillus. Furthermore, the emergence of simultaneous resistance to different anti-fungal drug classes (multidrug resistance) in different fungal strains, particularly in different *candida* species is also arising more distressing situation which creates the need for novel anti-fungal drugs [80].

1.6 REFERENCES

1. J.M. Coffin, HIV population dynamics in vivo: Implications for genetic variation, pathogenesis and therapy. Science, 267 (1995) 483-489.
2. C. Teixeira, R.B. Jose, B. Gomes, P. Gomes, F. Maurel, Viral surface glycoproteins, gp120 and gp41, as potential drug targets against HIV-1: brief overview one quarter of a century past the approval of zidovudine, the first anti-retroviral drug. European Journal of Medicinal Chemistry 46 (2011) 979-992.
3. http://www.unaids.org/sites/default/files/media_asset/global-AIDS-update-2016_en.pdf, accessed on 16th Dec, 2016.
4. Annual Report, NACO (2015-2016).
5. http://www.naco.gov.in/sites/default/files/India%20HIV%20Estimations%202015.pdf, accessed on 3rd Nov. 2016.
6. J.A. Levy, Pathogenesis of human immunodeficiency virus infection. Microbiological Reviews, 57 (1993) 183-289.
7. A. Engelman, P. Cherepanov, The structural biology of HIV-1: Mechanistic and therapeutic insights. Nature Reviews Microbiology 10 (2012) 279-290.
8. P. Zhu, J. Liu, J.J. Bess, E. Chertova, J.D. Lifson, H. Grise, G.A. Ofek, Distribution and three-dimensional structure of AIDS virus envelope spikes. Nature, 441(2006) 847-852.
9. I.O. Gleenberg, A. Herschhorn, A. Hizi, Inhibition of the activities of reverse transcriptase and integrase of Human Immunodeficiency Virus type-1 by peptides derived from the Homologous Viral Protein R (Vpr). Journal of Molecular Biology, 369 (2007) 1230-1243.
10. M. Ott, M. Geyer, Q. Zhou, The control of HIV transcription: Keeping RNA polymerase II on track. Cell Host & Microbe, 10 (2011) 426-435.
11. E.O. Freed, HIV-1 assembly, release and maturation. Nature Reviews Microbiology, 13 (2015) 484-496.
12. J.R. Brechtl, W. Breitbart, M. Galietta, S. Krivo, B. Rosenfeld, The use of highly active anti-retroviral therapy (HAART) in patients with advanced HIV infection: Impact on medical, palliative care and quality of life outcomes. Journal of Pain and Symptom Management 21(2001) 41-51.
13. L.Q. Sun, L. Zhu, K. Qian, B. Qin, L. Huang, C.H. Chen, K.H. Lee, Design synthesis and preclinical evaluations of novel 4-substituted 1,5-diarylanilines as potent HIV-1 Non-nucleoside reverse transcriptase inhibitor (NNRTI) drug candidates. Journal of Medicinal Chemistry, 55 (2012) 7219-7229.

14. P. Chong, P. Sebahar, M. Youngman, D. Garrido, H. Zhang, E.L. Stewart, R.T. Nolte, Rational design of potent non-nucleoside inhibitors of HIV-1 reverse transcriptase. Journal of Medicinal Chemistry, 55 (2012) 10601-10609.
15. J.A. Este, T. Cihlar, Current status and challenges of antiretroviral research and therapy. Antiviral Research, 85 (2010) 25-33.
16. M.J. Kozal, Drug-resistant Human Immunodeficiency Virus. Clinical Microbiology & Infectious Diseases, 15 (2009) 69-73.
17. W.C. Greene, Z. Debyser, Y. Ikeda, E.O. Freed, E. Stephens, W. Yonemoto, R.W. Buckheit, Novel targets for HIV therapy. Antiviral Research, 80 (2008) 251-265.
18. J. Ding, K. Das, C. Tantillo, W. Zhang, A.D. Clark, S. Jessen, X. Lu, Structure of HIV-1 reverse transcriptase in a complex with the non-nucleoside inhibitor α-APA R 95845 at 2.8 A resolution. Structure, 3 (1995) 365-379.
19. S.G. Sarafianos, B. Marchand, K. Das, D.M. Himmel, M.A. Parniak, S.H. Hughes, E. Arnold, Structure and function of HIV-1 reverse transcriptase: Molecular mechanisms of polymerization and inhibition. Journal of Molecular Biology 385 (2009) 693-713.
20. M.P. de Bethune, Non-nucleoside reverse transcriptase inhibitors (NNRTIs), their discovery, development and use in the treatment of HIV-1 infection: A review of the last 20 years (1989-2009). Antiviral Research, 85 (2010) 75-90.
21. F. Esposito, A. Corona, E. Tramontano, HIV-1 Reverse Transcriptase still remains a new drug target: Structure, function, classical inhibitors and new inhibitors with innovative mechanisms of actions. Molecular Biology International (2012) 586401, doi: 10.1155/2012/586401.
22. E. De Clercq, The design of drugs for HIV and HCV. Nature Reviews Drug Discovery 6 (2007) 1001-1018.
23. https://aidsinfo.nih.gov/education-materials/fact-sheets/21/58/fda-approved-hiv-medicines, accessed on 7th Nov. 2016.
24. T. Cihlar, A.S. Ray, Nucleoside and nucleotide HIV reverse transcriptase inhibitors: 25 years after zidovudine. Antiviral Research, 85 (2010) 39-58.
25. H.B. Fung, E.A. Stone, F.J. Piacenti, Tenofovir disoproxil fumarate: A nucleotide reverse transcriptase inhibitor for the treatment of HIV infection, Clinical Therapeutics, 24 (2002) 1515-1548.
26. https://aidsinfo.nih.gov/drugs/290/tenofovir-disoproxil-fumarate/0/patient, accessed on 4th Aug. 2016.
27. R. Scatena, P. Bottoni, G. Botta, G.E. Martorana, B. Giardina, The role of mitochondria in pharmacotoxicology: A re-evaluation of an old, newly emerging topic. American journal of physiology. Cell physiology. 293 (2007) C12–21.

28. S.E. Lim, W.C. Copeland. Differential incorporation and removal of antiviral deoxynucleotides by human DNA polymerase gamma. The Journal of biological chemistry, 276 (2001) 23616-23623.
29. A.J. Berdis, DNA Polymerases as therapeutic targets. Biochemistry, 47 (2008) 8253-8260.
30. S.J. Hecker, M.D. Erion, Prodrugs of phosphates and phosphonates, Journal of Medicinal Chemistry, 51 (2008) 2328-2345.
31. E. Taneva, K. Crooker, S.H. Park, J.T. Su, A. Ott, N. Cheshenko, I. Szleifer, Differential mechanisms of Tenofovir and Tenofovir Disoproxil Fumarate cellular transport and implications for topical pre-exposure prophylaxis. Antimicrobial agents and chemotherapy, 60 (2015) 1667-1675.
32. R.H. Smith, C.J. Michejda, S.H. Hughes, E. Arnold, P.J. Janssen, M.K. Smith, Structure and mechanism of action of non-nucleoside inhibitors of HIV-1 reverse transcriptase: strategies to combat drug resistance. Journal of Molecular Structure: THEOCHEM 423 (1998) 67-77.
33. E.D. Clercq, Anti-HIV drugs: 25 compounds approved within 25 years after the discovery of HIV. International Journal of Antimicrobial Agents, 33 (2009) 307-320.
34. J. Ghosn, M.L. Chaix, C. Delaugerre, HIV-1 resistance to first and second generation non-nucleoside reverse transcriptase inhibitors. AIDS Reviews, 11 (2009) 165-173.
35. A. Ivetac, S.E. Swift, P.L. Boyer, A. Diaz, J. Naughton, J.A. Young, S.H.Hughes, Discovery of novel inhibitors of HIV-1 reverse transcriptase through virtual screening of experimental and theoretical ensembles. Chemical Biology & Drug Design, 83 (2014) 521-531.
36. G. Moyle, M. Boffito, A. Stoehr, A. Rieger, Z. Shen, K. Manhard, B. Sheedy, Phase 2a randomized controlled trial of short-term activity, safety and pharmacokinetics of a novel non-nucleoside reverse transcriptase inhibitor, RDEA806, in HIV-1 positive, antiretroviral-naive subjects. Antimicrobial Agents and Chemotherapy, 54 (2010) 3170-3178.
37. D.A. Margolis, J.J. Eron, E. DeJesus, S. White, P. Wannamaker, B. Stancil, M. Johnson, Unexpected finding of delayed-onset seizures in HIV-positive, treatment-experienced subjects in the Phase IIb evaluation of fosdevirine (GSK2248761). Antiviral Therapy,19 (2014) 69-78.
38. M. Platten, G. Fatkenheuer, Lersivirinea new drug for HIV infection therapy. Expert Opinion on Investigational Drugs, 22 (2013)1687-94.
39. L.B. Johnson, L.D. Saravolatz, Etravirine, a next-generation non nucleoside reverse-transcriptase inhibitor. Clinical Infectious Diseases 48 (2009) 1123-1128.

40. H. Jeulin, M. Foissac, L. Boyer, N. Agrinier, P. Perrier, A. Kennel, A. Velay, Real-life rilpivirine resistance and potential emergence of an E138A-positive HIV strain in north-eastern France. The Journal of Antimicrobial Chemotherapy, 69 (2014) 3095-3102.
41. P. Zhan, C. Pannecouque, E. De Clercq, X. Liu, Anti-HIV drug discovery and development: Current innovations and future trends. Journal of Medicinal Chemistry 59 (2016) 2849-2878.
42. S.D. Patel, D.M. Kinariwala, T.B. Javadekar, Clinico-microbiological study of opportunistic infection in HIV seropositive patients. Indian journal of sexually transmitted diseases, 32 (2011) 90-93.
43. http://www.cdc.gov/hiv/basics/livingwithhiv/opportunisticinfections.html, accessed on 7th April 2016.
44. https://www.aids.gov/hiv-aids-basics/staying-healthy-with-hiv-aids/potential-related-health-problems/opportunistic-infections/, accessed on 13th April, 2015.
45. "Tuberculosis WHO global tuberculosis report 2015" http://www.who.int/tb/Global_TB_Facts.pdf?ua=1, accessed on 26th Dec. 2015.
46. A. Zumla, P. Nahid, S.T. Cole, Advances in the development of new tuberculosis drugs and treatment regimens. Nature Reviews Drug Discovery, 12 (2013) 388-404.
47. N. Chhabra, M.L. Aseri, R. Dixit, S. Gaur, Pharmacotherapy for multidrug resistant tuberculosis. Journal of Pharmacology & Pharmacotherapeutics, 3 (2012) 98-104.
48. S.K Parida, R. Axelsson-Robertson, M.V. Rao, N. Singh, I. Master, A. Lutckii, S. Keshavjee, Totally drug-resistant tuberculosis and adjunct therapies. Journal of Internal Medicine, 277 (2015) 388-405.
49. K.H. Mayer, D. Hamilton, Synergistic pandemics: Confronting the global HIV and tuberculosis epidemics, Clinical Infectious Diseases, 50 (2010) S67-70.
50. http://www.tbfacts.org/tb-hiv/#sthash.4UJJsvOd.dpuf, accessed on 14th March, 2016.
51. http://hivinsite.ucsf.edu/, accessed on 14th March, 2016.
52. H. Esmail, C.E. Barry, D.B. Young, R.J. Wilkinson, The ongoing challenge of latent tuberculosis. Philosophical Transactions of the Royal Society of London. Series B, Biological Sciences, 369 (2014).
53. C. Porwal, A. Kaushik, N. Makkar, J.N. Banavaliker, M. Hanif, R. Singla, A.K. Bhatnagar, Incidence and risk factors for extensively drug-resistant tuberculosis in Delhi region, PLoS One. 8 (2013) e55299.
54. G.B. Migliori, R. Loddenkemper, F. Blasi, M.C. Raviglione, 125 years after Robert Koch's discovery of the tubercle bacillus: The new XDR-TB threat. Is "science" enough to tackle the epidemic?" European Respiratory Journal, 29 (2007) 423-427.

55. A. Bhargava, Y. Jain, The revised national tuberculosis control programme in India: Time for revision of treatment regimens and rapid up-scaling of DOTS-plus initiative". The National Medical Journal of India, 21 (2008) 187-191.
56. S. Leone, E. Nicastri, S. Giglio, P. Narciso, G. Ippolito, N. Acone, Immune reconstitution inflammatory syndrome associated with *Mycobacterium tuberculosis* infection: A systematic review. International Journal of Infectious Diseases, 14 (2010) 283-291.
57. G. Brigden, C. Hewison, F. Varaine, New developments in the treatment of drug-resistant tuberculosis: Clinical utility of bedaquiline and delamanid. Infection and Drug Resistance, 8 (2015) 367-378.
58. N. Rockwood, E. du Bruyn, T. Morris, R.J. Wilkinson, Assessment of treatment response in tuberculosis. Expert Review of Respiratory Medicine, 31 (2016) 1-12.
59. J.B. Parr, M.L. Rich, S. Keshavjee, M.F. Franke, C.D. Mitnick, J. Bayona, M.C. Becerra, Presumptive treatment of multidrug-resistant tuberculosis in household contacts. The International Journal of Tuberculosis and Lung Disease, 20 (2016) 370-375.
60. F.D. Lowy, *Staphylococcus aureus* infections. New England Journal of Medicine, 339 (1998) 520-532.
61. A.S. Kumar, S. Kumar, J.N. Sheagren, Increased incidence of *Staphylococcus aureus* bacteremia in hospitalized patients with Acquired Immunodeficiency Syndrome. Clinical Infectious Diseases, 33 (2001) 1412-1416.
62. K. Podovich, R. Weinsein, A. Aroutcheva, T. Rice, B. Hota, Community associated methicillin-resistant *Staphylococuus aureus* and HIV: Interacting epidemics. Clinical Infectious Disease, 50 (2010) 979-987.
63. A.H. Gaur, C.C. Patrick, J.A. McCullers, P.M. Flynn, T.A. Pearson, B.I. Razzouk, S.J. Thompson, *Bacillus cereus* bacteremia and meningitis in immunocompromised children. Clinical Infectious Diseases, 32 (2001) 1456-1462.
64. M. Kartalija, M.A. Sande, Diarrhoea and AIDS in the era of highly active antiretroviral therapy. Clinical Infectious Diseases, 28 (1999) 701-705.
65. A.M Medina, F.P Rivera, L.M Romero, L.A. Kolevic, M.E. Castillo, E. Verne, R. Hernandez, Diarrheagenic *Escherichia coli* in Human Immunodeficiency Virus (HIV) pediatric patients in Lima, Peru. The American Journal of Tropical Medicine and Hygiene, 83 (2010) 158-163.
66. R.J. Carpenter, J.D. Hartzell, J.A. Forsberg, B.S. Babel, A. Ganesan, *Pseudomonas putida* war wound infection in a US Marine: A case report and review of the literature. Journal of Infection, 56 (2008) 234-240.
67. E. Dervisoglu, D.O. Dundar, I. Yegenaga, A. Willke, Peritonitis due to *Pseudomonas putida* in a patient receiving automated peritoneal dialysis, Infection. 36 (2008) 379-380.

68. C.L. Ventola, The antibiotic resistance crisis: Part 1: Causes and threats. Pharmacy and Therapeutics, 40 (2015) 277-83.
69. A.J. Wood, S.C. Piscitelli, K.D. Gallicano, Interactions among drugs for HIV and opportunistic infections. New England Journal of Medicine, 344 (2001) 984-996.
70. R. Kaur, M.S. Dhakad, R. Goyal, P. Bhalla, R. Dewan, Spectrum of opportunistic fungal infections in HIV/AIDS patients in tertiary care hospital in India. The Canadian Journal of Infectious Diseases & Medical Microbiology, (2016), doi:10.1155/2016/2373424
71. A. Cassone, R. Cauda, Candida and candidiasis in HIV-infected patients, AIDS. 26 (2012) 1457-1472.
72. E.I. Nweze, U.L. Ogbonnaya, Oral Candida isolates among HIV-infected subjects in Nigeria, Journal of Microbiology, Immunology and Infection, 44 (2011) 172–177.
73. K.P. Anwar, A. Malik, K.H. Subhan, Profile of candidiasis in HIV infected patients. Iranian Journal of Microbiology, 4 (2012) 204-209.
74. P. Latge, *Aspergillus fumigatus* and Aspergillosis. Clinical Microbiology Review, 12 (1999) 310-350.
75. D. Armstrong-James, G. Meintjes, G.D. Brown. A neglected epidemic: Fungal infections in HIV/AIDS. Trend in Microbiology, 22 (2014) 120-127.
76. S. Antinori, M. Nebuloni, C. Magni, M. Fasan, F. Adorni, A. Viola, C. Parravicini, Trends in the post-mortem diagnosis of opportunistic invasive fungal infections in patients with AIDS. American Journal of Clinical Pathology, 132 (2009) 221-227.
77. M. Richardson, C. Lass-Florl, Changing epidemiology of systemic fungal infections, Clinical Microbiology and Infection, 14 (2008) 5-24.
78. P. Vandeputte, S. Ferrari, A.T. Coste, P. Vandeputte, S. Ferrari, A.T. Coste, Antifungal resistance and new strategies to control fungal infections. International Journal of Microbiology. (2012) 713687, doi: 10.1155/2012/713687.
79. C. Spampinato, D. Leonardi, Candida infections, causes, targets and resistance mechanisms: Traditional and alternative antifungal agents. BioMed Research International. (2013) 204237, doi: 10.1155/2013/204237.
80. D.S. Perlin, E. Shor, Y. Zhao, Update on antifungal drug resistance. Current Clinical Microbiology Reports, 2 (2015) 84-95.

CHAPTER 2

Review of Literature

Nitrogen containing heterocyclic compounds obtained from synthetic as well as natural origin (like alkaloids) have been known for the diverse biological activity. Although, this family constitutes very large number of compounds, however in this dissertation work, we selected few members; like tetrahydroisoquinoline, tetrahydroquinoline, quinoline, piperazine and oxindole or indolin-2-one (Fig. **2.1**). Selection of the above heterocyclic nucleus was made based upon their feasibility of diversity orientated synthesis and their pharmacological potential, especially as anti-infective agents. In the present chapter, we summarized the pharmacological activity of compounds based upon the aforementioned nucleuses against HIV and other infectious microbes like bacteria, fungi, and mycobacterium.

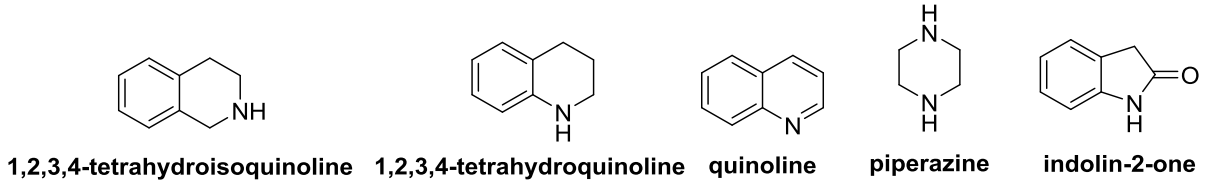

Fig. 2.1 Structure of selected nitrogen containing heterocyclic nucleus

2.1 Biological significance of tetrahydroisoquinoline based scaffold

1,2,3,4-tetrahydroisoquinoline (THIQ, Fig. **2.1**) is secondary amine with the chemical formula $C_9H_{11}N$. THIQ containing alkaloids are widely distributed in nature and more attention has been paid in the recent years on this type of alkaloid, owing to their diverse range of biological activities. Especially, THIQ based anti-tumor agents obtained from natural sources have been studied over the past four decades [1]. Some other typical examples of naturally occurring anti-tumor agents containing core THIQ includes indenoisoquinoline, saframycin, narciclasine, bioxalomycin, quinocarcin, tetrazomine and ecteinascidin-743 [2-4]. In addition to the anti-cancer activity, compounds containing this nucleus are reported for other diverse type of anti-parasitic activity, in the present dissertation work we summarized their anti-infective activity against diverse type of pathogens like HIV, bacteria, fungi, protozoan and mycobacterium.

2.1.1 Tetrahydroisoquinoline as anti-bacterial agents

Compounds based upon 6,7-dimethoxy-1,2,3,4-tetrahydroisoquinoline nucleus were synthesized and evaluated for *in-vitro* anti-microbial activities against different bacterial strains like *S. aureus, S. epidermidis, E. coli* and *P. aeruginosa*. Among the tested compounds, three analogs (**1a-c,** Fig. **2.2**) displayed good to moderate anti-bacterial activity against the all tested bacterial strains with MIC 3.5–20 µg/mL [5]. In another study, 1-benzyl-1,2,3,4-tetrahydroisoquinoline derivatives were synthesized and tested for anti-bacterial activity by Al-Hiari and co-workers, best active compound **2** (Fig. **2.2**) of this series, inhibited

the growth of methicillin-resistant *S. aureus* with MIC of 32 µg/mL [6]. Liu and team reported a series of 7-substitued-1,2,3,4-tetrahydroisoquinoline derivative as inhibitor of DNA gyrase, in which compounds **3a** and **3b** (Fig. **2.2**) strongly inhibited the DNA gyrase of *S. aureus* and *B. subtilis* with IC_{50} of 0.125 and 0.25 µg/mL, respectively [7].

In one more study, novel *bis*-heterocyclic compounds containing THIQ nucleus with thiazole ring were synthesized and investigated for anti-microbial activity against two Gram (+)ve strains; *S. aureus* and *B. cereus*. Among the newly synthesized compounds, two compounds **4** and **5** (Fig. **2.2**) showed prominent anti-bacterial activity in low micromolar concentration against both bacterial strains [8]. In an another study, Galan and co-workers generated different 6,7-dimethoxy-THIQ based compounds (Fig. **2.2**) varied at 1st position and subsequently evaluated for anti-bacterial activity against different strains like *B. cereus, S. aureus, E. faecalis*, *S. typhi* and *E. coli*. The result of the study revealed that compounds like fluorophenylpropanoate ester (**6**), halogenated phenyl (**7a** and **7b**) and phenethyl carbamates (**8a** and **8b**) exerted the bactericidal activity at low micromolar concentration against the tested strains [9].

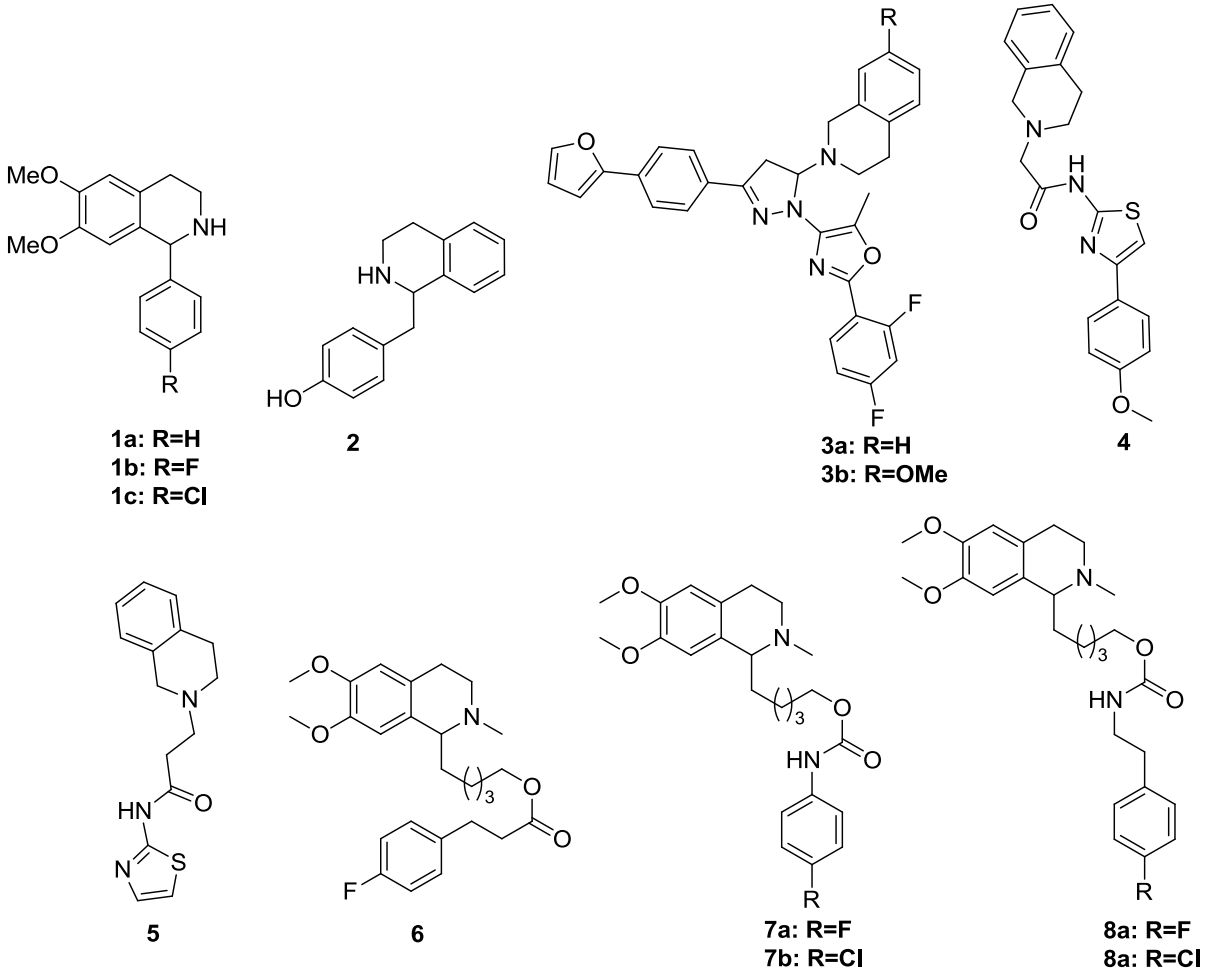

Fig. 2.2 Tetrahydroisoquinoline based compounds as anti-bacterial agents

2.1.2 Tetrahydroisoquinoline as anti-HIV agents

During the search for plant-derived compounds as anti-HIV agents, Kashiwada and team isolated some heterocyclic compounds from the leaves of *Nelumbo nucifera* and evaluated for the anti-HIV activity. Out of the tested compounds, two compounds (R)-Coclaurine **9** and (S)-norcoclaurine **10** (Fig. **2.3**), demonstrated potent anti-HIV activity with EC_{50} values of 0.8 and <0.82 µg/mL, respectively with therapeutic index (TI) values of >125 and >25, respectively [10]. Beside this, compounds based upon 1-aryl-1,2,3,4-tetrahydroisoquinoline were synthesized and assayed for anti-HIV-1 activity as well as cytotoxicity, among the series best active compound **11** (Fig. **2.3**) exhibited anti-HIV activity with EC_{50} 4.6 µM and cytotoxicity (CC_{50}) 727.3 µM [11].

De-novo hit-to-lead efforts involving the design of novel C-X-C chemokine receptor type 4 (CXCR4) antagonists, resulted in the discovery of a novel series of THIQ analogs as antagonist of CXCR4 receptor. Compound **12** (Fig. **2.3**) was proved as a potent and selective CXCR4 antagonist lead candidate (IC_{50} 5 nM) with a promising *in-vitro* profile. Further, ADME properties of compound **12** revealed its low metabolic liability potential and its *in-vivo* evaluations in rats demonstrated 63% bioavailability [12].

Swidorski and group performed lead optimization studies on BMS-663068, a known potent HIV-1 attachment inhibitor and synthesized series of compounds based upon THIQ and tetrahydropyrido[3,4-d]pyrimidine nucleus. Several THIQ based compounds exhibited sub-namomolar potency against HIV in pseudotype viral infection assay. Best active compound **13,** among the tested compounds (Fig. **2.3**) exhibited EC_{50} 0.02 nM [13].

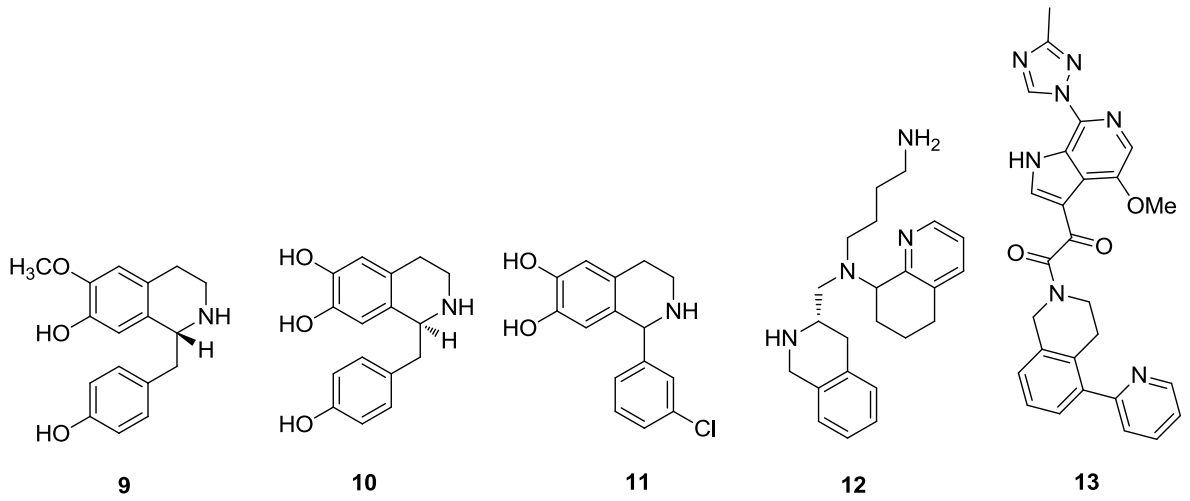

Fig. 2.3 Tetrahydroisoquinoline based compounds as anti-HIV agents

2.1.3 Tetrahydroisoquinoline as anti-fungal agents

Makarieva and co-workers isolated tetrahydroisoquinoline containing dimeric sphingolipid known as Oceanalin A (**14,** Fig. **2.4**) from an ethanolic extract of the marine sponge Oceanapia sp. The novel compound, oceanalin A exhibited anti-fungal activity (MIC 30 µg/mL) against the pathogenic fungus *C. glabrata* by inhibiting ceramide synthase enzyme, which consequently blocked the sphingolipid biosynthesis [14].

Novel THIQ compounds were designed using structure-based *de-novo* design, targeting the lanosterol 14a-demethylase (CYP51) enzyme. Designed compounds were synthesized and evaluated for anti-fungal activity against six different strains (*C. albicans, C. parapsilosis, C. neoformans, A. fumigates, T. rubrum* and *M. canis*). Most of the tested compounds showed potent anti-fungal activity against one or more tested strains, two compounds **15a** and **15b** (Fig. **2.4**) exhibited equal or potent anti-fungal activity against five tested strains (except *C. albicans*) than that of fluconazole [15].

In one more study, Krauss and team reported synthesis and anti-fungal activity of *N*-alkyl-1,2,3,4-tetrahydroisoquinoline and 6,7-dimethoxy-1,2,3,4-tetrahydroisoquinoline based compounds. The result of *in-vitro* testing revealed that compound **16** (Fig. **2.4**) having *N*-alkyl-1,2,3,4-tetrahydroisoquinoline with C11-alkyl chain showed anti-fungal potency against *C. glabrata, A. niger* and *H. burtonii* comparable to clotrimazole. Further, author proposed that the possible mechanism of action might be due to inhibition of ergosterol biosynthesis [16].

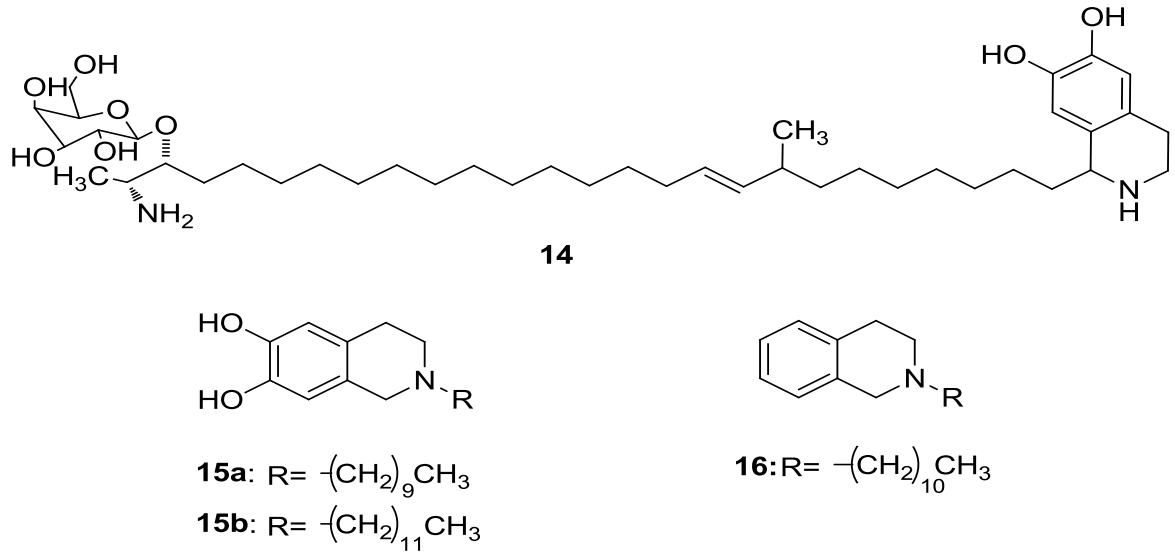

Fig. 2.4 Tetrahydroisoquinoline based compounds as anti-fungal agents

2.1.4 Tetrahydroisoquinoline as anti-tubercular agents

Tangallapally *et al.* performed lead optimization studies on a known potent anti-tubercular compound 5-nitro-furan-2-carboxylic acid 4-(4-benzyl-piperazin-1-yl)-benzylamide, which possessed low bioavailability. Series of compounds was prepared, among which compounds containing THIQ nucleus **17a, 17b** and **17c** (Fig. **2.5**) showed potent anti-tuberculosis activity (EC_{50} 0.006, 0.2 and 0.4 µg/mL, respectively) with better bioavailability [17].

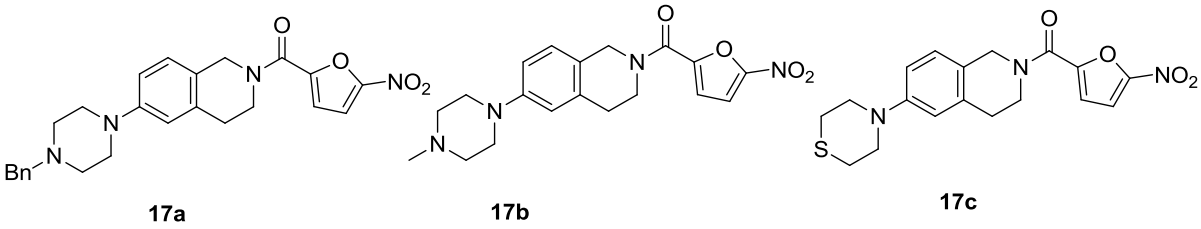

Fig. 2.5 Tetrahydroisoquinoline based compounds as anti-tubercular agents

2.2. Biological significance of Tetrahydroquinoline scaffold

Compound containing 1,2,3,4-tetrahydroquinoline entity (THQ, Fig. **2.1**), are known for wide range of pharmacological utility, due to which this nucleus has attracted the attention of several synthetic and medicinal chemists. The spectrum of biological activities includes anti-microbial, anti-viral, anti-fungal, anti-malarial, anti-leishmanial, anti-tubercular, anti-diabetic, anti-thrombotic and anti-cancer etc [18-20]. In the present dissertation work, we mainly summarized the anti-infective activity of THQ nucleus.

THQ based natural products are reported for their wide range of pharmacological application, for example, sumanirole (Fig. **2.6**) is widely used for basic research related to neurobiological mechanisms [21]. Naturally occurring angustureine (Fig. **2.6**) is a tetrahydroquinoline alkaloid, first isolated from the bark of *Galipea officinalis* has been used in traditional herbal medicine as an anti-septic [22]. Galipinine and cuspareine (Fig. **2.6**) are structurally related tetrahydroquinoline alkaloids which are known for their potent anti-malarial and anti-spasmodic activity, respectively [23, 24]. Compound flumequine (Fig. **2.6**) with tetrahydroquinoline nucleus exhibited broad-spectrum anti-bacterial activity and widely used as veterinary drug in food-producing animals [25]. Further, martinellic acid (Fig. **2.6**) bearing tetrahydroquinoline nucleus fused with pyrrolidine, have been reported as bradykinin receptor antagonist in several studies [26]. A cytotoxic alkaloid, aspernigerin (Fig. **2.6**) consisting of tetrahydroquinoline and piperazine moieties was isolated from the extract of a culture of *A. niger* which exhibited cytotoxic activity against cervical carcinoma and colorectal carcinoma cell lines with IC_{50} values of 46 and 35 µM, respectively [27].

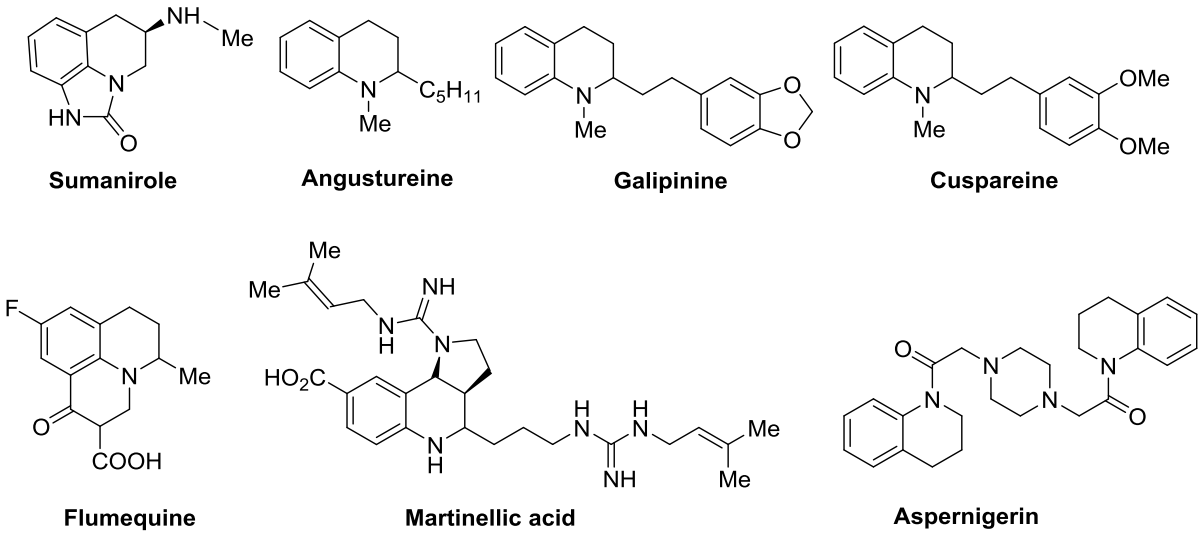

Fig 2.6 Structure of naturally occurring compounds containing tetrahydroquinoline nucleus

Elaborated study emphasize on anti-infective activity of THQ based compounds against pathogens like bacteria, HIV, fungi, and mycobacterium is given below;

2.2.1 Tetrahydroquinoline as anti-bacterial agents

In several scientific reports, THQ based compounds are reported for antibacterial activity against diverse bacterial strains, in one such study, compounds **18** and **19** (Fig. **2.7**) exhibited potent anti-bacterial activity against *E. faecalis* and *S. epidermidis* by inhibition of their enzymes farnecyl transferase and methionyltRNA synthetase, respectively [28, 29]. Compound containing *N*-benzenesulfonyl (BS) derivatives of THQ were synthesized and screened for anti-bacterial activity against methicillin-resistant *S. aureus, E. coli* and *P. aeruginosa.* Among the series of compounds, **20** (Fig. **2.7**) demonstrated moderate activity at 100 µg/mL concentration, against three selected bacterial strains [30].

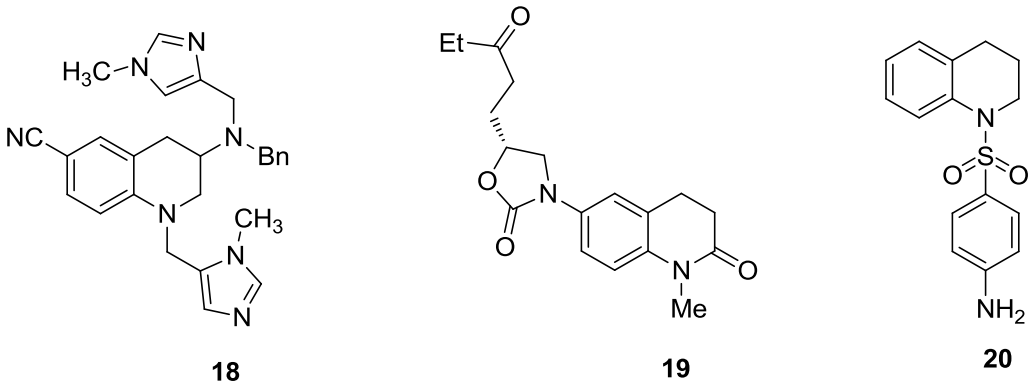

Fig. 2.7 Tetrahydroquinoline based compounds as anti-bacterial agents

2.2.2 Tetrahydroquinoline as anti-HIV agents

Su and team reported a series of THQ, which exhibited potent inhibitory activity against reverse transcriptase of HIV-1 by blocking its allosteric site. The most potent compound of the series **21a** (Fig. **2.8**) exhibited inhibitory activity against the wild, K103N and Y181C strains of HIV-1 RT with IC_{50} values of 1, 1 and 4 nM respectively. Another bioisostere of the same compound **21b** also inhibited the wild, K103N and Y181C strains of HIV-1 RT with IC_{50} values of 18, 18 and 99 nM, respectively [31].

Beside this, a novel series of 5-alkyl-2-arylthio-6-((3,4-dihydroquinolin-1(2*H*)-yl)methyl)pyrimidin-4(3*H*)-ones was synthesized and evaluated for HIV-1 RT inhibitory activity. Among the tested analogs, compounds **22a** and **22b** (Fig. **2.8**) exhibited potency comparable to nevirapine [32]. Derivatives of (S)-2-((2S,4R)-2-(3-aminophenyl)-1,2,3,4-tetrahydroquinolin-4-yl)cyclopentanone; **23a** and **23b** (Fig. **2.8**) are also reported for moderate anti-HIV activity in recombinant virus assay [33].

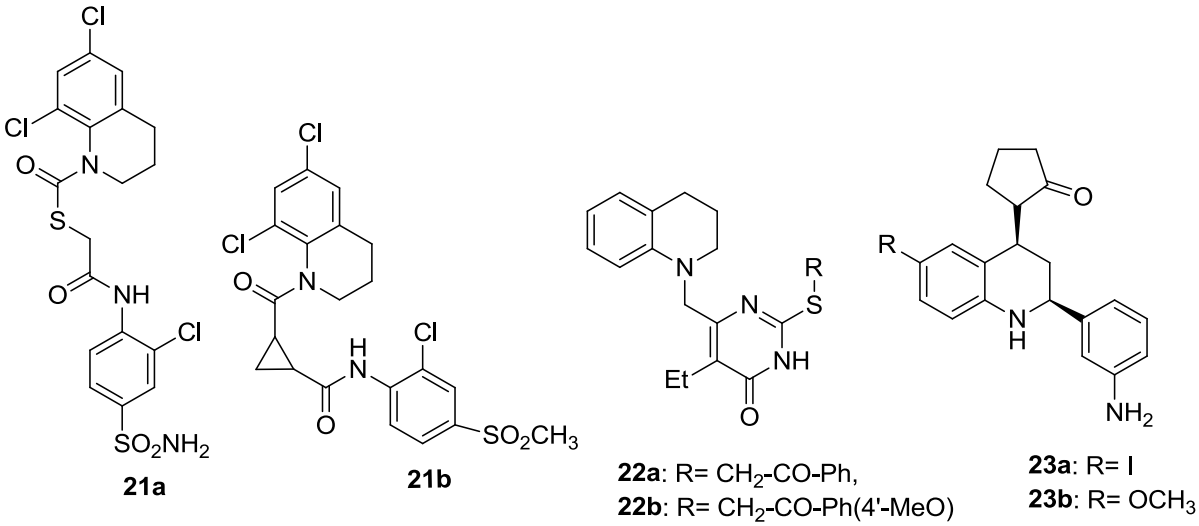

Fig. 2.8 Tetrahydroquinoline based compounds as anti-HIV agents

2.2.3. Tetrahydroquinoline as anti-fungal agents

Urbina *et al.* synthesized a series compounds and evaluated for anti-fungal activity, compounds **24a** and **24b** (Fig. **2.9**) of the series inhibited the growth of four fungal strains (*M. gypseum, T. mentagrophytes, T. rubrum, E. floccosum*) with MIC ranges from 12.5-25 µg/mL [34]. In another report, Gutierrez and team synthesized a series of 1-((2S,4S)-2-(furan-2-yl)-1,2,3,4-tetrahydroquinolin-4-yl)pyrrolidin-2-one derivatives and evaluated their activity against several phytopathogenic fungi. Compound **25** (Fig. **2.9**) of the series exhibited potent anti-fungal activity against *C. cladosporoide* comparable to the reference compound myclobutanil [35]. A series of *N*-alkyl substituted urea derivatives were synthesized and evaluated for *in-vitro* anti-fungal activity against *A. niger* and *T. rubrumi*,

compound **26** (Fig. **2.9**) containing urea conjugation of tetrahydroquinoline and morpholine inhibited the growth of both tested fungal strains with IC_{50} values 12.5 and 12.5 µg/mL, respectively [36].

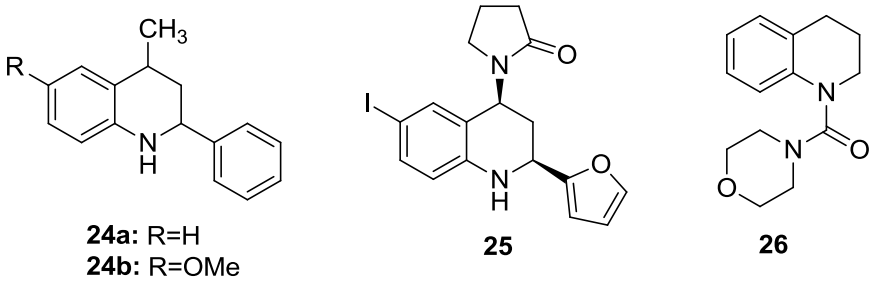

24a: R=H
24b: R=OMe

25

26

Fig. 2.9 Tetrahydroquinoline based compounds as anti-fungal agents

2.2.4 Tetrahydroquinoline as anti-tubercular agents

A series of nine hydrazone derivatives were synthesized *via* reaction of 2-(2-oxo-1,2,3,4-tetrahydroquinoline-7-yloxy)acetohydrazide with different o-hydroxyaldehyde. Further, hydrazone derivatives were complexed with Zn (II) yielded a series of nine complexes. Next, both series of compounds containing hydrazone derivatives as well as their Zn (II) complexes were evaluated for anti-tubercular activity. The Preliminary results of study showed that most of the hydrazone derivatives (without complex) exhibited weak to moderate activity (from 2.4 to 67.5% inhibition of *Mtb* at tested concentration of 6.25 µg/mL), best active compound **27** (Fig. **2.10**) exhibited 67.5% inhibition of *Mtb* at 6.25 µg/mL concentration. Interestingly, all Zn (II) complexes of hydrazones demonstrated good to potent anti-tubercular activity (>80% inhibition of *Mtb* at 6.25 µg/mL concentration). Among the tested compounds **28**, **29a** and **29b** (Fig. **2.10**) were found to be the most active with MIC 1.6 µg/mL against *Mtb* [37].

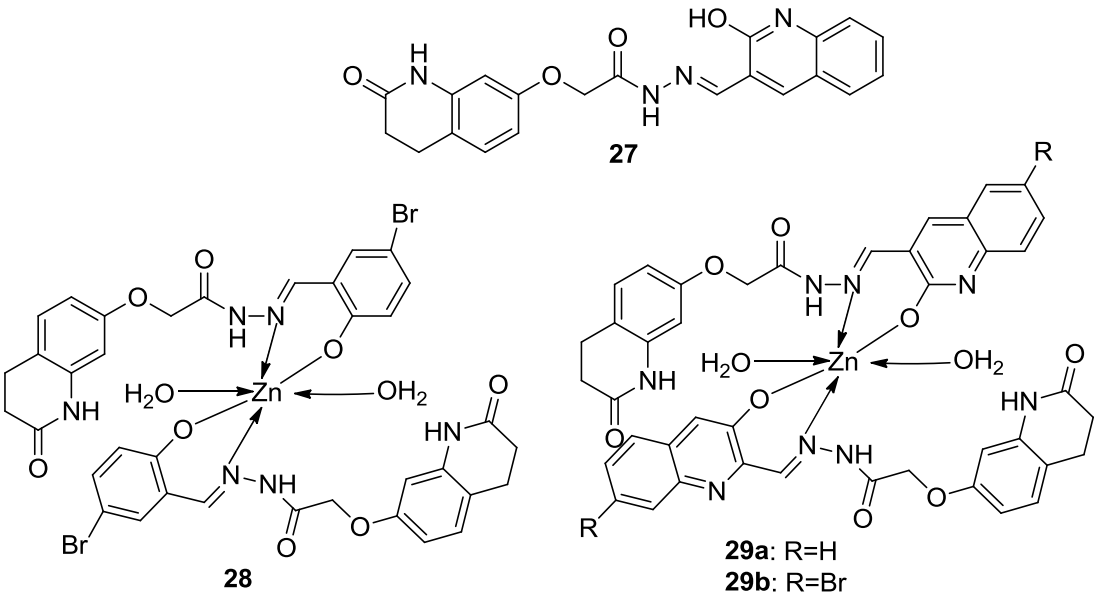

Fig. 2.10 Tetrahydroquinoline based compounds as anti-tubercular agents

2.3 Biological activity of quinoline scaffold

Quinoline also called 1-aza-naphthalene (Fig. **2.1**) is known for wide range of pharmacological activity. It is a weak tertiary base with log P value of 2.04, and has acidic pKb value of 4.85. Further, quinoline can form the salt with acids and follow the reaction pattern of pyridine and benzene [38]. Quinoline possess diverse activity like cardiotonic, anti-convulsant, anti-inflammatory, analgesic, anti-malarial, anti-bacterial, anti-fungal, anti-anthelmintic and anti-viral etc [39-41]. In this dissertation work, we emphasized on the anti-parasitic activity of quinoline scaffold.

2.3.1 Quinoline as anti-bacterial agents

Quinolone is a separate class of quinoline which constitute 1,4-dihydro-4-oxo-3-pyridine carboxylic acid fused with benzene ring as core nucleus. Quinolone based compounds are well known for anti-microbial activity and extensive studies on this nucleus resulted in the number of marketed anti-microbial agents like ciprofloxacin, ofloxacin and sparfloxacin etc. As plethora of reports are available which revealed the anti-bacterial potential of quinolones, however here we laid emphasis on compounds containing quinoline as core nucleus [42, 43].

Narender and group reported the synthesis of new multi substituted quinoline derivatives *via* Baylis–Hillman reaction and screened them against bacterial strians like *B. subtilis*, *B. sphaericus*, *S. aureus, C. violaceum, K. aerogenes,* and *P. aeruginosa*. Compounds exhibited varied response against different bacterial strains, particularly compounds **30a** and **30b** (Fig. **2.11**) showed significant inhibitory activity against *C. violaceum* and *P. aeruginosa*

comparable to standard drug Penicillin [44]. In another report, novel quinoline based compounds attached to various fused analogs such as triazole, pyrimidine, pyrazole and imidazole were synthesized and screened *in-vitro* for their anti-microbial activity against *B. cereus* and *E. coli*. Compound **31** (Fig. **2.11**) among the series predominantly inhibited the growth of both tested bacterial strains with ZOI 44 and 37 mm, respectively [45].

Compound bearing isoxazoline and cyanopyridine moieties over quinoline has been reported for anti-microbial activity, one such compound **32** (Fig. **2.11**) showed significant activity against *E.coli* and *S. aureus* [46]. A new class of compounds containing quinoline and pyrano[3,2-c]chromene was synthesized and *in-vitro* investigated against a representative panel of pathogenic strains like *B. subtilis, C. tetani, S. pneumoniae, E. coli, S. typhi* and *V. cholera.* Compounds **33a**, **33b** and **33c** (Fig. **2.11**) of the series exhibited moderate anti-bacterial activity against the tested bacterial strains [47].

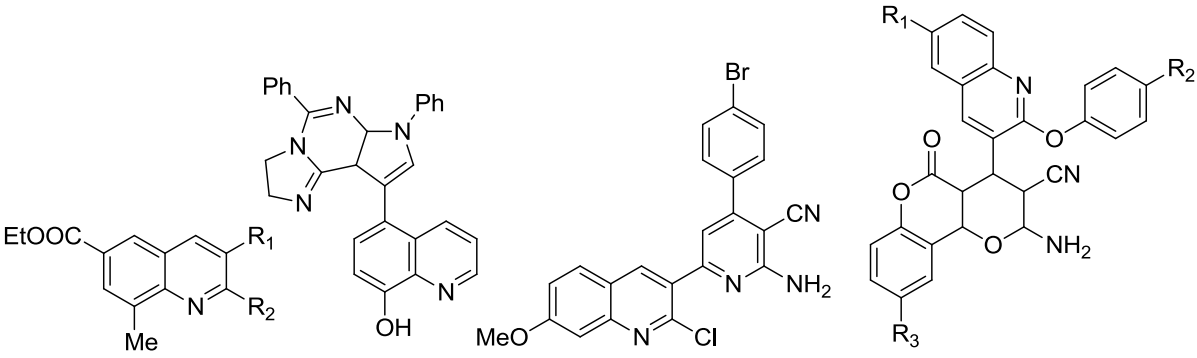

30a: R_1=Ph, R_2=H
30b: R_1=Me, R_2=Ph

31

32

33a: R_1=Me, R_2=Cl, R_3=H
33b: R_1=H, R_2=Cl, R_3=Me
33c: R_1=OMe, R_2=Me, R_3=Me

Fig. 2.11 Quinoline based compounds as anti-bacterial agents

2.3.2 Quinoline as anti-HIV agents

Fakhfakhe *et al.* reported the synthesis and biological activity (anti-HIV-1 and anti-protozoal) of substituted quinolines, compound **34** (Fig. **2.12**) of series inhibited the growth of HIV-1 in sub-micromolar concentration [48]. In another study, Chen and co-workers designed and synthesized thirty-two quinoline derivatives as HIV-1 inhibitors. The majority of compounds showed moderate to prominent anti-viral activity by inhibiting the formation of SIV-induced syncytium in CEM174 cells. Best active compound **35** (Fig. **2.12**) of the series showed EC_{50} 1.1 µM with safety index more than 100 [49]. In one more report, novel styrylquinoline class bearing aryl/acyl group at the C-7 position was synthesized and evaluated for HIV-1 replication inhibition, two best active compounds **36a** and **36b** (Fig. **2.12**) exhibited EC_{50} 2 µM against HIV-1 [50].

Moret and group reported the synthesis and anti-HIV properties of a new series of compounds containing quinoline moiety with polyamine backbones. Compound **37** (Fig.

2.12) of this series was found active with EC_{50} 0.7 and 3.5 µM against the LAV and BaL strains of HIV-1, respectively [51]. Zeng *et al.* synthesized ten 5,5'-(*p*-phenylenebisazo)-8-hydroxyquinoline based compounds and *in-vitro* evaluated for HIV-1 inhibitory activity. Tested compounds demonstrated diverse range of activity against HIV-1, two best active compounds **38a** and **38b** (Fig. **2.12**) showed EC_{50} values of 2.59 and 4.01 µg/mL with therapeutic index of 31.77 and 24.51, respectively [52].

Serrao *et al.* reported series of 8-hydroxyquinoline based compounds as novel inhibitor of the HIV integrase and lens epithelium-derived growth factor/p75 (IN−LEDGF/p75) interaction. Lead optimization studies at the C-5 and C-7 position of quinoline ultimately yielded several compounds with low micromolar activity. Two of quinolin-8-ol based compounds **39a** and **39b** (Fig. **2.12**) inhibited viral replication in MT-4 cells with EC_{50} 3.3 and 4.6 µM, respectively with safety index more than 33 [53]. Rev protein of HIV-1 facilitates the export of viral RNA from nucleus to cytoplasm, which is a key step in HIV-1 pathogenesis. Zhong and group screened a commercial library of compounds and identified a hit compound bearing a benzene sulfonamide quinoline scaffold which inhibited Rev activity and also possessed anti-HIV-1 potency. SAR studies afforded hit compound **40** with potent HIV-1 inhibitory activity (EC_{50} 0.27µM) with low toxicity [54].

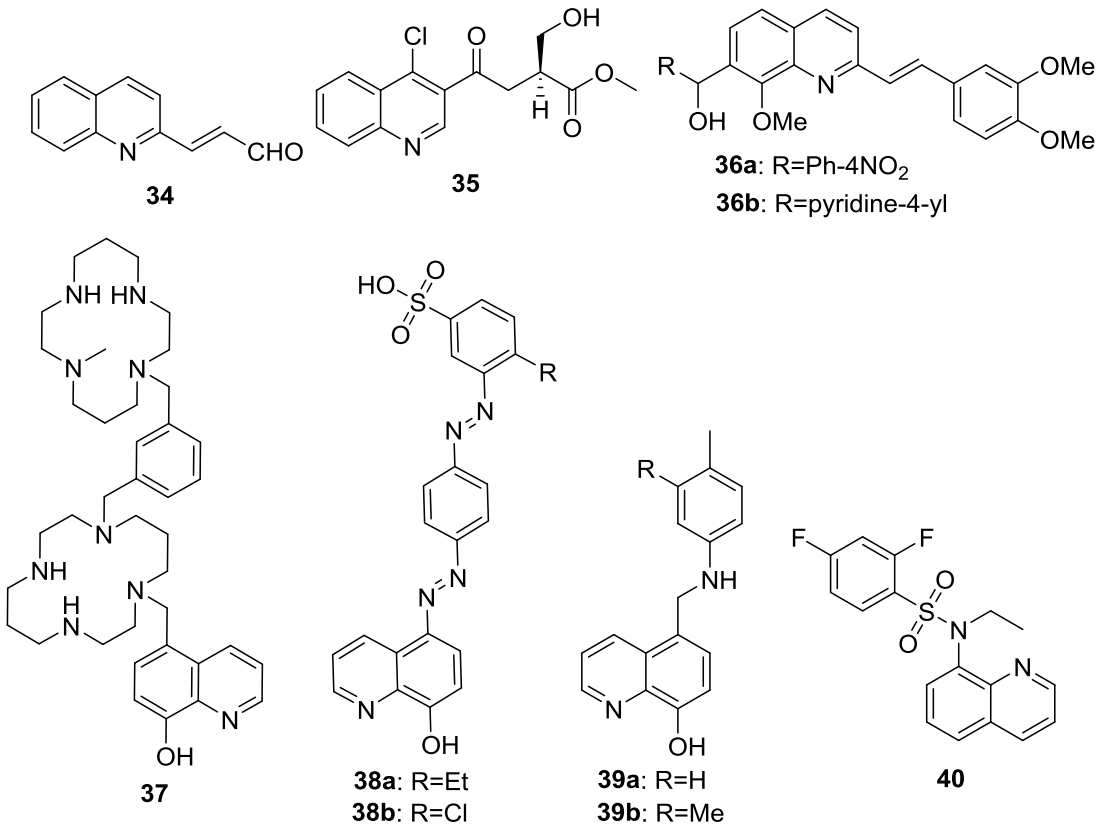

Fig. 2.12 Quinoline based compounds as anti-HIV agents

2.3.3 Quinoline as anti-fungal agents

A series of quinoline derivatives was synthesized and tested for *in-vitro* anti-fungal activity against eight strains of human pathogenic fungi. Among the series, compounds **41a** and **41b** (Fig. **2.13**) showed comparable or better anti-fungal activity than fluconazole against most of the tested fungal strains [55]. Holla *et al.* prepared conjugates of 1,2,3-triazole and quinoline and evaluated them against five fungal strains (*A. flavus, A. fumigates, C. albicans, P. marneffei, T. mentagrophytes*), compound **42** (Fig. **2.13**) of the series showed potent anti-fungal activity (MIC 6-12.5 µg/mL) against all tested fungal strains [56].

Ten quinoline derivatives were designed and screened for *in-vitro* anti-fungal activity against *C. albicans*, in which best active compounds **43a** and **43b** (Fig. **2.13**) inhibited the growth of tested fungal strain with MIC 4 and 8 µg/mL, respectively [57]. Kumar *et al.* synthesized certain non-azole secondary amines containing 2-chloroquinoline and evaluated for anti-fungal activity against *A. niger, A. flavus, M. purpureus and P. citrinum*. The result of the study revealed that compound **44a** and **44b** (Fig. **2.13**) exhibited significant growth inhibition of *A. niger* and *A. flavus* [58].

Series of compounds containing amide of quinoline, azaindole and pyridine were synthesized and tested for *in-vitro* anti-fungal activity against *C. albicans*, *A. fumigatus* and *S. cerevisiae*. One of best active compound **45** (Fig. **2.13**) of series inhibited the growth of *C. albicans* and S. *cerevisiae* with better potency compared to the standard drug amphotericin B [59]. In one more study, a series of new 6-quinolinyl and quinolinyl *N*-oxide chalcones were synthesized and evaluated for anti-fungal activity, compound **46** (Fig. **2.13**) of the series showed good to moderate activity against the tested fungal strains of *P. brasiliensis*, *C. tropicalis* and *C. gattii* with MIC 31.20, 15.60 and 7.80 µg/mL, respectively [60]. Garudachari *et al.* synthesized two series of quinoline based compounds and *in-vitro* evaluated their anti-fungal activity by well plate method (zone of inhibition). Compound **47** (Fig. **2.13**) was found to be potent anti-fungal comparable to flucanazole against the tested strain *A. niger* [61].

Patel *et. al.,* constructed 1,2,4-triazol-3-yl thio-acetamide based compounds and *in-vitro* analyzed for anti-fungal activity against *A. niger,* and *C. albicans,* compounds **48a** and **48b** (Fig. **2.13**) possessed anti-fungal activity against the both tested strains with potency comparable to fluconazole [62]. In more study, Vandekerckhove and team synthesized (hydroxy alkylamino) quinoline derivatives and tested against two yeast strains (*C. albicans* and *R. bogoriensis)* and one mold strain (*A. flavus*). The result of the study revealed that compound **49** (Fig. **2.13**) of series inhibited the growth of *A. flavus* with MIC 2 µg/mL [63].

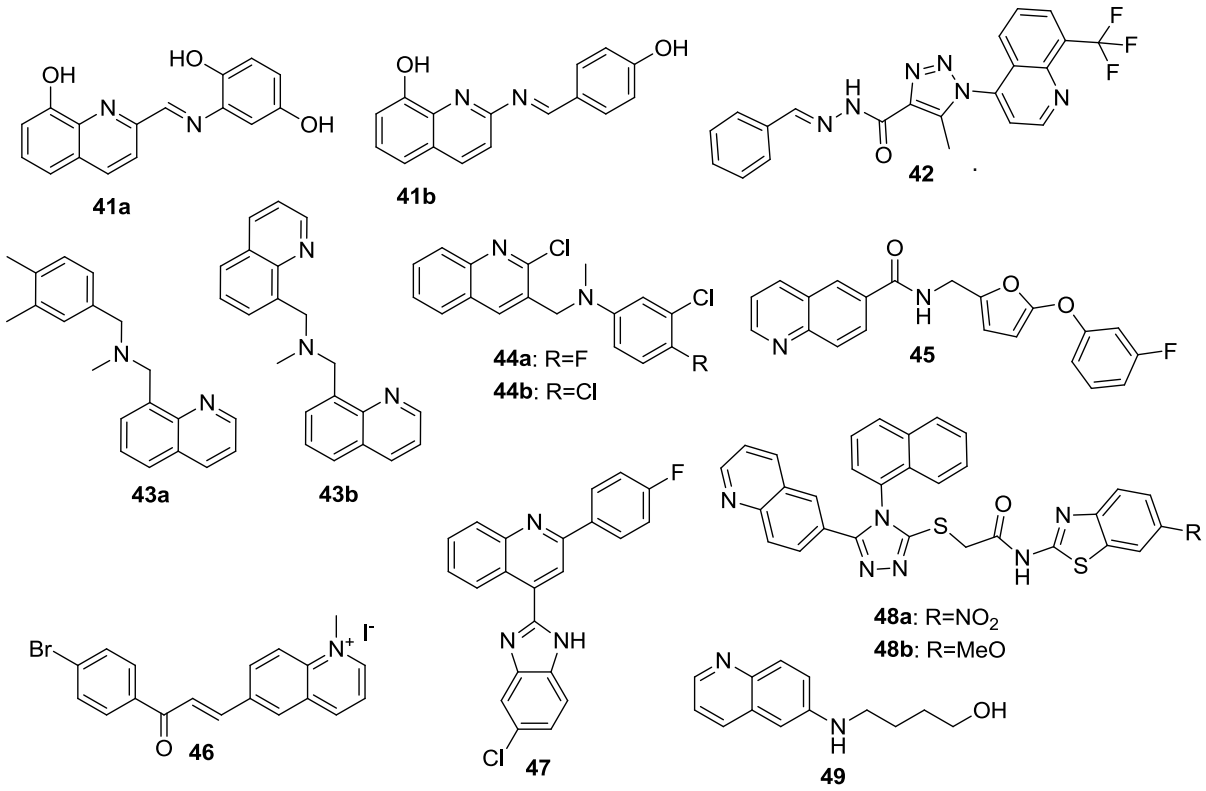

Fig. 2.13 Quinoline based compounds as anti-fungal agents

2.3.4 Quinoline as anti-tubercular agents

Diverse type of compounds containing quinoline nucleus are well known for anti-tubercular activity, moreover, recently approved anti-TB drug Bedaquiline (TMC-2017), sold under the brand name Sirturo also contain quinoline nucleus [64, 65]. TMC207 is a diarylquinoline compound with a novel mechanism of action which acts by the inhibition of bacterial ATP synthase and possess potent activity against drug-sensitive and drug-resistant strains [66].

In a study exploring the anti-tubercular potential of compounds containing quinoline nucleus, Vangapandu and team reported *in-vitro* activity of ring-substituted quinoline analogs against *M. tuberculosis* H37Rv strains. The best effective compound of series **50** (Fig. **2.14**) exhibited MIC value of 1 µg/mL against the tested strain, comparable to first line anti-tuberculosis drug isoniazid [67]. Researchers from the same group reported the synthesis and *in-vitro* evaluation of ring-substituted quinoline carbohydrazides as anti-mycobacterial agents, the result of the study demonstrated that three compounds **51a-51c** (Fig. **2.14**) exhibited the MIC value of 6.25 µ/mL against drug-sensitive *M. tuberculosis* H37Rv strain [68].

Upadhayaya *et al.* synthesized quinoline derivatives possessing triazolo, ureido and thioureido substituents and evaluated for anti-mycobacterial activity. Best active compounds **52** and **53** (Fig. **2.14**) of the series inhibited the growth of tested strain with MIC of 3.125

µg/mL [69]. Beside this, twenty six quinoline-3-carbohydrazone derivatives were synthesized and evaluated against *M. tuberculosis* H37Rv, *M. smegmatis* and *M. fortuitum* using broth micro-dilution assay method. Among the tested compounds, **54a** and **54b** (Fig. **2.14**) significantly inhibited the growth of all three tested mycobacterial strains with MIC 1, 10 and 1 µg/mL, respectively [70].

In another report, new series of quinoline-oxazolidinone hybrid molecules were synthesized based on the *in-silico* studies and subsequently screened for their anti-tubercular activity against three strains (*M. tuberculosis, M. smegmatis* and *M. fortuitum*). The result of the assay study revealed that compound **55** (Fig. **2.14**) overall possessed best anti-mycobacteria activity among the series against three selected strains with MIC 0.625, 2.5 and 10 µg/mL, respectively [71]. Tukulula and team designed and synthesized a series of arylamino quinoline derivatives based on the quinine and mefloquine scaffolds and evaluated *in-vitro* for anti-tubercular activity. Several synthesized compounds exhibited moderate to significant activity against *M. tuberculosis*, in which compound **56** (Fig. **2.14**) showed 98% growth inhibitory activity against replicating *M. tuberculosis* strain [72].

Jain *et al.* designed and synthesized novel arylquinoline derivatives based upon the pharmacophoric features of bedaquiline and subsequently evaluated for anti-mycobacterial activity using resazurin microtitre assay plate method, compounds were also tested for cytotoxicity. Several tested compounds exhibited good anti-tubercular activity during the assay, especially best active compound, **57** (Fig. **2.14**) exhibited MIC 5.18 µM with safety index 152.86 [73]. A series of quinoline-β-lactam-based hybrids was synthesized and tested for their anti-malarial and anti-tubercular activities. Anti-mycobacterial result of the study showed encouraging activity, especially two best active compounds **58a** and **58b** (Fig. **2.14**) showed three times better activity than ethionamide [74].

In one more study, Kos and group prepared ring-substituted 8-hydroxyquinoline-2-carboxanilide derivatives and *in-vitro* screened against *M. tuberculosis*, *M. avium* complex and *M. avium*. Some of the tested compounds showed anti-mycobacterial activity against one or more tested strains, especially compound **59** (Fig. **2.14**) showed MIC 24 µM against all three tested mycobacterial strains [75]. In the recent study, a series of forty-eight quinoline-aminopiperidine based urea and thiourea derivatives were designed and synthesized as DNA gyrase inhibitor of *Mycobacterium*. In biological studies, best active compound **60** (Fig. **2.14**) inhibited the activity of *Mtb* DNA gyrase with IC_{50} of 0.62 µM, moreover, same compound also exhibited promising inhibitory activity (IC_{50} 0.95 µM) against GyrB of *M. smegmatis* [76].

Medapi and team employed hit optimization approach upon the reported GyrB inhibitor of *Mycobacterium* and synthesized forty six novel quinoline derivatives. The compounds were evaluated for *in-vitro Mycobacterium* GyrB inhibitory ability as well as anti-tubercular activity against *Mtb* H37Rv strain. Among the series, three compounds emerged to be significantly active with IC_{50} values below 1 µM against GyrB, in which best active compound **61** (Fig. **2.14**) exhibited IC_{50} 0.86 µM, moreover **61** also inhibited the growth of *Mtb* with a MIC of 3.3 µM [77]. In one more report, novel quinoline-oxadiazole hybrid compounds were evaluated for anti-*Mtb* activity (against H37Rv strain) and cytotoxicity of the compounds was also evaluated over HepG2 cell line. In biological studies, best active compounds **62a**, **62b** and **62c** (Fig. **2.14**) showed MIC values <0.5 µM with selectivity index >500 [78].

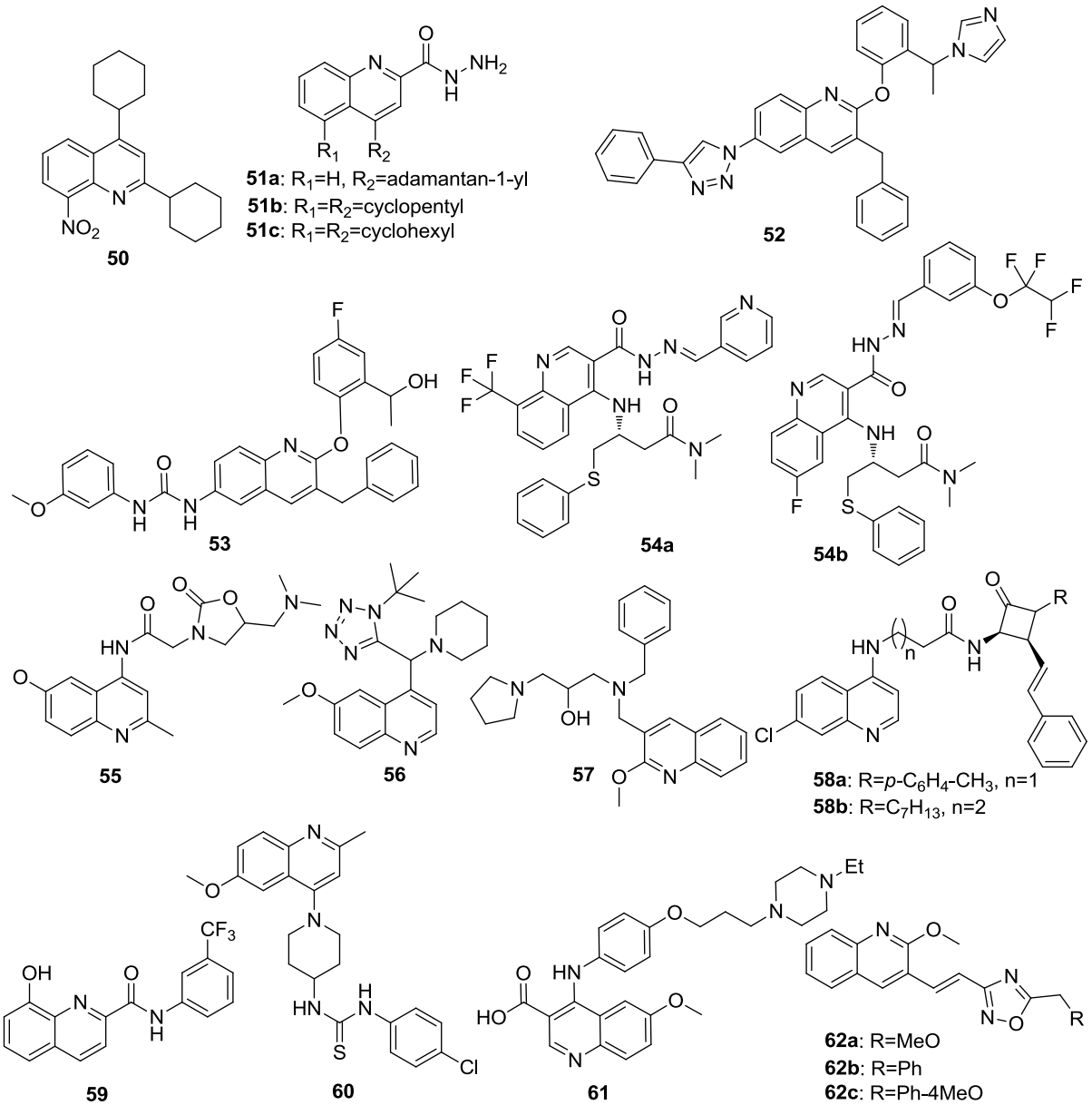

Fig. 2.14 Quinoline based compounds as anti-tubercular agents

2.4 Anti-infective activity of compounds containing piperazine

Piperazine (Fig. **2.1**) was being used from the 1900th century for the treatment of gout. Successful use of piperazine in the treatment of helminthiasis led to its extensive use as drug for human as well as other animals [79]. Piperazine in its different forms like hydrate, adipate and citrate are mainly used for the treatment of ascariasis and enterobiasis [80]. Piperazine ring is common widespread structural motifs in drug discovery and numbers of derivatives containing this nucleus are already encountered as positive hits against various biological targets [81]. Piperazine template deserves the molecular backbone due its versatile binding affinity while in certain ligands it acts as potent and selective inhibitor of biological targets [82, 83].

Piperazine moiety in drugs also helpful in the enhancement of solubility of parent compound, as it contains two nitrogen which can be converted into Ionizable forms using suitable acid entity [84]. Number of drugs containing piperazine nucleus have been approved clinically, which covers diverse pharmacological spectrum like anti-anginals (ranolazine and trimetazidine), anti-depressant (amoxapine, befuraline, buspirone, flesinoxan, ipsapirone and zalospirone), anti-histamine (meclozine, cinnarizine, cetirizine and levocetirizine), anti-psychotic (perphenazine, prochlorperazine and prochlorperazine), analgesic (antrafenine), anti-bacterial (gatifloxacin and ciprofloxacin), anti-tubercular (rifampicin), anti-fungal (itraconazole and ketoconazole), anti-HIV (delavirdine and indinavir) [85-87].

2.4.1 Piperazine as anti-bacterial agents

Compounds containing nucleus *N*-[5-(5-nitro-2-thienyl)-1,3,4-thiadiazole-2-yl]piperazinyl quinolone were synthesized and evaluated for *in-vitro* anti-bacterial activity against Gram (+)ve and Gram (-)ve bacterial strains. The result of the anti-bacterial study revealed that three compounds showed better activity compared to ciprofloxacin and norfloxacin against tested Gram (+)ve strains (*S. aureus*, *S. epidermidis* and *B. subtilis*). However, all three compounds were found to be very less active against Gram (-)ve bacteria. Compound **63** (Fig. **2.15**) was found to be the best active compound against Gram (+)ve bacterial strains with MIC 0.008-0.015 µg/mL [88]. In another report, novel compounds based upon isothiazolone nucleus were synthesized and tested for anti-bacterial activity, in which compound containing piperazine moiety **64** (Fig. **2.15**) exhibited bactericidal activity against four strains (*S. epidermidis*, *E. coli*, *S. typhimurium* and *P. aeruginosa*) with MIC 0.3 µg/mL [89].

Analogs of levofloxacin carrying a 2-aryl-2-oxoethyl or 2-aryl-2-oxyiminoethyl moiety attached to the piperazine ring at C-10 position were prepared and evaluated for anti-bacterial activity. Among the series of compound, **65** (Fig. **2.15**) exhibited promising

inhibitory activity against Gram (+)ve bacterial strains (*S. aureus, S. epidermidis, S. epidermidis, B. subtilis* and *E. feacalis*) with MIC 0.12-0.5 µg/mL [90]. Kumar *et al.* reported substituted 1-benzhydryl-piperazine sulfonamide based compounds for anti-bacterial activity against Gram (+)ve (*S. aureus, S. epidermis, B. cereus* and *B. substilis*) and Gram (-)ve (*E.coli, P. aeruginosa, P. vulgaris* and *S. typhi*) bacterial strains. Compound **66** (Fig. **2.15**) showed potent anti-microbial activity compared to the standard drug streptomycin against the tested strains [91].

Yu *et al.* synthesized derivatives of norfloxacin and evaluated them for their anti-microbial activity against plant pathogenic bacterial strains. Best active compound **67** (Fig. **2.15**) showed potent activity against *X. oryzae* even better than norfloxacin [92]. In another study, combined effect of 1-(1-naphthylmethyl)-piperazine (NMP) **68** (Fig. **2.15**) and ciprofloxacin (CPFX) in 12 fluoroquinolone (FQ)-resistant clinical isolates of *S. aureus* was assessed using a checkerboard microdilution method. In this study, a synergistic anti-microbial effect between NMP and CPFX was observed in all 12 FQ-resistant strains, the effect was further confirmed by the time-killing test and agar diffusion assay for the selected strain [93].

Chen and team synthesized a range of fluoroquinolone derivatives with 4-(carbopiperazin-1-yl)piperazinyl moieties at the C7 position and evaluated them for inhibition of bacterial pathogens commonly disseminated in the hospital environment. The results of the study indicated that compound **69** (Fig. **2.15**) showed activity against ciprofloxacin-resistant *P. aeruginosa* (CRPA) with MIC 16 µg/mL, around 16-fold more potent than ciprofloxacin, while the majority of other derivatives retained potency against methicillin-resistant *S. aureus* [94].
A series of compound containing 4-hydroxycoumarin moiety coupled with piperazine was designed and synthesized in order to search potent anti-bacterial drugs. Anti-bacterial activity of the compounds against *E. coli, P. aeruginosa, B. subtilis* and *S. aureus* was tested in which several compounds showed good anti-bacterial activity against Gram (+)ve strains. Compound **70** (Fig. **2.15**) presented the most potent anti-bacterial activity against *B. subtilis* and *S. aureus* with MIC of 0.236, 0.355 µg/mL, respectively [95].

Novel piperazine derivatives of phenothiazine were synthesized and evaluated for anti-microbial activity. Tested compounds exhibited good to potent activity against *S. aureus* and *B. subtilis*, moreover compound **71** (Fig. **2.15**) inhibited the growth of above mentioned bacterial strains comparable to standard drug streptomycin [92]. Beside this, a series of novel diarylmethylamines was synthesized, and anti-bacterial activity of the compounds was assessed against two bacterial strains *L. monocytogenes* and *E. coli*. Compound **72** of series (Fig. **2.15**) containing phenyl and *N*-methyl piperazine moiety showed moderate anti-bacterial activity against both pathogenic bacteria with MIC value of 31 µg/mL [96].

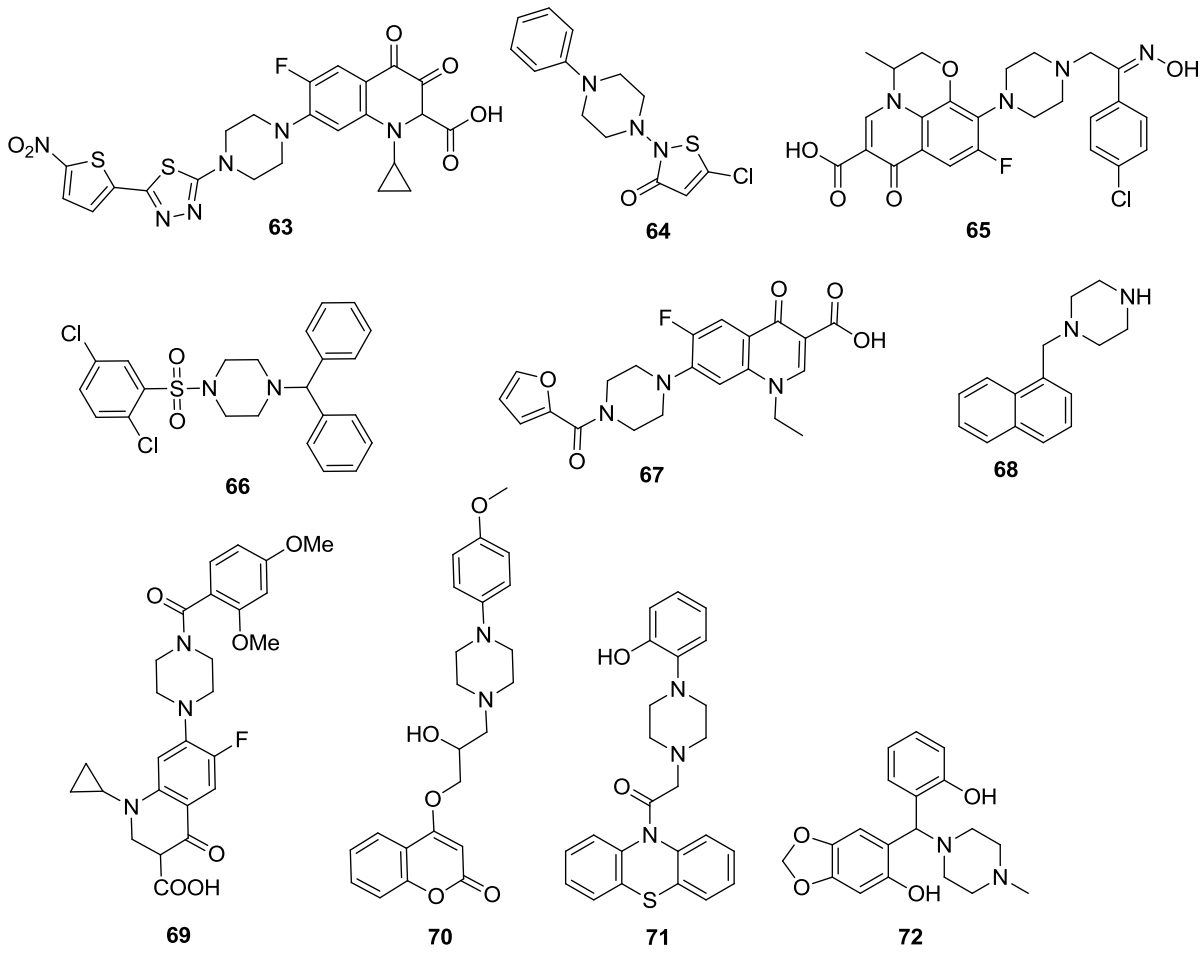

Fig. 2.15 Piperazine based compounds as anti-bacterial agents

2.4.2 Piperazine as anti-HIV agents

Tagat *et al.* performed lead optimization studies on scaffold piperidino-2(S)-methyl piperazine in order to search HIV-1 co-receptor CCR5 antagonist. The study resulted in the discovery of piperazine-based CCR5 antagonist (compound **73**, Fig. **2.16**), which was found to be a potent inhibitor of HIV-1 entry and as well as its replication with excellent oral bioavailability in the rat, dog and monkey [97]. In another study on development of CCR5 antagonist, McCombie *et. al.,* reported compound **74** (Fig. **2.16**) which possessed structural similarity to the above mentioned compound also exhibited CCR5 antagonistic activity with sub-nanomolar potency. Moreover, compound **74** also inhibited the entry of HIV at nano-molar concentration and displayed good oral absorption in rodents and primates [98].

In the late stage of HIV-1 infection, Platelet-Activating Factor (PAF) mediated neurotoxicity are commonly implicated, responsible for AIDS dementia complex [99]. Serradji and group reported that substituted piperazine derivative which showed the ability to diminish both HIV-1 replication in monocyte-derived macrophages as well as PAF-induced platelet aggregation. Among the series, compound **75** (Fig. **2.16**) displayed significant inhibition of

PAF-induced platelet aggregation (IC_{50} 2.5 µM) as well as growth of HIV-1 (75% inhibition at 10 µM) [100].

El-Faham *et al.* reported synthesis, anti-HIV evaluation and cytotoxicity studies of piperazine-based unsymmetrical bis-urea derivatives, best active compounds of the series **76** (Fig. **2.16**) showed anti-HIV activity (EC_{50}) 9.6 µg/mL and cytotoxicity (CC_{50}) 125 µg/mL in lymphoid MT-4 cells [101]. Wang *et al.* discovered attachment inhibitors using a high throughput cell-based screening approach, searched compounds **77a** and **77b** (Fig. **2.16**) exhibited attachment inhibition between viral gp-120 and host cell receptor CD4 at the low nanomolar concentration. Overall, SAR studies revealed piperazine ring act as the critical essential element for the attachment inhibitory activity [102].

A series of 1,4-disubstituted piperazine derivatives was designed, synthesized and evaluated for anti-HIV-1 activity. The majority of tested compounds showed potent anti-HIV-1 activity, best active compound **78** (Fig. **2.16**) showed nanomolar potency (EC_{50} 6.17 nM), which was found to be comparable to the reference compound TAK-220 hydrochloride. Moreover, compound **78** possessed much better water solubility as well as oral bioavailability compared to TAK-220 hydrochloride [103]. In one more study, a series of 4-azaindole oxoacetic acid piperazine benzamides was synthesized and evaluated as potential HIV-1 attachment inhibitor. Among the synthesized series, compound **79** (Fig. **2.16**) containing 5-membered heteroaryl ring at the 4-azaindole nucleus exhibited potent anti-HIV-1 activity (EC_{50} 0.34 µM). Compound **79** also possessed suitable pharmacokinetic profiles in a rat model with superior oral bioavailability and lower clearance as compared with BMS-378806 [104].

Liu *et al.* designed a novel piperazine derivatives by employing fragment-assembly strategy and bioisosteric-replacement principle as CCR5 fusion inhibitor. Target series was synthesized and evaluated for CCR5 fusion inhibitory activity, among the series majority of compounds exhibited medium to potent inhibitory activity. Best active compound **80** (Fig. **2.16**) was found to be a CCR5 antagonist with an IC_{50} value of 6.29 µM and it also possessed anti-HIV-1 activity with EC_{50} 0.44 µM [105]. Further, Bala and co-workers synthesized a series of fifteen compounds based upon the scaffold *N*-alkyl/aryl-4-(3-substituted-3-phenylpropyl) piperazine-1-carbothioamide and evaluated for anti-microbial as well as reverse transcriptase (RT) inhibition activities. Most promising active compound an oxo derivative **81** (Fig. **2.16**) displayed 72.30% inhibition of RT at tested 100 µg/mL concentration [106].

Bevirimat is an anti-HIV drug, which acts upon viral protease responsible for the division of gag precursor polyprotein into sub-domains, ultimately hampered HIV maturation [107]. Subsequent studies illustrated that effectiveness of Bevirimat reduced in the treatment of 40-

50% of patients who carried resistant in the SP1 region of HIV-1 Gag [108]. Zhao *et. al.,* integrated caffeic acid and piperazine moieties with bevirimat produced new derivatives, in which best active compound **82** (Fig. **2.16**) showed 3 and 51 folds improved activity against the most prevalent bevirimat-resistant strains; HIV-1/NL4-3 and NL4-3/V370A, respectively [109].

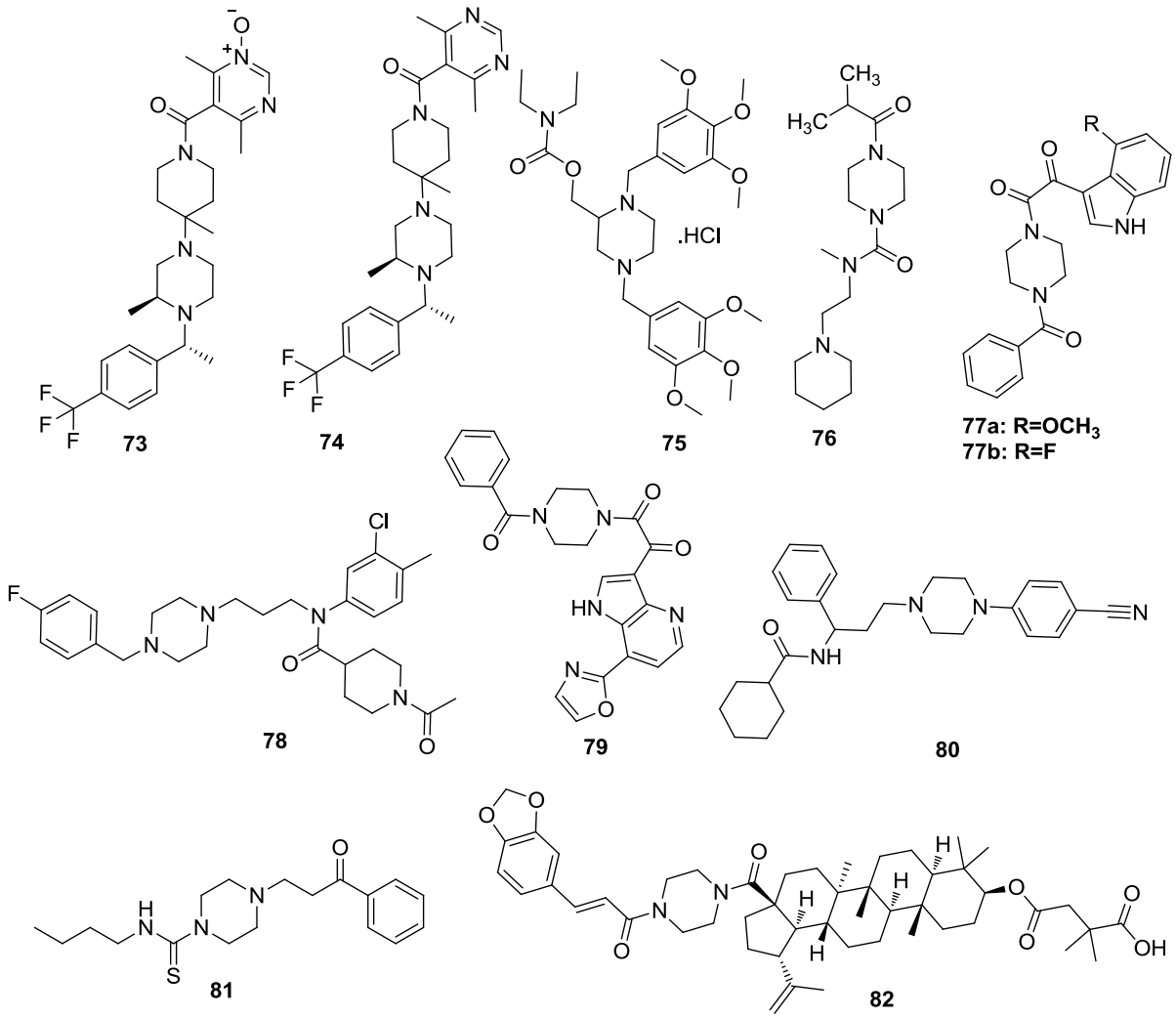

Fig. 2.16 Piperazine based compounds as anti-HIV agents

2.4.3 Piperazine as anti-fungal agents

Upadhayaya *et al.* synthesized tetrazole based compounds and evaluated for anti-fungal activity, best active compound **83** (Fig. **2.17**) showed MIC value of 0.12-0.25 µg/mL against *C. albicans, C. tropicalis, C. Parapsilosis* and *C. Krusei,* which was found to be comparable to itraconazole and better than fluoconazole [110]. Cushion *et. al.,* synthesized pentamidine based compounds constituted 1,4-piperazinediyl moiety and subsequently evaluated against *P. carinii* (fungal strain commonly causes pneumonia in AIDS patients). Out of the tested compounds, four were found to be potently active and exhibited IC_{50} values of <0.01 µg/mL,

moreover best active compound **84** (Fig. **2.17**) exhibited IC_{50} 0.001 µg/mL against *P. carinii* [111].

Kondoh and team screened a chemical library against fungal enzyme1,3-beta-D-glucan synthase, study resulted in the discovery of few hits in which one piperazine propanol derivative **85** (Fig. **2.17**) was identified as a potent inhibitor against target enzyme with an IC_{50} value of 0.16 µM. Compound **85** also exhibited excellent *in-vitro* anti-fungal activity against pathogenic fungi *C. albicans* and *A. fumigates* [112].

Quinazolinone linked piperazine compounds were explored as fungal efflux pump inhibitors of strains *C. albicans* and *C. glabrata*. The activity was expressed in minimum potentiating concentration (MPC_8), it was the lowest concentration achieving 8 fold reduction in MIC of Fluconazole. Compound **86** (Fig. **2.17**) of the series exhibited MPC_8 at 0.0625 and <0.03 µg/mL for *C. albicans* and *C. glabrata* fungal strains respectively [113]. Library of 500 compounds was screened for fungicidal activity *via* induction of endogenous reactive oxygen species (ROS) accumulation. SAR studies revealed that piperazine-1-carboxamidine analogs with bulky atoms or large side chains were characterized by a high ROS accumulation capacity in *C. albicans* and consequently for high fungicidal activity. Compound **87** (Fig. **2.17**) of series showed MIC 9.4 µg/mL against *C. albicans*, moreover **87** also resulted in high accumulation of ROS [114].

Novel 1,2,4-triazole derivatives with a substituted piperazine side chain were designed and synthesized targeting the lanosterol 14α-demethylase enzyme. Subsequently, compounds were evaluated for anti-fungal activity against several human pathogenic fungi, majority of compounds were found to be more potent against *C. albicans* compared to standard drug fluconazole. Two compounds **88a** and **88b** (Fig. **2.17**) displayed *in-vitro* anti-fungal activity against *C. neoformans* comparable to voriconazole with a MIC_{80} value of 0.0156 µg/mL [115].

Wang and team designed and synthesized triazole based compounds as inhibitor of cytochrome P450 14α-demethylase (CYP51) taking fluoconazole as core scaffold. Synthesized compounds were evaluated against different human pathogenic fungi, compound **89** (Fig. **2.17**) of series exhibited anti-funagl activity against seven strains (*C. albicans, C. parapsilosis, C. neoformans, C. glabrata, A. fumigates, T. rubrum* and *M. gypseum*) comparable or better to fluoconazole [116]. In one more study, piperazine based compounds were designed and synthesized as anti-fungal agents taking natural product 1,5-diphenyl-2-penten-1-one as a hit. Compounds were evaluated for *in-vitro* activity against certain plant pathogenic fungi and the results of study indicated that most of the tested compounds exhibited moderate activity, while best active compound **90** (Fig. **2.17**) exhibited

anti-fungal activity against *P. aphanidermatum* comparable to positive control difenoconazole [117].

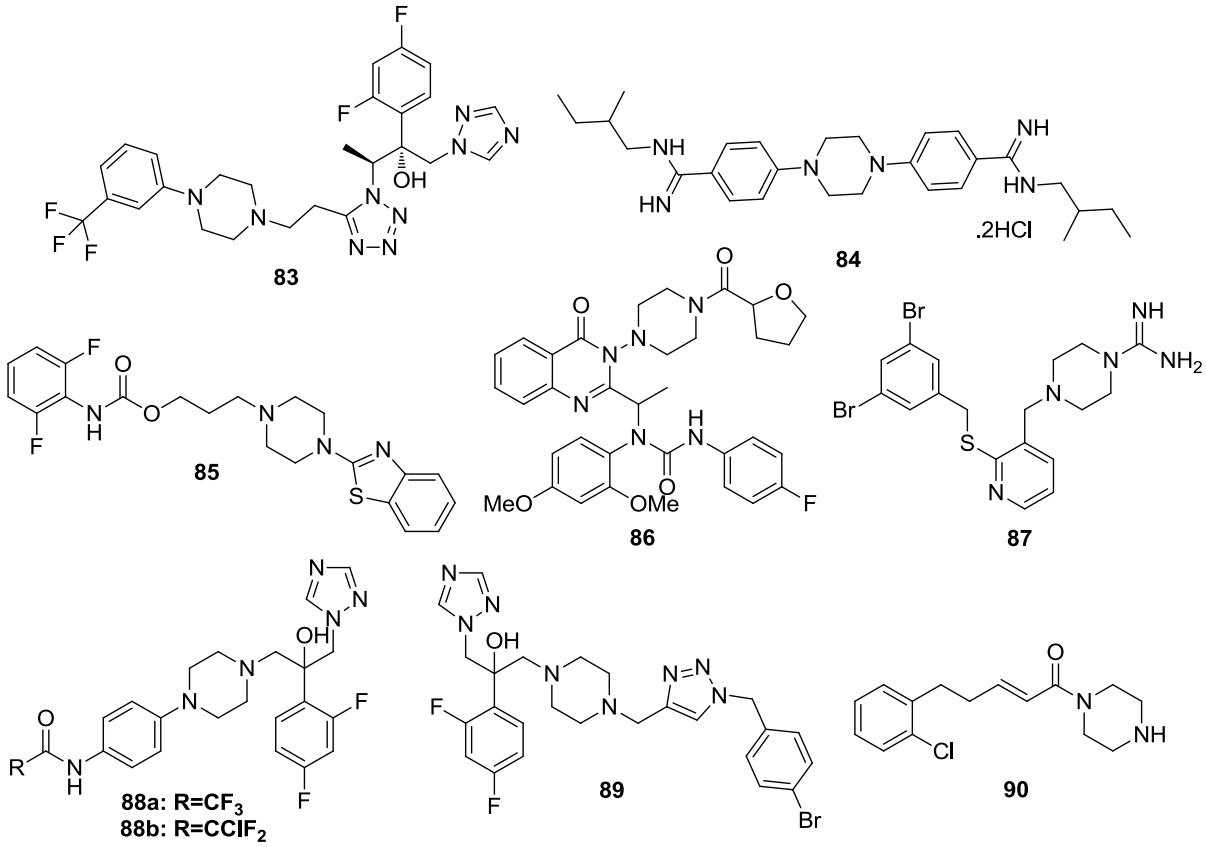

Fig. 2.17 Piperazine based compounds as anti-fungal agents

2.4.4. Piperazine as anti-tubercular agents

Novel 4-oxo-1,4-dihydroquinoline-3-carboxylic acid based compounds with substituents at the 4th position of piperazine were synthesized and evaluated *in-vivo* against *M. tuberculosis* in Swiss albino mice. Among the tested compounds, best active compound **91** (Fig. **2.18**) exhibited activity comparable to standard drug sparfloxacin (in terms of survival rate, reduction of splenomegaly and reduced tubercular lesions) at a dose of 200 mg/kg [118]. Bogatcheva and team synthesized a diverse library of five thousand compounds from commercially available diamines and tested for activity against *Mtb*, out of which one hundred forty-three hits exhibited MIC equal to or less than 12.5 µM. Compound **92** (Fig. **2.18**) showed significant *in-vitro* anti-tubercular activity against *Mtb* with MIC 0.13 µM [119].

Rakesh *et al.* performed SAR studies on 3,5-di-substituted isoxazoline core in order to search potential anti-tubercular agent. Substitution the at C-5 position of isoxazoline with piperazyl-urea and piperazyl-carbamate produced compounds with improved anti-tubercular activity, particularly best active compound **93** (Fig. **2.18**) inhibited the growth of *M. tuberculosis* with MIC 0.4 µg/mL [120]. Further, Blaser and group synthesized different

analogs of anti-tuberculosis drug PA-824 [121] by attaching different functionalities like amide, carbamate and urea. Generated compounds were assessed for anti-tubercular activity against *M. tuberculosis* and pharmacokinetic parameters of significantly active compounds were also accessed. Result of the study revealed that arylpiperazine based compound **94** (Fig. **2.18**) displayed an excellent MIC profile against *M. tuberculosis* (0.033 and 1.1 μM) in Microplate Alamar Blue Assay (MABA) and Low Oxygen Recovery Assay (LORA), respectively, moreover compound **94** also possessed favourable pharmacokinetic profiles [122].

Nagesh *et al.* reported nineteen phenanthridine based compounds for their anti-tubercular activity against *M. tuberculosis*. Among the tested compounds, three compounds exhibited good activity (MIC ≤3.125 μg/mL) against the tested strain, in which best active compound **95** (Fig. **2.18**) displayed excellent activity (MIC 1.56 μg/mL) with good selectivity index [123]. Chauhan and group described the synthesis and *in-vitro* anti-tubercular activity of thiazolone piperazine tetrazole derivatives. Out of the screened derivatives, the majority of compounds exhibited MIC values <24 μM against *M. tuberculosis,* in which compound **96** (Fig. **2.18**) inhibited the growth of tested strains with MIC 2.51μM, even better than ethambutol (MIC 9.78 μM). Furthermore, compound **96** displayed no toxicity against Vero cells and mouse bone marrow derived macrophages at tested concentration of 100 μM [124].

In one more report, derivatives of *N*-[4-(piperazin-1-yl)phenyl]cinnamamide were designed via molecular hybridization approach as anti-tubercular agents. Further, fifty two designed compounds were synthesized and evaluated for anti-tubercular activity against *Mtb* using Resazurin microtitre plate assay (REMA), in which compound **97** (Fig. **2.18**) with trifluoromethyl substitution exhibited good anti-tubercular activity with MIC 3.125 μg/mL [125]. Next, Peng *et al.* explored 1,3-benzothiazin-4-one based compounds as anti-*Mtb* agents and concluded that compounds having piperazine substituents in benzothiazinone scaffold were found to be well tolerated and one such compound **98** (Fig. **2.18**) showed potent anti-tubercular activity (MIC 0.008 μM). Moreover, compound **98** also possessed favourable aqueous solubility (104 μg/mL) [126].

Bobesh and team developed a series of 1-(2-(piperazin-1-yl)ethyl)-1,5-naphthyridin-2(*1H*)-one derivatives as topoisomerase II inhibitors of *Mtb.* Compounds were screened for DNA gyrase enzyme inhibitory activity and also for anti-*Mtb* activity. The most promising active compound of the series **99** (Fig. **2.18**) inhibited the DNA gyrase supercoiling with IC_{50} 0.29 μM and also displayed good anti-*Mtb* activity with MIC of 3.45 μM [127].

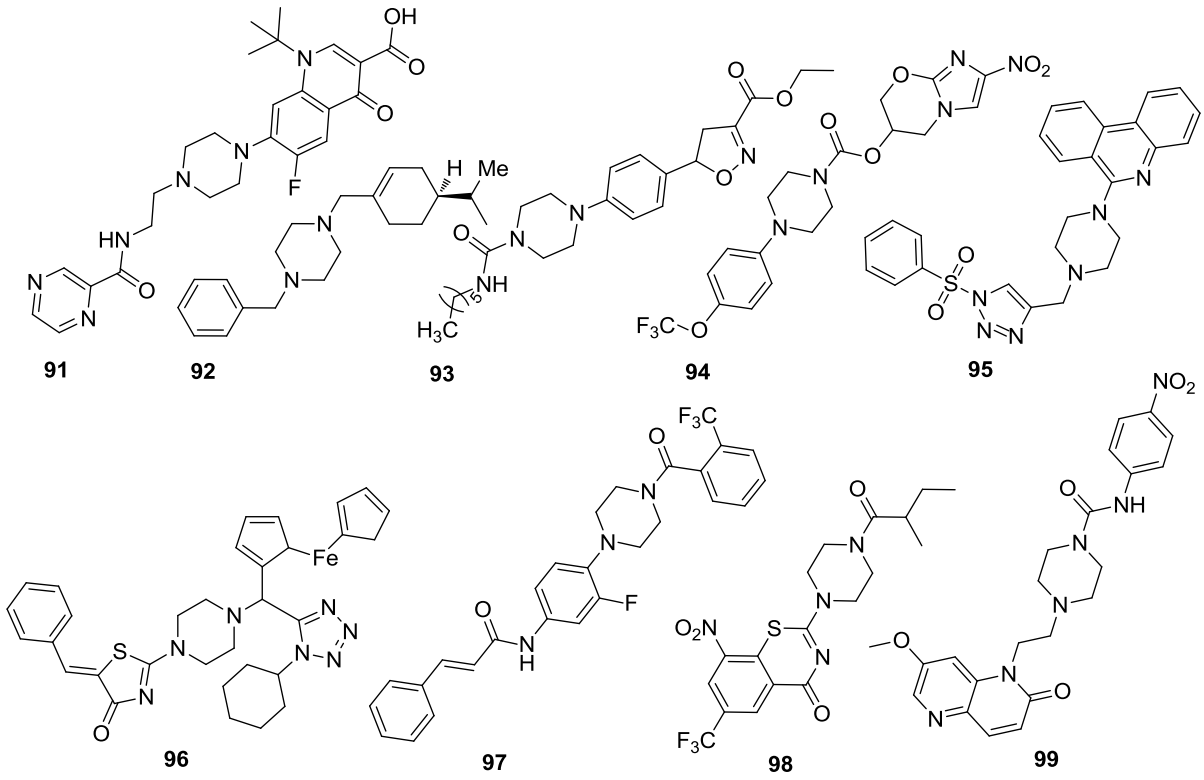

Fig. 2.18 Piperazine based compounds as anti-tubercular agents

2.5. Biological significance of oxindole or indolin-2-one

Structurally, oxindole or indolin-2-one (Fig. **2.19**) nucleus consists of a benzene ring fused with pyrrole ring having carbonyl group at the 2nd position. Oxindole exists in two tautomeric forms (Oxindole A and Oxindole B, Fig. **2.19**). Extract of plant *Uncaria tomentosa* contains oxindole alkaloids has been used traditionally for anti-inflammatory purpose [128, 129]. Various reports revealed the pharmacological potential of compounds containing oxindole ring against different ailments like gastric ulcer, arthritis, infection, cancer and other inflammatory processes [130-132].

Drug Sunitinib in clinical use for gastrointestinal, renal cell cancer also contains oxindole nucleus [133]. Further, optimization of the substituents around the oxindole nucleus resulted the discovery of several kinase inhibitors that are in clinical trials like SU6668, SU14813, SU4984 [134]. Furthermore, drugs like indolidan and adibendan possessed oxindole nucleus have been used for the treatment of congestive heart failure due to their strong vasodilatory and positive ionotropic effect [135, 136].

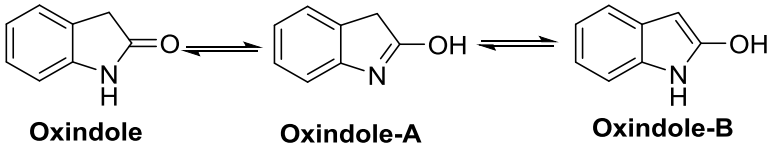

Fig. 2.19 Tautomerism in oxindole ring

Owing to its diverse pharmacological profile, researchers have shown huge interest in developing novel synthetic oxindole derivatives with fascinating biological activities. In this study, we summarized the anti-infective property of compounds based on oxindole nuleus.

2.5.1 Oxindole as anti-bacterial agents

Rindhe and team reported a series of oxindole based compounds as anti-bacterial agents against *S. aureus, S. pyrogenes, E. coli* and *P. aeruginosa.* Majority of the compounds showed moderate to significant anti-bacterial activity against the tested strains. Best active, compound **100** (Fig. **2.20**) inhibited the growth of *S. aureus* and *P. aeruginosa* at concentration 25 µg/mL [137]. In other similar study, compounds containing oxindole nucleus were synthesized and evaluated for anti-bacterial activity against pathogenic bacterial strains (*E. coli, S. dysenterie, S. aureus* and *B. cereus*). Most of the tested compounds were found to be moderate to significantly active against the tested strains. Compound **101** (Fig. **2.20**) of series possessed higher potency against Gram (+)ve bacteria *B. cereus* compared to the standard anti-bacterial agent sulphamethoxazole, whereas another compound **102** (Fig. **2.20**) exhibited potent activity against Gram (-)ve bacteria *S. dysenterie* comparable to sulphamethoxazole [138].

Singh *et al.* generated heterocycles comprising spiro-oxindole, 2-amino-*4H*-pyran and 1,2,3-triazole substructures using ultrasonic irradiation. The anti-bacterial activity of all compounds was also investigated against four bacterial strains (*S. aureus, B. subtilis, E. coli* and *P. aeruginosa*) in which majority of compounds showed weak to moderate anti-bacterial activity against one or more strains, whereas compound **103** (Fig. **2.20**) showed significant activity against *B. subtilis* with MIC 16 µg/mL [139]. In one more scientific report, a series of novel spirooxindoles was synthesized and evaluated for their anti-microbial activity, compound **104** (Fig. **2.20**) of series was found to be promisingly active against *S. aureus* bacteria with 1.6 times more potency compared to standard drug streptomycin. Moreover, compound **104** also exhibited 6.4 times more potency than standard drug ciprofloxacin against *M. luteus* and *S. typhimurium* [140].

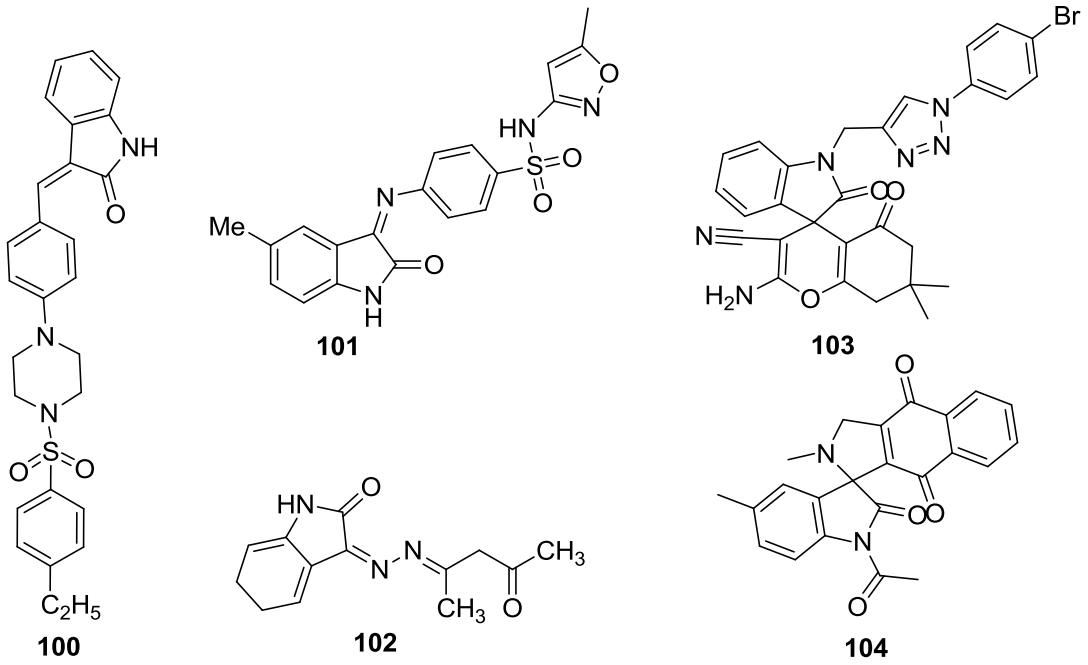

Fig. 2.20 Oxindole based compounds as anti-bacterial agents

2.5.2 Oxindole as anti-HIV agents

Jiang *et al.* discovered a novel oxindole based compound as HIV-1 non-nucleoside reverse transcriptase inhibitor *via* HTS using a cell-based assay. Further, structural modifications were made in order to improve the inhibitory activity of hit compound as well as to establish the SAR studies. This approach resulted in the identification of compound **105** (Fig. **2.21**) with low nanomolar (EC_{50} 15 nM) potency against HIV replication [141]. In the next phase of this study, same research group made further modification in order to further improve the potency against HIV, for example bromo at the 5th position of oxindole was replaced by chloro and instead of ester moiety, different heterocyclic rings were also tried. Subsequently, systematic efforts in this direction afforded more new compounds with nanomolar potency, especially compounds **106** and **107** (Fig. **2.21**) showed EC_{50} 6 and 8 nM, respectively against HIV-1. Moreover, compound **107** also possessed favourable pharmacokinetic profile [142].

Palomba *et al.* disclosed flexible synthetic approach to access the spirocyclopropyl oxindole derivatives. Some compounds of the series were selected for evaluation against HIV-1 RT as well as for anti-HIV-1 activity. Among the evaluated compounds **108** (Fig. **2.21**) inhibited the HIV-1 RT with IC_{50} 7.1 µg/mL, moreover compound **108** also showed anti-HIV-1 activity with EC_{50} 0.92 µg/mL [143].

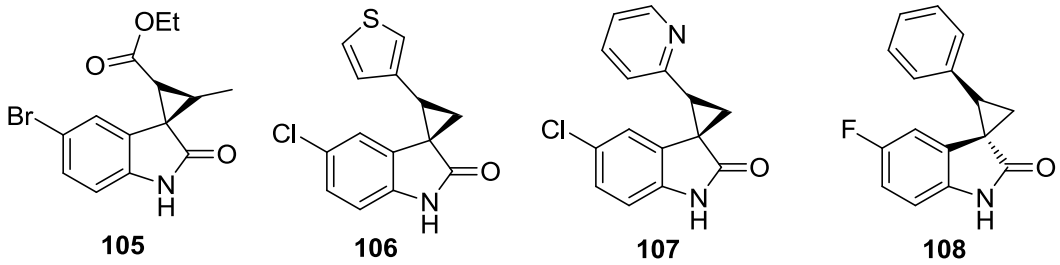

Fig. 2.21 Oxindole based compounds as anti-HIV agents

2.5.3 Oxindole as anti-fungal agents

Rindhe *et al.* described the synthesis and anti-microbial evaluation of ten 3(*Z*)-{4-[4-(arylsulfonyl)piperazin-1-ylbenzylidene)-1,3-dihydro-*2H*-indol-2-one derivatives. In the assay system, compound **109** (Fig. **2.22**) of series exhibited excellent anti-fungal activity against *A. clavatus* comparable to the standard drug gresiofulvin [137]. In one more study, novel compounds containing oxindole nucleus were synthesized and evaluated for anti-microbial activity, result of the study revealed that best active compound **110** (Fig. **2.22**) of series inhibited the growth of pathogenic fungi *A. flavus* and *C. albicans* with MIC 10 µg/mL and 5 µg/mL, respectively [138].

Wu and group synthesized a series of spirooxindole tetrahydrofuran derivatives and evaluated for anti-fungal activity against five phytopathogenic fungi (*R. solani, F. semitectum, A. solani, V. mali* and *F. graminearum*) using mycelium growth rate method. Compound **111** (Fig. **2.22**) of series showed potent activity against *F. graminearum* with IC_{50} value of 3.31 µg/mL, comparable to control drug cycloheximide (IC_{50} 3.3 µg/mL) [144]. Novel derivatives of spirooxindole-pyrazoline were synthesized and evaluated for fungicidal activity against several crop fungi. The result of the study showed that majority of the compounds possessed moderate to good activity against several fungal strains, particularly compound **112** (Fig. **2.22**) showed *in-vitro* fungicidal activity against two fungal strains (*G. zeae* and *P. sasakii*) comparable to standard drug azoxystrobin [145].

In a recent study, new 2,3-dihydrooxazole-spirooxindole derivatives were synthesized and evaluated for anti-fungal activity by Tiwari and group. The result of the study revealed that compounds **113a** and **113b** (Fig. **2.22**) exhibited fungicidal activity against *P. cubensis* and *P. oryzae* with MIC 8 µg/mL [146].

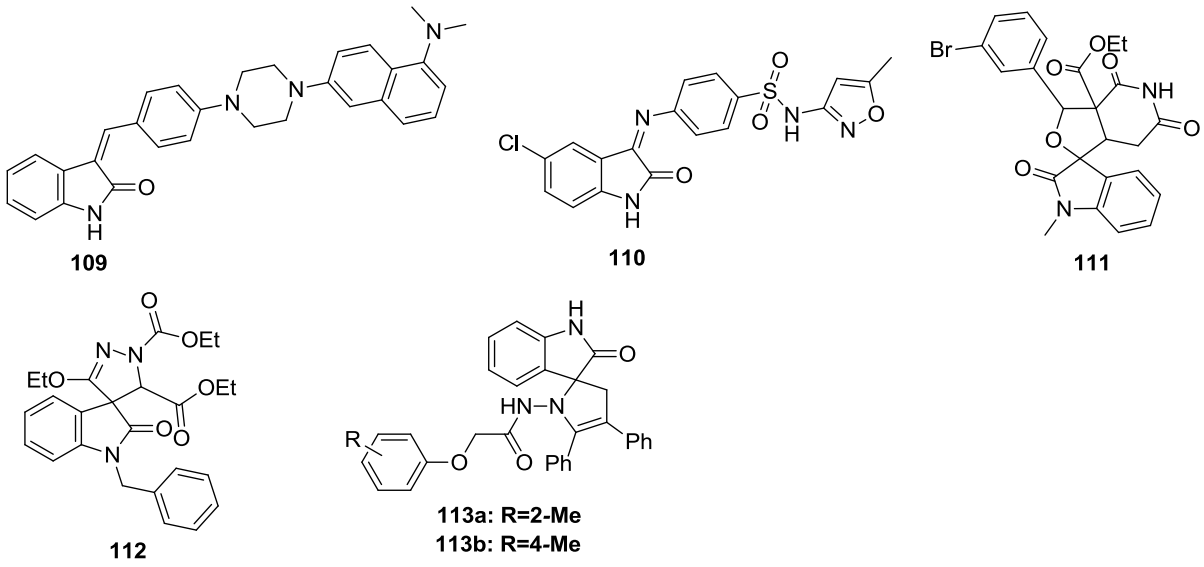

Fig. 2.22 Oxindole based compounds as anti-fungal agents

2.5.4 Oxindole as anti-tubercular agents

Chande *et. al.* synthesized spiro derivatives of oxindole and isoxazole-5-one using Michael addition reaction. Further, evaluation of compounds for anti-tubercular activity against *M. tuberculosis* revealed that majority of compounds showed moderate to potent activity, particularly two compounds **114a** and **114b** (Fig. **2.23**) exhibited MIC 0.05 µg/mL against the tested strain, which was found to be comparable to standard drug rifampicin [147].

In another report, Kumar *et. al.,* synthesized a series of 1-methyl-3,5-bis[(E)-arylmethylidene]tetrahydro-4(*1H*)-pyridinones derivatives and evaluated for their *in-vitro* and *in-vivo* activity against *M. tuberculosis.* Among the series, compound **115** (Fig. **2.23**) was found to be the best active with MIC value of 0.07 µM against *Mtb,* around 5.1 and 67.2 times more potent than isoniazid and ciprofloxacin, respectively. Moreover, compound **115** also effectively decreased the bacterial load in the lung and spleen tissues during *in-vivo* studies [148]. In one more study, similar research group synthesized a series of twenty nine novel spiro-pyrrolothiazolyl oxindoles and evaluated for anti-*Mtb* activity using agar dilution method, in which compound **116** (Fig. **2.23**) was found to be most active compound with MIC of 2.8 µM against MTB, around 2.70 times more active than standard drug ethambutol [149].

Mhiri *et al.* demonstrated the synthesis and anti-tubercular activity of benzofuranone oxindole hybrid compounds. Further, best active compounds were subjected to cytotoxicity studies against RAW cell lines. Among the series of compounds, twelve compounds showed potent anti-tubercular activity with MIC ranging from 1.56 to 6.25 µg/mL. In particular, two compounds **117a** and **117b** (Fig. **2.23**) were found to be significantly active (MIC of 1.56 µg/mL) with good safety profile [150].

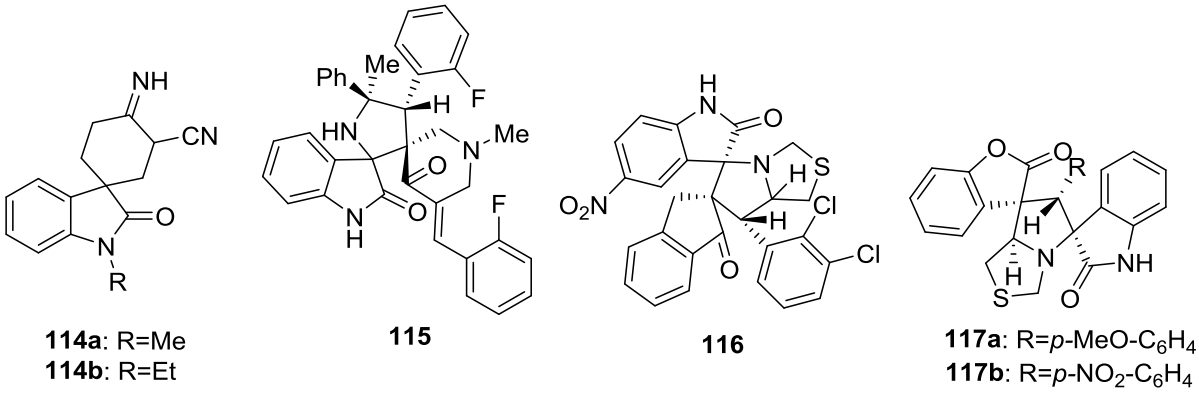

114a: R=Me
114b: R=Et

115

116

117a: R=*p*-MeO-C_6H_4
117b: R=*p*-NO_2-C_6H_4

Fig. 2.23 Oxindole based compounds as anti-tubercular agents

2.6 References

1. J.D. Scott, R.M. Williams, Chemistry and biology of the tetrahydroisoquinoline antitumor antibiotics. Chemical Reviews, 102 (2002) 1669-1730.
2. C. Avendano, J.C. Menendez, Medicinal Chemistry of Anti-cancer Drugs, Chapter 13: Cancer Chemoprevention, Elsevier, 1 (2000) 189-193.
3. C. Marchand, S. Antony, K.W. Kohn, M. Cushman, A. Ioanoviciu, B.L. Staker, A.B. Burgin, A novel norindenoisoquinoline structure reveals a common interfacial inhibitor paradigm for ternary trapping of the topoisomerase I-DNA covalent complex. Molecular Cancer Therapeutics, 5 (2006) 287-295.
4. G.R. Pettit, V. Gaddamidi, D.L. Herald, S.B. Singh, G.M. Cragg, J.M. Schmidt, F.E. Boettner, Antineoplastic Agents, 120. Pancratium littorale. Journal of Natural Products, 49 (1986) 995-1002.
5. R.K. Tiwari, D. Singh, J. Singh, A.K. Chhillar, R. Chandra, A.K. Verma, Synthesis, anti-bacterial activity and QSAR studies of 1,2-disubstituted-6,7-dimethoxy-1,2,3,4-tetrahydroisoquinolines. European Journal of Medicinal Chemistry, 41 (2006) 40-49.
6. Y.M. Al-Hiari, B.A. Sweileh, A.K. Shakya, G.A. Sheikha, S.I. Almuhtaseb, Synthesis of 1-benzyl-1,2,3,4-tetrahydroisoquinoline, Part I: Grignard synthesis of 1-(substituted benzyl)-1,2,3,4-tetrahydroisoquinoline models with potential anti-bacterial activity. Jordan Journal of Pharmaceutical Sciences, 2 (2009) 1-21.
7. X.H. Liu, J. Zhu, A. Zhou, B.A. Song, H.L. Zhu, L.S. Bai, P.S. Bhadury, Synthesis, structure and antibacterial activity of new 2-(1-(2-(substituted-phenyl)-5-methyloxazol-4-yl)-3-(2-substitued-phenyl)-4,5-dihydro-1H-pyrazol-5-yl)-7-substitued-1,2,3,4-tetrahydroisoquinoline derivatives, Bioorganic & Medicinal Chemistry, 17 (2009) 1207-1213.
8. A. Zablotskaya, I. Segal, A. Geronikaki, T. Eremkina, S. Belyakov, M. Petrova, I. Shestakova, Synthesis, physicochemical characterization, cytotoxicity, antimicrobial, anti-inflammatory and psychotropic activity of new *N*-[1,3-(benzo)thiazol-2-yl]-ω-[3,4-dihydroisoquinolin-2(1H)-yl]alkanamides. European Journal of Medicinal Chemistry, 70 (2013) 846–856.
9. A. Galan, L. Moreno, J. Parraga, A. Serrano, M.J. Sanz, D. Cortes, N. Cabedo Novel isoquinoline derivatives as anti-microbial agents. Bioorganic & Medicinal Chemistry, 21 (2013) 3221-3230.
10. Y. Kashiwada, A. Aoshima, Y. Ikeshiro, Y.P. Chen, H. Furukawa, M. Itoigawa, T. Fujioka, Anti-HIV benzylisoquinoline alkaloids and flavonoids from the leaves of Nelumbonucifera and structure–activity correlations with related alkaloids. Bioorganic & Medicinal Chemistry, 13 (2005) 443-448.

11. P. Cheng, N. Huang, Z.Y. Jiang, Q. Zhang, Y.T. Zheng, J.J. Chen, X.M. Zhang, 1-aryl-tetrahydroisoquinoline analogs as active anti-HIV agents *in- vitro*. Bioorganic & Medicinal Chemistry Letters, 18 (2008) 2475-2478.
12. V.M. Truax, H. Zhao, B.M. Katzman, A.R. Prosser, A.A. Alcaraz, M.T. Saindane, R.B. Howard, Discovery of tetrahydroisoquinoline-based CXCR4 antagonists. ACS Medicinal Chemistry Letters, 4 (2013) 1025-1030.
13. J.J. Swidorski, Z. Liu, Z. Yin, T. Wang, D.J. Carini, S. Rahematpura, M. Zheng, Inhibitors of HIV-1 attachment: The discovery and structure-activity relationships of tetrahydroisoquinolines as replacements for the piperazine benzamide in the 3-glyoxylyl 6-azaindole pharmacophore. Bioorganic & Medicinal Chemistry Letters, 26 (2016) 160-167.
14. T.N. Makarieva, V.A. Denisenko, P.S. Dmitrenok, A.G. Guzii, E.A. Santalova, V.A. Stonik, J.B. Macmillan, Oceanalin A, a hybrid alpha, omega-bifunctionalized sphingoid tetrahydroisoquinoline beta-glycoside from the marine sponge Oceanapia sp. Organic Letters, 7 (2005) 2897-2900.
15. J. Zhu, J. Lu, Y. Zhou, Y. Li, J. Cheng, C. Zheng, Design, synthesis and anti-fungal activities *in-vitro* of novel tetrahydroisoquinoline compounds based on the structure of lanosterol 14alpha-demethylase (CYP51) of fungi. Bioorganic & Medicinal Chemistry Letters, 16 (2006) 5285-5289.
16. J. Krauss, C. Muller, J. Kiebling, S. Richter, V. Staudacher, F. Bracher, Synthesis and biological evaluation of novel N-alkyl tetra and decahydroisoquinolines: Novel anti-fungals that target ergosterol biosynthesis. Archiv Der Pharmazie Chemistry in Life Sciences, 347 (2014) 283-290.
17. R.P. Tangallapallya, R.B. Leea, A.M. Lenaertsb, R.E. Leea, Synthesis of new and potent analogs of anti-tuberculosis agent 5-nitro-furan-2-carboxylic acid 4-(4-benzyl-piperazin-1-yl)-benzylamide with improved bioavailability. Bioorganic & Medicinal Chemistry Letters, 16 (2006) 2584-2589.
18. J.P. Michael, Quinoline, quinazoline and acridone alkaloids. Natural Product Reports, 25 (2008) 166-187.
19. V. Sridharan, P.A. Suryavanshi, J.C. Menendez, Advances in the chemistry of tetrahydroquinolines. Chemical Reviews, 111 (2011) 7157-7259.
20. M.L. Quan, P.C. Wong, C. Wang, F. Woerner, J.M. Smallheer, F.A. Barbera, J.M. Bozarth, Tetrahydroquinoline derivatives as potent and selective factor XIa inhibitors. Journal of Medicinal Chemistry, 57 (2014) 955-969.
21. R.B. McCall, K.J. Lookingland, P.J. Bedard, R.M. Huff, Sumanirole, a highly dopamine D2-selective receptor agonist: *in-vitro* and *in vivo* pharmacological characterization and

efficacy in animal models of Parkinson's disease. Journal of Pharmacology and Experimental Therapeutics, 314 (2005) 1248-1256.

22. C. Theeraladanon, M. Arisawa, M. Nakagawa, A. Nishida, Total synthesis of (+)-(S)-angustureine and the determination of the absolute configuration of the natural product angustureine. Tetrahedron: Asymmetry, 16 (2005) 827-831.
23. I. Jacquemond-Collet, F. Benoit-Vical, A. Valentin, E. Stanislas, M. Mallie, I. Fouraste, Anti-plasmodial and cytotoxic activity of galipinine and other tetrahydroquinolines from *Galipea officinalis*. Planta Medica, 68 (2002) 68-69.
24. I. Jacquemond-Collet, S. Hannedouche, N. Fabre, I. Fouraste, C. Moulis, Two tetrahydroquinoline alkaloids from *Galipea officinalis*. Phytochemistry, 51 (1999) 1167-1169.
25. E. Chalkidou, F. Perdih, I. Turel, D.P. Kessissoglou, G. Psomas, Copper (II) complexes with anti-microbial drug flumequine: structure and biological evaluation. Journal of Inorganic Biochemistry, 113 (2012) 55-65.
26. D. Ma, C. Xia, J. Jiang, J. Zhang, First total synthesis of martinellic acid, a naturally occurring bradykinin receptor antagonist. Organic Letters, 3 (2001) 2189-2191.
27. L. Shen, Y.H. Ye, X.T. Wang, H.L. Zhu, C. Xu, Y.C. Song, Structure and total synthesis of aspernigerin: a novel cytotoxic endophyte metabolite. Chemistry 12 (2006) 4393-4396.
28. L.J. Lombardo, A. Camuso, J. Clark, K. Fager, J. Gullo-Brown, J.T. Hunt, Design, synthesis and structure-activity relationships of tetrahydroquinoline-based farnesyltransferase inhibitors. Bioorganic & Medicinal Chemistry Letters, 15 (2005) 1895-1899.
29. R.L. Jarvest, S.A. Armstrong, J.M. Berge, P. Brown, J.S. Elder, M.J. Brown, Definition of the heterocyclic pharmacophore of bacterial methionyl tRNAsynthetase inhibitors: potent anti-bacterially active non-quinolone analogs. Bioorganic & Medicinal Chemistry Letters, 14 (2004) 3937-3941.
30. S.R. Martinez, G.E. Miana, I. Albesa, M.R. Mazzieri, M.C. Becerra, Evaluation of anti-bacterial activity and reactive species generation of N-benzenesulfonyl derivatives of heterocycles. Chemical and Pharmaceutical Bulletin, 64 (2016) 135-141.
31. D.S. Su, J.J. Lim, E. Tinney, B.L. Wan, M.B. Young, K.D. Anderson, Substituted tetrahydroquinolines as potent allosteric inhibitors of reverse transcriptase and its key mutants. Bioorganic & Medicinal Chemistry Letters, 19 (2009) 119-123.
32. J. Zhang, P. Zhan, J. Wu, Z. Li, Y. Jiang, W. Ge, C. Pannecouque, Synthesis and biological evaluation of novel 5-alkyl-2-arylthio-6-((3,4-dihydroquinolin-1(*2H*)-yl)methyl)pyrimidin-4(*3H*)-ones as potent non-nucleoside HIV-1 reverse transcriptase inhibitors. Bioorganic & Medicinal Chemistry Letters, 19 (2011) 4366-4376.

33. L.M. Bedoya, Quinoline-based compounds as modulators of HIV transcription through NF-kappa B and Sp1 inhibition. Antiviral Research, 87 (2010) 338-344.
34. J.M. Urbina, J.C. Cortes, A. Palma, S.N. Lopez, S.A. Zacchino, R.D. Enriz, Inhibitors of the fungal cell wall synthesis of 4-aryl-4-*N*-arylamine-1-butenes and related compounds with inhibitory activities on beta(1-3)glucan and chitin synthases. Bioorganic & Medicinal Chemistry, 8 (2000) 691-698.
35. M. Gutierrez, U. Carmona, G. Vallejos, L. Astudillo, Anti-fungal activity of tetrahydroquinolines against some phytopathogenic fungi. Zeitschrift für Naturforschung. C, Journal of biosciences, 67 (2012) 551-556.
36. Q.Z. Zheng, K. Cheng, X.M. Zhang, K. Liu, Q.C. Jiao, H.L. Zhu, Synthesis of some N-alkyl substituted urea derivatives as anti-bacterial and anti-fungal agents. European Journal of Medicinal Chemistry, 45 (2010) 3207-3212.
37. M.C. Mandewalea, S. Kokatea, B. Thorata, S. Sawanta, R. Yamgarb, Zinc complexes of hydrazone derivatives bearing 3,4-dihydroquinolin-2(*1H*)-one nucleus as new anti-tubercular agents. Arabian Journal of Chemistry, (2016) Under Press, doi.org/10.1016/j.arabjc.2016.07.016.
38. S.D. Joshi, N.M. Jangade, S.R. Dixit, A.S. Joshi, V.H. Kulkarni, Quinoline: a promising and versatile scaffold for future. Indo American Journal of Pharmaceutical Research 6 (2016) 5033-5044.
39. S. Kumar, S. Bawa, H. Gupta, Biological activities of quinoline derivatives. Mini-Reviews in Medicinal Chemistry, 9 (2009) 1648-1654.
40. A. Marella, O.P. Tanwar, R. Saha, M.R. Ali, S. Srivastava, M. Akhter, M. Shaquiquzzaman, Quinoline: A versatile heterocyclic. Saudi Pharmaceutical Journal, 21 (2013) 1-12.
41. S. Bawa, S. Kumar, S. Drabu, R. Kumar, Structural modifications of quinoline-based anti-malarial agents: Recent developments, Journal of Pharmacy and Bioallied Sciences, 2 (2010) 64-71.
42. https://www.drugs.com/drug-class/quinolones.html, accessed on 2nd Oct. 2016.
43. K.J. Aldred, R.J. Kerns, N. Osheroff, Mechanism of quinolone action and resistance. Biochemistry, 53 (2014) 1565-1574.
44. P. Narender, U. Srinivas, M. Ravinder, B.A. Rao, C. Ramesh, K. Harakishore, B. Gangadasu, Synthesis of multisubstituted quinolines from Baylis–Hillman adducts obtained from substituted 2-chloronicotinaldehydes and their anti-microbial activity. Bioorganic & Medicinal Chemistry, 14 (2006) 4600-4609.
45. S.A. Abdel-Mohsen. Synthesis, reactions and anti-microbial activity of 2-Amino-4-(8-quinolinol-5-yl)-1-(p-tolyl)-pyrrole-3-carbonitrile. Bulletin of the Korean Chemical Society, 26 (2005) 719-726.

46. R.C. Khunt, N.J. Datta, F.M. Bharmal, G.P. Mankad, A.R. Parikh, Synthesis and biological evaluation of cyanopyridine and isoxazole derivatives. Indian Journal of Heterocyclic Chemistry, 10 (2000) 97-100.
47. D.C. Mungra, M.P. Patel, D.P. Rajani, R.G. Patel, Synthesis and identification of β-aryloxyquinolines and their pyrano [3,2-c]chromene derivatives as a new class of anti-microbial and anti-tuberculosis agents. European Journal of Medicinal Chemistry, 46 (2011) 4192-4200.
48. M.A. Fakhfakh, A. Fournet, E. Prina, J.F. Mouscadet, X. Franck, R. Hocquemiller, B. Figadere, Synthesis and biological evaluation of substituted quinolines: potential treatment of protozoal and retroviral co-infections. Bioorganic & Medicinal Chemistry, 11 (2003) 5013–5023.
49. S. Chen, R. Chen, M. He, R. Pang, Z. Tan, M. Yang. Design, synthesis and biological evaluation of novel quinoline derivatives as HIV-1 Tat–TAR interaction inhibitors. Bioorganic & Medicinal Chemistry, 17 (2009) 1948-1956.
50. M. Normand-Bayle, C. Benard, F. Zouhiri, J.F. Mouscadet, H. Leh, C.M. Thomas, G. Mbemba, New HIV-1 replication inhibitors of the styryquinoline class bearing aroyl/acyl groups at the C-7 position: synthesis and biological activity. Bioorganic & Medicinal Chemistry Letters, 15 (2005) 4019-4022.
51. V. Moret, N. Dereudre-Bosquet, P. Clayette, Y. Laras, N. Pietrancosta, A. Rolland, C. Weck, Synthesis and anti-HIV properties of new hydroxyquinoline-polyamine conjugates on cells infected by HIV-1 LAV and HIV-1 BaL viral strains. Bioorganic & Medicinal Chemistry Letters, 16 (2006) 5988-5992.
52. X.W. Zeng, N. Huang, H. Xu, W.B. Yang, L.M. Yang, H. Qu, Y.T. Zheng. Anti- human immunodeficiency virus type 1 (HIV-1) agents 4. Discovery of 5,5'-(p-phenylenebisazo)-8-hydroxyquinoline sulfonates as new HIV-1 inhibitors *in-vitro*. Chemical and Pharmaceutical Bulletin, 58 (2010) 976-979.
53. E. Serrao, B. Debnath, H. Otake, Y. Kuang, F. Christ, Z. Debyser, N. Neamati, Fragment-based discovery of 8-hydroxyquinoline inhibitors of the HIV-1 integrase-lens epithelium-derived growth factor/p75 (IN-LEDGF/p75) interaction. Journal of Medicinal Chemistry, 56 (2013) 2311-2322.
54. F. Zhong, G. Geng, B. Chen, T. Pan, Q. Li, H. Zhang, C. Bai, Identification of benzenesulfonamide quinoline derivatives as potent HIV-1 replication inhibitors targeting Rev protein. Organic & Biomolecular Chemistry, 13 (2015) 1792-1799.
55. R. Musiol, J. Jampilek, V. Buchta, L. Silva, H. Niedbala, B. Podeszwa, A. Palka, Anti-fungal properties of new series of quinoline derivatives. Bioorganic & Medicinal Chemistry, 14 (2006) 3592-3598.

56. B.S. Holla, M. Mahalinga, M.S. Karthikeyan, B. Poojary, P.M. Akberali, N.S. Kumari, Synthesis, characterization and anti-microbial activity of some substituted 1,2,3-triazoles. European Journal of Medicinal Chemistry, 40 (2005) 1173-1178.
57. P.S. Kharkar, M.N. Deodhar, V.M. Kulkarni, Design, synthesis, anti-fungal activity and ADME prediction of functional analogs of terbinafine. Medicinal Chemistry Research, 18 (2009) 421-432.
58. S. Kumar, S. Bawa, S. Drabu, B.P. Panda, Design and synthesis of 2-chloroquinoline derivatives as non-azoles anti-mycotic agents. Medicinal Chemistry Research, 20 (2011) 1340-1348.
59. K. Nakamoto, I. Tsukada, K. Tanaka, M. Matsukura, T. Haneda, S. Inoue, N. Murai, Synthesis and evaluation of novel anti-fungal agents-quinoline and pyridine amide derivatives. Bioorganic & Medicinal Chemistry Letters, 20 (2010) 4624-4626.
60. L. de Carvalho Tavares, S. Johann, T. Maria de Almeida Alves, J.C. Guerra, E. Maria de Souza-Fagundes, P.S. Cisalpino, A.J. Bortoluzzi, Quinolinyl and quinolinyl N-oxide chalcones: synthesis, anti-fungal and cytotoxic activities. European Journal of Medicinal Chemistry, 46 (2011) 4448-4456.
61. B. Garudachari, M.N. Satyanarayana, B. Thippeswamy, C.K. Shivakumar, K.N. Shivananda, G. Hegde, A.M. Isloor, Synthesis, characterization and anti-microbial studies of some new quinoline incorporated benzimidazole derivatives. European Journal of Medicinal Chemistry, 54 (2012) 900-906.
62. R.V. Patel, S.W. Park, Access to a new class of biologically active quinoline based 1,2,4-triazoles. European Journal of Medicinal Chemistry, 71(2014) 24-30.
63. S. Vandekerckhove, S. Van Herreweghe, J. Willems, B. Danneels, T. Desmet, C. de Kock, P.J. Smith, Synthesis of functionalized 3-, 5-, 6- and 8-aminoquinolines via intermediate (3-pyrrolin-1-yl)- and (2-oxopyrrolidin-1-yl)quinolines and evaluation of their anti-plasmodial and anti-fungal activity. European Journal of Medicinal Chemistry, 92 (2015) 91-102.
64. https://www.drugs.com/search.php?searchterm=Bedaquiline, accessed on 7th Nov. 2016.
65. R. Mahajan, Bedaquiline: First FDA-approved tuberculosis drug in 40 years. International Journal of Applied & Basic Medical Research, 3 (2013) 1-2.
66. A. Matteelli, A.C. Carvalho, K.E. Dooley, A. Kritski, TMC207: the first compound of a new class of potent anti-tuberculosis drugs. Future Microbiology, 5 (2010) 849-858.
67. S. Vangapandu, M. Jain, R. Jain, S. Kaur, P.P. Singh, Ring-substituted quinolines as potential anti-tuberculosis agents. Bioorganic & Medicinal Chemistry, 12 (2004) 2501-2508.

68. V. Monga, A. Nayyar, B. Vaitilingam, P.B. Palde, S.S. Jhamb, S. Kaur, P.P. Singh, Ring-substituted quinolines. Part 2: Synthesis and anti-mycobacterial activities of ring-substituted quinolinecarbohydrazide and ring-substituted quinolinecarboxamide analogs. Bioorganic & Medicinal Chemistry, 12 (2004) 6465-6472.
69. R.S. Upadhayaya, G.M. Kulkarni, N.R. Vasireddy, J.K. Vandavasi, S.S. Dixit, V. Sharma, J. Chattopadhyaya, Design, synthesis and biological evaluation of novel triazole, urea and thiourea derivatives of quinoline against Mycobacterium tuberculosis. Bioorganic & Medicinal Chemistry, 17 (2009) 4681-4692.
70. S. Eswaran, A.V. Adhikari, N.K. Pal, I.H. Chowdhury, Design and synthesis of some new quinoline-3-carbohydrazone derivatives as potential anti-mycobacterial agents. Bioorganic & Medicinal Chemistry Letters, 20 (3) 1040-1044.
71. K.D. Thomas, A.V. Adhikari, I.H. Chowdhury, T. Sandeep, R. Mahmood, B. Bhattacharya, E. Sumesh, Design, synthesis and docking studies of quinoline-oxazolidinone hybrid molecules and their anti-tubercular properties. European Journal of Medicinal Chemistry, 46 (2011) 4834-4845.
72. M. Tukulula, S. Little, J. Gut, P.J. Rosenthal, B. Wan, S.G. Franzblau, K. Chibale, The design, synthesis, in silico ADME profiling, anti-plasmodial and anti-mycobacterial evaluation of new arylamino quinoline derivatives. European Journal of Medicinal Chemistry, 57 (2012) 259-267.
73. P.P. Jain, M.S. Degani, A. Raju, M. Ray, M.G. Rajan, Rational drug design based synthesis of novel arylquinolines as anti-tuberculosis agents. Bioorganic & Medicinal Chemistry Letters, 23 (2013) 6097-6105.
74. R. Raj, C. Biot, S. Carrere-Kremer, L. Kremer, Y. Guerardel, J. Gut, P.J. Rosenthal, V. Kumar, 4-Aminoquinoline-β-lactam conjugates: synthesis, anti-malarial and anti-tubercular evaluation. Chemical Biology & Drug Design, 83 (2014) 191-197.
75. J. Kos, I. Zadrazilova, E. Nevin, M. Soral, T. Gonec, P. Kollar, M. Oravec, Ring-substituted 8-hydroxyquinoline-2-carboxanilides as potential anti-mycobacterial agents. Bioorganic & Medicinal Chemistry, 23 (2015) 4188-4196.
76. B. Medapi, J. Renuka, S. Saxena, J.P. Sridevi, R. Medishetti, P. Kulkarni, P. Yogeeswari, Design and synthesis of novel quinoline-aminopiperidine hybrid analogs as Mycobacterium tuberculosis DNA gyraseB inhibitors. Bioorganic & Medicinal Chemistry, 23 (2015) 2062-2078.
77. B. Medapi, P. Suryadevara, J. Renuka, J.P. Sridevi, P. Yogeeswari, D. Sriram, 4 Aminoquinoline derivatives as novel Mycobacterium tuberculosis GyrB inhibitors: Structural optimization, synthesis and biological evaluation. European Journal of Medicinal Chemistry, 103 (2015) 1-16.

78. P.P. Jain, M.S. Degani, A. Raju, A. Anantram, M. Seervi, S. Sathaye, M. Ray, Identification of a novel class of quinoline-oxadiazole hybrids as anti-tuberculosis agents. Bioorganic & Medicinal Chemistry Letters, 26 (2016) 645-649.
79. V. Hahn, A. Mikolasch, K. Wende, H. Bartrow, U. Lindequist, F. Schauer, Synthesis of model morpholine derivatives with biological activities by laccase-catalysed reactions. Biotechnology and Applied Biochemistry, 4 (2009) 187-195.
80. http://apps.who.int/medicinedocs/en/d/Jh2922e/3.2.4.html, accessed on 12 March, 2016
81. R.V. Patel, S. W. Park, An evolving role of piperazine moieties in drug design and discovery. Mini Reviews in Medicinal Chemistry, 13, (2013) 1579-1601.
82. A.M. Amani, Synthesis and biological activity of piperazine derivatives of phenothiazine. Drug Research, 65 (2015) 5-8.
83. D.A. Horton, G.T. Bourne, M.L. Smythe, The combinatorial synthesis of bicyclic privileged structures or privileged substructures. Chemical Reviews, 103 (2003) 893-930.
84. J. Hecq, M. Deleers, D. Fanara, H. Vranckx, P. Boulanger, S. Le Lamer, K. Amighi, Preparation and *in-vitro*/*in-vivo* evaluation of nano-sized crystals for dissolution rate enhancement of ucb-35440-3, a highly dosed poorly water-soluble weak base. European Journal of Pharmaceutics and Biopharmaceutics, 64 (2006) 360-368.
85. C.P. Meher, A.M. Rao, M. Omar, Piperazine-pyrazine and their multiple biological activities. Asian Journal of Pharmaceutical Sciences and Research, 3 (2013) 43-60.
86. S. Jafari, F. Fernandez-Enright, X.F. Huang, Structural contributions of anti-psychotic drugs to their therapeutic profiles and metabolic side effects. Journal of Neurochemistry 120 (2012) 371-384.
87. A.K. Rathi, R. Syed, H.S. Shin, R.V. Patel, Piperazine derivatives for therapeutic use: a patent review, Expert Opinion on Therapeutic Patents, 26 (2016) 777-797.
88. A. Foroumadi, S. Mansouri, Z. Kiani, A. Rahmani. Synthesis and *in-vitro* antibacterial evaluation of *N*-[5-(5-nitro-2-thienyl)-1,3,4-thiadiazole-2-yl]piperazinyl quinolones. European Journal of Medicinal Chemistry, 38 (2003) 851-854.
89. A. Khalaj, N. Adibpour, A.R. Shahverdi, M. Daneshtalab, Synthesis and anti-bacterial activity of 2-(4-substituted phenyl)-3(*2H*)-isothiazolones. European Journal of Medicinal Chemistry, 39 (2004) 699-705.
90. A. Foroumadi, S. Emami, S. Mansouri, A. Javidnia, N. Saeid-Adeli, F.H. Shirazi, A. Shafiee, Synthesis and anti-bacterial activity of levofloxacin derivatives with certain bulky residues on piperazine ring. European Journal of Medicinal Chemistry, 42 (2007) 985-992.

91. C.S. Kumar, K. Vinaya, J.N. Chandra, N.R. Thimmegowda, S.B. Prasad, C.T. Sadashiva, K.S. Rangappa, Synthesis and anti-microbial studies of novel 1-benzhydryl-piperazine sulfonamide and carboxamide derivatives. Journal of Enzyme Inhibition and Medicinal Chemistry, 23 (2008) 462-469.
92. Z. Yu, G. Shi, Q. Sun, H. Jin, Y. Teng, K. Tao, G. Zhou, Design, synthesis and *in-vitro* anti-bacterial/anti-fungal evaluation of novel 1-ethyl-6-fluoro-1,4-dihydro-4-oxo-7(1-piperazinyl)quinoline-3-carboxylic acid derivatives. European Journal of Medicinal Chemistry, 44 (2009) 4726-4733.
93. L. Li, Z. Li, N. Guo, J. Jin, R. Du, J. Liang, Wu X, Synergistic activity of 1-(1-naphthylmethyl)-piperazine with ciprofloxacin against clinically resistant *Staphylococcus aureus*, as determined by different methods. Letters in Applied Microbiology, 52 (2011) 372-378.
94. P.T. Chen, W.P. Lin, A.R. Lee, M.K. Hu, New 7-[4-(4-(un)substituted)piperazine-1-carbonyl]-piperazin-1-yl] derivatives of fluoroquinolone: synthesis and anti-microbial evaluation. Molecules, 18 (2013) 7557-7569.
95. S.F. Wang, Y. Yin, X. Wu, F. Qiao, S. Sha, P.C. Lv, J. Zhao, Synthesis, molecular docking and biological evaluation of coumarin derivatives containing piperazine skeleton as potential anti-bacterial agents. Bioorganic & Medicinal Chemistry, 22 (2014) 5727-5737.
96. S. Mahato, A. Singh, L. Rangan, C.K. Jana, Synthesis, In silico studies and *In-vitro* evaluation for anti-oxidant and anti-bacterial properties of diarylmethylamines: A novel class of structurally simple and highly potent pharmacophore. European Journal of Pharmaceutical Sciences, 88 (2016) 202-209.
97. J.R. Tagat, R.W. Steensma, S.W. McCombie, D.V. Nazareno, S. Lin, B.R. Neustadt, K. Cox, Piperazine-based CCR5 antagonists as HIV-1 inhibitors. II. discovery of 1-[(2,4-dimethyl-3-pyridinyl)carbonyl]-4-methyl-4-[3(S)-methyl-4-[1(S)-[4-(trifluoromethyl)phenyl]ethyl]-1-piperazinyl]-piperidine-N1-oxide (Sch-350634), an orally bioavailable, potent CCR5 antagonist. Journal of Medicinal Chemistry. 44 (2001) 3343-3346.
98. S.W. McCombie, J.R. Tagat, S.F. Vice, S.I. Lin, R. Steensma, A. Palani, B.R. Neustadt, Piperazine-based CCR5 antagonists as HIV-1 inhibitors. III: synthesis, anti-viral and pharmacokinetic profiles of symmetrical heteroaryl carboxamides. Bioorganic & Medicinal Chemistry, 13 (2003) 567-571.
99. H.A. Gelbard, H.S. Nottet, S. Swindells, M. Jett, K.A. Dzenko, P. Genis, R. White, Platelet-activating factor: a candidate human immunodeficiency virus type 1-induced neurotoxin. Journal of Virology, 68 (1994) 4628-4635.

100. N. Serradji, O. Bensaid, M. Martin, W. Sallem, N. Dereuddre-Bosquet, H. Benmehdi, C. Redeuilh, Structure-activity relationships in platelet-activating factor. Part 13: synthesis and biological evaluation of piperazine derivatives with dual anti-PAF and anti-HIV-1 or pure anti-retroviral activity. Bioorganic & Medicinal Chemistry, 14 (2006) 8109-8125.
101. A. El-Faham, M. Armand-Ugon, J.A. Este, F. Albericio, Use of *N*-methylpiperazine for the preparation of piperazine-based unsymmetrical bis-ureas as anti-HIV agents. ChemMedChem, 3 (2008) 1034-1037.
102. T. Wang, J.F. Kadow, Z. Zhang, Z. Yin, Q. Gao, D. Wu, D.D. Parker, Inhibitors of HIV-1 attachment. Part 4: A study of the effect of piperazine substitution patterns on anti-viral potency in the context of indole-based derivatives. Bioorganic & Medicinal Chemistry Letters, 19 (2009) 5140-5145.
103. M.X. Dong, L. Lu, H. Li, X. Wang, H. Lu, S. Jiang, Q.Y. Dai, Design, synthesis, and biological activity of novel 1,4-disubstituted piperidine/piperazine derivatives as CCR5 antagonist-based HIV-1 entry inhibitors. Bioorganic & Medicinal Chemistry Letters, 22 (2012) 3284-3286.
104. T. Wang, Z. Yang, Z. Zhang, Y.F. Gong, K.A. Riccardi, P.F. Lin, D.D. Parker, Inhibitors of HIV-1 attachment. Part 10. The discovery and structure-activity relationships of 4-azaindole cores. Bioorganic & Medicinal Chemistry Letters, 23 (2013) 213-217.
105. T. Liu, Z. Weng, X. Dong, L. Chen, L. Ma, S. Cen, N. Zhou, Design, synthesis and biological evaluation of novel piperazine derivatives as CCR5 antagonists. PLoS One, 8 (2013) e53636.
106. V. Bala, D. Mandalapu, S. Gupta, S. Jangir, B. Kushwaha, Y.S. Chhonker, H. Chandasana, *N*-Alkyl/aryl-4-(3-substituted-3-phenylpropyl)piperazine-1-carbothioamide as dual-action vaginal microbicides with reverse transcriptase inhibition. European Journal of Medicinal Chemistry, 101 (2015) 640-650.
107. A.T. Nguyen, C.L. Feasley, K.W. Jackson, T.J. Nitz, K. Salzwedel, G.M. Air, M. Sakalian, The prototype HIV-1 maturation inhibitor, bevirimat, binds to the CA-SP1 cleavage site in immature Gag particles. Retrovirology. 8 (2011) 101.
108. N.A. Margot, C.S. Gibbs, M.D. Miller, Phenotypic susceptibility to bevirimat in isolates from HIV-1-infected patients without prior exposure to bevirimat. Antimicrobial Agents and Chemotherapy, 54 (2010) 2345-2353.
109. Y. Zhao, Q. Gu, S.L. Morris-Natschke, C.H. Chen, K.H. Lee, Incorporation of privileged structures into bevirimat can improve activity against wild-type and bevirimat-resistant HIV-1. Journal of Medicinal Chemistry, 59 (2016) 9262-9268.
110. R.S. Upadhayaya, N. Sinha, S. Jain, N. Kishore, R. Chandra, S.K. Arora, Optically active anti-fungal azoles: synthesis and anti-fungal activity of (2R,3S)-2-(2,4-

difluorophenyl)-3-(5-[2-[4-aryl-piperazin-1-yl]-ethyl]-tetrazol-2-yl/1-yl)-1-[1,2,4]-triazol-1-yl-butan-2-ol. Bioorganic & Medicinal Chemistry, 12 (2004) 2225-2238.

111. M.T. Cushion, P.D. Walzer, M.S. Collins, S. Rebholz, J.J. Vanden Eynde, A. Mayence, T.L. Huang, Highly active anti-Pneumocystis carinii compounds in a library of novel piperazine-linked bisbenzamidines and related compounds. Antimicrobial Agents and Chemotherapy, 48 (2004) 4209-4216.
112. O. Kondoh, Y. Inagaki, H. Fukuda, E. Mizuguchi, Y. Ohya, M. Arisawa, N. Shimma, Piperazine propanol derivative as a novel anti-fungal targeting 1,3-beta-D-glucan synthase. Biological and Pharmaceutical Bulletin, 28 (2005) 2138-2141.
113. W.J. Watkins, L. Chong, A. Cho, R. Hilgenkamp, M. Ludwikow, N. Garizi, N. Iqbal, Quinazolinone fungal efflux pump inhibitors. Part 3: (N-methyl) piperazine variants and pharmacokinetic optimization. Bioorganic & Medicinal Chemistry Letters, 17 (2007) 2802-2806.
114. I.E. Francois, K. Thevissen, K. Pellens, E.M. Meert, J. Heeres, E. Freyne, E. Coesemans, Design and synthesis of a series of piperazine-1-carboxamidine derivatives with anti-fungal activity resulting from accumulation of endogenous reactive oxygen species. ChemMedChem. 4 (2009) 1714-1721.
115. J. Xu, Y. Cao, J. Zhang, S. Yu, Y. Zou, X. Chai, Q. Wu, Design, synthesis and anti-fungal activities of novel 1,2,4-triazole derivatives. European Journal of Medicinal Chemistry, 46 (2011) 3142-3148.
116. Y. Wang, K. Xu, G. Bai, L. Huang, Q. Wu, W. Pan, S. Yu, Synthesis and anti-fungal activity of novel triazole compounds containing piperazine moiety. Molecules, 19 (2014) 11333-11340.
117. G. Xu, X. Yang, B. Jiang, P. Lei, X. Liu, Q. Wang, X. Zhang, Synthesis and bioactivities of novel piperazine-containing 1,5-diphenyl-2-penten-1-one analogs from natural product lead. Bioorganic & Medicinal Chemistry Letters, 26 (2016) 1849-1853.
118. A.V. Shindikar, C.L. Viswanathan, Novel fluoroquinolones: design, synthesis, and *in vivo* activity in mice against Mycobacterium tuberculosis H37Rv. Bioorganic & Medicinal Chemistry Letters, 15 (2005) 1803-1806.
119. E. Bogatcheva, C. Hanrahan, B. Nikonenko, R. Samala, P. Chen, J. Gearhart, F. Barbosa, Identification of new diamine scaffolds with activity against *Mycobacterium tuberculosis*. Journal of Medicinal Chemistry, 49 (2006) 3045-3048.
120. D.S. Rakesh, R.B. Lee, R. Tangallapally, R.E. Lee, Synthesis, optimization and structure-activity relationships of 3,5-disubstituted isoxazolines as new anti-tuberculosis agents. European Journal of Medicinal Chemistry, 44 (2009) 460-472.

121. U. Manjunatha, H.M. Boshoff, C.E Barry, The mechanism of action of PA-824 novel insights from transcriptional profiling. Communicative & Integrative Biology, 2 (2009) 215-218.
122. A. Blaser, B.D. Palmer, H.S. Sutherland, I. Kmentova, S.G. Franzblau, B. Wan, Y. Wang, Structure-activity relationships for amide, carbamate and urea-linked analogs of the tuberculosis drug (6*S*)-2-nitro-6-{[4-(trifluoromethoxy)benzyl]oxy}-6,7-dihydro-5*H*-imidazo[2,1-b][1,3]oxazine (PA-824). Journal of Medicinal Chemistry, 55 (2012) 312-326.
123. H.N. Nagesh, K.M. Naidu, D.H. Rao, J.P. Sridevi, D. Sriram, P. Yogeeswari, K.V. Chandra Sekhar, Design, synthesis and evaluation of 6-(4-((substituted-1H-1,2,3-triazol-4-yl)methyl)piperazin-1-yl)phenanthridine analogs as anti-mycobacterial agents. Bioorganic & Medicinal Chemistry Letters, 23 (2013) 6805-6810.
124. K. Chauhan, M. Sharma, P. Trivedi, V. Chaturvedi, P.M. Chauhan, New class of methyl tetrazole based hybrid of (Z)-5-benzylidene-2-(piperazin-1-yl)thiazol-4(%H)-one as potent anti-tubercular agents. Bioorganic & Medicinal Chemistry Letters, 24 (2014) 4166-4170.
125. K.N. Patel, V.N. Telvekar, Design, synthesis and anti-tubercular evaluation of novel series of *N*-[4-(piperazin-1-yl)phenyl]cinnamamide derivatives. European Journal of Medicinal Chemistry, 75 (2014) 43-56.
126. C.T. Peng, C. Gao, N.Y. Wang, X.Y. You, L.D. Zhang, Y.X. Zhu, Y. Xv, Synthesis and antitubercular evaluation of 4-carbonyl piperazine substituted 1,3-benzothiazin-4-one derivatives. Bioorganic & Medicinal Chemistry Letters, 25 (2015) 1373-1376.
127. K.A. Bobesh, J. Renuka, R.R. Srilakshmi, S. Yellanki, P. Kulkarni, P. Yogeeswari, D. Sriram, Replacement of cardiotoxic aminopiperidine linker with piperazine moiety reduces cardiotoxicity? *Mycobacterium tuberculosis* novel bacterial topoisomerase inhibitors. Bioorganic & Medicinal Chemistry, 24 (2016) 42-52.
128. A.A. Dreifuss, A.L. Bastos-Pereira, T.V. Avila, S. Soley Bda, A.J. Rivero, J.L. Aguilar, A. Acco. Anti-tumoral and anti-oxidant effects of a hydroalcoholic extract of cat's claw (Uncaria tomentosa) (Willd. Ex Roem. & Schult) in an in-vivo carcinosarcoma model. Journal of Ethnopharmacology, 130 (2010) 127-133.
129. T. Mammone, C. Akesson, D. Gan, V. Giampapa, R.W. Pero, A water soluble extract from *Uncaria tomentosa* (Cat's Claw) is a potent enhancer of DNA repair in primary organ cultures of human skin. Phytotherapy Research, 20 (2006) 178-183.
130. H. Guan, A.D. Laird, R.A. Blake, C. Tang, C. Liang. Design and synthesis of aminopropyl tetrahydroindole-based indolin-2-ones as selective and potent inhibitors of Src and Yes tyrosine kinase. Bioorganic & Medicinal Chemistry Letters, 14 (2004) 187-190.

131. M. Kaur, M. Singh, N. Chadha, O. Silakari, Oxindole: A chemical prism carrying plethora of therapeutic benefits. European Journal of Medicinal Chemistry, 123 (2016) 858-894.
132. R. Roskoski, Sunitinib: A VEGF and PDGF receptor protein kinase and angiogenesis inhibitor. Biochemical and Biophysical Research Communications, 356 (2007) 323-328.
133. https://www.clinicaltrials.gov/, accessed on 12 Nov. 2016.
134. C.R. Prakash, P. Theivendren, S. Raja, Indolin-2-ones in clinical trials as potential kinase inhibitors. Pharmacology & Pharmacy 3 (2012) 62-71.
135. R.F. Kauffman, D.W. Robertson, R.B. Franklin, G.E. Sandusky, F. Dies, J.L. McNay, J.S. Hayes, Indolidan: A potent, long-acting cardiotonic and inhibitor of type IV cyclic AMP phosphodiesterase. Cardiovascular Drug Reviews, 8 (1990) 303-322.
136. T. Bethke, D. Brunkhorst, H.V. der Leyen, W. Meyer, R. Nigbur, H. Scholz, Mechanism of action and cardiotonic activity of a new phosphodiesterase inhibitor, the benzimidazole derivative adibendan (BM 14.478), in guinea-pig hearts. Arch. Pharmacology, 337 (1988) 576-582.
137. S.S. Rindhe, B.K. Karale, R.C. Gupta, M.A. Rode, Synthesis, anti-microbial and anti-oxidant activity of some oxindoles. Indian Journal of Pharmaceutical Sciences, 73 (2011) 292-296.
138. N.G. Kandile, H.T. Zaky, M.I. Mohamed, H.M. Ismaeel, N.A. Ahmed, Synthesis, characterization and *in-vitro* anti-microbial evaluation of new compounds incorporating oxindole nucleus. Journal of Enzyme Inhibition and Medicinal Chemistry, 27 (2012) 599-608.
139. H. Singh, J. Sindhu, J.M. Khurana, C. Sharma, K.R. Aneja, Ultrasound promoted one pot synthesis of novel fluorescent triazolyl spirocyclic oxindoles using DBU based task specific ionic liquids and their anti-microbial activity. European Journal of Medicinal Chemistry, 77 (2014) 145-154.
140. G. Bhaskar, Y. Arun, C. Balachandran, C. Saikumar, P.T. Perumal, Synthesis of novel spirooxindole derivatives by one pot multicomponent reaction and their anti-microbial activity. European Journal of Medicinal Chemistry, 51 (2012) 79-91.
141. T. Jiang, K.L. Kuhen, K. Wolff, H. Yin, K. Bieza, J. Caldwell, B. Bursulaya, Design, synthesis and biological evaluations of novel oxindoles as HIV-1 non-nucleoside reverse transcriptase inhibitors. Part I. Bioorganic & Medicinal Chemistry Letters, 16 (2006) 2105-2108.
142. T. Jiang, K.L. Kuhen, K. Wolff, H. Yin, K. Bieza, J. Caldwell, B. Bursulaya, Design, synthesis and biological evaluations of novel oxindoles as HIV-1 non-nucleoside

reverse transcriptase inhibitors. Part II. Bioorganic & Medicinal Chemistry Letters, 16 (2006) 2109-2112.

143. M. Palomba, L. Rossi, L. Sancineto, E. Tramontano, A. Corona, L. Bagnoli, C. Santi, A new vinyl selenone-based domino approach to spirocyclopropyl oxindoles endowed with anti-HIV RT activity. Organic & Biomolecular Chemistry, 14 (2016) 2015-2024.
144. J.S. Wu, X. Zhang, Y.L. Zhang, J.W. Xie, Synthesis and anti-fungal activities of novel polyheterocyclic spirooxindole derivatives. Organic & Biomolecular Chemistry, 13 (2015) 4967-4975.
145. C. Yang, J. Li, R. Zhou, X. Chen, Y. Gao, Z. He, Facile synthesis of spirooxindole-pyrazolines and spirobenzofuranone-pyrazolines and their fungicidal activity. Organic & Biomolecular Chemistry, 1 (2015) 4869-4878.
146. S. Tiwaria, P. Pathaka, R. Sagarb, Efficient synthesis of new 2,3-dihydrooxazole-spirooxindoles hybrids as anti-microbial agents. Bioorganic & Medicinal Chemistry Letters, 26 (2016) 2513–2516.
147. M.S. Chande, R.S. Verma, P.A. Barve, R.R. Khanwelkar, R.B. Vaidya, K.B. Ajaikumar, Facile synthesis of active anti-tubercular, cytotoxic and anti-bacterial agents: a Michael addition approach. European Journal of Medicinal Chemistry, 40 (2005) 1143-1148.
148. R.R. Kumar, S. Perumal, P. Senthilkumar, P. Yogeeswari, D. Sriram, Discovery of anti-mycobacterial spiro-piperidin-4-ones: an atom economic, stereoselective synthesis and biological intervention. Journal of Medicinal Chemistry, 51 (2008) 5731-5735.
149. P. Prasanna, K. Balamurugan, S. Perumal, P. Yogeeswari, D. Sriram, A regio- and stereoselective 1,3-dipolar cycloaddition for the synthesis of novel spiro pyrrolothiazolyloxindoles and their anti-tubercular evaluation. European Journal of Medicinal Chemistry, 45 (2010) 5653-5661.
150. C. Mhiri, S. Boudriga, M. Askri, M. Knorr, D. Sriram, P. Yogeeswari, F. Nana, Design of novel dispirooxindolopyrrolidine and dispirooxindolopyrrolothiazole derivatives as potential anti-tubercular agents. Bioorganic & Medicinal Chemistry Letters, 25 (2015) 4308-4313.

CHAPTER 3

Objectives and Plan of Work

NNRTIs are an important class of anti-retroviral drugs which acts at the allosteric site of RT and subsequently inhibits its catalytic function. The major advantages of NNRTIs are that they specifically inhibit the viral reverse transcriptase without showing any effects on the host polymerases, further these do not show cross resistance with NRTIs [1]. NNRTIs are crucial components of Highly Active Anti-Retroviral Therapy (HAART), due to their high potency, low toxicity and good specificity. Unfortunately, the clinical effectiveness of NNRTIs, especially of the first generation (nevirapine, delavirdine and efavirenz) has been hampered due to continuous development of drug resistance [2]. Further, in recent clinical reports few strains of HIV-1 showed less sensitivity against second generation NNRTIs (etravirine and rilpivirine) also [3, 4]. So, all these factors compel the need for search of novel NNRTIs effective against drug sensitive as well as drugs resistance strains of RT with favourable pharmacokinetic profile.

People living with HIV/AIDS face major health threat due to their weak immune system, which makes them susceptible to numerous infections called “opportunistic infections”. Opportunistic infections are the most common cause of death among HIV/AIDS patients [5]. Such infections are predominantly caused by certain pathogens like virus, bacteria, fungus and protozoan etc, moreover, treatment of such infection among the HIV/AIDS patient is a challenging task [6, 7]. Furthermore, emerging drug resistance of above pathogens towards the currently available drugs and drug-drug interaction problems in multiple drug therapy, further drive the need for the search of new effective and safe drug [8]. Therefore, considering all the above factors, the following objectives were set for this dissertation work:

3.1. Objectives

To design, synthesize nitrogen containing heterocyclic compounds as novel NNRTIs and to evaluate their inhibitory potential against HIV-1 RT, HIV-1 and allied opportunistic bacterial including mycobacterial and fungal infections.

3.2. Plan of work

The plan of work is as follows:

3.2.1. Design of novel NNRTIs

Initially, twenty six nitrogen containing heterocyclic scaffolds (such as tetrahydroisoquinoline, tetrahydroquinoline, quinoline and piperazine) were designed as HIV-1 RT inhibitors by considering the required pharmacophoric features established from the literature reported potential hits. Further, five scaffolds containing oxindole nucleus were designed based upon the outcome of virtual screening studies [9]. Furthermore, all the above designed thirty one scaffolds were *in-silico* screened (via docking studies) against three strains of HIV-1 RT (one

wild and two mutant strains) and eleven scaffolds out of the above mentioned thirty one scaffolds were selected which exhibited significant *in-silico* inhibitory activity against all the three strains of HIV-1 RT. Finally, using the above selected eleven scaffolds, series of compounds were generated by making different substitutions.

In order to estimate the drug-likeness behavior of designed compounds, their physicochemical and pharmacokinetic parameters were *in-silico* predicted using three tools (Qik-prop, admetSAR and FAF-*Drugs*[3]). Different drug-likeness parameters predicted were; molecular weight, number of hydrogen bond donor groups, number of hydrogen bond acceptor groups, total solvent accessible surface area, number of rotatable bonds, octanol/water partition coefficient, aqueous solubility, apparent caco-2 cell permeability, brain/blood partition coefficient, acute oral toxicity and mutagenicity.

3.2.2. Synthesis of designed compounds

For the synthesis of target compounds, both conventional as well as non-conventional (microwave assisted) approaches were used. Several reaction conditions were evaluated for optimization of reaction and final optimized conditions were used for the synthesis of designed compounds. Synthesized compounds were further purified by various techniques like washing with suitable solvents, column chromatography and re-crystallization techniques as per requirement.

3.2.3. Characterization of synthesized compounds

Purified compounds were preliminarily characterized by physicochemical methods like melting point and thin layer chromatography to assess the purity of the compounds. The final structure of the compounds was further confirmed by spectral techniques like FTIR, ^{1}H NMR, ESI-MS and Elemental analysis.

3.2.4 Biological Activity

1. Synthesized compounds were *in-vitro* evaluated for HIV-1 RT inhibitory activity via colorimetric ELISA based assay.
2. Among the compounds screened against HIV-1 RT, four series of compounds displayed overall good to excellent RT inhibition activity. Three to four top active compounds from each of these series were selected and evaluated for anti-HIV-1 activity and cytotoxicity (against T cell lines).
3. Compounds were evaluated for *in-vitro* anti-bacterial activity against two Gram (-)ve negative (*Escherichia coli, Pseudomonas putida*) and two Gram (+)ve (*Staphylococcus aureus* and *Bacillus cereus*) strains.

4. The *in-vitro* anti-fungal activity of all compounds was evaluated against *Candida albicans* and *Aspergillus niger*.
5. Anti-tubercular activity of synthesized compounds was also evaluated against *Mycobacterium tuberculosis*.

3.2.5 Molecular docking studies

Docking studies were performed for the compounds which exhibited best and least inhibitory activity (from each series) during HIV-1 RT *in-vitro* assay in order to predict their putative binding modes as well as interaction pattern inside the NNIBP of HIV-1 RT.

3.3 References

1. M.P. de Bethune, Non-nucleoside reverse transcriptase inhibitors (NNRTIs), their discovery, development and use in the treatment of HIV-1 infection: A review of the last 20 years (1989-2009). Antiviral Research, 85 (2010) 75-90.
2. J. Ghosn, M.L. Chaix, C. Delaugerre, HIV-1 resistance to first and second generation non-nucleoside reverse transcriptase inhibitors. AIDS reviews, 11 (2009) 165-173.
3. E.L. Asahchop, M.A. Wainberg, R.D. Sloan, C.L. Tremblay, Antiviral drug resistance and the need for development of new HIV-1 reverse transcriptase inhibitors. Antimicrobial Agents and Chemotherapy, 56 (2012) 5000-5008.
4. K. Singh, B. Marchand, D.K. Rai, B. Sharma, E. Michailidis, E.M. Ryan, K.B. Matzek, Biochemical mechanism of HIV-1 resistance to rilpivirine. The Journal of Biological Chemistry, 287 (2012) 38110-38123.
5. M. Ghate, S. Deshpande, S. Tripathy, M. Nene, P. Gedam, S. Godbole, M. Thakar, Incidence of common opportunistic infections in HIV-infected individuals in Pune, India: Analysis by stages of immunosuppression represented by CD4 counts. International Journal of Infectious Diseases, 13 (2009) e1–e8.
6. F. Bonnet, C. Lewden, T. May, L. Heripret, E. Jougla, S. Bevilacqua, D. Costagliola, Opportunistic infections as causes of death in HIV-infected patients in the HAART era in France. Scandinavian Journal of Infectious Diseases, 37 (2005) 482–487.
7. M.A. Fischbach, C.T. Walsh, Antibiotics for emerging pathogens. Science, 325 (2009) 1089-1093.
8. C.A. Hughes, A. Tseng, R. Cooper, Managing drug interactions in HIV-infected adults with co-morbid illness. Canadian Medical Association Journal, 187 (2015) 36-43.
9. S. Chander, A. Penta, S. Murugesan, Structure-based virtual screening and docking studies for the identification of novel inhibitors against wild and drug resistance strains of HIV-1 RT. Medicinal Chemistry Research, 24 (2015) 1869-1883.

CHAPTER 4

Design and Prediction of Drug-likeness Properties

CHAPTER 4

Design and Prediction of Drug-likeness Properties

4.1 Design of HIV-1 RT inhibitors

The success of anti-HIV drug discovery is certainly based upon the fact that, HIV life cycle has been deeply investigated and several of its crucial steps have been validated as drug targets, subsequently, many potential inhibitors have been developed against some of these targets [1]. Reverse Transcriptase (RT) is one among the various HIV targets which has been deeply characterized due to its key role in viral replication. NNRTIs are key components of HAART, due to their high potency, low toxicity and high selectivity [2]. Nevertheless, like other anti-HIV drugs, resistance to NNRTIs arises as a result of mutations that affect their effective binding with target RT enzyme, subsequently allows HIV genome replication in an unrestricted manner. The specific mutations associated with resistance to NNRTIs correlate with amino acid changes in the pocket where NNRTIs preferentially bind [3]. Although, after the advent of HAART, a multidrug therapy, highly fatal AIDS became a chronic manageable disease, but still its management is complex and worrisome due to associated problems like development of drug resistance, monitoring of therapy, efficacy and poor drug tolerability [4]. Therefore, there is a compelling need for the search of novel anti-HIV drugs possessing favorable safety profile, improved potency and active against both wild as well as drug resistance strains of HIV-1.

NNRTIs inhibits the activity of RT by binding at the allosteric site, also known as Non Nucleoside Inhibitory Binding Pocket (NNIBP), which is located about 10 A˚ away from the DNA polymerase catalytic site of HIV-1 RT [5]. NNIBP is basically a hydrophobic pocket, surrounded by hydrophobic amino acids like Y181, Y188, W229, F227, V106, P236, L100, L234 and Y318 while the rim of NNIBP contains hydrophilic amino acids like K101 and K103 [6, 7]. Several mutations in the NNIBP are frequently observed and subsequently responsible for the emergence of drug resistance against available NNRTIs. For example, mutations like Y181C and Y188L generally result in loss or reduction of key hydrophobic interactions of the inhibitor at the NNIBP, other mutations like L100I and V106A generally creates steric hindrance at the central region of the NNIBP affecting the stability of inhibitor inside the pocket. Further, amino acid substitutions occur at the rim of NNIBP like K101E and K103N, may interfere with entry of inhibitors [8]. Compared to second generation NNRTIs (rilpivirine and etravirine), first generation NNRTIs (nevirapine, delavirdine and efavirenz) showed low genetic barrier to resistance, for example, single mutation like K103N confers high resistance around eighteen, forty and twenty eight fold to efavirenz, nevirapine and delavirdine, respectively [9,10]. Furthermore, two mutant strains of RT (K103N and K103N/Y181C) are frequently observed clinically in patients on NNRTIs therapy and responsible for high-level phenotypic resistance against available NNRTIs. HIV-1 RT strain having a dual mutation of K103N and Y181C inside the NNIBP of HIV RT exhibits the high

level of resistance against first generation NNRTIs, moreover their susceptibility also reduces towards second generation NNRTIs [11]. The availability of crystal structures of HIV-1 RT, the discovery of potent NNRTIs as well as information of mutations responsible for drug resistance can be taken basis for the discovery of novel ligands active against wild as well as drug resistance strains of RT.

Although, NNRTIs are structurally diverse group of compounds; still they possessed numerous ubiquitous fragments in their structures and possess a common pharmacophoric model. This model at one terminal includes an aromatic ring able to participate in *pi-pi* stacking interactions with RT, connected to linker generally having amide or thio-amide moieties capable of hydrogen bonding and at second terminal one or more hydrocarbon-rich domain that participate in hydrophobic interactions [12]. In chapter **2**, (Review of Literature) pharmacological potential of various heterocyclic moieties containing nuclei like tetrahydroisoquinoline, tetrahydroquinoline, quinoline, piperazine and oxindole were discussed with main emphasizing on their activity against the pathogenic organisms. In the present dissertation, attempts were made to design novel NNRTIs against wild as well resistant strains of HIV-1 RT using rational drug design approach (including both ligand as well as structure based).

4.1.1 Ligand based design of novel NNRTIs

In the first phase, heterocyclic moieties containing THIQ nucleus were designed as inhibitors of HIV-1 RT. In this direction, for the design of novel NNRTIs, crucial pharmacophoric features were taken from the literature reported NNRTIs (Fig. **4.1**) having potent anti-HIV-1 RT activity (IC_{50}: low micromolar to nanomolar) like nevirapine, efavirenz, loviride [13], R00943 (14), **A, B** [15] and **C** [16]. As shown in Fig. **4.1**, despite the structural diversity of NNRTIs, these shared the pharmacophoric similarity like all possessed aromatic or heterocyclic moieties at opposite terminals as hydrophobic wings (blue dotted lines) connected via a hydrophilic linker (red color portion with red dotted lines). Inspired by these findings, we planned to generate a library of compounds containing 6,7-dimethoxy tetrahydroisoquinoline nucleus as one hydrophobic wing and phenyl with different substitutions as second wing, connecting via different hydrophilic linkers (Fig. **4.2**). Rationality for taking 6,7-dimethoxy substituted tetrahydroisoquinoline nucleus in designed ligands was that methoxy group constitutes methyl as non-polar head and oxygen as polar heteroatom, former group (methyl) may participate in hydrophobic interactions with hydrophobic residues of NNIBP, while oxygen imparts hydrophilic property to the designed ligand.

Subsequently, based upon the above concept, a series of compounds (**THIQ-A-I**) was generated as NNRTIs, while considering their synthetic feasibility, novelty and pharmacophoric requirement.

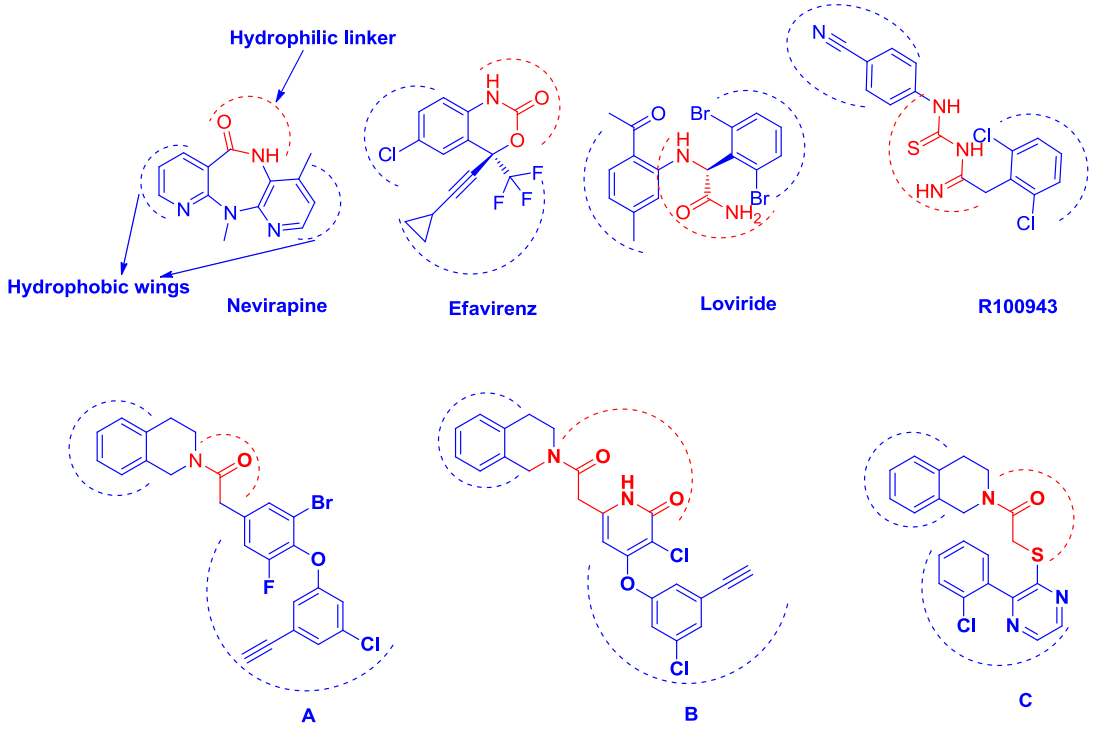

Fig. 4.1 Structure of some reported potential inhibitors of HIV-1 RT

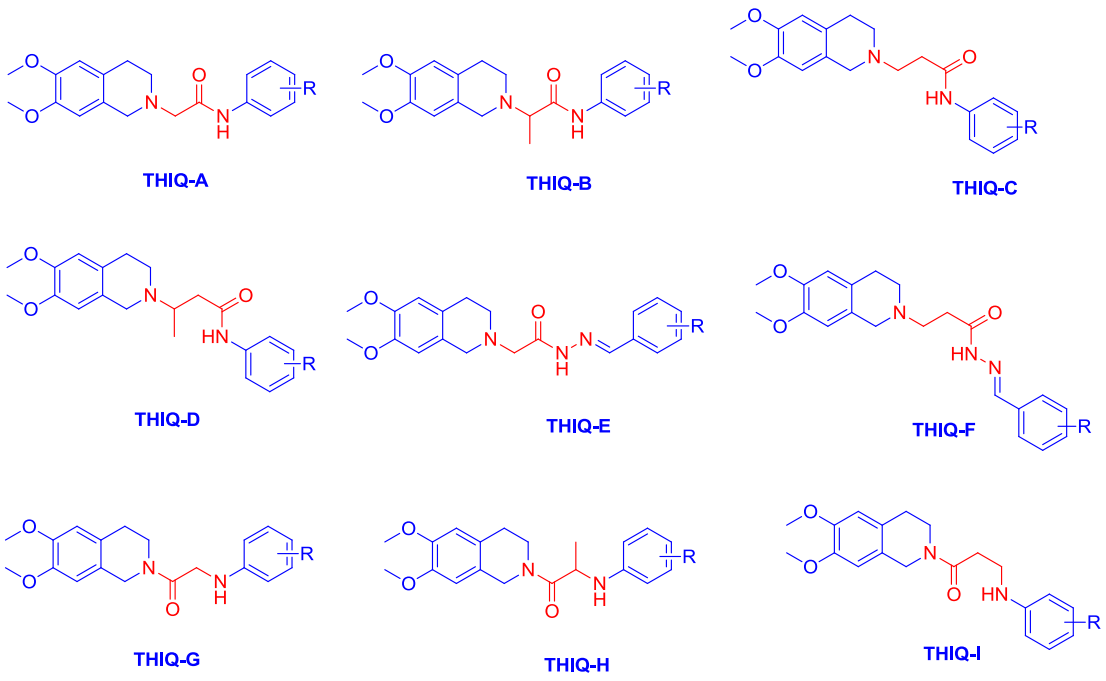

Fig. 4.2 Structure of designed THIQ prototype compound as inhibitors of HIV-1 RT

Similarly, in the second phase of designing, heterocyclic moieties containing THQ and quinoline nucleus were designed as HIV-1 RT inhibitors using pharmacophoric features from literature reported (Fig. **4.3**) potent RT inhibitors like **D** [12], **E** [17], **F**, **G** [18], **H** [19] and **I** [20]. Like earlier discussed compounds (Fig. **4.1**), reported compounds **D** to **I** (Fig. **4.3**) also shared similar pharmacophoric features, which includes aromatic or heterocyclic moieties at opposite terminals connected via a hydrophilic linker. Using this approach, virtual library of compounds was generated (**THQ-A-I**, **Q-A**, and **Q-B** Fig. **4.4**) while considering their synthetic feasibility, novelty and pharmacophoric requirement.

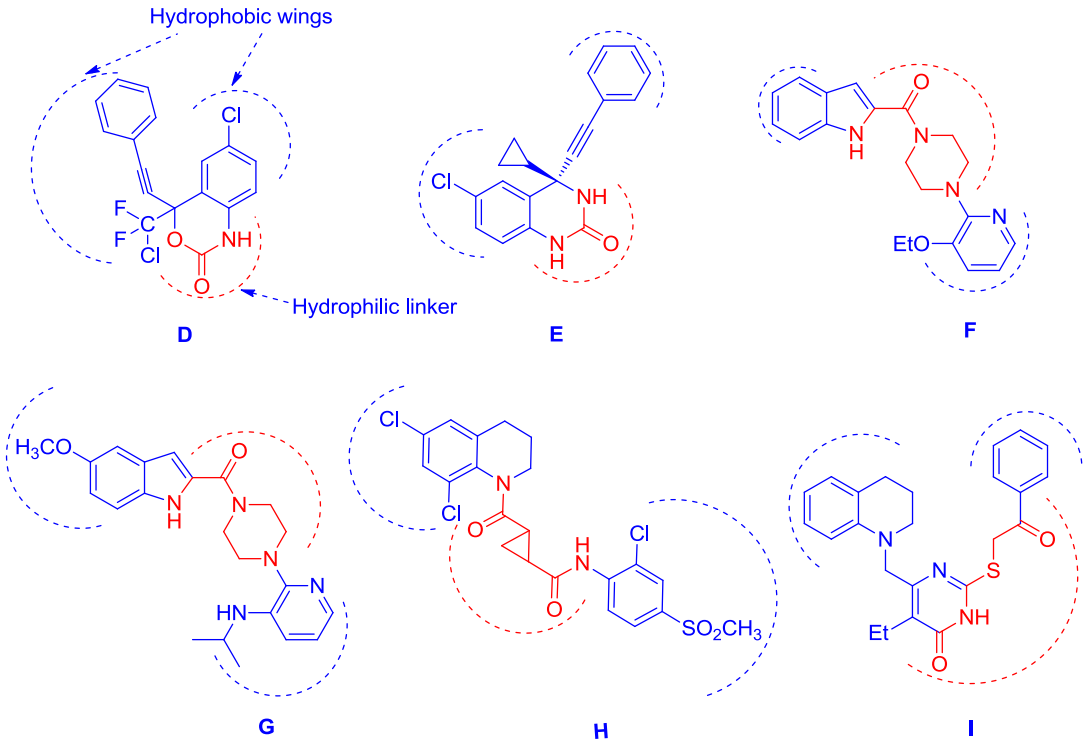

Fig. 4.3 Structure of some reported potential HIV-1 RT inhibitors

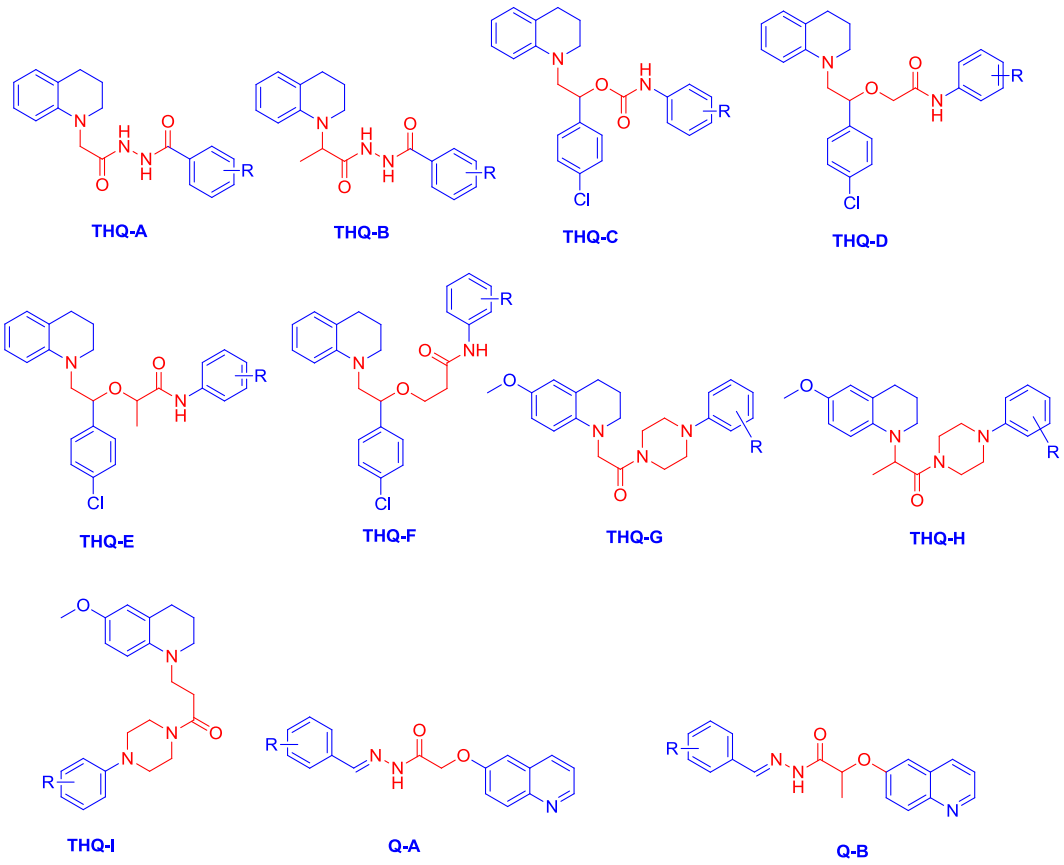

Fig. 4.4 Structure of designed prototype (**THQ-A** to **I**, **Q-A** to **Q-B**) compounds as inhibitors of HIV-1 RT

4.1.2 Design of HIV-1 RT inhibitors by molecular hybridization technique

Molecular hybridization is a rational approach to design novel ligands against a specific target, which involves the combination of two or more pharmacophoric subunits of known bioactive moieties [21, 22]. Similar approach has been successfully utilized for the search of potent HIV-1 RT inhibitors [23, 24]. Several literature reports revealed that, compounds containing diaryl alkylidene **J** [25], diarylmethane **K** [26] and diaryl ethers **L** [15] are known for the potent inhibition of HIV-1 RT (Green colour highlight, Fig. **4.5**). In the present study, biaryl amines as bioisosteres of above mentioned moieties (alkylidene, diarylmethane and diaryl ethers) was attached with 1-(4-phenylpiperazin-1-yl)ethanone (Coral colour highlight, Fig. **4.5**) a bioisosteres component of compound **G** (already reported for RT inhibition) [18] in order to design novel pharmacophore. Using this approach, six hybrid prototype molecules (**BBA-A** to **F**) were designed as inhibitors of HIV-1 RT.

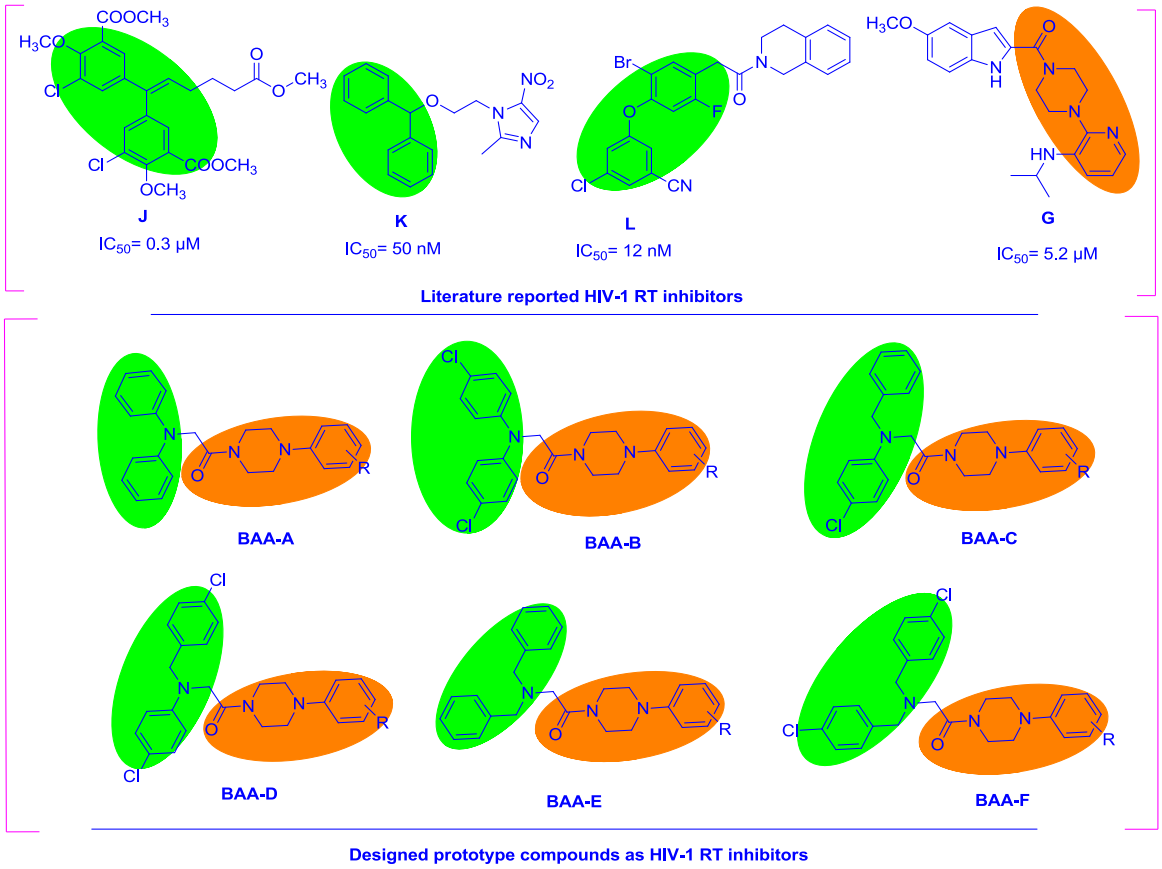

Fig. 4.5 Structure of reported HIV-1 RT inhibitors (**J** to **G**) and designed hybrid prototype compounds (**BBA-A** to **F**)

4.1.3 Design of HIV-1 RT inhibitors by *in-silico* based lead optimization studies

In computational studies, using structure-based virtual screening on Maybridge database, we shortlisted nine potential hits which exhibited significant *in-silico* activity against three strains of HIV-1 RT (one wild (PDB ID: 4G1Q) and two mutant strains (PDB ID: 3TAM and 4I2Q) [27]. Further, based upon the desired interaction pattern, pharmacophoric requirement and synthetic feasibility, we selected hit **MB** (Fig. **4.6**) for further studies. Selected hit **MB** possessed bromo at the 5th position of indolin-2-one nucleus, which provoked our interest to explore the compounds for anti-HIV-1 RT potential which containing different halogens like fluoro, chloro and iodo at the 5th position of indolin-2-one. For comparison scaffold without halogen substitution was also incorporated in the study. Overall, five prototype scaffolds were designed as NNRTIs with or without halogens at the 5th position of indolin-2-one, while keeping the phenyl ring reserved for different substitutions (**MB-A-E,** Fig. **4.6**).

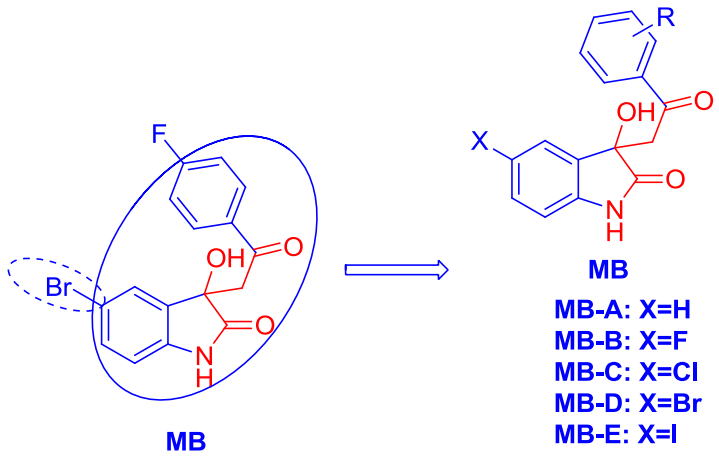

Fig. 4.6 Selected hit **MB** and designed prototype scaffolds **MB-A** to **E**

4.1.4 *In-silico* screening of the designed scaffolds using docking studies

Using different drug design approaches like ligand based, molecular hybridization, virtual screening, thirty one (**THIQ-A** to **I**, **THQ-A** to **I**, **Q-A** to **B**, **BAA-A** to **F**, **MB-A** to **E**) scaffolds were generated. In the next step, designed thirty one scaffolds were evaluated for their *in-silico* inhibitory activity against one wild (3MEE) and two mutant strains (3TAM and 4I2Q) of HIV RT. Docking studies were performed using the core nucleus (without any substitution, R=H) of designed scaffolds. Parameters considered while selection of different RT strains for the *in-silico* studies were; type of mutation involved, drug resistance profile and their clinical abundance.

Among the patients administered with NNRTIs therapy, two mutant RT strains; K103N and K103N/Y181C are frequently observed clinically [11]. Single mutation K103N in HIV-1 RT generally reduces its sensitivity towards the first line drugs (especially efavirenz), while dual mutation (K103N/Y181C) generally confer high resistance against all first line drugs and it also reduces the potency of second line drug especially etravirine [28]. Fortunately, the crystal structures of the above mentioned mutant HIV-1 RT strains (K103N and K103N/Y181C) as well as wild strain are available at protein data bank (PDB ID: 3TAM, 4I2Q and 3MEE respectively). So, in order to *in-silico* evaluate the potency of the designed scaffolds against drug sensitive and drugs resistant strains of HIV-1 RT, docking studies were performed using rilpivirine as the reference compound.

4.1.4.1 Docking studies: Experimental and Protocol

Docking studies of thirty one core scaffolds (Table **4.1**) along with reference compound rilpivirine were performed using Glide 5.9 in 'Extra Precision' mode [29], running on maestro version 9.4. The enzyme used for the docking studies were wild HIV-1 RT (PDB ID: 3MEE), and mutant strains involved are K103N (PDB ID: 3TAM) and K103N/Y181C mutations (PDB ID: 4I2Q). All three selected proteins were retrieved from Protein Data Bank (RCSB) in

complex with their co-crystallized ligands. Protein preparation wizard of Schrödinger suite was used for the preparation of selected proteins. Proteins were pre-processed separately by deleting the substrate co-factor as well as the crystallographically observed water molecules (water without H bonds), followed by optimization of hydrogen bonds. After assigning charge and protonation states, finally energy was minimized with root mean square deviation (RMSD) value of 0.30 Å using Optimized Potentials for Liquid Simulations-2005 (OPLS-2005) force field [30]. Finally, energy minimized proteins and co-crystallized ligands were employed to build energy grids using the default value of protein atom scaling (1.0 Å) within a cubic box centered on the centroid of the X-ray ligand poses. The structure of designed ligands and rilpivirine was drawn using ChemSketch and converted to 3D with the help of 3D optimization tool. By using LigPrep 2.6 module [31], the drawn ligands were geometry optimized; partial atomic charges were computed using OPLS-2005 force field. Finally, 32 poses were included with different tautomeric and steric features for docking studies. RMSD values were calculated between the experimental binding mode of co-crystallized ligands and their re-docked poses in their respective proteins to ensure accuracy and reliability of the docking procedure. Finally, prepared ligands were docked with prepared proteins using Glide 5.9 module in extra precision mode (XP). The binding affinity of tested ligands with respective targets was estimated in terms of XP score.

4.1.4.2 Analysis of docking results and selection of scaffolds for further studies

The value of RMSD obtained between experimental binding mode as in X-ray and re-docked poses of co-crystallized ligands of three proteins (3MEE, 3TAM and 4I2Q) were found to be 0.6, 1.1 and 0.9 Å respectively. So, overall validation studies demonstrated that, docking procedure could be relied on for further docking studies. Superimposed view of rilpivirine X-ray pose and its re-docked pose in 3MEE is shown in Fig. **4.7** as one of representative.

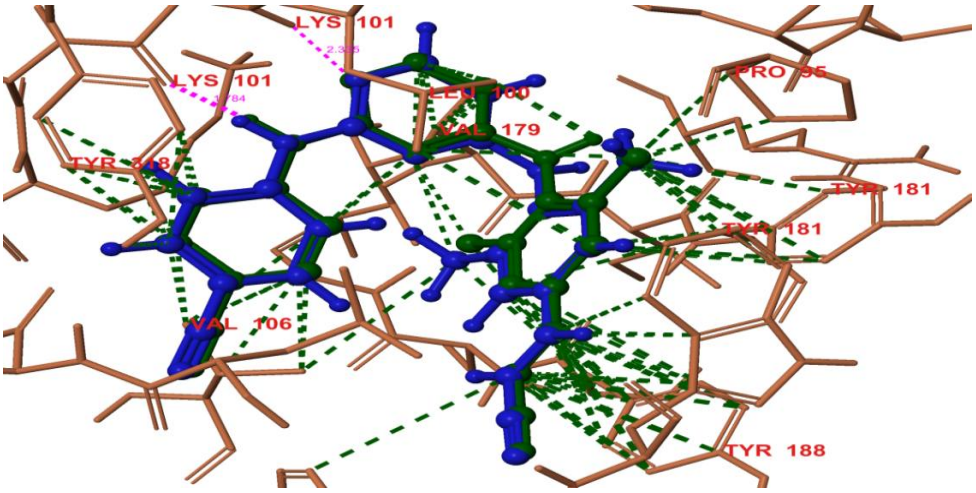

Fig. 4.7 Superimposed view of best scoring pose of rilpivirine (blue) with its X-ray pose (green) inside the NNIBP of 3MEE

The results of the docking studies are shown in Table **4.1,** in terms of XP score, basically, it revealed the *in-silico* binding affinities between the ligand and receptor, in general, more is the value of XP score (in negative terms), greater will be the binding affinities between the tested molecules. In docking studies, compounds which exhibited Glide XP score ≥ 80% (in negative terms) of the reference drug rilpivirine against the respective targets were considered significantly active. For example, rilpivirine exhibited XP score -14.32, -11.83 and -11.36 against 3MEE, 3TAM and 4I2Q respectively, so cut off XP score threshold set for a compound to be significantly active were -11.45, -9.46 and -9.08 respectively, for the three selected targets.

In the study, designed compounds which exhibited XP score equal or more than the set threshold are highlighted by bold fonts in Table **4.1**. Furthermore, scaffolds which exhibited significant *in-silico* activity against all three selected strains (compounds **THIQ-A, THIQ-B, THIQ-E, THIQ-G, THQ-B, THQ-C, THQ-D, THQ-I, Q-B, BBA-C** and **MB-C**) were selected for further studies.

Table 4.1 Glide XP scores of the designed prototype ligands

Scaffold	XP score (3MEE)	XP score (3TAM)	XP score (4I2Q)
THIQ-A	**-13.24**	**-10.94**	**-10.13**
THIQ-B	**-12.92**	**-11.17**	**-10.62**
THIQ-C	**-12.12**	**-10.57**	-8.09
THIQ-D	**-12.42**	-9.26	-8.71
THIQ-E	**-11.74**	**-11.87**	**-10.11**
THIQ-F	-9.39	**-10.05**	-8.37
THIQ-G	**-13.32**	**-10.31**	**-11.12**
THIQ-H	-10.69	-9.42	-8.20
THIQ-I	**-11.87**	-7.99	-8.53
THQ-A	-**11.93**	**-11.05**	-8.18
THQ-B	**-12.19**	**-11.94**	**-10.04**
THQ-C	**-13.76**	**-10.95**	**-11.21**
THQ-D	**-11.87**	**-10.86**	**-10.89**
THQ-E	-11.12	**-10.89**	**-9.42**
THQ-F	-9.63	-8.54	**-10.14**
THQ-G	**-11.72**	-7.63	-7.59
THQ-H	**-11.98**	-7.87	-8.12
THQ-I	**-12.22**	**-9.49**	**-9.24**
Q-A	-10.72	-9.32	-**9.28**
Q-B	**-11.91**	**10.15**	-**9.97**
BBA-A	-11.31	**-9.69**	-8.87
BBA-B	**-12.21**	**-9.88**	**-10.18**
BBA-C	**-12.08**	**-10.18**	**-9.68**
BBA-D	-10.47	-9.22	**-9.23**
BBA-E	-11.17	**-9.83**	-7.41
BBA-F	-9.81	-8.47	-8.34
MB-A	**-11.63**	-8.88	**-10.18**
MB-B	**-12.39**	-9.05	**-9.36**
MB-C	**-13.28**	**-11.49**	**-10.18**
MB-D	**-13.07**	**-10.29**	-8.96
MB-E	-**11.53**	-9.17	-8.19
Rilpivirine	**-14.32**	**-11.83**	**-11.36**
Cut off value	**-11.45**	**-9.46**	**-9.08**

So, based upon the results of *in-silico* studies, scaffolds **THIQ-A, THIQ-B, THIQ-E, THIQ-G, THQ-B, THQ-C, THQ-D, THQ-I, Q-B, BAA-C** and **MB-C** were found to be *in-silico* active against all three tested strains of HIV-1 RT, so these were selected for further generation of series of compounds. Considering the selected compounds as core nucleus, series of compounds were generated by making different substitutions with different functionalities like methyl, methoxy, fluoro, chloro, bromo, nitro and cyano etc at different position of phenyl

ring. Rationality for substitution with different above mentioned functionalities was to expand the diversity of the core scaffolds, each selected substituent impose a unique effect on the ring system, for example, methyl and methoxy groups exhibit weak and strong electron donating effect, respectively, while halogens like fluoro, chloro and bromo are overall weak electron withdrawing in nature (due to simultaneous inductive and mesomeric effect). In addition to this, substitutions like nitro and cyano are strong electron withdrawing in nature and act as strong ring deactivator. Therefore, diverse type of substituents at different positions of phenyl ring imparts variance in the physico-chemical properties of the designed ligands, which can be helpful to establish the SAR studies.

Furthermore, in some series particularly based upon core compounds **THQ-B, THQ-I** and **BAA-C,** apart from the substituted phenyl rings some extra bioisosteres of phenyl like pyridine, benzyl etc were also generated to expand the diversity of compounds. Finally, series of compounds **5a-o, 9a-o, 14a-k, 17a-o, 23a-o, 28a-l, 32a-n, 38a-o, 43a-p, 51a-n** and **54a-k** were generated based upon the shortlisted core nucleus **THIQ-A, THIQ-B, THIQ-E, THIQ-G, THQ-B, THQ-C, THQ-D, THQ-I, Q-B, BAA-C** and **MB-C,** respectively (Fig. **4.8**)**.**

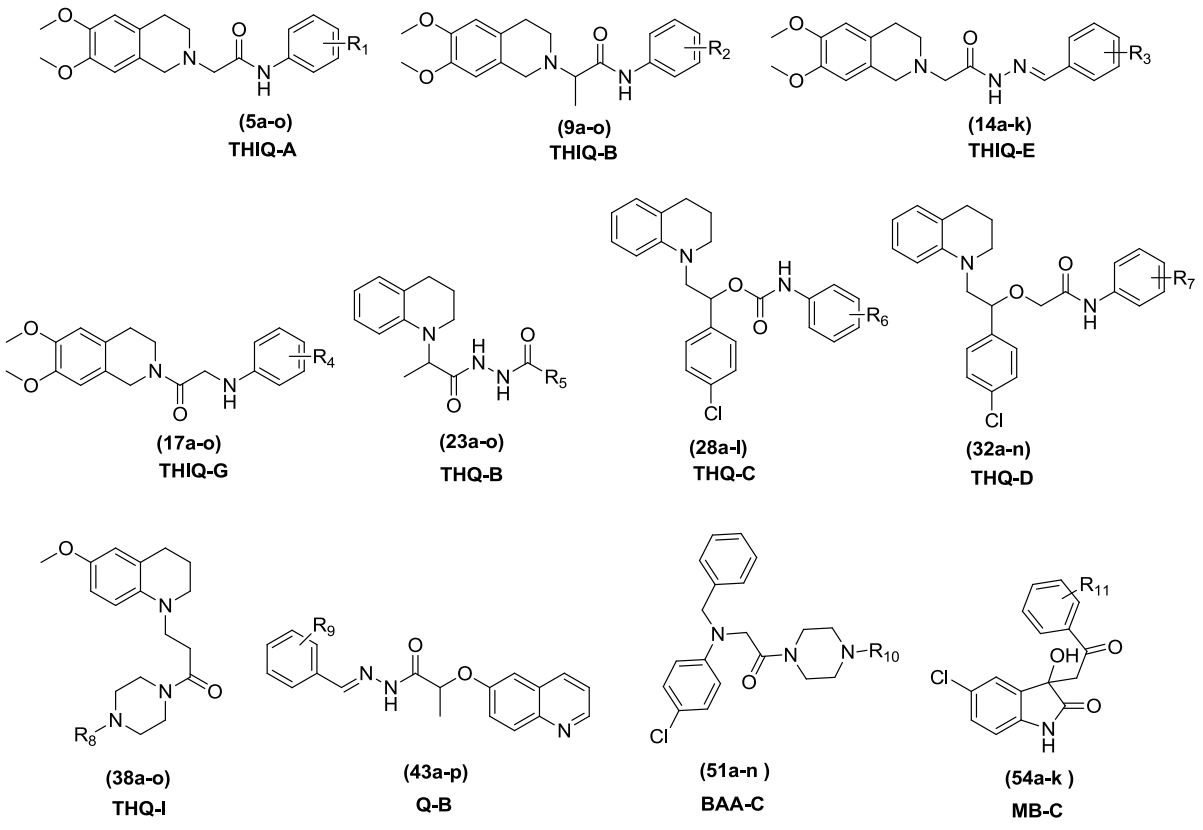

Fig. 4.8 Scaffolds shortlisted after docking studies and generated series of compounds

4.2 *In-silico* prediction of drug-likeness properties

Physicochemical and pharmacokinetic (Absorption, Distribution, Metabolism, Excretion and Toxicity, abbreviated as ADMET) properties play very crucial role in the discovery and development of new drugs. Currently available drugs in the market possess a balance of desirable ADMET properties and intrinsic potency [32]. Moreover, calculation of ADMET of all new compounds using *in-vivo* model is very challenging, time consuming and costly task. In order to predict the drug-likeness behavior of the designed compounds, their physicochemical and ADMET properties were *in-silico* predicted using three different tools; Qik-prop module of Schrödinger [33], admetSAR [34] and FAF-*Drugs*^{3} [35].

Different parameters generated for the prediction of physicochemical and ADMET properties were; molecular weight (Mol wt), total solvent accessible surface area (SASA), number of hydrogen bond donor groups (HBD), number of hydrogen bond acceptor groups (HBA), octanol/water partition coefficient (logP), aqueous solubility (logS), apparent caco-2 cell permeability (PCaco), brain/blood partition coefficient (log BB), number of rotatable bonds (Rot) and oral acute toxicity (acute tox).

Molecular weight and SASA are important parameters which influence the membrane diffusion and permeability of a compound. Generally, molecular weight is directly proportional to the molecular size of the compound [36]. Hydrogen-bonds play an important role in binding of ligand with receptor and also in determining the specificity of ligand. However, increase in the no. of hydrogen bond donor groups or hydrogen bond acceptor groups in ligand, may adversely affect the specificity of the ligand [37].

LogP is a crucial parameter which decides the lipophilicity of the molecule and also plays an important role in membrane permeability. Very high as well as very low LogP values of ligand negatively affect its membrane permeability; generally compound with high logP values possessed poor aqueous solubility. Furthermore, parameters like PCaco represents apparent Caco-2 cell permeability in nm/sec, which correlates with permeability of compound across the membrane of gut cell wall. Parameters like logBB gives an idea regarding the relative bio-distribution of compound in brain and plasma. Rotatable bonds in a molecule specify about the non-ring single bond attached to non-hydrogen atoms, no. of rotatable bonds of ligand also influence their ADMET profile [38]. Designed compounds were *in-silico* evaluated for oral acute toxicity and carcinogenicity (in qualitative terms).

Optimum range of drug-likeness parameters followed by 95% of approved drug molecules are given in the Table **4.2** [39] while their predicted values are summarized in Tables **4.3-4.13**, (except Mol. Wt. which is shown in Tables **5.1-5.3, 5.5-5.11** and **5.13**). Values of descriptors which exceeded the prescribed optimum range are highlighted by bold fonts.

Table 4.2 Optimum range of physicochemical and ADMET parameters

S. No	Molecular descriptor	Optimum range
1	Molecular weight (Mol wt)	130 to 725
2	Total solvent accessible surface area in square angstroms (SASA)	300 to1000
3	No. of hydrogen bond donor groups (HBD)	0 to 6
4	No. of hydrogen bond acceptor groups (HBA)	2 to 20
5	Octanol/water partition coefficient (logP)	-2 to 6.5
6	Aqueous solubility, in mol dm^{-3} (logS)	-6.5 to 0.5
7	Brain/blood partition coefficient (logBB)	-3.0 to1.2
8	No. of rotatable bonds (Rot)	0 to 15
9	Caco-2 cell permeability in nm/sec (PCaco)	<25 poor, >500 great

The predicted values of parameters like Mol Wt, SASA, HBD and HBA were found within their optimum range for all series of compounds. Predicted logP values of all compounds also lied within the optimum range of drug-likeness, although majority of compounds of series **28a-l, 31a-n** and **51a-n** displayed the high value of predicted logP (>5), which revealed that, compounds of these series might be overall more hydrophobic in nature as compared to the compounds of other series. Furthermore, majority of designed compounds displayed the predicted logS value within the optimum range, although compounds like **28d**, **28l** and **51n** exhibited low value of logS (highlighted by bold fonts) than the optimum range, but predicted logS value deviated by a very small margin from the optimum range, which might not change their ADMET properties much significantly. So, considering these facts three compounds (**28d**, **28l** and **51n**) were also included and preceded for further studies.

Compounds having substitution with functionalities like nitro and cyano exhibited moderate Caco-2 cell permeability (<500 nm/sec), while rest of the compounds displayed excellent Caco-2 cell permeability with predicted value >500 nm/sec, moreover value >500 nm/sec is generally considered desirable for druggability [39]. Values of parameters like logBB and Rot were also found within the optimum range. Based upon the predicted value of acute oral toxicity, all the designed compounds lied in class III, which means predicted LD_{50} of these compounds lied in ranges between 0.5-5 g/Kg, which can be considered suitable for druggability point of view [34]. Carcinogenicity of all compounds were predicted in qualitative terms, interestingly all compounds were found to be non-carcinogenic. So, overall based upon the predicted drug-likeness parameters, the designed compounds were found to be possessed drug-likeness behaviour and can be preceded further for synthesis and other studies.

Table 4.3 *In-silico* predicted drug-likeness parameters of compounds **5a-o**

Com. Code	SASA[a]	HBD[b]	HBA[c]	logP	logS	PCaco[d]	logBB[e]	Rot[f]	Acute tox[g]
5a	640.08	1	5	3.16	-3.71	873.02	0.17	5	class III
5b	648.12	1	5	3.38	-3.85	951.82	0.22	5	class III
5c	672.67	1	5	3.47	-4.28	869.92	0.16	5	class III
5d	670.73	1	5	3.47	-4.25	888.45	0.17	5	class III
5e	673.05	1	6	3.25	-3.84	922.54	0.13	6	class III
5f	674.76	1	6	3.24	-3.87	884.91	0.11	6	class III
5g	647.40	1	5	3.39	-4.04	884.99	0.29	5	class III
5h	633.15	1	5	3.41	-3.75	895.09	0.30	5	class III
5i	662.52	1	5	3.65	-4.41	887.14	0.35	5	class III
5j	662.34	1	5	3.65	-4.41	887.67	0.35	5	class III
5k	677.08	1	8	2.45	-3.82	105.78	-0.92	6	class III
5l	690.63	1	5	4.14	-5.11	886.48	0.45	5	class III
5m	667.55	1	5	3.70	-4.19	1119.43	0.30	5	class III
5n	694.07	1	5	3.74	-4.66	886.85	0.16	5	class III
5o	683.35	1	5	3.98	-4.78	1030.68	0.42	5	class III

[a]Solvent accessible surface area, [b]No. of hydrogen bond donors, [c]No. of hydrogen bond acceptors, [d]Predicted apparent Caco-2 cell permeability, [e]Predicted brain/blood partition coefficient, [f]No. of rotatable bonds, [g]Acute oral toxicity

Table 4.4 *In-silico* predicted drug-likeness parameters of compounds **9a-o**

Com. Code	SASA[a]	HBD[b]	HBA[c]	logP	logS	PCaco[d]	logBB[e]	Rot[f]	Acute tox[g]
9a	661.85	1	5	3.57	-4.09	1196.69	0.32	5	class III
9b	668.66	1	5	3.76	-4.21	1201.46	0.33	5	class III
9c	679.98	1	5	3.78	-4.41	1168.67	0.31	5	class III
9d	679.80	1	5	3.78	-4.41	1167.44	0.31	5	class III
9e	683.04	1	6	3.57	-4.02	1215.41	0.27	6	class III
9f	684.45	1	6	3.55	-4.04	1161.95	0.24	6	class III
9g	656.62	1	5	3.70	-4.20	1162.82	0.43	5	class III
9h	640.69	1	5	3.69	-3.90	1071.75	0.40	5	class III
9i	671.49	1	5	3.96	-4.57	1161.55	0.48	5	class III
9j	671.49	1	5	3.96	-4.57	1161.74	0.48	5	class III
9k	649.65	1	5	4.03	-4.19	1228.43	0.53	5	class III
9l	698.71	1	5	4.44	-5.25	1162.95	0.59	5	class III
9m	685.37	1	8	2.75	-3.96	138.81	-0.77	6	class III
9n	686.62	1	5	3.94	-4.53	1064.01	0.27	5	class III
9o	694.78	1	5	3.97	-4.67	1073.07	0.27	5	class III

[a]Solvent accessible surface area, [b]No. of hydrogen bond donors, [c]No. of hydrogen bond acceptors, [d]Predicted apparent Caco-2 cell permeability, [e]Predicted brain/blood partition coefficient, [f]No. of rotatable bonds, [g]Acute oral toxicity

Table 4.5 *In-silico* predicted drug-likeness parameters of compounds **14a-k**

Com. Code	SASA[a]	HBD[b]	HBA[c]	logP	logS	PCaco[d]	logBB[e]	Rot[f]	Acute tox[g]
14a	725.43	1	6	3.94	-4.89	599.01	-0.18	7	class III
14b	735.04	1	7	3.75	-4.59	599.61	-0.24	8	class III
14c	735.40	1	7	3.75	-4.60	599.46	-0.24	8	class III
14d	709.64	1	6	3.90	-4.80	592.74	-0.07	7	class III
14e	714.00	1	6	4.10	-4.85	690.70	0.03	7	class III
14f	724.69	1	6	4.16	-5.13	592.83	-0.01	7	class III
14g	729.24	1	6	4.24	-5.29	595.70	0.00	7	class III
14h	727.23	1	6	4.24	-5.26	599.74	0.01	7	class III
14i	736.38	1	9	2.95	-4.53	72.01	-1.33	8	class III
14j	736.51	1	7	2.90	-5.34	124.47	-1.06	8	class III
14k	806.75	1	9	3.95	-4.96	594.41	-0.39	10	class III

[a]Solvent accessible surface area, [b]No. of hydrogen bond donors, [c]No. of hydrogen bond acceptors, [d]Predicted apparent Caco-2 cell permeability, [e]Predicted brain/blood partition coefficient, [f]No. of rotatable bonds, [g]Acute oral toxicity

Table 4.6 *In-silico* predicted drug-likeness parameters of compounds **17a-o**

Com. Code	SASA[a]	HBD[b]	HBA[c]	logP	logS	PCaco[d]	logBB[e]	Rot[f]	Acute tox[g]
17a	677.02	1	6	3.35	-4.37	1944.68	-0.33	6	class III
17b	675.73	1	6	3.30	-4.32	1775.94	-0.36	6	class III
17c	675.85	1	6	3.30	-4.33	1774.45	-0.36	6	class III
17d	647.59	1	5	3.45	-4.48	1775.06	-0.18	5	class III
17e	647.61	1	5	3.45	-4.48	1775.62	-0.18	5	class III
17f	651.56	1	5	3.61	-4.69	1942.39	-0.14	5	class III
17g	662.73	1	5	3.71	-4.85	1774.83	-0.13	5	class III
17h	662.91	1	5	3.71	-4.85	1775.66	-0.13	5	class III
17i	654.16	1	5	3.68	-4.78	2005.25	-0.12	5	class III
17j	667.70	1	5	3.78	-4.96	1775.12	-0.12	5	class III
17k	667.74	1	5	3.78	-4.96	1775.51	-0.11	5	class III
17l	676.75	1	6	2.45	-5.06	368.53	-1.14	6	class III
17m	702.12	1	6	2.68	-4.31	566.50	-0.94	6	class III
17n	690.61	1	5	4.20	-5.55	1776.93	-0.03	5	class III
17o	695.91	1	5	3.88	-5.24	2363.77	-0.20	5	class III

[a]Solvent accessible surface area, [b]No. of hydrogen bond donors, [c]No. of hydrogen bond acceptors, [d]Predicted apparent Caco-2 cell permeability, [e]Predicted brain/blood partition coefficient, [f]No. of rotatable bonds, [g]Acute oral toxicity

Table 4.7 *In-silico* predicted drug-likeness parameters of compounds **23a-o**

Com. Code	SASA[a]	HBD[b]	HBA[c]	logP	logS	PCaco[d]	logBB[e]	Rot[f]	Acute tox[g]
23a	634.91	2	5	4.12	-5.54	1367.87	-0.60	4	class III
23b	670.63	2	6	4.30	-5.72	1624.93	-0.59	5	class III
23c	671.36	2	6	4.22	-5.73	1403.32	-0.67	5	class III
23d	673.48	2	6	4.22	-5.77	1365.18	-0.68	5	class III
23e	643.23	2	5	4.35	-5.85	1469.41	-0.48	4	class III
23f	644.89	2	5	4.37	-5.93	1367.84	-0.49	4	class III
23g	644.95	2	5	4.37	-5.93	1367.72	-0.49	4	class III
23h	659.89	2	8	3.62	-5.42	351.05	-1.29	5	class III
23i	674.42	2	8	3.41	-5.68	163.84	-1.71	5	class III
23j	674.47	2	8	3.41	-5.68	164.03	-1.71	5	class III
23k	717.03	2	7	4.37	-6.08	1365.55	-0.78	6	class III
23l	679.88	2	5	4.94	-6.42	1617.92	-0.23	4	class III
23m	741.31	2	8	4.42	-6.03	1404.80	-0.82	7	class III
23n	692.42	2	5	4.73	-6.26	1132.42	-0.86	6	class III
23o	731.29	2	8	4.02	-6.39	136.31	-2.03	7	class III

[a]Solvent accessible surface area, [b]No. of hydrogen bond donors, [c]No. of hydrogen bond acceptors, [d]Predicted apparent Caco-2 cell permeability, [e]Predicted brain/blood partition coefficient, [f]No. of rotatable bonds, [g]Acute oral toxicity

Table 4.8 *In-silico* predicted drug-likeness parameters of compounds **28a-l**

Com. Code	SASA[a]	HBD[b]	HBA[c]	logP	logS	PCaco[d]	logBB[e]	Rot[f]	Acute tox[g]
28a	666.92	1	4	5.41	-5.96	4364.71	0.08	5	class III
28b	695.19	1	4	5.81	-6.36	5415.96	0.17	5	class III
28c	698.84	1	4	5.72	-6.43	4388.60	0.07	5	class III
28d	698.55	1	4	5.72	**-6.62**	4385.09	0.07	5	class III
28e	670.72	1	4	5.60	-6.15	4731.37	0.19	5	class III
28f	675.51	1	4	5.66	-6.21	4386.54	0.19	5	class III
28g	675.50	1	4	5.66	-6.21	4387.41	0.20	5	class III
28h	690.12	1	4	5.90	-6.38	4383.63	0.25	5	class III
28i	704.16	1	7	5.10	-6.08	524.68	-0.95	6	class III
28j	704.31	1	7	5.10	-6.08	526.00	-0.95	6	class III
28k	753.13	1	6	6.10	-6.37	2422.50	-0.33	7	class III
28l	794.67	1	6	5.54	**-6.73**	1313.13	-0.68	7	class III

[a]Solvent accessible surface area, [b]No. of hydrogen bond donors, [c]No. of hydrogen bond acceptors, [d]Predicted apparent Caco-2 cell permeability, [e]Predicted brain/blood partition coefficient, [f]No. of rotatable bonds, [g]Acute oral toxicity

Table 4.9 *In-silico* predicted drug-likeness parameters of compounds **32a-n**

Com. Code	SASA[a]	HBD[b]	HBA[c]	logP	logS	PCaco[d]	logBB[e]	Rot[f]	Acute tox[g]
32a	676.14	1	4	5.30	-5.85	4027.37	-0.07	7	class III
32b	674.88	1	4	5.46	-5.83	4310.01	-0.03	7	class III
32c	691.35	1	4	5.56	-6.12	4098.20	-0.06	7	class III
32d	700.66	1	4	5.59	-6.09	4082.31	-0.07	7	class III
32e	692.37	1	5	5.53	-5.69	6654.45	0.09	8	class III
32f	706.36	1	5	5.38	-5.94	4212.55	-0.12	8	class III
32g	705.16	1	5	5.37	-5.92	4081.79	-0.13	8	class III
32h	683.82	1	4	5.53	-6.19	4026.22	0.04	7	class III
32i	691.19	1	4	5.72	-6.13	4087.68	0.11	7	class III
32j	692.09	1	4	5.74	-6.08	4079.53	0.11	7	class III
32k	696.15	1	4	5.85	-6.12	4090.30	0.12	7	class III
32l	697.12	1	4	5.85	-6.06	4080.61	0.12	7	class III
32m	706.26	1	7	4.57	-5.84	490.08	-1.06	8	class III
32n	726.11	1	4	5.92	-6.14	4320.49	-0.05	7	class III

[a]Solvent accessible surface area, [b]No. of hydrogen bond donors, [c]No. of hydrogen bond acceptors, [d]Predicted apparent Caco-2 cell permeability, [e]Predicted brain/blood partition coefficient, [f]No. of rotatable bonds, [g]Acute oral toxicity

Table 4.10 *In-silico* predicted drug-likeness parameters of compounds **38a-o**

Com. Code	SASA[a]	HBD[b]	HBA[c]	logP	logS	PCaco[d]	logBB[e]	Rot[f]	Acute tox[g]
38a	690.49	0	5	4.14	-4.77	2585.16	-0.07	4	class III
38b	723.60	0	5	4.40	-5.53	2579.47	-0.09	4	class III
38c	733.17	0	5	4.41	-5.68	2397.01	-0.13	4	class III
38d	744.73	0	6	4.35	-5.25	2576.60	-0.16	5	class III
38e	733.78	0	6	4.22	-5.04	2404.41	-0.18	5	class III
38f	738.23	0	6	4.22	-5.12	2397.01	-0.19	5	class III
38g	705.34	0	5	4.34	-5.20	2467.31	-0.02	4	class III
38h	710.01	0	5	4.40	-5.35	2398.53	0.00	4	class III
38i	722.55	0	5	4.66	-5.62	2585.25	0.05	4	class III
38j	724.89	0	5	4.67	-5.73	2397.39	0.05	4	class III
38k	725.02	0	5	4.67	-5.74	2398.21	0.05	4	class III
38l	739.36	0	8	3.41	-5.01	287.89	-1.21	5	class III
38m	738.53	0	5	3.62	-3.61	643.76	0.18	6	class III
38n	696.67	0	6	3.81	-4.64	2186.13	-0.16	4	class III
38o	742.58	0	5	4.97	-6.25	2585.43	0.18	4	class III

[a]Solvent accessible surface area, [b]No. of hydrogen bond donors, [c]No. of hydrogen bond acceptors, [d]Predicted apparent Caco-2 cell permeability, [e]Predicted brain/blood partition coefficient, [f]No. of rotatable bonds, [g]Acute oral toxicity

Table 4.11 *In-silico* predicted drug-likeness parameters of compounds **43a-p**

Com. Code	SASA[a]	HBD[b]	HBA[c]	logP	logS	PCaco[d]	logBB[e]	Rot[f]	Acute tox[g]
43a	641.79	1	5	3.54	-4.01	1571.25	-0.68	5	class III
43b	667.75	1	5	3.90	-4.30	1581.83	-0.69	5	class III
43c	680.90	1	6	3.51	-4.08	1572.47	-0.76	6	class III
43d	681.64	1	6	3.51	-4.08	1570.94	-0.76	6	class III
43e	650.82	1	5	3.64	-4.18	1573.77	-0.59	5	class III
43f	653.41	1	5	3.64	-4.18	1571.80	-0.57	5	class III
43g	663.54	1	5	4.17	-4.62	1580.58	-0.54	5	class III
43h	668.44	1	5	4.17	-4.62	1571.71	-0.52	5	class III
43i	673.39	1	5	4.23	-4.82	1571.64	-0.51	5	class III
43j	673.48	1	5	4.23	-4.87	1571.82	-0.51	5	class III
43k	680.76	1	8	3.37	-4.10	217.23	-1.74	6	class III
43l	682.49	1	8	3.37	-4.10	188.35	-1.82	6	class III
43m	682.63	1	8	3.37	-4.10	188.74	-1.82	6	class III
43n	682.52	1	6	3.26	-3.98	326.21	-1.56	5	class III
43o	688.80	1	5	4.80	-5.23	1571.85	-0.39	5	class III
43p	750.77	1	8	3.45	-4.25	1570.67	-0.91	8	class III

[a]Solvent accessible surface area, [b]No. of hydrogen bond donors, [c]No. of hydrogen bond acceptors, [d]Predicted apparent Caco-2 cell permeability, [e]Predicted brain/blood partition coefficient, [f]No. of rotatable bonds, [g]Acute oral toxicity

Table 4.12 *In-silico* predicted drug-likeness parameters of compounds **51a-n**

Com. Code	SASA[a]	HBD[b]	HBA[c]	logP	logS	PCaco[d]	logBB[e]	Rot[f]	Acute tox[g]
51a	726.04	0	4	5.57	-6.23	5164.05	0.24	6	class III
51b	748.46	0	4	5.88	-6.36	5606.61	0.28	6	class III
51c	758.24	0	4	5.90	-6.44	5161.92	0.24	6	class III
51d	764.68	0	5	5.68	-6.21	5417.31	0.20	7	class III
51e	763.21	0	5	5.63	-6.18	5165.21	0.18	7	class III
51f	763.04	0	5	5.63	-6.18	5197.91	0.18	7	class III
51g	732.21	0	4	5.74	-6.24	5344.61	0.32	6	class III
51h	735.05	0	4	5.81	-6.40	5165.42	0.36	6	class III
51i	750.13	0	4	6.07	-6.27	5161.12	0.45	6	class III
51j	750.10	0	4	6.08	-6.27	5165.16	0.42	6	class III
51k	781.60	0	7	4.87	-6.19	429.54	-0.99	7	class III
51l	778.21	0	4	6.34	-6.37	5521.95	0.55	7	class III
51m	765.82	0	4	5.02	-5.10	1274.70	0.51	6	class III
51n	852.75	0	4	6.38	**-6.61**	1355.44	0.47	8	class III

[a]Solvent accessible surface area, [b]No. of hydrogen bond donors, [c]No. of hydrogen bond acceptors, [d]Predicted apparent Caco-2 cell permeability, [e]Predicted brain/blood partition coefficient, [f]No. of rotatable bonds, [g]Acute oral toxicity

Table 4.13 *In-silico* predicted drug-likeness parameters of compounds **54a-k**

Com. Code	SASA[a]	HBD[b]	HBA[c]	logP	logS	PCaco[d]	logBB[e]	Rot[f]	Acute tox[g]
54a	275.91	2	3	2.75	-3.98	1.035	-0.05	3	class III
54b	293.47	2	4	2.76	-4.20	1.05	-0.43	4	class III
54c	295.48	2	4	2.76	-4.20	1.05	-0.44	4	class III
54d	281.28	2	3	2.89	-4.22	1.03	-0.06	3	class III
54e	288.36	2	3	3.40	-4.76	1.018	-0.05	3	class III
54f	289.34	2	3	3.40	-4.76	1.08	-0.05	2	class III
54g	322.25	2	3	3.51	-4.89	1.013	-0.059	3	class III
54h	310.69	2	5	2.66	-4.83	0.30	-0.74	4	class III
54i	308.24	2	5	2.76	-4.44	1.067	-0.66	5	class III
54j	319.41	2	3	4.05	-5.52	0.90	-0.06	3	class III
54k	328.63	2	4	3.38	-5.14	1.057	-0.54	3	class III

[a]Solvent accessible surface area, [b]No. of hydrogen bond donors, [c]No. of hydrogen bond acceptors, [d]Predicted apparent Caco-2 cell permeability, [e]Predicted brain/blood partition coefficient, [f]No. of rotatable bonds, [g]Acute oral toxicity

4.3 References

1. E. Ballana, J.A. Este, Insights from host genomics into HIV infection and disease: Identification of host targets for drug development. Antiviral Research, 100 (2013) 473-486.
2. F.W. Bell, A.S. Cantrell, M. Hoegberg, S.R. Jaskunas, N.G. Johansson, C.L. Jordan, M.D. Kinnick, Phenethylthiazolethiourea (PETT) compounds, a new class of HIV-1 reverse transcriptase inhibitors. Synthesis and basic structure activity relationship studies of PETT analogs. Journal of Medicinal Chemistry, 38 (1995) 4929-4936.
3. S. Emamzadeh-Fard, S. Esmaeeli, K. Arefi, M. Moradbeigi, B. Heidari, S.E. Fard, K. Paydary, Mechanisms of anti-retroviral drug resistance: Implications for novel drug discovery and development. Infectious Disorders-Drug Targets, 13 (2013) 330-336.
4. P. Chong, P. Sebahar, M. Youngman, Rational design of potent non-nucleoside inhibitors of HIV-1 Reverse Transcriptase. Journal of Medicinal Chemistry, 55 (2012) 10601-10609.
5. R.F. Freitas, S.E. Galembeck, Computational study of the interaction between TIBO inhibitors and Y181 (C181), K101 and Y188 amino acids. Journal of Physical Chemistry, 110 (2006) 21287–21298.
6. A.J. Paul, P.J. Janssen, P.J. Lewi, E. Arnold, F. Daeyaert, M. Jonge, J. Heeres, In search of a novel anti-HIV drug: Multidisciplinary coordination in the discovery of 4-[[4-[[4-[(1E)-2-cyanoethenyl]-2,6-dimethylphenyl]amino]-2-pyrimidinyl]amino]benzonitrile (R278474, rilpivirine). Journal of Medicinal Chemistry, 48 (2005)1901-1909.
7. A.L. Hopkins, J. Ren, R.M. Esnouf, B.E. Willcox, E.Y. Jones, C. Ross, T. Miyasaka, Complexes of HIV-1 reverse transcriptase with inhibitors of the HEPT series reveal conformational changes relevant to the design of potent non-nucleoside inhibitors. Journal of Medicinal Chemistry, 39 (1996)1589-1600.
8. J. Ren, C.E. Nichols, P.P. Chamberlain, Relationship of potency and re-silience to drug resistance mutations for GW420867X revealed by crystal structures of inhibitor complexes for wild-type, Leu100Ile, Lys101Glu and Tyr188Cys mutant HIV-1 reverse transcriptases. Journal of Medicinal Chemistry, 50 (2007) 2301-2309.
9. C. Reynolds, C.B. Koning, S.C. Pelly, W.A. Otterlo, M.L. Bode, In search of a treatment for HIV current therapies and the role of Non-Nucleoside Reverse Transcriptase Inhibitors (NNRTIs). Chemical Society Reviews, 41 (2012) 4657-4670.
10. C. Delaugerre, R. Rohban, A. Simon, Resistance profile and cross-resistance of HIV-1 among patients failing a non-nucleoside reverse transcriptase inhibitor-containing regimen. Journal of Medical Virology, 65 (2001) 445-448.

11. E.L. Asahchop, M.A. Wainberg, M. Oliveira, H. Xu, B.G. Brenner, D. Moisi, I.R. Ibanescu, Distinct resistance patterns to etravirine and rilpivirine in viruses containing non-nucleoside reverse transcriptase inhibitor mutations at baseline. AIDS (London, England), 27 (2013) 879-887.
12. A. Yang S, Pannecouque C, Daelemans D, X.D. Ma, Y. Liu, F.E. Chen, E. De Clercq, Molecular design, synthesis and biological evaluation of BP-O-DAPY and O-DAPY derivatives as non-nucleoside HIV-1 reverse transcriptase inhibitors. European Journal of Medicinal Chemistry, 65 (2013)134-143.
13. P. Zhan, X. Chen, D. Li, Z. Fang, E. De Clercq, X. Liu, HIV-1 NNRTIs: Structural diversity, pharmacophore similarity and implications for drug design. Medicinal Research Reviews, 33 (2013) E1-E72.
14. D.W. Ludovici, M.J. Kukla, P.G. Grous, S. Krishnan, K. Andries, M.P. de Bethune, H. Azijn, Evolution of anti-HIV drug candidates. Part 1: From α-Anilinophenylacetamide (α-APA) to imidoyl thiourea (ITU). Bioorganic & Medicinal Chemistry Letters, 11 (2001) 2225-2228.
15. J.J. Smith, N. Arora, J.R. Billedeau. J. Fretland, J. Q. Hang, G.M. Heilek, S.F. Harris, Synthesis and biological activity of new pyridone diaryl ether non-nucleoside inhibitors of HIV-1 reverse transcriptase. Medicinal Chemistry Communications, 1 (2010) 79-83.
16. P. Zhan, W. Chen, X. Liu, X. Li, X. Chen, Y. Tian, C. Pannecouque, Discovery of novel 2-(3-(2-chlorophenyl)pyrazin-2-ylthio)-*N*-arylacetamides as potent HIV-1 inhibitors using a structure-based bioisosterism approach. Bioorganic & Medicinal Chemistry, 20 (2012) 6795-6802.
17. T.J. Tucker, T.A. Lyle, C.M. Wiscount, S.F. Britcher, S.D. Young, W.M. Sanders, W.C. Lumma, Synthesis of a series of 4-(arylethynyl)-6-chloro-4-cyclopropyl-3,4-dihydroquinazolin-2(*1H*)-ones as novel non-nucleoside HIV-1 reverse transcriptase inhibitors. Journal of Medicinal Chemistry, 37 (1994) 2437–2444.
18. D.L. Romero, M. Busso, C.K. Tan, F. Reusser, J.R. Palmer, S.M. Poppe, P.A. Aristoff, Non-nucleoside reverse transcriptase inhibitors that potently and specifically block Human Immunodeficiency Virus type 1 replication, Proceedings of the National Academy of Sciences of the United States of America, 88 (1991) 8806-8810.
19. D.S. Su, J.J. Lim, E. Tinney, B.L. Wan, M.B. Young, K.D. Anderson, Substituted tetrahydroquinolines as potent allosteric inhibitors of reverse transcriptase and its key mutants. Bioorganic & Medicinal Chemistry Letters, 19 (2009) 119-123.
20. J. Zhang, P. Zhan, J. Wu, Z. Li, Y. Jiang, W. Ge, C. Pannecouque, Synthesis and biological evaluation of novel 5-alkyl-2-arylthio-6-((3,4-dihydroquinolin-1(*2H*)-yl)methyl)pyrimidin-4(*3H*)-ones as potent non-nucleoside HIV-1 reverse transcriptase inhibitors. Bioorganic & Medicinal Chemistry, 19 (2011) 4366-4376.

21. C. Lazar, A. Kluczyk, T. Kiyota, Y. Konishi, Drug evolution concept in drug design: 1. Hybridization method, Journal of Medicinal Chemistry 47 (2004) 6973-6982.
22. C. Viegas-Junior, A. Danuello, V. da Silva Bolzani, E.J. Barreiro, C.A. Fraga, Molecular hybridization: A useful tool in the design of new drug prototypes. Current Medicinal Chemistry, 14 (2007) 1829-1852.
23. J.W. Corbett, K.J. Kresge, S. Pan, B.C. Cordova, R.M. Klabe, J.D. Rodgers, S.K. Erickson-Viitanen, Trifluoromethyl-containing 3-alkoxymethyl and 3-aryloxymethyl-2-pyridinones are potent inhibitors of HIV-1 non-nucleoside reverse transcriptase. Bioorganic & Medicinal Chemistry Letters, 11 (2001) 309–312.
24. M. Patel, R.J. McHugh, B.C. Cordova, R.M. Klabe, S. Erickson-Viitanen, G.L. Trainor, J.D. Rodgers. Synthesis and evaluation of quinoxalinones as HIV-1 reverse transcriptase inhibitors. Bioorganic & Medicinal Chemistry Letters, 10 (2000) 1729-1731.
25. M. Cushman, A. Casimiro-Garcia, E. Hejchman, J.A. Ruell, M. Huang, C.A. Schaeffer, K. Williamson, New alkenyldiarylmethanes with enhanced potencies as anti-HIV agents which act as non-nucleoside reverse transcriptase inhibitors. Journal of Medicinal Chemistry, 41 (1998) 2076–2089.
26. R. Silvestri, M. Artico, S. Massa, T. Marceddu, F. De Montis, P. La Colla, 1-[2-(Diphenylmethoxy)ethyl]-2-methyl-5-nitroimidazole: A potent lead for the design of novel NNRTIs. Bioorganic & Medicinal Chemistry Letters, 10 (2000) 253-256.
27. S. Chander, A. Penta, S. Murugesan, Structure-based virtual screening and docking studies for the identification of novel inhibitors against wild and drug resistance strains of HIV-1 RT. Medicinal Chemistry Research, 24 (2015) 1869–1883.
28. K. Das, J.D. Bauman, A.D. Clark, Y.V. Frenkel, P.J. Lewi, A.J. Shatkin, S.H. Hughes, High-resolution structures of HIV-1 reverse transcriptase/TMC278 complexes: Strategic flexibility explains potency against resistance mutations, Proceedings of the National Academy of Sciences of the United States of America, 105 (2008) 1466-1471.
29. Glide, Schrödinger, LLC, New York, Version 5.9, (2013).
30. W.L. Jorgensen, D.S. Maxwell, R.J. Tirado, Development and testing of the OPLS all-atom force field on conformational energetics and properties of organic liquids, Journal of American Chemical Society, 118 (1996) 11225-11236.
31. Lig-Prep, Schrödinger, LLC, New York, Version 2.6, (2013).
32. M.M. Hann, G.M. Keseru, Finding the sweet spot: The role of nature and nurture in medicinal chemistry. Nature Reviews Drug Discovery, 11 (2012) 355-365.
33. Qik-prop, Schrödinger, LLC, New York, Version 3.7, (2013).

34. F. Cheng, W. Li, Y. Zhou, J. Shen, Z. Wu, G. Liu, admetSAR: A comprehensive source and free tool for assessment of chemical ADMET properties. Journal of Chemical Information and Modeling, 52 (2012) 3099-3105.
35. D. Lagorce, O. Sperandio, J.B. Baell, M.A. Miteva, B.O. Villoutreix, FAF-Drugs: A web server for compound property calculation and chemical library design. Nucleic Acids Research, 43 (2015) W200-W207.
36. M.V.S. Varma, K. Sateesh, R. Panchagnula, Functional role of P-glycoprotein in limiting intestinal absorption of drugs: contribution of passive permeability to P-glycoprotein mediated efflux transport. Molecular Pharmaceutics, 2 (2005) 12-21.
37. H. Pajouhesh, G.R. Lenz, Medicinal chemical properties of successful central nervous system drugs. Neurotherapeutics, 2 (2005) 541-553.
38. P.D. Leeson, B. Springthorpe, The influence of drug-like concepts on decision-making in medicinal chemistry, Nature Reviews Drug Discovery, 6 (2007) 881-890.
39. Qikprop, User Manual, Schrödinger, LLC, Chapter-1, Version 3.8 (2013) 2-5.

CHAPTER 5

Synthesis and Characterization

5.1 Experimental and General Methodology

All solvents and reagents purchased from Sigma, Merck and Spectrochem companies were used as received without further purification. The solvent system used throughout experimental work for running TLC was ethyl acetate and hexane mixture (in suitable proportion) in order to monitor the progress of reactions. Melting points were uncorrected and determined in open capillary tubes on a Precision Buchi B530 (Flawil, Switzerland) melting point apparatus containing silicon oil. IR spectra of the synthesized compounds were recorded using FTIR spectrophotometer (Shimadzu IR Prestige 21, India). ^{1}H NMR and ^{13}C NMR spectra were recorded on Bruker DPX-400 spectrometer (Bruker India Scientific Pvt. Ltd., Mumbai) using TMS as an internal standard (chemical shifts in *δ*). Elemental analysis was performed on Vario EL III M/s Elementar C, H, N and S analyzer (Elementar Analysensysteme GmbH, Hanau, Germany). ES-MS were recorded on MICROMASS Quattro-II LCMS system (Waters Corporation, Milford, USA).

5.2 Synthesis and characterization of designed compounds

Conventional as well as non-conventional (microwave assisted synthesis) approaches were used for the synthesis of designed series. Several reaction conditions were evaluated for optimization of reaction and final optimized conditions were used for the synthesis of target compounds (Scheme **1-11**). Synthesized compounds were further purified by various techniques like washing with suitable solvents, column chromatography and re-crystallization techniques as per requirement. Purified compounds were characterized by preliminary physicochemical methods like melting point and thin layer chromatography to assess the purity of the compounds. The structure of the compounds was further confirmed by spectral techniques like IR, ^{1}H NMR, ^{13}C NMR, Mass spectral and elemental analysis.

5.2.1 Synthesis and characterization of 2-(6,7-dimethoxy-3,4-dihydroisoquinolin-2(*1H*)-yl)-*N*-phenylacetamide derivatives (5a-o)

The synthesis of target compounds **5a-o** was achieved using the route outlined in scheme **1**. Initially, the reaction of different anilines **1a-o** and chloroacetyl chloride **2** in DCM, in the presence of triethylamine as a base afforded 2-chloro-*N*-phenylacetamide derivatives (**3a-o**) as intermediates. Further, treatment of compounds **3a-o** with hydrochloride salt of 6,7-dimethoxy tetrahydroisoquinoline (**4**), in acetonitrile in the presence of potassium carbonate as base afforded the titled compounds (**5a-o**).

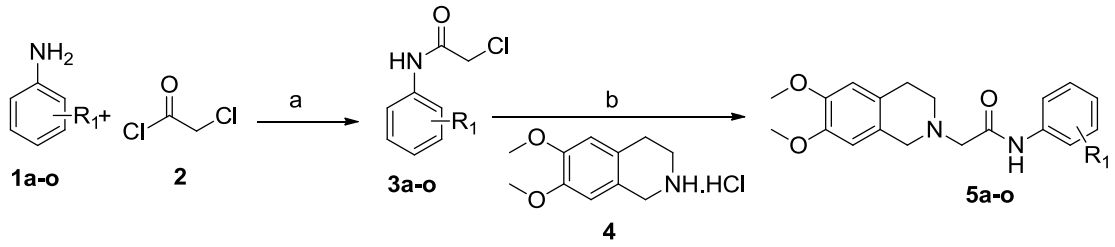

Scheme 1. Reagents and conditions: (a) DCM, Et_3N, 0˚C-rt, 1-2 h (b) ACN, K_2CO_3, Reflux 3-5 h

General procedure for the synthesis of 2-chloro-*N*-phenylacetamide derivatives (3a-o)

Chloroacetyl chloride **2** (1.68 g, 15 mmol) was added dropwise to the ice-cold stirred solution of anilines (**1a-o,** 15 mmol) in DCM, in the presence of triethylamine (45 mmol, 0.63 ml) as base, reaction was further stirred at rt for 1-2 h, the progress of the reaction was monitored by TLC. After completion of reaction, DCM layer was washed with saturated bicarbonate solution (50 ml), then again twice washed with distilled water (2 x 50ml), collected DMC layer was dried over sodium sulphate and evaporated on the rotary evaporator to obtain the intermediates **3a-o** [1, 2].

General procedure for the synthesis of 2-(6,7-dimethoxy-3,4-dihydroisoquinolin-2(*1H*)-yl)-*N*-phenylacetamide derivatives (5a-o)

2-chloro-*N*-phenylacetamide derivatives **3a-o** (10 mmol) was added to the stirred reaction mass of 6,7-dimethoxy tetrahydroisoquinoline **4** (10 mmol, 0.23 g), in acetonitrile in the presence of potassium carbonate as a base (25 mmol, 0.34 g). The reaction mass was further allowed to reflux, the progress of the reaction was monitored by TLC (Scheme **1**). After completion of reaction (after 3-5 h), solvent acetonitrile was evaporated on the rotary evaporator; water (25 ml) was added to the reaction mixture and extracted twice with equal volume of ethyl acetate (2x25 ml). Combined ethyl acetate layer was washed with brine water (50 ml), dried over sodium sulphate and evaporated on rotary evaporator to afford the final compounds **5a-o** [1, 2]. Synthesized compounds were purified by first washing with hexane, followed by diethyl ether. Preliminary characteristics data of the synthesized compounds **(5a-o)** are shown in Table **5.1**.

Table 5.1 Preliminary characteristics data of compounds **5a-o**

Comp. code	R_1	Mol. formula	Mol. Wt	% yield	Melting point (˚C)
5a	H	$C_{19}H_{22}N_2O_3$	326.16	73	152-154
5b	2-CH_3	$C_{20}H_{24}N_2O_3$	340.18	76	136-138
5c	3-CH_3	$C_{20}H_{24}N_2O_3$	340.18	78	130-131
5d	4-CH_3	$C_{20}H_{24}N_2O_3$	340.18	81	150-153
5e	3-OCH_3	$C_{20}H_{24}N_2O_4$	356.17	76	138-140
5f	4-OCH_3	$C_{20}H_{24}N_2O_4$	356.17	84	152-154
5g	4-F	$C_{19}H_{21}FN_2O_3$	344.15	71	150-151
5h	2-Cl	$C_{19}H_{21}ClN_2O_3$	360.12	64	108-110
5i	3-Cl	$C_{19}H_{21}ClN_2O_3$	360.12	69	176-178
5j	4-Cl	$C_{19}H_{21}ClN_2O_3$	360.12	74	178-180
5k	4-NO_2	$C_{19}H_{21}N_3O_5$	371.15	67	192-194
5l	3-CF_3	$C_{20}H_{21}F_3N_2O_3$	394.15	68	176-178
5m	2,6-di-Me	$C_{21}H_{26}N_2O_3$	354.19	77	154-157
5n	3,4-di-Me	$C_{21}H_{26}N_2O_3$	354.19	75	158-160
5o	2-Me,5-Cl	$C_{20}H_{23}ClN_2O_3$	374.14	68	116-119

Spectral characterization of compounds 5a-o

Synthesized compounds were characterized by spectral analysis such as IR, ^{1}H NMR and Mass. The IR spectra of **5a-o** showed the absorption bands corresponding to the stretching of amidic hydrogen (−CO**NH**-) at the region 3200–3350 cm^{-1} (strong, broad). Further, a prominent absorption at the region 1663-1703 cm^{-1} appeared corresponding to the stretching of the carbonyl group (−**CO**NH-). ^{1}H NMR of compounds **5a-o**, showed the merged peak of four protons present at the 3rd and 4th position of tetrahydroisoquinoline (THIQ) ring at around δ~2.8-2.9. Two protons present at the carbon between nitrogen and carbonyl group appeared at around δ~3.3-3.4. The pair of protons at the first carbon of THIQ displayed characteristic peak at δ~3.7-3.8. Furthermore, six methoxy protons (at the 6th and 7th carbon of THIQ) appeared around δ~3.8-3.9. Two aromatic protons present at the 5th and 8th position of THIQ showed corresponding peaks at δ~6.5-6.6. Amidic protons (-CON**H**-) in most of the compounds appeared between δ~9-10, except compound **5m** in which it appeared at δ~8.76. Counting and position of other protons present at the phenyl ring also appeared in accordance with their proposed structures. Further, mass spectra of titled compounds showed the corresponding M+1 peak. Detailed spectral data of compounds **5a-o** is given below;

2-(6,7-dimethoxy-3,4-dihydroisoquinolin-2(1H)-yl)-N-phenylacetamide (5a)

White solid; IR (KBr, v, cm^{-1}): 3288, 3001, 2821, 2775, 1693, 1517, 1423, 1228, 1139, 1105; ^{1}H NMR (400 MHz, $CDCl_3$): δ 9.21 (s, 1H), 7.59 (dd, *J* = 8.6, 1.1 Hz, 2H), 7.39 – 7.31 (m,

2H), 7.14 (d, *J* = 7.4 Hz, 1H), 6.67 (s, 1H), 6.55 (s, 1H), 3.88 (d, *J* = 12.2 Hz, 6H), 3.77 (s, 2H), 3.34 (s, 2H), 2.92 (s, 4H); MS: m/z 327.2 (M+1).

2-(6,7-dimethoxy-3,4-dihydroisoquinolin-2(1H)-yl)-N-o-tolylacetamide (5b)

White solid; IR (KBr, v, cm^{-1}): 3294, 2975, 2914, 2829, 1670, 1490, 1251, 1226, 1139, 1013; ^{1}H NMR (400 MHz, $CDCl_3$): δ 9.33 (s, 1H), 8.14 (d, *J* = 8.1 Hz, 1H), 7.25 (s, 1H), 7.17 (d, *J* = 7.2 Hz, 1H), 7.06 (td, *J* = 7.5, 1.2 Hz, 1H), 6.66 (s, 1H), 6.54 (s, 1H), 3.89 (s, 3H), 3.86 (s, 3H), 3.79 (s, 2H), 3.38 (s, 2H), 2.95 (d, *J* = 3.8 Hz, 4H), 2.20 (s, 3H); MS: m/z 341.2 (M+1).

2-(6,7-dimethoxy-3,4-dihydroisoquinolin-2(1H)-yl)-N-m-tolylacetamide (5c)

White solid; IR (KBr, v, cm^{-1}): 3286, 3010, 2949, 2833, 1683, 1519, 1489, 1220, 1143, 1024; 1H NMR (400 MHz, CDCl3): δ 9.17 (s, 1H), 7.40 (d, *J* = 11.8 Hz, 2H), 7.23 (t, *J* = 7.7 Hz, 1H), 6.95 (d, *J* = 7.6 Hz, 1H), 6.67 (s, 1H), 6.55 (s, 1H), 3.88 (d, *J* = 12.3 Hz, 6H), 3.74 (d, *J* = 17.9 Hz, 2H), 3.33 (s, 2H), 2.98 – 2.80 (m, 4H), 2.36 (s, 3H); MS: m/z 341.2 (M+1).

2-(6,7-dimethoxy-3,4-dihydroisoquinolin-2(1H)-yl)-N-p-tolylacetamide (5d)

White solid; IR (KBr, v, cm^{-1}): 3267, 2943, 2827, 2779, 1685, 1517, 1462, 1253, 1196; ^{1}H NMR (400 MHz, $CDCl_3$): δ 9.14 (s, 1H), 7.51 – 7.42 (m, 2H), 7.15 (d, *J* = 8.2 Hz, 2H), 6.67 (s, 1H), 6.55 (s, 1H), 3.88 (d, *J* = 12.1 Hz, 6H), 3.76 (s, 2H), 3.32 (s, 2H), 2.91 (d, *J* = 3.1 Hz, 4H), 2.33 (s, 3H); MS: m/z 341.2 (M+1).

2-(6,7-dimethoxy-3,4-dihydroisoquinolin-2(1H)-yl)-N-(3-methoxyphenyl) acetamide (5e)

White solid; IR (KBr, v, cm^{-1}): 3277, 2922, 2829, 1685, 1597, 1523, 1465, 1255, 1139, 1005; 1H NMR (400 MHz, CDCl3): δ 9.17 (s, 1H), 7.42 (d, *J* = 11.7 Hz, 2H), 7.24 (t, *J* = 7.8 Hz, 1H), 6.93 (d, *J* = 7.8 Hz, 1H), 6.66 (s, 1H), 6.54 (s, 1H), 3.88 (d, *J* = 12.3 Hz, 6H), 3.82 (s, 3H), 3.72 (d, *J* = 17.9 Hz, 2H), 3.32 (s, 2H), 2.96 – 2.78 (m, 4H); MS: m/z 357.2 (M+1).

2-(6,7-dimethoxy-3,4-dihydroisoquinolin-2(1H)-yl)-N-(4-methoxyphenyl) acetamide (5f)

White solid; IR (KBr, v, cm^{-1}): 3317, 2957, 2920, 2821, 1688, 1615, 1517, 1467, 1253, 1134, 1103; ^{1}H NMR (400 MHz, $CDCl_3$): δ 9.09 (s, 1H), 7.51 (s, 1H), 7.48 (s, 1H), 6.89 (d, *J* = 2.2 Hz, 1H), 6.87 (d, *J* = 2.2 Hz, 1H), 6.67 (s, 1H), 6.55 (s, 1H), 3.90 (s, 3H), 3.87 (s, 3H), 3.81 (s, 3H), 3.76 (s, 2H), 3.32 (s, 2H), 2.92 (s, 4H); MS: m/z 357.2 (M+1).

2-(6,7-dimethoxy-3,4-dihydroisoquinolin-2(1H)-yl)-N-(4-fluorophenyl)acetamide (5g)

White solid; IR (KBr, v, cm^{-1}): 3302, 3070, 2991, 2816, 1687, 1612, 1508, 1469, 1228, 1136, 1101; ^{1}H NMR (400 MHz, $CDCl_3$): δ 9.20 (s, 1H), 7.65 – 7.49 (m, 2H), 7.08 – 7.00 (m, 2H), 6.67 (s, 1H), 6.55 (s, 1H), 3.88 (d, *J* = 11.6 Hz, 6H), 3.76 (s, 2H), 3.33 (s, 2H), 2.92 (s, 4H), 1.60 (s, 2H); MS: m/z 345.2 (M+1).

N-(2-chlorophenyl)-2-(6,7-dimethoxy-3,4-dihydroisoquinolin-2(1H)-yl)acetamide 5h)

White solid; IR (KBr, v, cm^{-1}): 3298, 2993, 2889, 2833, 1701, 1519, 1436, 1230, 1139, 1103; ^1H NMR (400 MHz, $CDCl_3$): δ 9.97 (s, 1H), 8.48 (dd, *J* = 8.3, 1.5 Hz, 1H), 7.37 (dd, *J* = 8.0, 1.4 Hz, 1H), 7.32 (dd, *J* = 7.5, 1.0 Hz, 1H), 7.10 – 7.01 (m, 1H), 6.67 (s, 1H), 6.55 (s, 1H), 3.90 (s, 3H), 3.86 (s, 3H), 3.81 (s, 2H), 3.38 (s, 2H), 2.94 (s, 4H); MS: m/z 361.1 (M+1), 363.1 (M+3).

N-(3-chlorophenyl)-2-(6,7-dimethoxy-3,4-dihydroisoquinolin-2(1H)-yl)acetamide (5i)

White solid; IR (KBr, v, cm^{-1}): 3228, 3001, 2821, 2752, 1663, 1517, 1423, 1228, 1138, 1005; 1H NMR (400 MHz, CDCl3): δ 9.27 (s, 1H), 7.69 (t, *J* = 2.0 Hz, 1H), 7.45 (ddd, *J* = 8.2, 2.0, 0.9 Hz, 1H), 7.10 (ddd, *J* = 8.0, 2.0, 1.0 Hz, 1H), 6.67 (s, 1H), 6.55 (s, 1H), 3.89 (d, *J* = 12.4 Hz, 6H), 3.76 (s, 2H), 3.33 (s, 2H), 2.92 (d, *J* = 3.5 Hz, 4H); MS: m/z 361.1 (M+1), 363.1 (M+3).

N-(4-chlorophenyl)-2-(6,7-dimethoxy-3,4-dihydroisoquinolin-2(1H)-yl)acetamide (5j)

White solid; IR (KBr, v, cm^{-1}): 3269, 2941, 2900, 2825, 2785, 1680, 1517, 1492, 1396, 1253, 1220, 1141, 1105; ^1H NMR (400 MHz, $CDCl_3$): δ 9.25 (s, 1H), 7.56 – 7.53 (m, 2H), 7.31 (s, 2H), 6.67 (s, 1H), 6.55 (s, 1H), 3.90 (s, 3H), 3.87 (s, 3H), 3.76 (s, 2H), 3.33 (s, 2H), 2.92 (s, 4H); MS: m/z 361.1 (M+1), 363.1 (M+3).

2-(6,7-dimethoxy-3,4-dihydroisoquinolin-2(1H)-yl)-N-(4-nitrophenyl)acetamide (5k)

Pale yellow solid; IR (KBr, v, cm^{-1}): 3273, 2933, 2829, 1703, 1504, 1336, 1226; ^1H NMR (400 MHz, $CDCl_3$): δ 9.62 (s, 1H), 8.23 (d, *J* = 9.2 Hz, 2H), 7.77 (d, *J* = 9.2 Hz, 2H), 6.68 (s, 1H), 6.55 (s, 1H), 3.89 (d, *J* = 14.3 Hz, 6H), 3.78 (s, 2H), 3.38 (s, 2H), 2.94 (s, 4H); MS: m/z 372.2 (M+1).

2-(6,7-dimethoxy-3,4-dihydroisoquinolin-2(1H)-yl)-N-(3-(trifluoromethyl)phenyl) acetamide (5l)

White solid, IR (KBr, v, cm^{-1}): 3302, 3070, 2991, 2816, 1687, 1612, 1508, 1469, 1228, 1136, 1101; ^1H NMR (400 MHz, $CDCl_3$): δ 9.54 (s, 1H), 7.90 (s, 1H), 7.77 (d, *J* = 7.9 Hz, 1H), 7.45 (t, *J* = 7.9 Hz, 1H), 7.36 (d, *J* = 7.8 Hz, 1H), 6.68 (s, 1H), 6.58 (s, 1H), 3.90 (s, 2H), 3.87 (s, 6H), 3.73 (d, *J* = 14.1 Hz, 1H), 3.50 – 3.43 (m, 1H), 2.91 (d, *J* = 5.3 Hz, 2H), 2.88 – 2.76 (m, 2H); MS: m/z 395.2 (M+1).

2-(6,7-dimethoxy-3,4-dihydroisoquinolin-2(1H)-yl)-N-(2,6-dimethylphenyl) acetamide (5m)

White solid; IR (KBr, v, cm^{-1}): 3315, 2956, 2920, 2821, 1691, 1610, 1517, 1467, 1253, 1132, 1103; ^1H NMR (400 MHz, $CDCl_3$): δ 8.76 (s, 1H), 7.10 (d, *J* = 1.6 Hz, 3H), 6.66 (s, 1H), 6.56 (s, 1H), 3.88 (d, *J* = 3.5 Hz, 6H), 3.83 (s, 2H), 3.40 (s, 2H), 2.99 (d, *J* = 5.0 Hz, 2H), 2.95 (d, *J* = 5.2 Hz, 2H), 2.26 (s, 6H); MS: m/z 355.2 (M+1).

2-(6,7-dimethoxy-3,4-dihydroisoquinolin-2(1H)-yl)-N-(3,4-dimethylphenyl) acetamide (5n)

White solid; IR (KBr, v, cm^{-1}): 3332, 3045, 2997, 2831, 2773, 1693, 1519, 1489, 1225, 1230, 1138, 1101; ^1H NMR (400 MHz, $CDCl_3$): δ 9.11 (s, 1H), 7.35 (s, 2H), 7.09 (d, *J* = 7.9 Hz, 1H), 6.67 (s, 1H), 6.55 (s, 1H), 3.90 (s, 3H), 3.87 (s, 3H), 3.76 (s, 2H), 3.33 (s, 2H), 2.92 (s, 4H), 2.25 (d, *J* = 9.1 Hz, 6H); MS: m/z 355.2 (M+1).

N-(5-chloro-2-methylphenyl)-2-(6,7-dimethoxy-3,4-dihydroisoquinolin-2(1H)-yl) acetamide (5o)

White solid; IR (KBr, v, cm^{-1}): 3277, 3016, 2937, 2900, 2829, 1701, 1514, 1445, 1259, 1228, 1190, 1136; 1H NMR (400 MHz, CDCl3): δ 9.44 (s, 1H), 8.02 (dd, *J* = 6.7, 2.7 Hz, 1H), 7.22 – 7.12 (m, 2H), 6.67 (s, 1H), 6.54 (s, 1H), 3.88 (d, *J* = 11.5 Hz, 6H), 3.80 (s, 2H), 3.38 (s, 2H), 3.04 – 2.86 (m, 4H), 2.25 (s, 3H); MS: m/z 375.1 (M+1).

5.2.2 Synthesis and characterization of 2-(6,7-dimethoxy-3,4-dihydroisoquinolin-2(*1H*)-yl)-*N*-phenylpropanamide derivatives (9a-o)

Target compounds **9a-o** were achieved in two steps, details of the reaction conditions are described in scheme **2**. The first step involved reaction of different anilines (**6a-o)** with 2-chloropropionyl chloride **7**, which afforded substituted 2-chloro-*N*-phenylpropanamide (**8a-o)** as intermediates. In the second step, the reaction of intermediates (**8a-o)** with 6,7-dimethoxy-1,2,3,4-tetrahydroisoquinoline **4** afforded the titled compounds (**9a-o**).

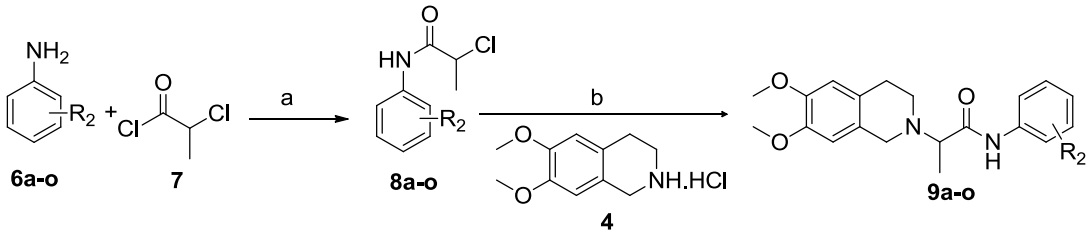

Scheme 2. Reagents and conditions: (a) DCM, Et_3N, 0˚C-rt, 2-2.5 h (b) ACN, K_2CO_3, Reflux 3-5 h

General procedure for the synthesis of 2-chloro-*N*-phenylpropanamide derivatives (8a-o)

2-chloropropionyl chloride **7** (1.87 g, 15 mmol) was added dropwise to the ice-cold stirred solution of anilines **6a-o** (15 mmol) in DCM, in the presence of triethylamine (45 mmol, 4.6 g) as a base, the reaction was further stirred at rt for 1.5-2 h. After completion of reaction as per TLC, DCM layer was washed with saturated bicarbonate water (50 ml), and then again twice washed with distilled water (2 x 50ml). DCM layer was separated and dried over sodium sulphate and evaporated on the rotary evaporator to yield the intermediates **(8a-o)** [1, 2].

General procedure for the synthesis of 2-(6,7-dimethoxy-3,4-dihydroisoquinolin-2(1*H*)-yl)-*N*-phenylpropanamide derivatives (9a-o)

Substituted 2-chloro-*N*-phenylpropanamide derivatives (intermediates **8a-o,** 10 mmol) were added to the stirred reaction mass of **4** (10 mmol, 0.23 g) in acetonitrile in the presence of potassium carbonate as base (25 mmol, 0.34 g). The reaction mass was refluxed for 3 to 5 h, and the progress of reaction was monitored by TLC. After completion of reaction, solvent acetonitrile was evaporated on the rotary evaporator; water was added to the reaction mixture (25 ml) and extracted twice with equal volume of ethyl acetate (2x25 ml). Combined ethyl acetate layer was washed with brine water (50 ml), dried over sodium sulphate and evaporated on rotary evaporator to afford the final compounds **9a-o** [1, 2]. All the synthesized compounds were purified by first washing with hexane, followed by diethyl ether. Preliminary characteristics data of the synthesized compounds **9a-o** are shown in Table **5.2**

Table 5.2 Preliminary characteristics data of compounds **9a-o**

Comd. code	R_2	Mol. formula	Mol. Wt	% yield	Melting point (˚C)
9a	H	$C_{20}H_{24}N_2O_3$	340.18	68	146-149
9b	2-CH_3	$C_{21}H_{26}N_2O_3$	354.19	73	148-150
9c	3-CH_3	$C_{21}H_{26}N_2O_3$	354.19	71	132-135
9d	4-CH_3	$C_{21}H_{26}N_2O_3$	354.19	77	120-122
9e	3-OCH_3	$C_{21}H_{26}N_2O_4$	370.19	81	136-138
9f	4-OCH_3	$C_{21}H_{26}N_2O_4$	370.19	84	152-153
9g	4-F	$C_{20}H_{23}FN_2O_3$	358.17	73	144-146
9h	2-Cl	$C_{20}H_{23}ClN_2O_3$	374.14	69	148-150
9i	3-Cl	$C_{20}H_{23}ClN_2O_3$	374.14	74	162-164
9j	4-Cl	$C_{20}H_{23}ClN_2O_3$	374.14	75	156-157
9k	2-CF_3	$C_{21}H_{23}F_3N_2O_3$	408.17	69	152-155
9l	3-CF_3	$C_{21}H_{23}F_3N_2O_3$	408.17	72	220-222
9m	4-NO_2	$C_{20}H_{23}N_3O_5$	385.16	66	192-194
9n	2,4-di-Me	$C_{22}H_{28}N_2O_3$	368.21	74	128-130
9o	3,4-di-Me	$C_{22}H_{28}N_2O_3$	368.21	71	142-143

Spectral characterization of compounds 9a-o

Synthesized compounds were characterized by spectral analysis such as IR, ^{1}H NMR and Mass. The IR spectra of compounds (**9a-o)** showed the expected absorption bands corresponding to stretching of amidic hydrogen (-CO**NH**-) at 3200-3350 cm^{-1} (strong, broad) and characteristic amide carbonyl stretching (**C=O)** at 1680-1697 cm^{-1}. ^{1}H NMR spectra of compounds **9a-o**, showed the characteristic peak (as doublet) of three methyl protons (attached at carbon adjacent to the carbonyl group) at δ~1.43-1.46. Single proton present at

the carbon between nitrogen and carbonyl group appeared as quartet or multiplet at around δ~3.3-3.4. Protons at the 3rd and 4th position of THIQ appeared either as separate peaks or merged at δ~2.8-2.9. Further, dual protons at the first carbon of THIQ appeared as two discrete peaks at δ~3.7-3.8. Six methoxy protons (at the 6th and 7th carbon of THIQ) appeared around δ~3.8-3.9. Two aromatic protons present at the 5th and 8th position of THIQ showed corresponding peaks at δ~6.5-6.6. Amidic protons (-CONH-) in most of the compounds appeared between δ~9-10. Counting and position of other protons present at the phenyl ring also appeared in accordance with their proposed structures. Further, mass spectra of titled compounds showed the corresponding M+1 peak. Detailed spectral data of compounds **9a-o** is given below;

2-(6,7-dimethoxy-3,4-dihydroisoquinolin-2(1H)-yl)-N-phenylpropanamide (9a)

White solid; IR (KBr, v, cm^{-1}): 3302, 3049, 2991, 2920, 2831, 1691, 1598, 1571, 1435, 1382, 1220, 1111; ^{1}H NMR (400 MHz, $CDCl_3$): δ 9.35 (s, 1H), 7.58 (dd, *J* = 8.6, 1.0 Hz, 2H), 7.34 (t, *J* = 8.0 Hz, 2H), 7.11 (dd, *J* = 10.6, 4.3 Hz, 1H), 6.67 (s, 1H), 6.58 (s, 1H), 3.88 (d, *J* = 9.4 Hz, 7H), 3.84 (s, 1H), 3.42 (d, *J* = 7.0 Hz, 1H), 2.90 (d, *J* = 5.9 Hz, 2H), 2.87 – 2.79 (m, 2H), 1.44 (d, *J* = 7.0 Hz, 3H); MS: m/z 341.2 (M+1).

2-(6,7-dimethoxy-3,4-dihydroisoquinolin-2(1H)-yl)-N-o-tolylpropanamide (9b)

White solid; IR (KBr, v, cm^{-1}): 3288, 2941, 2910, 2831, 1672, 1610, 1517, 1490, 1294, 1257, 1222; ^{1}H NMR (400 MHz, CDCl3): δ 9.43 (s, 1H), 8.16 (t, *J* = 6.8 Hz, 1H), 7.24 (d, *J* = 7.9 Hz, 1H), 7.16 (d, *J* = 7.2 Hz, 1H), 7.05 (t, *J* = 7.0 Hz, 1H), 6.66 (s, 1H), 6.56 (s, 1H), 3.90 – 3.86 (m, 7H), 3.78 – 3.67 (m, 1H), 3.45 (t, *J* = 6.9 Hz, 1H), 2.89 (d, *J* = 14.3 Hz, 4H), 2.16 (s, 3H), 1.46 (d, *J* = 7.0 Hz, 3H); MS: m/z 355.2 (M+1).

2-(6,7-dimethoxy-3,4-dihydroisoquinolin-2(1H)-yl)-N-m-tolylpropanamide (9c)

White solid; IR (KBr, v, cm^{-1}): 3288, 2978, 2943, 2833, 2775, 1674, 1608, 1516, 1489, 1257, 1222, 1112; ^{1}H NMR (400 MHz, $CDCl_3$): δ 9.29 (s, 1H), 7.43 (s, 1H), 7.37 (d, *J* = 8.1 Hz, 1H), 7.22 (t, *J* = 7.8 Hz, 1H), 6.93 (d, *J* = 7.5 Hz, 1H), 6.67 (s, 1H), 6.58 (s, 1H), 3.87 (t, *J* = 12.3 Hz, 7H), 3.71 (d, *J* = 14.2 Hz, 1H), 3.41 (d, *J* = 7.0 Hz, 1H), 2.90 (d, *J* = 5.9 Hz, 2H), 2.82 (d, *J* = 6.5 Hz, 2H), 2.35 (s, 3H), 1.43 (d, *J* = 7.0 Hz, 3H); MS: m/z 355.2 (M+1).

2-(6,7-dimethoxy-3,4-dihydroisoquinolin-2(1H)-yl)-N-p-tolylpropanamide (9d)

White solid; IR (KBr, v, cm^{-1}): 3296, 2989, 2941, 2904, 2831, 1680, 1587, 1514, 1253, 1038, 1111; ^{1}H NMR (400 MHz, CDCl3): δ 9.28 (s, 1H), 7.46 (d, *J* = 8.4 Hz, 2H), 7.14 (d, *J* = 8.2 Hz, 2H), 6.66 (s, 1H), 6.57 (s, 1H) 3.88 (d, *J* = 9.5 Hz, 6H), 3.83 (d, *J* = 5.8 Hz, 1H), 3.70 (d, *J* = 14.2 Hz, 1H), 3.41 (q, *J* = 7.0 Hz, 1H), 2.84 (ddd, *J* = 17.8, 11.2, 5.7 Hz, 4H), 2.33 (s, 3H), 1.43 (d, *J* = 7.0 Hz, 3H); MS: m/z 355.2 (M+1).

2-(6,7-dimethoxy-3,4-dihydroisoquinolin-2(1H)-yl)-N-(3-methoxyphenyl)propanamide (9e)

White solid; IR (KBr, v, cm^{-1}): 3290, 3005, 2941, 2818, 1685, 1608, 1517, 1433, 1255, 1157, 1114; ^1H NMR (400 MHz, $CDCl_3$): δ 9.36 (s, 1H), 7.40 (t, *J* = 2.2 Hz, 1H), 7.22 (t, *J* = 8.1 Hz, 1H), 7.01 (dd, *J* = 8.0, 1.1 Hz, 1H), 6.69 – 6.65 (m, 2H), 6.58 (s, 1H), 3.88 (d, *J* = 9.3 Hz, 7H), 3.83 (s, 3H), 3.75 – 3.68 (m, 1H), 3.43 (q, *J* = 6.9 Hz, 1H), 2.90 (d, *J* = 6.0 Hz, 2H), 2.86 – 2.77 (m, 2H), 1.43 (d, *J* = 7.0 Hz, 3H); MS: 371.2 m/z (M+1).

2-(6,7-dimethoxy-3,4-dihydroisoquinolin-2(1H)-yl)-N-(4-methoxyphenyl)propanamide (9f)

White solid; IR (KBr, v, cm^{-1}): 3302, 3074, 2914, 2835, 2783, 1680, 1514, 1411, 1255, 1220, 1138; ^1H NMR (400 MHz, CDCl3): δ 9.23 (s, 1H), 7.54 – 7.44 (m, 2H), 6.92 – 6.83 (m, 2H), 6.67 (s, 1H), 6.58 (s, 1H), 3.90 (s, 3H), 3.87 (s, 3H), 3.83 (s, 1H), 3.81 (s, 3H), 3.41 (q, J = 7.0 Hz, 1H), 2.89 (t, J = 7.0 Hz, 2H), 2.86 – 2.77 (m, 2H), 1.43 (d, J = 7.0 Hz, 3H); MS: m/z 371.2 (M+1).

2-(6,7-dimethoxy-3,4-dihydroisoquinolin-2(1H)-yl)-N-(4-fluorophenyl)propanamide (9g)

White solid; IR (KBr, v, cm^{-1}): 3388, 3059, 2941, 2906, 2831, 2777, 1691, 1612, 1517, 1224, 1161, 1112; ^1H NMR (400 MHz, $CDCl_3$): δ 9.37 (s, 1H), 7.56 – 7.51 (m, 2H), 7.02 (t, *J* = 8.7 Hz, 2H), 6.66 (s, 1H), 6.58 (s, 1H), 3.88 (d, *J* = 8.8 Hz, 7H), 3.74 – 3.69 (m, 1H), 3.43 (t, *J* = 7.1 Hz, 1H), 2.90 (d, *J* = 5.7 Hz, 2H), 2.84 (dd, *J* = 11.2, 5.2 Hz, 2H), 1.43 (d, *J* = 7.0 Hz, 3H); MS: m/z 359.2 (M+1).

N-(2-chlorophenyl)-2-(6,7-dimethoxy-3,4-dihydroisoquinolin-2(1H)-yl)propanamide (9h)

White solid; IR (KBr, v, cm^{-1}): 3283, 3115, 2983, 2949, 2831, 1687, 1593, 1517, 1344, 1255, 1214, 1109; ^1H NMR (400 MHz, $CDCl_3$): δ 10.07 (s, 1H), 8.49 (dd, *J* = 8.3, 1.5 Hz, 1H), 7.38 – 7.29 (m, 2H), 7.04 (td, *J* = 7.8, 1.5 Hz, 1H), 6.66 (s, 1H), 6.57 (s, 1H), 3.87 (s, 7H), 3.73 (d, *J* = 14.2 Hz, 1H), 3.48 (d, *J* = 7.0 Hz, 1H), 2.95 (dd, *J* = 8.8, 5.2 Hz, 2H), 2.85 (dd, *J* = 10.9, 5.4 Hz, 2H), 1.46 (d, *J* = 7.0 Hz, 3H); MS: m/z 375.1 (M+1), 377.1 (M+3).

N-(3-chlorophenyl)-2-(6,7-dimethoxy-3,4-dihydroisoquinolin-2(1H)-yl)propanamide (9i)

White solid; IR (KBr, v, cm^{-1}): 3287, 2923, 2842, 1691, 1588, 1527, 1334, 1245, 1223, 1151; ^1H NMR (400 MHz, $CDCl_3$): δ 9.44 (s, 1H), 7.70 (t, *J* = 2.0 Hz, 1H), 7.42 (ddd, *J* = 8.2, 2.0, 0.9 Hz, 1H), 7.24 (t, *J* = 8.1 Hz, 1H), 7.08 (ddd, *J* = 8.0, 2.0, 1.0 Hz, 1H), 6.67 (s, 1H), 6.57 (s, 1H), 3.88 (d, *J* = 9.8 Hz, 7H), 3.73 (s, 1H), 3.44 (s, 1H), 2.90 (d, *J* = 5.8 Hz, 2H), 2.82 (td, *J* = 11.0, 5.2 Hz, 2H), 1.43 (d, *J* = 7.0 Hz, 3H); MS: m/z 375.1 (M+1), 377.1 (M+3).

N-(4-chlorophenyl)-2-(6,7-dimethoxy-3,4-dihydroisoquinolin-2(1H)-yl)propanamide (9j)

White solid; IR (KBr, v, cm^{-1}): 3286, 3066, 2987, 2941, 2831, 1680, 1583, 1517, 1396, 1255, 1222; ^1H NMR (400 MHz, CDCl3): δ 9.41 (s, 1H), 7.53 (d, *J* = 8.8 Hz, 2H), 7.30 (s, 2H), 6.67

(s, 1H), 6.57 (s, 1H), 3.90 (s, 3H), 3.85 (d, *J* = 17.3 Hz, 4H), 3.71 (d, *J* = 14.0 Hz, 1H), 3.43 (q, *J* = 7.0 Hz, 1H), 2.93 – 2.88 (m, 2H), 2.86 – 2.77 (m, 2H), 1.43 (d, J = 7.0 Hz, 3H); MS: m/z 375.1 (M+1), 377.1 (M+3).

2-(6,7-dimethoxy-3,4-dihydroisoquinolin-2(1H)-yl)-N-(2-(trifluoromethyl)phenyl) propanamide (9k)

White solid; IR (KBr, v, cm^{-1}): 3290, 2920, 2846, 1693, 1598, 1517, 1334, 1255, 1222, 1161; ^1H NMR (400 MHz, $CDCl_3$): δ 9.53 (s, 1H), 7.89 (s, 1H), 7.77 (d, *J* = 8.2 Hz, 1H), 7.45 (t, *J* = 7.9 Hz, 1H), 7.36 (d, *J* = 7.8 Hz, 1H), 6.68 (s, 1H), 6.58 (s, 1H), 3.89 (d, *J* = 10.7 Hz, 7H), 3.74 (s, 1H), 3.46 (d, *J* = 7.0 Hz, 1H), 2.94 – 2.89 (m, 2H), 2.84 (dd, *J* = 10.9, 5.4 Hz, 2H), 1.44 (d, *J* = 7.0 Hz, 3H); MS: m/z 409.2 (M+1).

2-(6,7-dimethoxy-3,4-dihydroisoquinolin-2(1H)-yl)-N-(3-(trifluoromethyl)phenyl)-propanamide (9l)

White solid; IR (KBr, v, cm^{-1}): 3292, 2943, 2904, 2767, 2563, 1697, 1614, 1517, 1228, 1122; ^1H NMR (400 MHz, $CDCl_3$): δ 9.42 (s, 1H), 7.30 (t, *J* = 2.0 Hz, 1H), 7.40 (ddd, *J* = 8.2, 2.0, 0.9 Hz, 1H), 7.24 (t, *J* = 8.1 Hz, 1H), 7.06 (ddd, *J* = 8.0, 2.0, 1.0 Hz, 1H), 6.67 (s, 1H), 6.67 (s, 1H), 3.78 (d, *J* = 9.8 Hz, 7H), 3.73 (s, 1H), 3.42 (s, 1H), 2.60 (d, *J* = 5.8 Hz, 2H), 2.84 (td, *J* = 11.0, 5.2 Hz, 2H), 1.42 (d, *J* = 7.0 Hz, 3H); MS: m/z 409.2 (M+1).

2-(6,7-dimethoxy-3,4-dihydroisoquinolin-2(1H)-yl)-N-(4-nitrophenyl) propanamide (9m)

Pale yellow solid; IR (KBr, v, cm^{-1}): 3280, 3113, 2989, 2949, 2831, 1697, 1593, 1517, 1334, 1255, 1224, 1109, 1028; ^1H NMR (400 MHz, $CDCl_3$): δ 9.80 (s, 1H), 8.25 – 8.21 (m, 2H), 7.75 (d, *J* = 9.2 Hz, 2H), 6.68 (s, 1H), 6.58 (s, 1H), 3.89 (d, *J* = 11.5 Hz, 7H), 3.75 (s, 1H), 3.49 (d, *J* = 7.0 Hz, 1H), 2.93 – 2.89 (m, 2H), 2.87 – 2.79 (m, 2H), 1.45 (d, *J* = 7.0 Hz, 3H); MS: m/z 386.2 (M+1).

2-(6,7-dimethoxy-3,4-dihydroisoquinolin-2(1H)-yl)-N-(2,4-dimethylphenyl) propanamide (9n)

White solid; IR (KBr, v, cm^{-1}): 3263, 2985, 2933, 2825, 1680, 1589, 1517, 1255, 1220, 1112; ^1H NMR (400 MHz, $CDCl_3$): δ 9.30 (s, 1H), 7.95 (d, *J* = 8.2 Hz, 1H), 7.04 (d, *J* = 8.0 Hz, 1H), 6.98 (s, 1H), 6.65 (s, 1H), 6.55 (s, 1H), 3.86 (t, *J* = 14.6 Hz, 7H), 3.73 (s, 1H), 3.44 (d, *J* = 7.0 Hz, 1H), 2.90 (dd, *J* = 8.9, 6.3 Hz, 4H), 2.30 (s, 3H), 2.13 (s, 3H), 1.46 (d, *J* = 7.0 Hz, 3H); MS: m/z 369.1 (M+1).

2-(6,7-dimethoxy-3,4-dihydroisoquinolin-2(1H)-yl)-N-(3,4-dimethylphenyl) propanamide (9o)

White solid; IR (KBr, v, cm^{-1}): 3307, 2995, 2937, 2904, 2831, 2779, 1680, 1616, 1517, 1463, 1253, 1222, 1138; ^1H NMR (400 MHz, $CDCl_3$): δ 9.22 (s, 1H), 7.37 (d, *J* = 2.0 Hz, 1H), 7.33 – 7.29 (m, 1H), 7.09 (d, *J* = 8.1 Hz, 1H), 6.67 (s, 1H), 6.57 (s, 1H), 3.88 (d, *J* = 9.9 Hz, 7H),

3.70 (d, *J* = 14.3 Hz, 1H), 3.40 (d, *J* = 7.0 Hz, 1H), 2.89 (d, *J* = 5.8 Hz, 2H), 2.82 (d, *J* = 6.4 Hz, 2H), 2.25 (d, *J* = 9.1 Hz, 6H), 1.43 (d, *J* = 7.0 Hz, 3H); MS: m/z 369.1 (M+1).

5.2.3 Synthesis and characterization of *N*'-benzylidene-2-(6,7-dimethoxy-3,4-dihydroisoquinolin-2(*1H*)-yl)acetohydrazide derivatives (14a-k)

The synthetic route followed for the target compounds **14a-k,** is illustrated in scheme **3**. Synthesis of target compounds involved sequence of reactions, first step involved reaction between 6,7-dimethoxy tetrahydroisoquinoline hydrochloride (**4**) with ethyl-2-bromoacetate (**10**), which afforded intermediate **11.** In further step, intermediate **11** was treated with hydrazine hydrate which involved the replacement of ethoxy group with hydrazine and afforded the intermediate **12.** Final reaction involved the formation of Schiff base between intermediate **12** and different aldehydes **(13a-k)**, which afforded the final compounds (**14a-k**) in moderate to excellent yield.

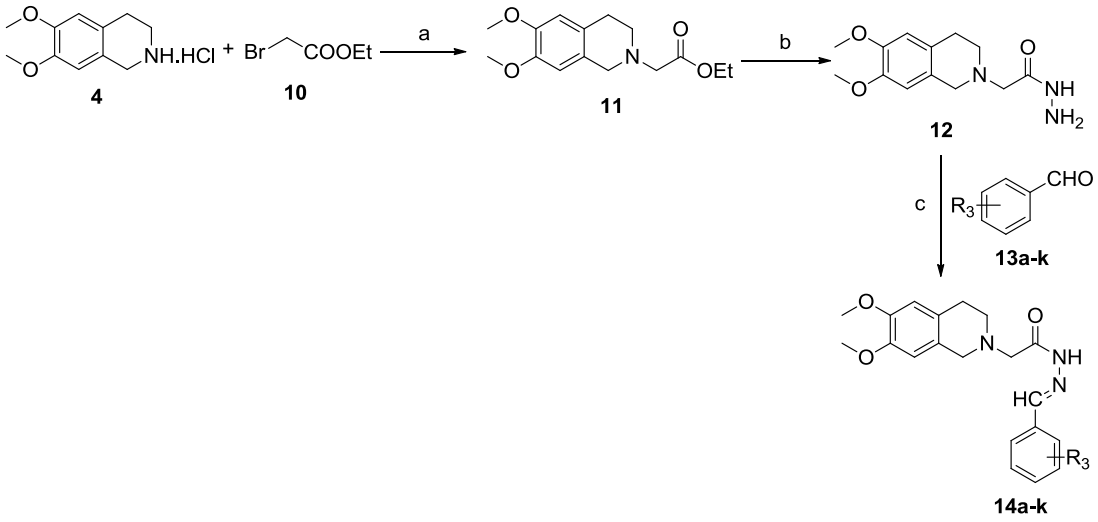

Scheme 3. Reagents and conditions: (a) DMF, Et_3N, K_2CO_3, 100˚C, 6 h (b) NH_2-NH_2.H_2O, EtOH, catalytic glacial AcOH, reflux 12 h (c) EtOH, catalytic AcOH, reflux 1-2 h

Synthesis of ethyl 2-(6,7-dimethoxy-3,4-dihydroisoquinolin-2(*1H*)-yl)acetate (**11**)

Potassium carbonate (6.94 g, 50 mmol) and triethylamine (4.04 g, 40 mmol) was added to stirred reaction mixture of starting material **4** (4.58g, 20 mmol) in DMF. Reaction was stirred at 80˚C for half an hour, after that allowed to stir at room temperature. Ethyl-2-bromoacetate (**10**) (1.65g, 10 mmol) was added dropwise to the stirring reaction mixture, reaction was further stirred at 100˚C, the progress of the reaction was monitored by TLC. After completion of reaction (after six hours), the reaction mass was cooled to rt and poured into conical flask containing ice-cold water (100 ml). The reaction mixture was twice extracted with ethyl acetate (2x100 ml) and combined ethyl acetate layer was washed with brine (200 ml), dried

over sodium sulphate and evaporated on rotatory evaporator to afford the intermediate **11** as oily liquid with 92% yield.

Synthesis of 2-(6,7-dimethoxy-3,4-dihydroisoquinolin-2(*1H*)-yl)acetohydrazide (12)

To the stirring reaction mixture of intermediate **11** (4.18 g, 15 mmol) in ethanol, hydrazine hydrate (2.25 g, 45 mmol) was added dropwise, followed by catalytic amount of glacial acetic acid was added. The reaction mixture was refluxed and progress of the reaction was monitored by TLC. After completion of reaction as per TLC (after 12 hours refluxing), ethanol was evaporated under reduced pressure, water was added (75 ml) to the reaction mass. Further, the reaction mass was extracted with 2% methanol in DCM four times (4x75 ml). Combined organic layer was dried over anhydrous sodium sulfate and evaporated under reduced pressure to afford the desired product **12** as white solid with 84% yield [3].

General procedure for the synthesis of *N′*-benzylidene-2-(6,7-dimethoxy-3,4-dihydroisoquinolin-2(*1H*)-yl)acetohydrazide derivatives (14a-k)

Intermediate acetohydrazide **12** (0.265g, 1 mmol) was added to the stirring solution of respective aldehyde (**13a-k**, 1 mmol) in ethanol containing catalytic amount of glacial acetic acid. The reaction mixture was refluxed for 1 to 2 hours; the progress of the reaction was monitored by TLC. After completion of the reaction, ethanol was evaporated; ethyl acetate (20 ml) was added to the reaction mass. Ethyl acetate layer was twice washed with distilled water (2x20 ml) and then with brine water (20 ml). The organic layer was dried over anhydrous sodium sulphate and finally evaporated on the rotary evaporator to afford the final derivatives **14a-k** [4]. Preliminary characteristics data of the synthesized compounds **14a-k** are shown in Table **5.3.**

Table 5.3 Preliminary characteristics data of compounds **14a-k**

Comp. code	R_3	Mol. formula	Mol. Wt	% yield	Melting point (˚C)
14a	2-CH_3	$C_{21}H_{25}N_3O_3$	367.19	72	152-155
14b	3-OCH_3	$C_{21}H_{25}N_3O_4$	383.18	77	136-138
14c	4-OCH_3	$C_{21}H_{25}N_3O_4$	383.18	72	94-96
14d	4-F	$C_{20}H_{22}FN_3O_3$	371.16	82	136-137
14e	2-Cl	$C_{20}H_{22}ClN_3O_3$	387.13	83	170-173
14f	4-Cl	$C_{20}H_{22}ClN_3O_3$	387.13	78	98-100
14g	3-Br	$C_{20}H_{22}BrN_3O_3$	431.08	75	96-99
14h	4-Br	$C_{20}H_{22}BrN_3O_3$	431.08	72	86-88
14i	4-NO_2	$C_{20}H_{22}N_4O_5$	398.16	81	162-164
14j	4-CN	$C_{21}H_{22}N_4O_3$	378.17	68	140-143
14k	3,4,5-tri-MeO	$C_{23}H_{29}N_3O_6$	443.21	66	156-157

Spectral characterization of compounds (14a-k)

Synthesized compounds were characterized by spectral analysis such as IR, Mass and three compounds were characterized by ^{1}H NMR. The IR spectra of compounds **14a-k** showed the absorption peak at 3196–3248 cm^{-1} (strong, broad) corresponding to the stretching of amidic hydrogen (−CO**NH**-). Further, a prominent absorption at the region 1674-1703 cm^{-1} appeared due to stretching of the carbonyl group (−**CO**NH-). ^{1}H proton NMR of six representative compounds (**14c, 14d, 14e, 14g, 14i, 14j,** and **14k**) showed peak of four protons present at the 3rd and 4th position of THIQ ring at around δ~2.6-3.1. Two protons present at the carbon between nitrogen and carbonyl group appeared at around δ~3.1-3.6. A pair of protons at the first carbon of THIQ appeared at δ~3.7-3.9, merged with six methoxy protons (at the 6th and 7th carbon of THIQ) in majority of compounds. Two aromatic protons present at 5th and 8th position of THIQ showed corresponding peaks at δ~6.4-6.6. One benzylidene proton (-N=C**H**-) appeared at δ~8.2 and amidic proton (-CON**H**-) appeared at δ~8-10. Counting and position of other protons present at the phenyl ring also appeared in accordance with their proposed structures. Further, mass spectra of compounds showed the corresponding M+1 peak. Detailed spectral data of compounds **14a-k** are given below;

2-(6,7-dimethoxy-3,4-dihydroisoquinolin-2(1H)-yl)-N'-(2-methylbenzylidene) acetohydrazide (14a)

White solid; IR (KBr, v, cm^{-1}): 3244, 2939, 2908, 2567, 1697, 1517, 1454, 1369, 1255, 1217, 1141; MS: m/z 368.3 (M+1).

2-(6,7-dimethoxy-3,4-dihydroisoquinolin-2(1H)-yl)-N'-(3-methoxybenzylidene) acetohydrazide (14b)

White solid; IR (KBr, v, cm^{-1}): 3242, 2997, 2941, 2902, 1703, 1571, 1517, 1317, 1288, 1253, 1083; MS: m/z 384.2 (M+1).

(2-(6,7-dimethoxy-3,4-dihydroisoquinolin-2(1H)-yl)-N'-(4-methoxybenzylidene) acetohydrazide (14c)

White solid; IR (KBr, v, cm^{-1}): 3211, 2904, 2831, 1701, 1503, 1333, 1251, 1165, 1026; 1H NMR (400 MHz, $CDCl_3$) δ 8.20 (s, 1H), 7.65 (d, *J* = 8.4 Hz, 2H), 7.45 (d, *J* = 7.7 Hz, 1H), 6.87 (d, *J* = 8.4 Hz, 2H), 6.65 (s, 1H), 6.55 (s, 1H), 3.88 – 3.82 (m, 11H), 3.28 (s, 2H), 3.08 (d, *J* = 24.0 Hz, 4H); MS: m/z 384.2 (M+1).

2-(6,7-dimethoxy-3,4-dihydroisoquinolin-2(1H)-yl)-N'-(4-fluorobenzylidene) acetohydrazide (14d)

White solid; IR (KBr, v, cm^{-1}): 3215, 3055, 2991, 2939, 2827, 1674, 1506, 1257, 1234, 1076; 1H NMR (400 MHz, $CDCl_3$) δ 8.20 (s, 1H), 7.74 (dd, *J* = 8.7, 5.4 Hz, 2H), 7.55 (d, *J* = 9.0 Hz,

1H), 7.08 (t, *J* = 8.6 Hz, 2H), 6.66 (s, 1H), 6.55 (s, 1H), 3.87 (dd, *J* = 11.8, 6.2 Hz, 8H), 3.56 (s, 2H), 3.07 (s, 2H), 2.99 (d, *J* = 5.1 Hz, 2H); MS: m/z 372.2 (M+1).

N'-(2-chlorobenzylidene)-2-(6,7-dimethoxy-3,4-dihydroisoquinolin-2(1H)-yl) acetohydrazide (14e)

White solid; IR (KBr, v, cm^{-1}): 3196, 2993, 2931, 2900, 2810, 1680, 1517, 1367, 1230, 1143, 1047; 1H NMR (400 MHz, $CDCl_3$) δ 10.05 (s, 1H), 8.33 – 8.22 (m, 1H), 7.96 (d, J = 7.3 Hz, 1H), 7.14 – 7.11 (m, 1H), 7.07 – 7.05 (m, 1H), 6.43 (s, 1H), 6.31 (s, 1H), 3.70 – 3.58 (m, 7H), 3.50 (s, 2H), 3.16 (t, J = 3.8 Hz, 2H), 2.68 (d, J = 3.9 Hz, 4H); MS: m/z 388.1 (M+1), 390.2 (M+3).

N'-(4-chlorobenzylidene)-2-(6,7-dimethoxy-3,4-dihydroisoquinolin-2(1H)-yl) acetohydrazide (14f)

White solid; IR (KBr, v, cm^{-1}): 3205, 3190, 2991, 2941, 2831, 1680, 1517, 1359, 1257, 1228, 1122, 1087; MS: m/z 388.1 (M+1), 390.2 (M+3).

N'-(3-bromobenzylidene)-2-(6,7-dimethoxy-3,4-dihydroisoquinolin-2(1H)-yl) acetohydrazide (14g)

White solid; IR (KBr, v, cm^{-1}): 3226, 3055, 2922, 2821, 1691, 1517, 1467, 1259, 1120, 1022; 1H NMR (400 MHz, $CDCl_3$) δ 10.05 (s, 1H), 10.29 (s, 1H), 8.51 (d, J = 6.4 Hz, 1H), 8.22 – 8.19 (m, 1H), 7.37 – 7.28 (m, 3H), 6.67 (s, 1H), 6.55 (s, 1H), 3.89 (s, 3H), 3.87 (s, 3H), 3.75 (s, 2H), 3.41 (s, 2H), 2.94-2.90 (m, 4H); MS: m/z 432.1 (M+1), 434.1 (M+3).

N'-(4-bromobenzylidene)-2-(6,7-dimethoxy-3,4-dihydroisoquinolin-2(1H)-yl) acetohydrazide (14h)

White solid; IR (KBr, v, cm^{-1}): 3248, 3012, 2900, 1691, 1517, 1359, 1261, 1228, 1120, 1066; MS: m/z 432.1 (M+1), 434.1 (M+3).

2-(6,7-dimethoxy-3,4-dihydroisoquinolin-2(1H)-yl)-N'-(4-nitrobenzylidene) acetohydrazide (14i)

White solid; IR (KBr, v, cm^{-1}): 3213, 2999, 2935, 2833, 1680, 1517, 1346, 1230, 1141, 1107; 1H NMR (400 MHz, $CDCl_3$) δ 10.43 (s, 1H), 8.35 (s, 1H), 8.26 (d, *J* = 8.1 Hz, 2H), 7.92 (d, *J* = 8.2 Hz, 2H), 6.67 (s, 1H), 6.54 (s, 1H), 3.88 (d, *J* = 12.6 Hz, 6H), 3.74 (s, 2H), 3.42 (s, 2H), 2.93 (s, 4H); MS: m/z 399.3 (M+1).

(4-cyanobenzylidene)-2-(6,7-dimethoxy-3,4-dihydroisoquinolin-2(1H)-yl) acetohydrazide (14j)

White solid; IR (KBr, v, cm^{-1}): 3207, 2945, 2831, 2223, 1691, 1517, 1274, 1255, 1141, 1074; 1H NMR (400 MHz, $CDCl_3$) δ 8.30 (s, 1H), 7.86 (d, J = 8.4 Hz, 2H), 7.70 (d, J = 8.4 Hz, 2H), 6.67 (s, 1H), 6.55 (s, 1H), 3.95 – 3.79 (m, 8H), 3.51 (s, 2H), 2.99 (s, 4H); MS: m/z 379.2 (M+1).

2-(6,7-dimethoxy-3,4-dihydroisoquinolin-2(1H)-yl)-N'-(3,4,5-trimethoxy benzylidene)acetohydrazide (14k)

White solid, IR (KBr, v, cm^{-1}): 3213, 2924, 2835, 1676, 1577, 1517, 1415, 1336, 1230, 1126, 1001; 1H NMR (400 MHz, $CDCl_3$) δ 8.59 (s, 1H), 8.18 (s, 1H), 6.97 (s, 2H), 6.65 (s, 1H), 6.54 (s, 1H), 3.89 (s, 15H), 3.85 (s, 2H), 3.60 (s, 2H), 3.11 (s, 2H), 3.00 (s, 2H); MS: m/z 444.3 (M+1).

5.2.4 Synthesis and characterization of 1-(6,7-dimethoxy-3,4-dihydroisoquinolin-2(*1H*)-yl)-2-(phenylamino)ethanone derivatives (17a-o)

Synthesis of final compounds **17a-o** was achieved in two steps, the first step involved the reaction of starting material 6,7-dimethoxy tetrahydroisoquinoline hydrochloride (**4**) with chloroacetyl chloride (**2**) which afforded the chloro ethanone intermediate (**15**) in good yield. Further, in order to optimize the second step, several reaction conditions were tried (details are given in table **4.4**) but finally microwave assisted synthesis under neat condition (b9, table **4.4**) was found to be suitable. Hence the titled compounds **(17a-o)** were synthesized using this approach.

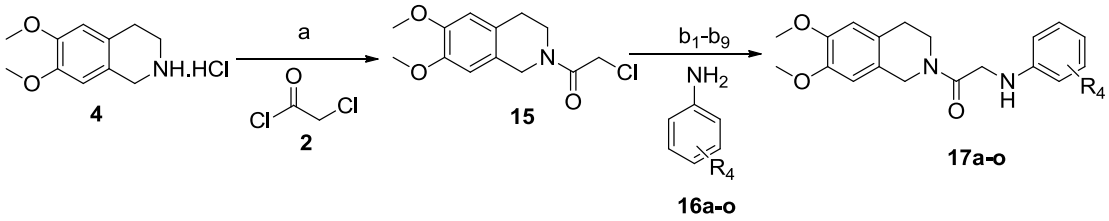

Scheme 4. Reagents and conditions: (a) DCM, Et_3N, 0˚C-rt, 2.5 h (b_1-b_9) Different conditions were tried using conventional as well as microwave assisted approach (Table **4.4**)

General procedure for the synthesis of 2-chloro-1-(6,7-dimethoxy-3,4 dihydro isoquinolin-2(*1H*)-yl)ethanone (15)

Chloroacetyl chloride **2** (2.24 g, 20 mmol) was added dropwise to the ice-cold stirring solution of starting material **4** (4.6 g, 20 mmol) in DCM, containing triethylamine (5.05 g, 50 mmol) as a base. The reaction was further stirred at room temprature for two hours until completion of reaction as per TLC. After completion of reaction, DCM layer was twice washed with distilled water (2x100 ml) and then with brine water (100 ml). DCM layer was dried over sodium sulphate and finally evaporated on rotary evaporator to afford the crude intermediate **15.** Crude intermediate compound **15** was purified by column chromatogrphy using ethyl acetate and hexane as mobile phase (5% ethyl acetate in hexane) and silica as

stationary phase (mesh size 100-200), which afforded intermediate **15** as pure white solid with 83% yield.

Optimization of the reaction conditions to obtain titled compounds (17a-o) using different conditions (exemplified as 17a)

For the synthesis of titled compounds **17a-o**, the second step was planned via reaction of intermediate **15** with substituted anilines **(16a-o)**. In order to attain suitable reaction conditions, both conventional and microwave assisted synthetic approaches using different reaction conditions were tried. As a model reaction, for the synthesis of compound **17a**, intermediate **15** and o-methoxy aniline **(16a)** were taken in the molar ratio (1:1). Several reaction conditions were evaluated (entry b_1-b_9, Table **4.4**) for optimization of reaction depicted in scheme **4**. In the first attempt, conventional approach was tried in acetonitrile using potassium carbonate as a base (2.5 equivalents). After refluxing for 10 h, no new spot was appeared in TLC. When the same condition was tried in ethanol as solvent, one new spot was detected with low intensity in TLC but after refluxing for 10 h also no significant increment in the product was observed. Above formed new spot was isolated, subjected to column chromatography which afforded the desired product but in very low yield (10%). Again no significant improvement in reaction was noticed when the reaction was tried in THF as solvent using triethylamine as base. When reaction was tried in DMF after taking potassium carbonate as a base (2.5 equivalents), no significant conversion took place at rt, however, upon heating the reaction mixture at 100˚C for 6 h, around 15% of the desired product was obtained. When the reaction was again tried in DMF as solvent by extending reaction time to 12 h under similar conditions, multiple spots appeared on the TLC.

Further, the two conventional approaches in which desired product in low yield was obtained (Entry no. 2 and 5 of Table **5.4**) were subjected under microwave irradiation to 300 W at 100˚C with same solvent and base. Slight enhancement in the yield was observed as compared to the conventional method but it was not significant. When the reaction was tried using solvent free microwave irradiation under similar conditions taking potassium carbonate as base, surprisingly in a short time of 3 min, good yield of **17a** was obtained (73%). Further, similar microwave approach was applied (entry **b_9**) for the reaction of intermediate **15** with substituted anilines (**16b-o**) which afforded the final products **17b-o** in moderate to good yield (66–84%) (Table **5.5**).

Table 5.4 Optimization of reaction conditions (scheme **4**, b_1-b_9) to obtain compound **17a**

Entry ID	Method	Condition	T (˚C)	Time	Yield %
b_1	Conventional	K_2CO_3,CH_3CN	85	10 h	No reaction[a]
b_2	Conventional	K_2CO_3, EtOH	90	10 h	11
b_3	Conventional	Et_3N, THF	80	10 h	No reaction[a]
b_4	Conventional	K_2CO_3, DMF	rt	10 h	No reaction[a]
b_5	Conventional	K_2CO_3, DMF	100	6 h	15
b_6	Conventional	K_2CO_3, DMF	100	12 h	Multiple spots on TLC
b_7	Microwave	K_2CO_3, EtOH	100	3 min	21
b_8	Microwave	K_2CO_3, DMF	100	3 min	27
b_9	Microwave	K_2CO_3, Neat	100	3 min	73

[a] Starting material recovered

General procedure (optimized) for the synthesis of compounds 17a-o by microwave irradiation method

Substituted aniline (**16a-o**, 1 mmol) and chloro intermediate **15** (0.27g, 1 mmol) was taken in microwave reaction vial in the presence of potassium carbonate as a base (0.347g, 2.5 mmol). The microwave oven was programmed at 300 W at 100˚C, the progress of the reaction was monitored using TLC. After completion of reaction (2-4.5 min), ice-cold water (15 ml) was added to the reaction mixture which resulted in precipitation of the product. The solid product was filtered off and washed thrice with cold water (3×20 ml), then washed with hexane (10 ml) and dried to afford the final products **17a-o** [5]**.** Preliminary characteristics data of the synthesized compounds **17a-o** are shown in Table **5.5**.

Table 5.5 Preliminary characteristics data of compounds **17a-o**

Comp. code	R_4	Mol. formula	Mol. Wt	% yield	Melting point (˚C)
17a	2-OCH_3	$C_{20}H_{24}N_2O_4$	356.17	73	90-92
17b	3-OCH_3	$C_{20}H_{24}N_2O_4$	356.17	79	118-121
17c	4-OCH_3	$C_{20}H_{24}N_2O_4$	356.17	83	116-117
17d	3-F	$C_{19}H_{21}FN_2O_3$	344.15	76	144-146
17e	4-F	$C_{19}H_{21}FN_2O_3$	344.15	81	126-128
17f	2-Cl	$C_{19}H_{21}ClN_2O_3$	360.12	68	104-105
17g	3-Cl	$C_{19}H_{21}ClN_2O_3$	360.12	84	136-138
17h	4-Cl	$C_{19}H_{21}ClN_2O_3$	360.12	75	116-118
17i	2-Br	$C_{19}H_{21}BrN_2O_3$	404.07	68	108-110
17j	3-Br	$C_{19}H_{21}BrN_2O_3$	404.07	75	124-127
17k	4-Br	$C_{19}H_{21}BrN_2O_3$	404.07	72	116-118
17l	4-CN	$C_{20}H_{21}N_3O_3$	351.16	68	146-148
17m	3-$COCH_3$	$C_{21}H_{24}N_2O_4$	368.17	66	112-114
17n	3-CF_3	$C_{20}H_{21}F_3N_2O_3$	394.15	76	134-137
17o	2,5-di-Me	$C_{21}H_{26}N_2O_3$	354.19	75	140-143

Spectral characterization of compounds (17a-o)

Synthesized compounds (**17a-o**) were characterized by IR, ^{1}H NMR, ESI-MS and elemental analysis, while four representative compounds were also characterized by ^{13}C NMR. IR spectra of titled compounds showed the characteristic absorption peak at 1640-1665 cm^{-1} (strong) corresponding to C=O stretching of the amide group. Apart from this, absorption peaks in the region 3350-3420 cm^{-1} (strong, sharp) appeared in spectra of all compounds corresponding to N-H stretching. Other distinguishable strong absorption peak appeared at 2208 cm^{-1} in the IR spectra of compound **17l** due to presence of nitrile (CN) group. In the ^{1}H NMR spectra of titled compounds, a pair of aliphatic protons at the 4th position of THIQ ring appeared at δ~2.8-2.9, while two protons present at the 3rd position of THIQ exhibited two different peaks with δ value around 3.6-3.8. Characteristics peaks corresponding to six methoxy hydrogens (at 6th and 7th position of THIQ) appeared between δ values 3.80-3.95. A pair of non-cyclic protons at the carbon between carbonyl and NH appeared as singlet at δ~3.9-4.0. Furthermore, pair of protons at the 1st position of THIQ appeared as two discrete singlets at δ~4.5-4.8, this may be due to the fact that presence of adjacent amide linkage at 2th position hindered the free movement of this proton pair. Two aromatic protons of THIQ (at 5th and 8th position) appeared at δ~6.6-6.7. Apart from this, depending upon the type and position of substitution present on aniline ring, corresponding peaks were noticed in the ^{1}H NMR spectra. Numbers of peak counting as well as their position in the ^{13}C NMR of four representative compounds (**17a, 17d, 17j** and **17n**) were found in accordance with the proposed structure, for example, a peak at δ~164-167 appeared in the ^{13}C NMR spectra of above compounds corresponding to the carbon of amide group. The elemental compositions determined using C H N analyzer revealed that experimental values were found in agreement with the calculated ones. ESI-MS of the synthesized compounds showed the corresponding M+1 peak. The purity of one compound **17b** (as a representative compound) was assured by LCMS (>99% purity).

1-(6,7-dimethoxy-3,4-dihydroisoquinolin-2(1H)-yl)-2-(2-methoxyphenylamino) ethanone (17a)

White solid; IR (KBr, v, cm^{-1}): 3419, 3062, 2991, 2833, 1656, 1604, 1514, 1415, 1263, 1234, 1118; ^{1}H NMR (400 MHz, $CDCl_3$) δ 7.32 (dd, *J* = 9.4, 4.5 Hz, 1H), 7.12 (s, 1H), 6.69 – 6.64 (m, 2H), 6.64 – 6.53 (m, 2H), 4.76 (s, 1H), 4.58 (s, 1H), 4.06 (s, 1H), 3.93 (t, *J* = 5.9 Hz, 1H), 3.91 – 3.83 (m, 7H), 3.76 (s, 3H), 3.70 (t, *J* = 5.9 Hz, 1H), 2.92 (t, *J* = 5.7 Hz, 1H), 2.86 (t, *J* = 5.7 Hz, 1H); ^{13}C NMR (100 MHz, $CDCl_3$, ppm) 25.64, 36.91, 39.03, 40.99, 52.28, 52.81, 105.77, 106.43, 106.82, 113.79, 117.88, 120.28, 121.76, 122.43, 123.72, 134.36, 144.13, 144.66, 164.87; Anal. Calcd. for $C_{20}H_{24}N_2O_4$: C, 67.40; H, 6.79; N, 7.86. Found: C, 67.52; H, 6.84; N, 7.83; MS: m/z 357.2 (M+1).

1-(6,7-dimethoxy-3,4-dihydroisoquinolin-2(1H)-yl)-2-(3-methoxyphenylamino) ethanone (17b)

White solid; IR (KBr, v, cm^{-1}): 3361, 2999, 2953, 2833, 1643, 1606, 1517, 1421, 1224, 1163, 1112; ^{1}H NMR (400 MHz, $CDCl_3$) δ 7.13 (t, *J* = 8.1 Hz, 1H), 6.74 – 6.60 (m, 2H), 6.32 (dt, *J* = 5.8, 3.0 Hz, 2H), 6.22 (d, *J* = 1.7 Hz, 1H), 4.74 (s, 1H), 4.56 (s, 1H), 3.97 (s, 2H), 3.94 – 3.86 (m, 7H), 3.81 (s, 3H), 3.68 (t, *J* = 5.9 Hz, 1H), 2.89 (t, *J* = 5.9 Hz, 1H), 2.83 (t, *J* = 5.9 Hz, 1H); Anal. Calcd. for $C_{20}H_{24}N_2O_4$: C, 67.40; H, 6.79; N, 7.86. Found: C, 67.43; H, 6.85; N, 7.85; MS: m/z 357.2 (M+1).

1-(6,7-dimethoxy-3,4-dihydroisoquinolin-2(1H)-yl)-2-(4-methoxyphenylamino) ethanone (17c)

White solid; IR (KBr, v, cm^{-1}): 3356, 2951, 2833, 1643, 1517, 1365, 1253, 1211, 1114, 821; ^{1}H NMR (400 MHz, $CDCl_3$) δ 6.83 (d, *J* = 8.5 Hz, 2H), 6.72 – 6.58 (m, 4H), 4.74 (s, 1H), 4.57 (s, 1H), 3.96 (s, 2H), 3.93 – 3.86 (m, 7H), 3.78 (s, 3H), 3.69 (t, *J* = 5.9 Hz, 1H), 2.89 (t, *J* = 5.6 Hz, 1H), 2.83 (t, *J* = 5.7 Hz, 1H); Anal. Calcd. for $C_{20}H_{24}N_2O_4$: C, 67.40; H, 6.79; N, 7.86 Found: C, 67.45; H, 6.82; N, 7.89; MS: m/z 357.2 (M+1).

1-(6,7-dimethoxy-3,4-dihydroisoquinolin-2(1H)-yl)-2-(3-fluorophenylamino) ethanone (17d)

White solid; IR (KBr, v, cm^{-1}): 3361, 2981, 2910, 2833, 1656, 1612, 1517 1433, 1365, 1253, 1222, 1112; ^{1}H NMR (400 MHz, $CDCl_3$) δ 7.19 – 7.08 (m, 1H), 6.69 – 6.65 (m, 2H), 6.49 – 6.38 (m, 2H), 6.34 (dq, *J* = 11.5, 2.3 Hz, 1H), 4.75 (s, 1H), 4.57 (s, 1H), 3.96 (d, *J* = 2.4 Hz, 2H), 3.93 – 3.88 (m, 7H), 3.69 (t, *J* = 5.9 Hz, 1H), 2.87 (dt, *J* = 25.9, 5.8 Hz, 2H); ^{13}C NMR (100 MHz, $CDCl_3$, ppm) 28.73, 40.19, 42.11, 44.23, 56.01, 56.05, 99.35, 99.60, 103.74, 103.92, 108.93, 109.40, 111.23, 111.65, 123.19, 124.70, 125.50, 126.76, 130.28, 148.99, 162.91, 165.33, 167.41; Anal. Calcd. for $C_{19}H_{21}FN_2O_3$: C, 66.26; H, 6.15; N, 8.13 Found: C, 66.24; H, 6.19; N, 8.15; MS: m/z 345.2 (M+1).

1-(6,7-dimethoxy-3,4-dihydroisoquinolin-2(1H)-yl)-2-(4-fluorophenylamino) ethanone (17e)

White solid; IR (KBr, v, cm^{-1}): 3365, 2939, 1837, 1643, 1514, 1440, 1265, 1222, 1116; ^{1}H NMR (400 MHz, $CDCl_3$) δ 6.93 (t, *J* = 8.7 Hz, 2H), 6.69 – 6.64 (m, 2H), 6.61 (ddd, *J* = 8.9, 4.3, 2.1 Hz, 2H), 4.85 (s, 1H), 4.74 (s, 1H), 4.57 (s, 1H), 3.95 (s, 2H), 3.91 – 3.85 (m, 7H), 3.69 (t, *J* = 5.9 Hz, 1H), 2.90 (t, *J* = 5.8 Hz, 1H), 2.83 (t, *J* = 5.9 Hz, 1H); Anal. Calcd. for $C_{19}H_{21}FN_2O_3$: C, 66.26; H, 6.15; N, 8.13 Found: C, 66.31; H, 6.18; N, 8.17; MS: m/z 345.2 (M+1).

2-(2-chlorophenylamino)-1-(6,7-dimethoxy-3,4-dihydroisoquinolin-2(1H)-yl) ethanone (17f)

White solid; IR (KBr, v, cm^{-1}): 3379, 2999, 2933, 2835, 1665, 1517, 1485, 1415, 1257, 1228, 1209, 1111; ^1H NMR (400 MHz, $CDCl_3$) δ 7.31 (dd, *J* = 7.9, 1.4 Hz, 1H), 7.17 (t, *J* = 7.7 Hz, 1H), 6.68 (s, 2H), 6.66 – 6.58 (m, 2H), 4.76 (s, 1H), 4.59 (s, 1H), 4.03 (d, *J* = 1.9 Hz, 2H), 3.93 (s, 1H), 3.89 (d, *J* = 3.2 Hz, 6H), 3.70 (t, *J* = 5.9 Hz, 1H), 2.91 (t, *J* = 5.7 Hz, 1H), 2.85 (t, *J* = 5.9 Hz, 1H); Anal. Calcd. for $C_{19}H_{21}ClN_2O_3$: C, 63.24; H, 5.87; N, 7.76 Found: C, 63.14; H, 5.82; N, 7.81; MS: m/z 361.3 (M+1), 363.3 (M+3).

2-(3-chlorophenylamino)-1-(6,7-dimethoxy-3,4-dihydroisoquinolin-2(1H)-yl) ethanone (17g)

White solid; IR (KBr, v, cm^{-1}): 3367, 3053, 2954, 2933, 2833, 1656, 1593, 1514, 1392, 1261, 1228, 1116; ^1H NMR (400 MHz, $CDCl_3$) δ 7.14 – 7.06 (m, 1H), 6.71 (dd, *J* = 7.9, 1.2 Hz, 1H), 6.67 (d, *J* = 3.2 Hz, 2H), 6.63 – 6.60 (m, 1H), 6.56 (dt, *J* = 8.2, 2.2 Hz, 1H), 4.73 (d, *J* = 15.0 Hz, 1H), 4.57 (s, 1H), 3.97 – 3.92 (m, 2H), 3.89 (dd, *J* = 8.1, 5.4 Hz, 7H), 3.68 (t, *J* = 5.9 Hz, 1H), 2.90 (t, *J* = 5.9 Hz, 1H), 2.84 (t, *J* = 5.8 Hz, 1H); Anal. Calcd. for $C_{19}H_{21}ClN_2O_3$: C, 63.24; H, 5.87; N, 7.76 Found: C, 63.27; H, 5.83; N, 7.79; MS: m/z 361.3 (M+1), 363.3 (M+3).

2-(4-chlorophenylamino)-1-(6,7-dimethoxy-3,4-dihydroisoquinolin-2(1H)-yl) ethanone (17h)

White solid; IR (KBr, v, cm^{-1}): 3360, 2927, 2906, 2833, 1658, 1600, 1511, 1433, 1265, 1226, 1124; ^1H NMR (400 MHz, $CDCl_3$) δ 7.16 (d, *J* = 8.7 Hz, 2H), 6.69 – 6.63 (m, 2H), 6.59 (dd, *J* = 8.9, 2.3 Hz, 2H), 4.74 (s, 1H), 4.57 (s, 1H), 3.95 (d, *J* = 2.9 Hz, 2H), 3.92 – 3.87 (m, 7H), 3.68 (s, 1H), 2.90 (t, *J* = 5.9 Hz, 1H), 2.84 (s, 1H); Anal. Calcd. for $C_{19}H_{21}ClN_2O_3$: C, 63.24; H, 5.87; N, 7.76 Found: C, 63.22; H, 5.82; N, 7.72; MS: m/z 361.3 (M+1), 363.3 (M+3).

2-(2-bromophenylamino)-1-(6,7-dimethoxy-3,4-dihydroisoquinolin-2(1H)-yl) ethanone (17i)

White solid; IR (KBr, v, cm^{-1}): 3379, 2999, 2931, 2837, 1649, 1517, 1433, 1442, 1257, 1228, 1207; ^1H NMR (400 MHz, $CDCl_3$) δ 7.50 (dd, *J* = 9.4, 4.5 Hz, 1H), 7.22 (s, 1H), 6.69 – 6.64 (m, 2H), 6.64 – 6.53 (m, 2H), 4.76 (s, 1H), 4.58 (s, 1H), 4.06 (s, 1H), 3.93 (t, *J* = 5.9 Hz, 1H), 3.91 – 3.83 (m, 7H), 3.70 (t, *J* = 5.9 Hz, 1H), 2.91 (t, *J* = 5.7 Hz, 1H), 2.85 (t, *J* = 5.7 Hz, 1H); Anal. Calcd. for $C_{19}H_{21}BrN_2O_3$: C, 56.31; H, 5.22; N, 6.91 Found: C, 56.32; H, 5.18; N, 6.96; MS: m/z 405.1 (M+1), 407.1 (M+2).

2-(3-bromophenylamino)-1-(6,7-dimethoxy-3,4-dihydroisoquinolin-2(1H)-yl) ethanone (17j)

White solid; IR (KBr, v, cm^{-1}): 3369, 2954, 2931, 2833, 1649, 1591, 1514, 1485, 1433, 1259, 1228, 1112; ^1H NMR (400 MHz, $CDCl_3$) δ 7.06 (t, J = 8.0 Hz, 1H), 6.86 (dd, J = 7.8, 1.0 Hz, 1H), 6.77 (dd, J = 4.0, 2.0 Hz, 1H), 6.67 (d, J = 2.7 Hz, 2H), 6.61 (dd, J = 8.2, 2.3 Hz, 1H),

4.75 (s, 1H), 4.57 (s, 1H), 3.95 (d, J = 1.2 Hz, 2H), 3.92 (s, 2H), 3.91 – 3.88 (m, 5H), 3.69 (t, J = 5.9 Hz, 1H), 2.91 (t, J = 5.8 Hz, 1H), 2.84 (t, J = 5.9 Hz, 1H); ^{13}C NMR (100 MHz, $CDCl_3$, ppm) 28.73, 40.21, 42.12, 44.24, 56.01, 56.06, 108.96, 109.40, 111.25, 111.64, 112.09, 114.99, 120.17, 123.30, 124.67. 125.50, 126.73, 130.52, 147.91, 148.53, 167.34; Anal. Calcd. for $C_{19}H_{21}BrN_2O_3$: C, 56.31; H, 5.22; N, 6.91 Found: C, 56.34; H, 5.17; N, 6.88; MS: m/z 405.1 (M+1), 407.1 (M+2).

2-(4-bromophenylamino)-1-(6,7-dimethoxy-3,4-dihydroisoquinolin-2(1H)-yl) ethanone (17k)

White solid; IR (KBr, v, cm^{-1}): 3358, 2985, 2902, 2833, 1643, 1517, 1433, 1396, 1285, 1224, 1124; ^{1}H NMR (400 MHz, $CDCl_3$) δ 7.31 (s, 1H), 6.67 (d, *J* = 5.2 Hz, 2H), 6.64 – 6.45 (m, 3H), 5.02 (s, 1H), 4.74 (s, 1H), 4.57 (s, 1H), 3.94 (s, 2H), 3.91 – 3.87 (m, 7H), 3.68 (t, *J* = 5.8 Hz, 1H), 2.90 (t, *J* = 5.8 Hz, 1H), 2.84 (t, *J* = 6.0 Hz, 1H); Anal. Calcd. for $C_{19}H_{21}BrN_2O_3$: C, 56.31; H, 5.22; N, 6.91 Found: C, 56.32; H, 5.18; N, 6.86; MS: m/z MS: m/z 405.1 (M+1), 407.1 (M+2).

4-(2-(6,7-dimethoxy-3,4-dihydroisoquinolin-2(1H)-yl)-2-oxoethylamino) benzonitrile (17l)

White solid; IR (KBr, v, cm^{-1}): 3358, 2985, 2902, 2833, 2208, 1643, 1517, 1433, 1396, 1285, 1224, 1124; ^{1}H NMR (400 MHz, $CDCl_3$) δ 7.48 (d, *J* = 8.5 Hz, 2H), 6.68 (d, *J* = 4.6 Hz, 2H), 6.65 – 6.62 (m, 2H), 5.60 (s, 1H), 4.75 (s, 1H), 4.57 (s, 1H), 4.00 (t, *J* = 4.0 Hz, 2H), 3.91 (s, 1H), 3.89 (t, *J* = 2.7 Hz, 6H), 3.68 (s, 1H), 2.91 (t, *J* = 5.7 Hz, 1H), 2.85 (t, *J* = 5.7 Hz, 1H); Anal. Calcd. for $C_{20}H_{21}N_3O_3$: C, 68.36; H, 6.02; N, 11.96 Found: C, 68.34; H, 6.07; N, 11.90; MS: m/z 352.0 (M+1).

2-(3-acetylphenylamino)-1-(6,7-dimethoxy-3,4-dihydroisoquinolin-2(1H)-yl) ethanone (17m)

White solid; IR (KBr, v, cm^{-1}): 3365, 2937, 2835, 1672, 1643, 1598, 1517, 1359, 1315, 1259, 1224, 1116; ^{1}H NMR (400 MHz, $CDCl_3$) δ 7.36 – 7.30 (m, 2H), 7.22 – 7.20 (m, 1H), 6.94 – 6.90 (m, 1H), 6.68 (s, 2H), 4.75 (s, 1H), 4.60 (s, 1H), 4.03 (s, 2H), 3.94 (s, 1H), 3.90 – 3.88 (m, 6H), 3.71 (t, *J* = 5.9 Hz, 1H), 2.91 (t, *J* = 5.8 Hz, 1H), 2.84 (t, *J* = 5.9 Hz, 1H), 2.61 (s, 3H); Anal. Calcd. for $C_{21}H_{24}N_2O_4$: C, 68.46; H, 6.57; N, 7.60 Found: C,: 68.47; H, 6.62; N, 7.56; MS: m/z 369.4 (M+1).

(6,7-dimethoxy-3,4-dihydroisoquinolin-2(1H)-yl)-2-(3(trifluoromethyl) phenylamino)ethanone (17n)

White solid; IR (KBr, v, cm^{-1}): 3350, 2910, 2835, 1643, 1612, 1514, 1431, 1359, 1284, 1261, 1222, 1109; ^{1}H NMR (400 MHz, $CDCl_3$) δ 7.30 (s, 1H), 6.99 (d, *J* = 7.7 Hz, 1H), 6.84 (s, 2H), 6.68 (t, *J* = 3.1 Hz, 2H), 4.76 (s, 1H), 4.59 (s, 1H), 4.00 (s, 2H), 3.92 (s, 1H), 3.90 (d, *J* = 2.5

Hz, 6H), 3.71 (t, *J* = 5.9 Hz, 1H), 2.92 (t, *J* = 5.9 Hz, 1H), 2.85 (t, *J* = 5.8 Hz, 1H); ^{13}C NMR (100 MHz, $CDCl_3$, ppm) 28.74, 40.26, 42.15, 44.29, 56.01, 56.06, 108.55, 108.94, 109.39, 111.23, 116.64, 113.99, 116.57, 123.12, 124.62, 125.64, 126.71, 129.62, 147.32, 148.09. 167.24; Anal. Calcd. for $C_{20}H_{21}F_3N_2O_3$: C, 60.91; H, 5.37; N, 7.10 Found: C, 60.92; H, 5.33; N, 7.15; MS: m/z 395.2 (M+1).

1-(6,7-dimethoxy-3,4-dihydroisoquinolin-2(1H)-yl)-2-(2,5-dimethylphenylamino) ethanone (17o)

White solid; IR (KBr, v, cm^{-1}): 3402, 2995, 2833, 1643, 1517, 1415, 1255, 1232, 1207, 1112; ^{1}H NMR (400 MHz, $CDCl_3$) δ 6.67 (d, *J* = 4.6 Hz, 2H), 6.44 (s, 1H), 6.35 (s, 2H), 4.74 (s, 1H), 4.58 (s, 1H), 3.98 (s, 2H), 3.91 (s, 1H), 3.89 (t, *J* = 4.3 Hz, 6H), 3.70 (t, *J* = 5.9 Hz, 1H), 2.90 (t, *J* = 5.9 Hz, 1H), 2.83 (t, *J* = 6.0 Hz, 1H), 2.28 (s, 6H); Anal. Calcd. for $C_{21}H_{26}N_2O_3$: C, 71.16; H, 7.39; N, 7.90. Found: C, 71.20; H, 7.42; N, 7.88; MS: m/z 355.2 (M+1).

5.2.5 Synthesis and characterization of *N'*-(2-(3,4-dihydroquinolin-1(*2H*)-yl) propanoyl)benzohydrazide derivatives and related analogs (23a-o)

The synthetic route and reaction conditions used for the synthesis of designed hydrazides **23a-o** are depicted in Scheme **5**. The first step involved reaction of tetrahydroquinoline (**18**) with ethyl-2-bromopropanoate (**19**) which afforded intermediate ester **20**. In next step, intermediate **20** was treated with hydrazine hydrate which resulted in replacement of ethoxy group with hydrazine and afforded the second intermediate compound **21**. Final coupling reaction between intermediate **21** and different substituted carboxylic acids (**22a-o**), afforded the final compounds (**23a-o**) in good to excellent yield.

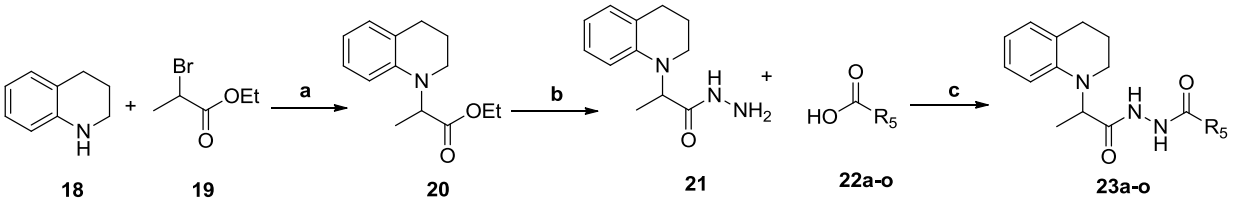

Scheme 5. Reagents and conditions: (a) DMF, K_2CO_3, 100 ˚C 4 h (b) NH_2-NH_2.H_2O, EtOH, catalytic glacial AcOH, reflux 12 hrs (c) HOBt, EDC.HCl, Et_3N, DCM, 6-9 h rt

Procedure for the synthesis of ethyl 2-(3,4-dihydroquinolin-1(*2H*)-yl)propanoate (20)

Ethyl 2-bromopropanoate **19** (5.15 ml, 40 mmol) was added dropwise to the stirring solution of 1,2,3,4-tetrahydroquinoline **18** (5.32 g, 40 mmol) in DMF, containing potassium carbonate (13.8 g, 100 mmol) as base. Reaction was further stirred at 100˚C for four hours until completion as per TLC. After completion of reaction, 200 ml ice-cold water was added to the reaction mixture and reaction mixture was twice extracted with ethyl acetate using

separating funnel (2x200 ml). Combined ethyl acetate layer was twice washed with ice cold water (2x400 ml), followed by brine water (400 ml). Ethyl acetate layer was dried over anhydrous sodium sulphate and finally evaporated on the rotary evaporator to afford compound **20** as viscous oil with 87% yield.

Procedure for the synthesis of 2-(3,4-dihydroquinolin-1(*2H*)-yl)propanehydrazide (21)

To the stirred reaction mixture of intermediate **20** (6.99 g, 30 mmol) in ethanol, hydrazine hydrate (4.36 ml, 90 mmol) was added dropwise, followed by addition of catalytic amount of glacial acetic acid. The reaction mixture was refluxed and the progress of reaction was monitored by TLC. After completion of reaction as per TLC (after 12 hours refluxing), ethanol was evaporated up to half of its original volume under reduced pressure. The reaction mass was allowed to cool at room temperature, then 100 ml of ice water was added to the reaction which induced solid precipitation in the reaction mass. The solid product was filtered out in Buchner funnel under vacuum filtration and then washed with 150 ml cold water: ethanol (4:1) mixture. Solid was dried and then washed with 100 ml of hexane, finally dried over on the rotary evaporator to afford the desired product **21** as a white solid with 78% yield [3].

General procedure for the synthesis of *N'*-(2-(3,4-dihydroquinolin-1(*2H*)-yl) propanoyl)benzohydrazide derivatives (**23a-o)**

To the stirred solution of acids (**22a-o,** 1 mmol) in dry DCM, HOBt (0.16 g, 1.2 mmol) and EDCI. HCl (0.23 g, 1.2 mmol) were added and stirring was continued for 30 min. Further, to the reaction mixture, 2-(3,4-dihydroquinolin-1(*2H*)-yl)propanehydrazide (**21**) was added portion wise and the reaction mixture was further stirred at room temperature for 6-9 h. After completion of reaction as per TLC, the reaction mass was taken in a separating funnel, to this 25 ml more DCM was added and washed with saturated sodium bicarbonate solution (50 ml). The organic layer was further washed with distilled water (50ml), followed by brine (50 ml). DCM layer was separated and dried over anhydrous sodium sulphate to afford the final compounds **(23a-o)** [6]. Preliminary characteristics data of the synthesized compounds **23a-o** are shown in Table **5.6**.

Table 5.6 Preliminary characteristics data of compounds **23a-o**

Comp code	R_5	Mol. formula	Mol. Wt	% Yield	Melting Point (˚C)
23a	Ph	$C_{19}H_{21}N_3O_2$	323.39	78	136-139
23b	2-MeO-Ph	$C_{20}H_{23}N_3O_3$	353.41	81	142-144
23c	3-MeO-Ph	$C_{20}H_{23}N_3O_3$	353.41	84	150-153
23d	4-MeO-Ph	$C_{20}H_{23}N_3O_3$	353.41	75	144-146
23e	2-F-Ph	$C_{19}H_{20}FN_3O_2$	341.38	72	140-142
23f	3-F-Ph	$C_{19}H_{20}FN_3O_2$	341.38	80	134-135
23g	4-F-Ph	$C_{19}H_{20}FN_3O_2$	341.38	82	138-141
23h	2-NO_2-Ph	$C_{19}H_{20}N_4O_4$	368.39	68	158-160
23i	3-NO_2-Ph	$C_{19}H_{20}N_4O_4$	368.39	74	166-168
23j	4-NO_2-Ph	$C_{19}H_{20}N_4O_4$	368.39	78	170-172
23k	3,4-DMeO-Ph	$C_{21}H_{25}N_3O_4$	383.44	83	154-156
23l	2,4-DCl-Ph	$C_{19}H_{19}Cl_2N_3O_2$	391.09	77	148-150
23m	3,4,5-tri-MeO-Ph	$C_{22}H_{27}N_3O_5$	413.47	62	166-168
23n	Styrene	$C_{21}H_{23}N_3O_2$	349.43	65	146-148
23o	Styrene-3-NO_2	$C_{21}H_{22}N_4O_4$	394.42	63	156-159

Spectral characterization of compounds (23a-o)

Synthesized compounds were characterized by spectral techniques like FT-IR, ^{1}H NMR, Mass and elemental analysis. FT-IR spectra of the tested compounds exhibited characteristic peaks in the expected absorption region, for example, all compounds possessed the dicarbonyl group (-**CO**-HN-NH-**CO**-), a corresponding stretching peak (broad with strong intensity) appeared in the IR spectrum at 1683-1710 cm^{-1}. Another characteristic peak (broad with moderate intensity) appeared at the region 3220-3317 cm^{-1} corresponding to the stretching of dual amidic hydrogen (-CO-**H**N-N**H-CO-**). The ^{1}H NMR spectrum of the test compounds (**23a-o**) showed characteristic doublet around δ~1.51 corresponding to the methyl group (attached at the carbon connecting carbonyl and nitrogen of THQ), while single proton at the same carbon appeared as quartet δ~4.57. Two protons at the 2nd position of THQ exhibited two distinct peaks as triplet around δ 3.25-3.35. Furthermore, proton pair at 3rd position of THQ appeared as multiplet in the upfield region δ~2.1, while protons pair at 4th position appeared around δ~2.85. Counting and peak pattern of signals corresponding to the aromatic protons of all compound were also observed in compliance with the proposed structure. Mass spectrum (ESI-MS) of the synthesized compounds exhibited corresponding M+1 peak. Details of spectral data of compounds (**23a-o**) is given below;

N'-(2-(3,4-dihydroquinolin-1(2H)-yl)propanoyl)benzohydrazide (23a)

White solid; IR (KBr, v, cm^{-1}): 3282, 2966, 2581, 1703, 1493, 1268, 1196, 925,873, 730; ^{1}H NMR (400 MHz, $CDCl_3$) δ 9.20 (s, 1H), 7.84 (d, *J* = 7.5 Hz, 2H), 7.52 (t, *J* = 7.4 Hz, 1H), 7.42 (t, *J* = 7.6 Hz, 2H), 7.07 (dd, *J* = 18.7, 7.4 Hz, 2H), 6.73 (t, *J* = 7.2 Hz, 1H), 6.67 (d, *J* =

8.2 Hz, 1H), 4.54 (q, *J* = 6.9 Hz, 1H), 3.41 – 3.29 (m, 1H), 3.23 (t, *J* = 9.9 Hz, 1H), 2.84 (t, *J* = 6.4 Hz, 2H), 2.13 – 2.00 (m, 2H), 1.47 (d, *J* = 7.0 Hz, 3H); MS: m/z 324.2 (M+1).

N'-(2-(3,4-dihydroquinolin-1(2H)-yl)propanoyl)-2-methoxybenzohydrazide (23b)

White solid; IR (KBr, v, cm^{-1}): 3288, 3207, 2933, 2600, 1917, 1504, 1469, 1288, 1234, 1016, 750; ^{1}H NMR (400 MHz, $CDCl_3$) δ 10.53 (d, *J* = 6.0 Hz, 1H), 9.42 (s, 1H), 8.19 (d, *J* = 6.6 Hz, 1H), 7.52 (s, 1H), 7.17 – 6.99 (m, 4H), 6.79 – 6.62 (m, 2H), 4.57 (q, *J* = 6.9 Hz, 1H), 4.07 (s, 3H), 3.40 – 3.19 (m, 2H), 2.86 (t, *J* = 6.4 Hz, 2H), 2.16 – 2.05 (m, 2H), 1.53 (t, *J* = 6.8 Hz, 3H); MS: m/z 354.2 (M+1).

N'-(2-(3,4-dihydroquinolin-1(2H)-yl)propanoyl)-3-methoxybenzohydrazide (23c)

White solid; IR (KBr, v, cm^{-1}): 3286, 2933, 2875, 2586, 1697, 1487, 1305, 1259, 1193, 1082, 935, 881, 752; ^{1}H NMR (400 MHz, $CDCl_3$) δ 9.11 (s, 1H), 7.34 (dd, *J* = 16.7, 8.7 Hz, 3H), 7.14 – 7.01 (m, 3H), 6.74 (t, *J* = 7.3 Hz, 1H), 6.68 (d, *J* = 8.3 Hz, 1H), 4.55 (q, *J* = 7.0 Hz, 1H), 3.83 (s, 3H), 3.34 (dd, *J* = 8.2, 7.7 Hz, 1H), 3.30 – 3.20 (m, 1H), 2.85 (t, *J* = 6.5 Hz, 2H), 2.15 – 2.04 (m, 2H), 1.49 (d, *J* = 7.0 Hz, 3H); MS: m/z 354.2 (M+1).

N'-(2-(3,4-dihydroquinolin-1(2H)-yl)propanoyl)-4-methoxybenzohydrazide (23d)

White solid; IR (KBr, v, cm^{-1}): 3244, 2935, 1693, 1494, 1311, 1256, 1172, 1022, 846, 748; ^{1}H NMR (400 MHz, $CDCl_3$) δ 9.08 (s, 1H), 8.70 (s, 1H), 7.80 (d, *J* = 8.9 Hz, 2H), 7.13 – 7.07 (m, 1H), 7.06 (d, *J* = 7.4 Hz, 1H), 6.97 – 6.91 (m, 2H), 6.74 (td, *J* = 7.3, 0.9 Hz, 1H), 6.68 (d, *J* = 8.2 Hz, 1H), 4.56 (q, *J* = 7.0 Hz, 1H), 3.87 (s, 3H), 3.39 – 3.31 (m, 1H), 3.29 – 3.22 (m, 1H), 2.86 (t, *J* = 6.5 Hz, 2H), 2.14 – 2.05 (m, 2H), 1.51 (d, *J* = 7.1 Hz, 3H); MS: m/z 354.2 (M+1).

N'-(2-(3,4-dihydroquinolin-1(2H)-yl)propanoyl)-2-fluorobenzohydrazide (23e)

White solid; IR (KBr, v, cm^{-1}): 3248, 2829, 2601, 1648, 1494, 1292, 1471, 1292, 1222, 1099, 1041, 754; ^{1}H NMR (400 MHz, $CDCl_3$) δ 9.12 (d, *J* = 17.9 Hz, 2H), 8.11 (td, *J* = 7.8, 1.8 Hz, 1H), 7.55 (dddd, *J* = 8.3, 7.3, 5.3, 1.9 Hz, 1H), 7.31 (td, *J* = 7.8, 1.0 Hz, 1H), 7.19 (ddd, *J* = 12.0, 8.3, 0.9 Hz, 1H), 7.14 – 7.04 (m, 2H), 6.75 (td, *J* = 7.4, 0.9 Hz, 1H), 6.70 (d, *J* = 8.3 Hz, 1H), 4.57 (q, *J* = 7.0 Hz, 1H), 3.39 – 3.31 (m, 1H), 3.30 – 3.22 (m, 1H), 2.86 (t, *J* = 6.5 Hz, 2H), 2.14 – 2.06 (m, 2H), 1.52 (d, *J* = 7.1 Hz, 3H); MS: m/z 342.90 (M+1).

N'-(2-(3,4-dihydroquinolin-1(2H)-yl)propanoyl)-3-fluorobenzohydrazide (23f)

white solid; IR (KBr, v, cm^{-1}): 3217, 2986, 2855, 1940, 1703, 1683, 1305, 1261, 1157, 950, 873, 754; ^{1}H NMR (400 MHz, $CDCl_3$) δ 9.11 (s, 1H), 7.59 (d, *J* = 7.7 Hz, 1H), 7.53 (d, *J* = 9.1 Hz, 1H), 7.41 (dt, *J* = 13.4, 6.7 Hz, 1H), 7.24 (t, *J* = 8.3 Hz, 1H), 7.14 – 7.01 (m, 2H), 6.75 (t, *J* = 7.4 Hz, 1H), 6.68 (d, *J* = 8.3 Hz, 1H), 4.55 (q, *J* = 6.9 Hz, 1H), 3.34 (d, *J* = 11.5 Hz, 1H), 3.24 (d, *J* = 7.6 Hz, 1H), 2.86 (t, *J* = 6.4 Hz, 2H), 2.14 – 2.05 (m, 2H), 1.50 (d, *J* = 7.0 Hz, 3H); MS: m/z 342.9 (M+1).

N'-(2-(3,4-dihydroquinolin-1(2H)-yl)propanoyl)-4-fluorobenzohydrazide (23g)

White solid; IR (KBr, v, cm^{-1}): 3250, 2991, 1697, 1483, 1240, 1157, 1096, 842, 761; ^1H NMR (400 MHz, $CDCl_3$) δ 9.08 (s, 1H), 7.84 (dd, *J* = 8.6, 5.3 Hz, 2H), 7.08 (dd, *J* = 19.5, 8.3 Hz, 4H), 6.75 (t, *J* = 7.3 Hz, 1H), 6.68 (d, *J* = 8.2 Hz, 1H), 4.55 (q, *J* = 7.0 Hz, 1H), 3.41 – 3.30 (m, 1H), 3.30 – 3.19 (m, 1H), 2.85 (t, *J* = 6.3 Hz, 2H), 2.15 – 2.05 (m, 2H), 1.50 (dd, *J* = 5.9, 4.3 Hz, 3H); MS: m/z 342.9 (M+1).

N'-(2-(3,4-dihydroquinolin-1(2H)-yl)propanoyl)-2-nitrobenzohydrazide (23h)

Pale yellow solid; IR (KBr, v, cm^{-1}): 3216, 2829, 1665, 1494, 1367, 1296, 1190, 1082, 935, 775; ^1H NMR (400 MHz, $CDCl_3$) δ 9.05 (s, 1H), 8.13 (d, *J* = 8.1 Hz, 1H), 7.78 – 7.69 (m, 2H), 7.69 – 7.64 (m, 1H), 7.14 – 7.03 (m, 2H), 6.75 (t, *J* = 7.4 Hz, 1H), 6.66 (d, *J* = 8.3 Hz, 1H), 4.51 (q, *J* = 7.0 Hz, 1H), 3.35 – 3.28 (m, 1H), 3.27 – 3.20 (m, 1H), 2.86 (t, *J* = 6.4 Hz, 2H), 2.10 (ddd, *J* = 10.9, 8.4, 4.4 Hz, 2H), 1.44 (d, *J* = 7.0 Hz, 3H); MS: m/z 369.26 (M+1).

N'-(2-(3,4-dihydroquinolin-1(2H)-yl)propanoyl)-3-nitrobenzohydrazide (23i)

Pale yellow solid; IR (KBr, v, cm^{-1}): 3261, 3164, 2691, 1629, 1553, 1392, 1256, 1226, 1063, 806; ^1H NMR (400 MHz, $CDCl_3$) δ 8.68 (s, 1H), 8.37 (d, *J* = 8.2 Hz, 1H), 8.14 (d, *J* = 7.8 Hz, 1H), 7.61 (t, *J* = 8.0 Hz, 1H), 7.14 – 7.04 (m, 2H), 6.79 – 6.69 (m, 2H), 4.66 – 4.55 (m, 1H), 3.36 (dd, *J* = 9.8, 4.2 Hz, 1H), 3.29 (dd, *J* = 11.6, 7.6 Hz, 1H), 2.86 (t, *J* = 6.2 Hz, 2H), 2.16 – 2.08 (m, 2H), 1.52 (d, *J* = 7.0 Hz, 3H); MS: m/z 369.2 (M+1).

N'-(2-(3,4-dihydroquinolin-1(2H)-yl)propanoyl)-4-nitrobenzohydrazide (23j)

Pale yellow solid; IR (KBr, v, cm^{-1}): 3313, 2933, 2862, 1701, 1667, 1529, 1449, 1307, 1197, 1078, 869, 736; ^1H NMR (400 MHz, $CDCl_3$) δ 9.35 (s, 1H), 9.13 (s, 1H), 8.29 (d, *J* = 8.7 Hz, 2H), 8.00 (d, *J* = 8.7 Hz, 2H), 7.10 (dd, *J* = 19.5, 7.4 Hz, 2H), 6.77 (t, *J* = 7.3 Hz, 1H), 6.68 (d, *J* = 8.2 Hz, 1H), 4.57 (q, *J* = 6.8 Hz, 1H), 3.40 – 3.21 (m, 2H), 2.87 (t, *J* = 6.5 Hz, 2H), 2.16 – 2.06 (m, 2H), 1.52 (d, *J* = 7.0 Hz, 3H); MS: m/z 369.2 (M+1).

N'-(2-(3,4-dihydroquinolin-1(2H)-yl)propanoyl)-3,4-dimethoxybenzohydrazide (23k)

White solid; IR (KBr, v, cm^{-1}): 3241, 2931, 1689, 1493, 1313, 1253, 1171, 1012, 842, 745; ^1H NMR (400 MHz, $CDCl_3$) δ 9.17 (s, 1H), 9.06 (s, 1H), 7.45 – 7.38 (m, 2H), 7.13 – 7.03 (m, 2H), 6.85 (d, *J* = 8.3 Hz, 1H), 6.77 – 6.66 (m, 2H), 4.57 (q, *J* = 7.0 Hz, 1H), 3.93 (s, 3H), 3.90 (s, 3H), 3.36 (dd, *J* = 11.4, 4.7 Hz, 1H), 3.28 – 3.22 (m, 1H), 2.85 (t, *J* = 6.4 Hz, 2H), 2.14 – 2.03 (m, 2H), 1.50 (d, *J* = 7.1 Hz, 3H); MS: m/z 384.27 (M+1).

2,4-dichloro-N'-(2-(3,4-dihydroquinolin-1(2H)-yl)propanoyl)benzohydrazide (23l)

White solid; IR (KBr, v, cm^{-1}): 3234, 2868, 1906, 1770, 1494, 1454, 1303, 1190, 1047, 866, 752; ^1H NMR (400 MHz, $CDCl_3$) δ 9.09 (s, 1H), 7.74 (d, *J* = 8.4 Hz, 1H), 7.48 (d, *J* = 1.9 Hz, 1H), 7.37 (d, *J* = 2.0 Hz, 1H), 7.13 – 7.05 (m, 2H), 6.75 (t, *J* = 7.5 Hz, 1H), 6.68 (d, *J* = 8.3 Hz, 1H), 4.55 (q, *J* = 7.0 Hz, 1H), 3.35 – 3.30 (m, 1H), 3.27 (dd, *J* = 7.9, 4.1 Hz, 1H), 2.86 (t,

J = 6.5 Hz, 2H), 2.12 – 2.04 (m, 2H), 1.50 (d, *J* = 7.1 Hz, 3H); MS: m/z 392.1 (M+1), 394.1 (M+3).

N'-(2-(3,4-dihydroquinolin-1(2H)-yl)propanoyl)-3,4,5-trimethoxybenzohydrazide (23m)

White solid; IR (KBr, v, cm^{-1}): 3279, 3201, 2928, 1917, 1883, 1501, 1465, 1283, 1232, 1012, 746; ^{1}H NMR (400 MHz, $CDCl_3$) δ 8.97 (s, 1H), 7.13 – 7.04 (m, 4H), 6.79 – 6.74 (m, 1H), 6.69 (d, *J* = 8.3 Hz, 1H), 4.57 (q, *J* = 7.1 Hz, 1H), 3.87 (d, *J* = 9.9 Hz, 9H), 3.37 (dd, *J* = 10.9, 5.0 Hz, 1H), 3.29 – 3.23 (m, 1H), 2.86 (t, *J* = 6.5 Hz, 2H), 2.14 – 2.07 (m, 2H), 1.49 (d, *J* = 7.1 Hz, 3H); MS: m/z 414.2 (M+1).

N'-(2-(3,4-dihydroquinolin-1(2H)-yl)propanoyl)cinnamohydrazide (23n)

White solid; IR (KBr, v, cm^{-1}): 3246, 2981, 1691, 1482, 1238, 1154, 1092, 842, 758; ^{1}H NMR (400 MHz, $CDCl_3$) δ 9.20 (s, 1H), 7.71 (d, *J* = 15.7 Hz, 1H), 7.51 (dd, *J* = 6.6, 2.7 Hz, 2H), 7.40 – 7.36 (m, 3H), 7.11 – 7.04 (m, 2H), 6.74 (dd, *J* = 8.9, 5.3 Hz, 1H), 6.67 (d, *J* = 8.2 Hz, 1H), 6.56 (d, *J* = 15.7 Hz, 1H), 4.55 (q, *J* = 7.0 Hz, 1H), 3.34 – 3.29 (m, 1H), 3.23 (dd, *J* = 9.8, 6.3 Hz, 1H), 2.85 (t, *J* = 6.5 Hz, 2H), 2.12 – 2.05 (m, 2H), 1.49 (d, *J* = 7.1 Hz, 3H); MS: m/z 350.2 (M+1).

(E)-N'-(2-(3,4-dihydroquinolin-1(2H)-yl)propanoyl)-3-(3-nitrophenyl) acrylohydrazide (23o)

Pale yellow solid; IR (KBr, v, cm^{-1}): 3256, 2872, 2605, 1714, 1504, 1454, 1309, 1192, 1172, 1078, 977, 746; ^{1}H NMR (400 MHz, $CDCl_3$) δ 9.30 (s, 1H), 8.38 (d, *J* = 14.7 Hz, 1H), 8.22 (dd, *J* = 8.2, 1.3 Hz, 1H), 7.75 (dd, *J* = 21.8, 11.7 Hz, 2H), 7.57 (t, *J* = 7.9 Hz, 1H), 7.08 (dd, *J* = 16.6, 7.6 Hz, 2H), 6.81 – 6.72 (m, 2H), 6.68 (d, *J* = 8.2 Hz, 1H), 4.58 (q, *J* = 7.0 Hz, 1H), 3.36 – 3.30 (m, 1H), 3.29 – 3.22 (m, 1H), 2.86 (t, *J* = 6.4 Hz, 2H), 2.09 (ddd, *J* = 13.3, 7.9, 3.3 Hz, 2H), 1.52 (d, *J* = 7.0 Hz, 3H); MS: m/z 395.2 (M+1).

5.2.6 Synthesis and characterization of 1-(4-chlorophenyl)-2-(3,4-dihydroquinolin-1(*2H*)-yl)ethyl phenylcarbamate derivatives (28a-l)

Designed compounds **28a-l** were synthesized in three steps, details of the reaction conditions used for the synthesis of target compounds are given below (scheme **6)**. The first step involved the reaction of tetrahydroquinoline (**18)** with 4-chlorophenacyl bromide (**24**), which afforded compound (**25)** as first intermediate. In the second step, keto group of intermediate (**25)** was reduced to hydroxyl using sodium borohydride as reducing agent yielded compound (**26)** as IInd intermediate. Further, the reaction of intermediate (**26)** with different substituted phenyl isocyanates (**27a-l**) in the presence of sodium hydride as base afforded the final compounds (**28a-l**) in good to excellent yield.

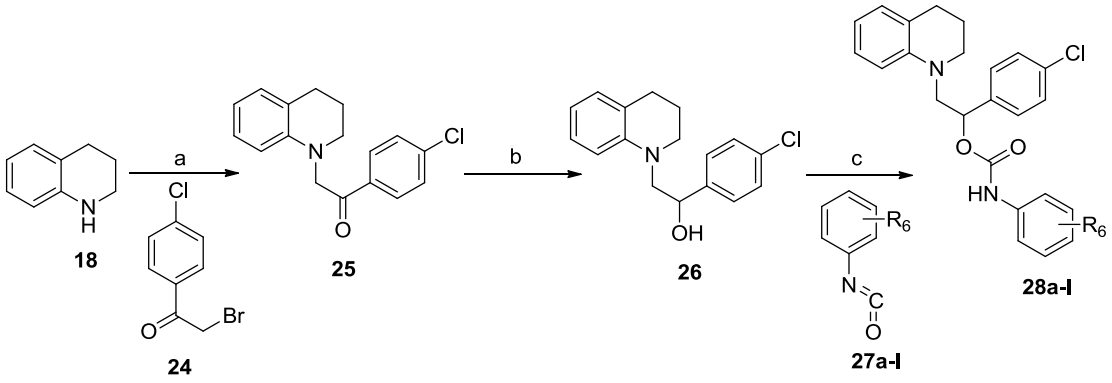

Scheme 6. Reagents and conditions: (a) DMF, Et_3N, 0 ˚C-rt, 12 h (b) $NaBH_4$, dry MeOH, 0 ˚C- rt, 6 h (c) NaH, dry THF, 0 ˚C-rt, 5-8 h

Procedure for synthesis of 1-(4-chlorophenyl)-2-(3,4-dihydroquinolin-1(*2H*)-yl)ethanone (25)

2-bromo-1-(4-chlorophenyl) ethanone **24** (9.28 g, 40 mmol) was added portion wise to the stirred ice cold solution of 1,2,3,4-tetrahydroquinoline **18** (5.32 g, 40 mmol) in DMF, containing triethylamine (14.42 ml, 100 mmol) as a base. The reaction was further stirred at rt and the progress of reaction was monitored using TLC. After completion of reaction as per TLC (after 12 h), 350 ml of water was added to the reaction mixture and then twice extracted with ethyl acetate using separating funnel (2x250 ml). Combined ethyl acetate layer was twice washed with ice cold water (2x500 ml) and then washed with brine water (500 ml). Ethyl acetate layer was dried over anhydrous sodium sulphate and finally evaporated on the rotary evaporator to afford the crude compound **25**. Crude compound **25** was further purified by column chromatography using ethyl acetate and hexane as solvent system (3% ethyl acetate in hexane) and silica gel (mess size 100-200) as a stationary phase which afforded the intermediate compound **25** as pale yellow solid with 68% yield.

Procedure for synthesis of 1-(4-chlorophenyl)-2-(3,4-dihydroquinolin-1(2*H*)-yl) ethanol (26)

To the ice-cold stirring solution of intermediate **25** (7.0 g, 24.40 mmol) in dry methanol, sodium borohydride (2.70 g, 73.20 mmol) was added portion wise, after complete addition, the reaction mixture was stirred at rt and the progress of reaction was monitored by TLC. After completion of reaction as per TLC (after 6 h), methanol was evaporated using rotary evaporator and 200 ml of ice water was slowly added to the reaction mass. Further, the reaction mixture was twice extracted with ethyl acetate using separating funnel (2x250 ml). Combined ethyl acetate layer was first washed with ice cold water (500 ml) and then washed with brine water (500 ml). Ethyl acetate layer was dried over anhydrous sodium sulphate and finally evaporated using rotary evaporator to afford the IInd intermediate compound **26**, as a white solid with 92% yield [7].

General procedure for the synthesis of 1-(4-chlorophenyl)-2-(3,4-dihydroquinolin-1(*2H*)-yl)ethyl phenylcarbamate derivatives (28a-l)

Sodium hydride (hexane washed, 0.052 g, 2.2 mmol) was added portion wise to the ice-cold stirred solution of intermediate **26** (0.574 g, 2 mmol) in dry THF. Further, corresponding isocyanate (**27a-l**) was slowly added under ice-cold condition. After that, reaction mixture was stirred at rt for next 5-8 h; the progress of reaction was monitored by TLC. After completion of the reaction, the reaction mixture was quenched with 0.1 N HCl (1 ml) under ice-cold condition. Further, THF was evaporated from the reaction mass, ethyl acetate (20 ml) was added. Ethyl acetate layer was twice washed with distilled water (2x20 ml), and then with brine water (20 ml). The organic layer was dried over anhydrous sodium sulphate and finally evaporated on the rotary evaporator to afford the final compounds **28a-l** [8]. Preliminary characteristics data of the synthesized compounds **28a-l** are shown in table **5.7**.

Table 5.7 Preliminary characteristics data of the synthesized compounds **28a-l**

Comp. Code	R_6	Mol. formula	Mol. Wt	% Yield	Melting point (˚C)
28a	H	$C_{24}H_{23}ClN_2O_2$	406.14	88	106-108
28b	2-CH_3	$C_{25}H_{25}ClN_2O_2$	420.16	82	76-79
28c	3-CH_3	$C_{25}H_{25}ClN_2O_2$	420.16	85	120-122
28d	4-CH_3	$C_{25}H_{25}ClN_2O_2$	420.16	83	138-141
28e	2-F	$C_{24}H_{22}ClFN_2O_2$	424.14	78	88-90
28f	3-F	$C_{24}H_{22}ClFN_2O_2$	424.14	79	106-109
28g	4-F	$C_{24}H_{22}ClFN_2O_2$	424.14	81	124-126
28h	4-Cl	$C_{24}H_{22}Cl_2N_2O_2$	440.11	87	166-168
28i	3-NO_2	$C_{24}H_{22}ClN_3O_4$	451.13	73	164-165
28j	4-NO_2	$C_{24}H_{22}ClN_3O_4$	451.13	75	166-168
28k	2-COOEt	$C_{27}H_{27}ClN_2O_4$	478.17	78	76-79
28l	4-COOEt	$C_{27}H_{27}ClN_2O_4$	478.17	76	132-134

Spectral characterization of compounds (28a-l)

All the synthesized compounds were characterized by spectral analysis like IR, ^{1}H NMR and Mass, while four representative compounds (**28a, 28c, 28f** and **28l**) were also characterized by ^{13}C NMR. IR spectra of the synthesized compounds showed the expected absorption bands, for example all compounds possessed hydrogen attached to nitrogen (−OCON**H**-), a corresponding stretching peak (sharp, strong) appeared in IR spectra of compounds at region 3200–3350 cm^{-1}. Another characteristic peak (sharp, strong), appeared in the region 1700-1750 cm^{-1} corresponding to the stretching of carbonyl group (-O**C=O**NH-). In the ^{1}H NMR spectra of compounds **28a-l,** two protons at 3rd carbon of THQ ring displayed peaks with δ ~1.9-1.7. Further, two benzylic proton at the fourth position of THQ ring appeared at δ

~2.70-2.72. Interestingly, two protons at 2nd position of THQ appeared as two discrete peaks at δ ~3.0-3.3. Two protons adjacent to nitrogen, outside the ring also appeared in two discrete peaks (dd) at δ ~3.40 and 3.87. Further, single proton at benzylic carbon connected with highly electronegative oxygen atom is highly de-shielded, which appeared (dd) at δ ~6.02. Further, all aromatic protons appeared at their expected region, moreover nitrogen proton of carbamate (N**H)** appeared in the aromatic region δ ~6.5-6.9 due to strong de-shielding effect. Further, number of peak counting as well as their position in ^{13}C NMR of compounds **28a, 28c, 28f** and **28l** were found in accordance with the proposed structure, for example all four compounds possessed carbonyl group (carbamate), corresponding to this a characteristics peak at δ ~152 appeared in ^{13}C NMR. Moreover, a peak at δ ~166.30 appeared in the ^{13}C NMR spectrum of compound **28l** due to presence of extra carbonyl group. ESI-MS of the synthesized compounds showed the corresponding M+1 peak. Details of spectral data of compounds **28a-l** is given below;

1-(4-chlorophenyl)-2-(3,4-dihydroquinolin-1(2H)-yl)ethyl phenylcarbamate (28a)

Light brown solid; IR (KBr, v, cm^{-1}): 3338, 2933, 1732, 1597, 1496, 1220, 1112, 1060, 850, 775; ^{1}H NMR (400 MHz, $CDCl_3$) δ 7.40 – 7.36 (m, 4H), 7.36 – 7.29 (m, 4H), 7.10 (dt, *J* = 11.4, 7.0 Hz, 2H), 6.96 (dd, *J* = 7.3, 1.4 Hz, 1H), 6.78 (d, *J* = 8.2 Hz, 1H), 6.66 – 6.59 (m, 2H), 6.02 (dd, *J* = 7.3, 6.2 Hz, 1H), 3.87 (dd, *J* = 15.0, 7.4 Hz, 1H), 3.40 (dd, *J* = 15.0, 6.2 Hz, 1H), 3.21 (ddd, *J* = 11.3, 7.5, 3.9 Hz, 1H), 3.02 (ddd, *J* = 11.0, 6.5, 4.2 Hz, 1H), 2.71 (dd, *J* = 12.1, 5.7 Hz, 2H), 1.89 – 1.73 (m, 2H); ^{13}C NMR (100 MHz, $CDCl_3$) δ 152.57, 144.93, 137.55, 134.09, 129.41, 129.08, 128.82, 127.96, 127.27, 123.75, 123.42, 122.42, 118.83, 116.26, 110.77, 73.60, 57.19, 50.70, 28.07, 21.99; MS: m/z 407.2 (M+1), 409.2 (M+3).

1-(4-chlorophenyl)-2-(3,4-dihydroquinolin-1(2H)-yl)ethyl o-tolylcarbamate (28b)

White solid; IR (KBr, v, cm^{-1}): 3308, 2864, 1730, 1506, 1234, 1180, 1051, 1010, 819, 740; ^{1}H NMR (400 MHz, $CDCl_3$) δ 7.35 (s, 4H), 7.20 (d, *J* = 8.2 Hz, 2H), 7.13 (d, *J* = 8.2 Hz, 3H), 6.93 (d, *J* = 7.0 Hz, 1H), 6.75 (d, *J* = 8.0 Hz, 1H), 6.61 (t, *J* = 7.1 Hz, 1H), 6.51 (s, 1H), δ 6.07 – 5.98 (m, 1H), 5.02 (dd, *J* = 8.5, 4.7 Hz, 1H), 4.96 (dd, *J* = 9.7, 6.3 Hz, 1H), 3.17 (d, *J* = 7.3 Hz, 1H), 3.01 (dd, *J* = 7.7, 3.3 Hz, 1H), 2.71 (dd, *J* = 11.9, 5.3 Hz, 2H), 2.32 (s, 3H), 1.79 (dd, *J* = 12.8, 7.7 Hz, 2H); MS: m/z 421.2 (M+1), 423.2 (M+3).

1-(4-chlorophenyl)-2-(3,4-dihydroquinolin-1(2H)-yl)ethyl m-tolylcarbamate (28c)

White solid; IR (KBr, v, cm^{-1}): 3305, 2943, 1732, 1703, 1568, 1504, 1296, 1228, 1053, 833, 748; ^{1}H NMR (400 MHz, $CDCl_3$) δ 7.37 (s, 4H), 7.22 – 7.16 (m, 2H), 7.10 (d, *J* = 7.6 Hz, 2H), 6.96 (d, *J* = 6.0 Hz, 1H), 6.90 (d, *J* = 7.4 Hz, 1H), 6.78 (d, *J* = 8.2 Hz, 1H), 6.66 – 6.60 (m, 1H), 6.56 (s, 1H), 6.01 (dd, *J* = 7.3, 6.3 Hz, 1H), 3.86 (dd, *J* = 15.0, 7.4 Hz, 1H), 3.40 (dd, *J* = 15.0, 6.2 Hz, 1H), 3.20 (ddd, *J* = 11.3, 7.7, 3.9 Hz, 1H), 3.04 – 2.96 (m, 1H), 2.71 (dd, *J* = 12.2, 5.8 Hz, 2H), 2.33 (s, 3H), 1.86 – 1.75 (m, 2H); ^{13}C NMR (100 MHz, $CDCl_3$) δ 152.54,

144.91, 139.03, 137.58, 137.40, 134.08, 129.38, 128.87, 128.81, 127.94, 127.26, 124.55, 122.40, 119.44, 116.24, 115.93, 110.75, 73.57, 57.18, 50.70, 28.06, 21.97, 21.52; MS: m/z 421.2 (M+1), 423.2 (M+3).

1-(4-chlorophenyl)-2-(3,4-dihydroquinolin-1(2H)-yl)ethyl p-tolylcarbamate (28d)

White solid; IR (KBr, v, cm^{-1}): 3305, 2922, 1714, 1697, 1508, 1226, 1070, 812, 746; ^{1}H NMR (400 MHz, $CDCl_3$) δ 7.37 (s, 4H), 7.22 (d, *J* = 8.3 Hz, 2H), 7.11 (d, *J* = 8.2 Hz, 3H), 6.95 (d, *J* = 7.0 Hz, 1H), 6.78 (d, *J* = 8.2 Hz, 1H), 6.63 (t, *J* = 7.2 Hz, 1H), 6.54 (s, 1H), 6.01 (t, *J* = 6.8 Hz, 1H), 3.86 (dd, *J* = 15.0, 7.3 Hz, 1H), 3.39 (dd, *J* = 15.0, 6.2 Hz, 1H), 3.19 (d, *J* = 7.5 Hz, 1H), 3.00 (dd, *J* = 7.7, 3.5 Hz, 1H), 2.70 (dd, *J* = 11.9, 5.6 Hz, 2H), 2.31 (s, 3H), 1.80 (dd, *J* = 12.9, 7.5 Hz, 2H); MS: m/z 421.2 (M+1), 423.2 (M+3).

1-(4-chlorophenyl)-2-(3,4-dihydroquinolin-1(2H)-yl)ethyl-2-fluorophenyl carbamate (28e)

White solid; IR (KBr, v, cm^{-1}): 3334, 3057, 2927, 2856, 1733, 1703, 1504, 1456, 1244, 1190, 1064; ^{1}H NMR (400 MHz, $CDCl_3$) δ 8.04 (s, 1H), 7.38 (s, 4H), 7.15 – 7.01 (m, 4H), 6.96 (d, *J* = 7.3 Hz, 1H), 6.89 (s, 1H), 6.76 (d, *J* = 8.2 Hz, 1H), 6.63 (td, *J* = 7.3, 0.9 Hz, 1H), 6.02 (dd, *J* = 7.2, 6.3 Hz, 1H), 3.86 (dd, *J* = 15.0, 7.3 Hz, 1H), 3.43 (dd, *J* = 15.0, 6.2 Hz, 1H), 3.23 (ddd, *J* = 11.3, 7.7, 3.9 Hz, 1H), 3.06 – 2.96 (m, 1H), 2.72 (dd, *J* = 11.6, 5.5 Hz, 2H), 1.81 (ddd, *J* = 9.1, 6.8, 3.8 Hz, 2H); MS: m/z 425.1 (M+1), 427.1 (M+3).

1-(4-chlorophenyl)-2-(3,4-dihydroquinolin-1(2H)-yl)ethyl-3-fluorophenyl carbamate (28f)

White solid; IR (KBr, v, cm^{-1}): 3292, 2918, 2831, 1736, 1505, 1494, 1269, 1230, 1089, 970; ^{1}H NMR (400 MHz, $CDCl_3$) δ 7.37 (s, 4H), 7.23 (dd, *J* = 8.2, 6.5 Hz, 1H), 7.12 (t, *J* = 8.5 Hz, 1H), 6.97 (t, *J* = 8.6 Hz, 2H), 6.82 – 6.73 (m, 2H), 6.64 (dd, *J* = 13.6, 5.3 Hz, 2H), 6.04 – 5.99 (m, 1H), 3.88 (dd, *J* = 15.0, 7.5 Hz, 1H), 3.40 (dd, *J* = 15.0, 6.0 Hz, 1H), 3.21 (ddd, *J* = 11.3, 7.4, 4.0 Hz, 1H), 3.04 (d, *J* = 6.9 Hz, 1H), 2.71 (dd, *J* = 12.1, 5.7 Hz, 2H), 1.88 – 1.75 (m, 2H); ^{13}C NMR (100 MHz, $CDCl_3$) δ 163.12 (d, *J* = 244.7 Hz), 152.28, 144.88, 139.13 (d, *J* = 10.9 Hz), 137.26, 134.22, 130.16 (d, *J* = 9.5 Hz), 129.44, 128.87, 127.92, 127.22, 122.47, 116.32, 114.06, 110.72, 110.38 (d, *J* = 21.3 Hz, 106.22 (d, *J* = 29.6 Hz), 73.90, 57.10, 50.65, 28.04, 21.96; MS: m/z 425.1 (M+1), 427.1 (M+3).

1-(4-chlorophenyl)-2-(3,4-dihydroquinolin-1(2H)-yl)ethyl-4-fluorophenyl carbamate (28g)

White solid; IR (KBr, v, cm^{-1}): 3336, 3058, 2930, 2856, 1736, 1699, 1506, 1446, 1244, 1192, 1067; ^{1}H NMR (400 MHz, $CDCl_3$) δ 7.38 (d, *J* = 5.2 Hz, 4H), 7.27 – 7.18 (m, 2H), 7.11 (t, *J* = 7.7 Hz, 1H), 7.04 – 6.95 (m, 3H), 6.78 (d, *J* = 7.9 Hz, 1H), 6.63 (t, *J* = 7.2 Hz, 1H), 6.55 (s, 1H), 6.01 (dd, *J* = 7.4, 6.1 Hz, 1H), 3.87 (dd, *J* = 15.0, 7.5 Hz, 1H), 3.39 (dd, *J* = 15.0, 6.0

Hz, 1H), 3.19 (dd, *J* = 15.2, 7.8 Hz, 1H), 3.07 – 2.97 (m, 1H), 2.71 (dd, *J* = 12.1, 5.8 Hz, 2H), 1.88 – 1.74 (m, 2H); MS: m/z 425.1 (M+1), 427.1 (M+3).

1-(4-chlorophenyl)-2-(3,4-dihydroquinolin-1(2H)-yl)ethyl-4-chlorophenyl carbamate (28h)

White solid; IR (KBr, v, cm^{-1}): 3294, 2924, 2877, 1901, 1714, 1697, 1539, 1494, 1228, 1055, 833, 746; ^{1}H NMR (400 MHz, $CDCl_3$) δ 7.42 – 7.33 (m, 4H), 7.27 (d, *J* = 7.2 Hz, 4H), 7.11 (t, *J* = 7.8 Hz, 1H), 6.95 (d, *J* = 6.0 Hz, 1H), 6.77 (d, *J* = 8.2 Hz, 1H), 6.63 (td, *J* = 7.3, 0.8 Hz, 1H), 6.57 (s, 1H), 6.01 (dd, *J* = 7.5, 6.1 Hz, 1H), 3.87 (dd, *J* = 15.0, 7.6 Hz, 1H), 3.39 (dd, *J* = 15.0, 6.0 Hz, 1H), 3.20 (ddd, *J* = 11.3, 7.4, 3.9 Hz, 1H), 3.08 – 2.99 (m, 1H), 2.70 (dd, *J* = 12.2, 5.8 Hz, 2H), 1.89 – 1.73 (m, 2H); MS: m/z 441.2 (M+1), 443.2 (M+3).

1-(4-chlorophenyl)-2-(3,4-dihydroquinolin-1(2H)-yl)ethyl-3-nitrophenyl carbamate (28i)

Pale yellow solid; IR (KBr, v, cm^{-1}): 3341, 2931, 2835, 1739, 1693, 1504, 1493, 1273, 1233, 1091, 970; ^{1}H NMR (400 MHz, $CDCl_3$) δ 8.21 (t, *J* = 2.1 Hz, 1H), 7.93 (ddd, *J* = 8.2, 2.1, 0.8 Hz, 1H), 7.68 (d, *J* = 8.0 Hz, 1H), 7.39 (s, 4H), 7.13 (t, *J* = 7.1 Hz, 1H), 6.95 (d, *J* = 7.3 Hz, 1H), 6.81 – 6.74 (m, 2H), 6.67 – 6.61 (m, 1H), 6.06 (dd, *J* = 7.8, 5.8 Hz, 1H), 3.92 (dd, *J* = 15.0, 7.9 Hz, 1H), 3.40 (dd, *J* = 15.1, 5.7 Hz, 1H), 3.22 (ddd, *J* = 11.2, 7.1, 3.9 Hz, 1H), 3.09 (ddd, *J* = 11.0, 6.6, 4.2 Hz, 1H), 2.77 – 2.63 (m, 2H), 1.91 – 1.77 (m, 2H); MS: m/z 452.2 (M+1), 453.2 (M+3).

1-(4-chlorophenyl)-2-(3,4-dihydroquinolin-1(2H)-yl)ethyl-4-nitrophenyl carbamate (28j)

Pale yellow solid; IR (KBr, v, cm^{-1}): 3338, 2933, 1732, 1597, 1496, 1301, 1220, 1112, 1060, 850,775; ^{1}H NMR (400 MHz, $CDCl_3$) δ 8.23 – 8.15 (m, 2H), 7.51 – 7.46 (m, 2H), 7.43 – 7.35 (m, 4H), 7.13 (t, *J* = 7.0 Hz, 1H), 6.94 (d, *J* = 6.8 Hz, 2H), 6.78 (d, *J* = 8.2 Hz, 1H), 6.64 (t, *J* = 7.3 Hz, 1H), 6.05 (dd, *J* = 7.8, 5.8 Hz, 1H), 3.91 (dd, *J* = 15.1, 7.9 Hz, 1H), 3.40 (dd, *J* = 15.1, 5.7 Hz, 1H), 3.22 (ddd, *J* = 11.2, 7.2, 4.0 Hz, 1H), 3.09 (ddd, *J* = 11.1, 6.6, 4.2 Hz, 1H), 2.70 (dd, *J* = 12.3, 5.9 Hz, 2H), 1.88 – 1.77 (m, 2H); MS: m/z 452.2 (M+1), 453.2 (M+3).

Ethyl-2-((1-(4-chlorophenyl)-2-(3,4-dihydroquinolin-1(2H)-yl)ethoxy)carbonyl amino)benzoate (28k)

White solid; IR (KBr, v, cm^{-1}): 3346, 2927, 1732, 1697, 1504, 1213, 1041, 835, 752; ^{1}H NMR (400 MHz, $CDCl_3$) δ 8.38 (d, *J* = 7.7 Hz, 1H), 8.04 (dd, *J* = 8.0, 1.5 Hz, 1H), 7.55 – 7.49 (m, 1H), 7.44 – 7.32 (m, 4H), 6.95 (d, *J* = 7.4 Hz, 2H), 6.84 (d, *J* = 7.4 Hz, 2H), 6.77 (d, *J* = 8.1 Hz, 1H), 6.00 (t, *J* = 6.7 Hz, 1H), 5.80 (s, 1H), 4.42 (q, *J* = 7.1 Hz, 2H), 3.83 (dd, *J* = 14.9, 7.3 Hz, 1H), 3.44 (dd, *J* = 15.0, 6.3 Hz, 1H), 3.32 – 3.24 (m, 1H), 3.04 – 2.97 (m, 1H), 2.71 (dd, *J* = 11.6, 5.4 Hz, 2H), 1.81 (dd, *J* = 11.5, 7.7 Hz, 2H), 1.45 (t, *J* = 7.1 Hz, 3H); MS: m/z 425.2 (daughter ion).

Ethyl-4-((1-(4-chlorophenyl)-2-(3,4-dihydroquinolin-1(2H)-yl)ethoxy)carbonyl amino)benzoate (28l)

White solid; IR (KBr, v, cm^{-1}): 3323, 2937, 2881, 1733, 1504, 1415, 1286, 1029, 1014, 856; ^{1}H NMR (400 MHz, $CDCl_3$) δ 8.01 – 7.97 (m, 2H), 7.41 (s, 1H), 7.38 (d, *J* = 4.0 Hz, 4H), 7.13 (dd, *J* = 11.2, 4.4 Hz, 1H), 6.95 (d, *J* = 7.3 Hz, 1H), 6.77 (d, *J* = 8.4 Hz, 2H), 6.63 (t, *J* = 7.3 Hz, 1H), 6.03 (dd, *J* = 7.5, 6.0 Hz, 1H), 4.37 (q, *J* = 7.1 Hz, 2H), 3.89 (dd, *J* = 15.0, 7.6 Hz, 1H), 3.40 (dd, *J* = 15.0, 6.0 Hz, 1H), 3.21 (ddd, *J* = 11.3, 7.5, 4.0 Hz, 1H), 3.09 – 3.01 (m, 1H), 2.70 (dd, *J* = 12.2, 5.8 Hz, 2H), 1.88 – 1.74 (m, 2H), 1.40 (t, *J* = 7.1 Hz, 3H); ^{13}C NMR (100 MHz, $CDCl_3$) δ 166.30, 152.16, 144.84, 141.88, 137.19, 134.24, 130.85, 129.44, 128.87, 127.90, 127.21, 125.28, 122.47, 117.74, 116.33, 110.69, 73.96, 60.95, 57.08, 50.65, 28.02, 21.95, 14.39; MS: m/z 425.2 (daughter ion).

5.2.7 Synthesis and characterization of 2-(1-(4-chlorophenyl)-2-(3,4-dihydroquinolin-1(*2H*)-yl)ethoxy)-*N*-phenylacetamide derivative (32a-n)

Designed compounds **32a-n** were synthesized in three steps (scheme **7**). First step involved the reaction of **26** (intermediate, scheme **6**) with ethyl-2-bromoacetate (**10**), was optimized using different conditions (a1-a2). Overall, second condition (a2) that involves the use of THF as solvent and sodium hydride as base was found to be suitable for the synthesis of intermediate compound **29**. Subsequent hydrolysis of compound **29** under basic condition afforded intermediate acid (**30**). Coupling reaction of intermediate **30** with various anilines (**31a-n**) afforded titled compounds (**32a-n**) in moderate to good yield.

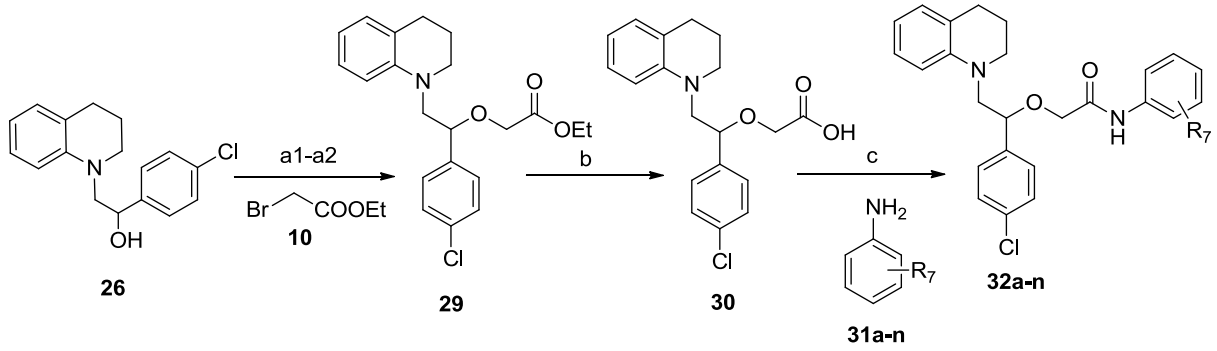

Scheme 7. Reagents and conditions: (a1) DMF, K_2CO_3, KI (catalytic amount), rt-100˚C 12h (a2) Dry THF, NaH, rt, 4 h, (b) 10% aq. NaOH:MeOH (1:1), reflux 5 h (c) HOBT, EDC.HCl, Et_3N, DCM, rt, 6-9 h

Optimization of reaction condition (a1-a2) for the synthesis of 2-(1-(4-chlorophenyl)-2-(3,4-dihydroquinolin-1(2*H*)-yl)ethoxy)acetate (29)

Two reaction conditions were tried for the synthesis of intermediate compound **29** from the compound **26** (intermediate obtained in scheme **6**). In the first condition, ethyl-2-

bromoacetate (**10**) was added to the stirred equimolar solution of intermediate **26,** and potassium carbonate (2.5 equivalents) in DMF, catalytic amount of potassium iodide was also added to the reaction mass. The reaction was stirred at room temperature, but till six hours no significant conversion took place and starting material remained almost intact. Further, reaction was stirred at 100˚C, but after six hours multiple spots appeared on the TLC, also starting material was not consumed completely. In the second condition (**a2**), base potassium carbonate was replaced by sodium hydride and THF was taken as solvent instead of DMF, this condition afforded compound **29**, in good yield. Detailed procedure is given in the below paragraph.

Synthesis of ethyl 2-(1-(4-chlorophenyl)-2-(3,4-dihydroquinolin-1(*2H*)-yl)ethoxy)acetate (29) using optimized reaction condition

Sodium hydride (hexane washed, 0.52 g, 22 mmol) was added portion wise to the ice-cold stirring solution of intermediate **26** (5.74 g, 20 mmol) in dry THF. Further, ethyl 2-bromoacetate **10** (2.19 ml, 20 mmol) was slowly added under ice-cold condition. The reaction mixture was stirred at rt for 4 h; progress of the reaction was monitored by TLC. After completion, the reaction was quenched with 0.1 N HCl (3 ml) under ice-cold condition. Further, THF was evaporated on the rotary evaporator and ethyl acetate (150 ml) was added to the reaction mass. Ethyl acetate layer was twice washed with distilled water (2x150 ml), and then with brine water (150 ml). The organic layer was dried over anhydrous sodium sulphate and finally evaporated on the rotary evaporator to afford the compound **29** as viscous oil with 87% yield.

Synthesis of 2-(1-(4-chlorophenyl)-2-(3,4-dihydroquinolin-1(*2H*)-yl)ethoxy)acetic acid (30)

To the stirred solution of ethyl 2-(1-(4-chlorophenyl)-2-(3,4-dihydroquinolin-1(*2H*)-yl)ethoxy)acetate **29** (5g, 13.4 mmol) in methanol (50 ml), 10 % aqueous sodium hydroxide solution was added (50 ml), and the reaction was refluxed. After completion of reaction as per TLC (after 5 h), methanol was evaporated, 100 ml of distilled water was added to the reaction mixture. Further, the reaction mixture was taken in a separating funnel and washed with hexane (150 ml), aqueous layer was separated and its pH was made slightly acidic (around 6). Further, aqueous portion was again extracted twice with ethyl acetate (200 ml). Combined ethyl acetate layer was first washed with ice cold water (400 ml), and then with brine water (400 ml). Ethyl acetate layer was dried over anhydrous sodium sulphate and finally evaporated on the rotary evaporator to afford the intermediate compound **30** as white solid with 93% yield.

General procedure for the synthesis of 2-(1-(4-chlorophenyl)-2-(3,4-dihydroquinolin-1(*2H*)-yl)ethoxy)-*N*-phenylacetamide derivative (**32a-n)**

To the stirred solution of 2-(1-(4-chlorophenyl)-2-(3,4-dihydroquinolin-1(*2H*)-yl)ethoxy)acetic acid **30** (0.345 g, 1 mmol) in dry DCM, HOBt (0.16 g, 1.2 mmol) and EDCI. HCl (0.23 g, 1.2 mmol), triethylamine (0.253 g, 2.5 mmol) were added and stirring was continued for 30 min. To the reaction mixture, corresponding anilines (**31a-n**, 1 mmol) were added and further stirred at room temperature for 6-9 h. After completion of reaction as per TLC, the reaction mass was taken in a separating funnel, to this 25 ml more DCM was added and washed with saturated sodium bicarbonate solution (50 ml), the organic layer was further washed with distilled water, followed by brine water (50ml). DCM layer was separated and dried over anhydrous sodium sulphate, finally evaporated on the rotary evaporator to afford the final titled compounds **32a-n** [6]. Preliminary characteristics data of the synthesized compounds **32a-n** is shown in Table **5.8**.

Table 5.8. Preliminary characteristics data of compounds **32a-n**

Comp. code	R_7	Mol. formula	Mol. Wt	% Yield	Melting point (˚C)
32a	H	$C_{25}H_{25}ClN_2O_2$	420.16	87	Semisolid
32b	2-CH_3	$C_{26}H_{27}ClN_2O_2$	434.18	73	Semisolid
32c	3-CH_3	$C_{26}H_{27}ClN_2O_2$	434.18	78	Semisolid
32d	4-CH_3	$C_{26}H_{27}ClN_2O_2$	434.18	82	Semisolid
32e	2-OCH_3	$C_{26}H_{27}ClN_2O_3$	450.17	79	Semisolid
32f	3-OCH_3	$C_{26}H_{27}ClN_2O_3$	450.17	77	Semisolid
32g	4-OCH_3	$C_{26}H_{27}ClN_2O_3$	450.17	83	Semisolid
32h	4-F	$C_{25}H_{24}ClFN_2O_2$	438.15	72	Semisolid
32i	3-Cl	$C_{25}H_{24}Cl_2N_2O_2$	454.12	76	Semisolid
32j	4-Cl	$C_{25}H_{24}Cl_2N_2O_2$	454.12	84	Semisolid
32k	3-Br	$C_{25}H_{24}BrClN_2O_2$	498.07	74	Semisolid
32l	4-Br	$C_{25}H_{24}BrClN_2O_2$	498.07	84	Semisolid
32m	4-NO_2	$C_{25}H_{24}ClN_3O_4$	465.15	67	Semisolid
32n	2,4-di-Me	$C_{27}H_{29}ClN_2O_2$	448.19	82	Semisolid

Spectral characterization of compounds 32a-n

Synthesized compounds were characterized by spectral analysis like IR and Mass, while six compounds (**32b, 32f, 32i, 32j, 32k** and **32n**) were characterized by ^{1}H NMR as representative of series. IR spectra of compounds **32a-n** displayed peak at 3444-3673 cm^{-1} (broad, intense) certainly due to the stretching of amidic hydrogen (−CON**H**-). Another characteristic peak (sharp, strong) appeared in the region 1683-1702 cm^{-1} corresponding to the stretching of carbonyl group (--**C=O**NH-). In the ^{1}H NMR spectra of four compounds**,** two protons at 3rd carbon of THQ ring displayed two separate peaks at δ ~1.75-1.99. Two

benzylic proton at the fourth position of THQ ring appeared at δ ~2.69-2.81. Protons pair at 2nd position of THQ and two protons adjacent to nitrogen (outside the THQ ring) appeared at δ ~3.20-3.84. Furthermore, proton pairs at carbon connecting carbonyl and oxygen atom exhibited two distinct peaks (dd) at δ ~3.85-4.14. Further, single proton at benzylic carbon connected with highly electronegative oxygen atom is highly de-shielded, which appeared (dd) between δ values 4.68-4.76. Nitrogen proton of amide linkage (-CON**H**-**)** appeared in highly downfield region with δ values 8.32-8.82. Further, counting as well as the position of aromatic protons of above four compounds was also found in accordance with the proposed structures. ESI-MS of the synthesized compounds showed the corresponding M+1 peak.

2-(1-(4-chlorophenyl)-2-(3,4-dihydroquinolin-1(2H)-yl)ethoxy)-N-phenyl acetamide (32a)

Pale yellow semisolid; IR (KBr, v, cm^{-1}): 3644, 3024, 2924, 2861, 1921, 1689, 1514, 1478, 1233, 1187, 1106, 985; MS: m/z 421.1(M+1), 423.1 (M+3).

2-(1-(4-chlorophenyl)-2-(3,4-dihydroquinolin-1(2H)-yl)ethoxy)-N-o-tolyl acetamide (32b)

Pale yellow semisolid; IR (KBr, v, cm^{-1}): 3645, 3614, 3449, 2926, 2864, 1697, 1519, 1458, 1301, 1196, 1101, 1012, 962, 827, 750; ^{1}H NMR (400 MHz, $CDCl_3$) δ 8.43 (s, 1H), 7.62 – 7.58 (m, 1H), 7.47 – 7.39 (m, 2H), 7.36 (d, *J* = 8.4 Hz, 2H), 7.18 (d, *J* = 7.1 Hz, 2H), 7.10 (ddd, *J* = 11.4, 4.7, 2.0 Hz, 2H), 6.94 (d, *J* = 6.1 Hz, 1H), 6.77 (d, *J* = 8.1 Hz, 1H), 6.64 (td, *J* = 7.3, 0.8 Hz, 1H), 4.76 (dd, *J* = 8.4, 4.1 Hz, 1H), 4.11 (d, *J* = 15.6 Hz, 1H), 3.97 (d, *J* = 15.6 Hz, 1H), 3.72 (dd, *J* = 15.2, 8.5 Hz, 1H), 3.44 – 3.28 (m, 2H), 3.20 (ddd, *J* = 11.0, 7.1, 3.6 Hz, 1H), 2.69 (dd, *J* = 11.9, 5.6 Hz, 2H), 2.10 (s, 3H), 1.87 – 1.82 (m, 1H), 1.78 (dd, *J* = 6.5, 2.8 Hz, 1H); MS: m/z 435.3 (M+1), 437.2 (M+3).

2-(1-(4-chlorophenyl)-2-(3,4-dihydroquinolin-1(2H)-yl)ethoxy)-N-m-tolyl acetamide (32c)

Pale yellow semisolid; IR (KBr, v, cm^{-1}): 3643, 2895, 1687, 1519, 1456, 1417, 1317, 1234, 1083, 1012, 987; MS: m/z 435.3 (M+1), 437.2 (M+3).

2-(1-(4-chlorophenyl)-2-(3,4-dihydroquinolin-1(2H)-yl)ethoxy)-N-p-tolyl acetamide (32d)

Pale yellow semisolid; IR (KBr, v, cm^{-1}): 3654, 3024, 2920, 2862, 1901, 1687, 1516, 1458, 1236, 1197, 1107, 987; MS: m/z 435.3 (M+1), 437.2 (M+3).

2-(1-(4-chlorophenyl)-2-(3,4-dihydroquinolin-1(2H)-yl)ethoxy)-N-(2-methoxy phenyl)acetamide (32e)

Pale yellow semisolid; IR (KBr, v, cm^{-1}): 3647, 2895, 1683, 1539, 1506, 1458, 1338, 1249, 1174, 1045; MS: m/z 451.3 (M+1), 453.2 (M+3).

2-(1-(4-chlorophenyl)-2-(3,4-dihydroquinolin-1(2H)-yl)ethoxy)-N-(3-methoxy phenyl)acetamide (32f)

Pale yellow semisolid; IR (KBr, v, cm^{-1}): 3647, 2924, 2850, 1697, 1539, 1489, 1415, 1267, 1230, 1155, 1122, 1039, 989, 840; ^1H NMR (400 MHz, $CDCl_3$) δ 8.60 (s, 1H), 7.45 – 7.41 (m, 2H), 7.39 – 7.34 (m, 2H), 7.18 – 7.02 (m, 4H), 6.96 (d, *J* = 8.0 Hz, 1H), 6.75 – 6.69 (m, 1H), 6.64 (ddd, *J* = 8.3, 2.5, 0.8 Hz, 1H), 6.51 (ddd, *J* = 8.0, 1.9, 0.8 Hz, 1H), 4.70 (dd, *J* = 9.4, 3.2 Hz, 1H), 4.13 (d, *J* = 16.0 Hz, 1H), 3.84 (d, *J* = 16.0 Hz, 1H), 3.76 – 3.67 (m, 4H), 3.32 (ddd, *J* = 18.6, 9.7, 2.9 Hz, 3H), 2.78 (dd, *J* = 12.6, 6.5 Hz, 2H), 1.93 (dd, *J* = 11.5, 5.2 Hz, 1H), 1.88 – 1.82 (m, 1H); MS: m/z 451.3 (M+1), 453.2 (M+3).

2-(1-(4-chlorophenyl)-2-(3,4-dihydroquinolin-1(2H)-yl)ethoxy)-N-(4-methoxy phenyl)acetamide (32g)

Pale yellow semisolid; IR (KBr, v, cm^{-1}): 3653, 2956, 1692, 1556, 1506, 1456, 1338, 1244, 1105, 1035; MS: m/z 451.3 (M+1), 453.2 (M+3).

2-(1-(4-chlorophenyl)-2-(3,4-dihydroquinolin-1(2H)-yl)ethoxy)-N-(4-fluoro phenyl)acetamide (32h)

Pale yellow semisolid; IR (KBr, v, cm^{-1}): 3673, 2929, 2874, 1699, 1558, 1523, 1288, 1097, 1016, 826, 745; MS: m/z 439.2 (M+1), 441.2 (M+3).

N-(3-chlorophenyl)-2-(1-(4-chlorophenyl)-2-(3,4-dihydroquinolin-1(2H)-yl) ethoxy)acetamide (32i)

Pale yellow semisolid; IR (KBr, v, cm^{-1}): 3646, 2956, 2924, 2866, 1697, 1520, 1274, 1238, 1107, 1089, 1014, 910; ^1H NMR (400 MHz, $CDCl_3$) δ 8.62 (s, 1H), 7.48 – 7.41 (m, 2H), 7.37 (d, *J* = 8.4 Hz, 2H), 7.19 – 7.13 (m, 1H), 7.12 – 7.07 (m, 2H), 7.05 – 7.01 (m, 2H), 6.99 (d, *J* = 2.1 Hz, 1H), 6.77 – 6.72 (m, 1H), 4.68 (dd, *J* = 9.8, 3.0 Hz, 1H), 4.14 (d, *J* = 16.2 Hz, 1H), 3.82 (d, *J* = 16.2 Hz, 1H), 3.77 – 3.71 (m, 1H), 3.34 (ddd, *J* = 22.1, 12.9, 9.5 Hz, 2H), 3.25 (dd, *J* = 15.4, 3.0 Hz, 1H), 2.80 (dd, *J* = 12.6, 6.4 Hz, 2H), 1.97 – 1.92 (m, 1H), 1.83 (dd, *J* = 7.7, 4.6 Hz, 1H); MS: m/z 455.2 (M+1), 457.2 (M+3).

N-(4-chlorophenyl)-2-(1-(4-chlorophenyl)-2-(3,4-dihydroquinolin-1(2H)-yl) ethoxy)acetamide (32j)

Pale yellow semisolid; IR (KBr, v, cm^{-1}): 3670, 2926, 2864, 1697, 1556, 1519, 1286, 1091, 1012, 827, 746; ^1H NMR (400 MHz, $CDCl_3$) δ 8.63 (s, 1H), 7.45 – 7.42 (m, 2H), 7.39 – 7.35 (m, 2H), 7.14 – 7.11 (m, 3H), 6.98 (d, *J* = 8.0 Hz, 1H), 6.96 – 6.89 (m, 2H), 6.74 (td, *J* = 7.3, 0.9 Hz, 1H), 6.64 – 6.61 (m, 2H), 4.69 (dd, *J* = 9.8, 3.0 Hz, 1H), 4.15 (d, *J* = 16.2 Hz, 1H), 3.84 (s, 1H), 3.73 (dd, *J* = 15.4, 9.8 Hz, 1H), 3.36 (t, *J* = 5.6 Hz, 2H), 3.27 (dd, *J* = 15.4, 3.1 Hz, 1H), 2.78 (dd, *J* = 12.6, 6.3 Hz, 2H), 1.93 (dd, *J* = 9.3, 3.9 Hz, 1H), 1.85 (dd, *J* = 7.5, 5.5 Hz, 1H); MS: m/z 455.2 (M+1), 457.2 (M+3).

N-(3-bromophenyl)-2-(1-(4-chlorophenyl)-2-(3,4-dihydroquinolin-1(2H)-yl) ethoxy)acetamide (32k)

Pale yellow semisolid; IR (KBr, v, cm^{-1}): 3666, 2940, 2806, 1696, 1519, 1417, 1338, 1236, 1107, 987; ^{1}H NMR (400 MHz, CDCl3) δ 8.61 (s, 1H), 7.44 (d, J = 8.5 Hz, 2H), 7.39 – 7.34 (m, 2H), 7.22 – 7.16 (m, 2H), 7.15 – 7.05 (m, 4H), 7.02 (t, J = 7.9 Hz, 1H), 6.79 – 6.74 (m, 1H), 4.68 (dd, J = 9.8, 2.9 Hz, 1H), 4.14 (d, J = 16.2 Hz, 1H), 3.82 (d, J = 16.2 Hz, 1H), 3.77 – 3.71 (m, 1H), 3.35 (dd, J = 10.5, 6.0 Hz, 2H), 3.25 (dd, J = 15.4, 3.0 Hz, 1H), 2.81 (dd, J = 11.6, 5.6 Hz, 2H), 1.99 – 1.91 (m, 1H), 1.88 – 1.79 (m, 1H); MS: m/z 499.2 (M+1), 501.19 (M+3).

N-(4-bromophenyl)-2-(1-(4-chlorophenyl)-2-(3,4-dihydroquinolin-1(2H)-yl) ethoxy)acetamide (32l)

Pale yellow semisolid; IR (KBr, v, cm^{-1}): 3486, 2924, 1699, 1519, 1456, 1286, 1236, 1107, 1012, 827, 748; MS: m/z 499.2 (M+1), 501.19 (M+3).

2-(1-(4-chlorophenyl)-2-(3,4-dihydroquinolin-1(2H)-yl)ethoxy)-N-(4-nitrophenyl) acetamide (32m)

Yellow semisolid; IR (KBr, v, cm^{-1}): 3444, 3242, 1923, 1702, 1506, 1471, 1305, 1112, 1001, 842. MS: m/z 466.3 (M+1), 468.3 (M+3).

2-(1-(4-chlorophenyl)-2-(3,4-dihydroquinolin-1(2H)-yl)ethoxy)-N-(2,4-dimethyl phenyl)acetamide (32n)

Pale yellow semisolid; IR (KBr, v, cm^{-1}): 3641, 2923, 2843, 1689, 1539, 1489, 1415, 1267, 1230, 1155, 1122, 1039, 989, 840; ^{1}H NMR (400 MHz, $CDCl_3$) δ 8.36 (s, 1H), 7.39 (dt, *J* = 12.0, 8.4 Hz, 5H), 7.09 (t, *J* = 7.6 Hz, 1H), 7.01 – 6.92 (m, 3H), 6.76 (dd, *J* = 13.2, 8.6 Hz, 1H), 6.64 (t, *J* = 7.2 Hz, 1H), 4.75 (dd, *J* = 8.5, 4.0 Hz, 1H), 4.11 (d, *J* = 15.6 Hz, 1H), 3.96 (d, *J* = 15.6 Hz, 1H), 3.71 (dd, *J* = 15.3, 8.5 Hz, 1H), 3.41 – 3.31 (m, 2H), 3.21 (ddd, *J* = 11.0, 7.1, 3.6 Hz, 1H), 2.69 (t, *J* = 7.9 Hz, 2H), 2.31 (s, 3H), 2.05 (s, 3H), 1.85 (dd, *J* = 10.1, 6.3 Hz, 1H), 1.81 – 1.74 (m, 1H); MS: m/z 449.3 (M+1), 451.3 (M+3).

5.2.8 Synthesis and characterization of 3-(6-methoxy-3,4-dihydroquinolin-1(*2H*)-yl)-1-(piperazin-1-yl)propan-1-one derivatives (38a-o)

Designed compounds **38a-o** were synthesized using three step synthetic route, reaction conditions used for the synthesis of target compounds are shown in scheme **8**. The first step involved the reduction of 6-methoxyquinoline (**33**) to 6-methoxytetrahydroquinoline (**34)** using Nickel-aluminium alloy under basic condition. Further, the reaction of intermediate **34** with 3-bromopropanoic acid (**35)** afforded intermediate compound **36.** Finally, the coupling of intermediate compound **36** with different piperazines (**37a-o**) afforded titled compounds **38a-o**.

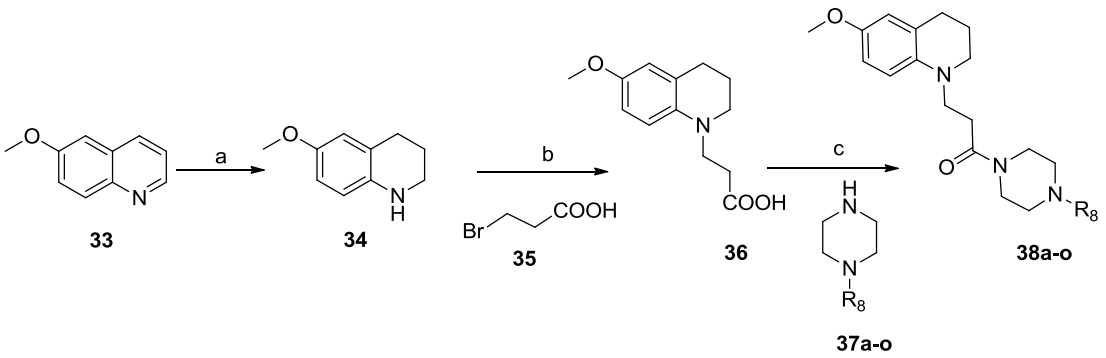

Scheme 8. Reagents and conditions: (a) EtOH, 10% aq. NaOH, Ni-Al alloy, 0˚C-rt, 6h (b) ACN, Et_3N, reflux, 5 h (c) HOBT, EDC. HCl, Et_3N, DCM, rt, 6-8 h

Synthesis of 6-methoxy-1,2,3,4-tetrahydroquinoline (34)

To the stirred solution of 6-methoxyquinoline **33** (4.34 ml, 31.44 mmol) in ethanol (50 ml), Ni-Al alloy (2.5 g) was added and stirring was continued for 30 min. Further, the reaction mass was cooled to 0-4˚C and then aqueous sodium hydroxide solution (10% w/v, 50 ml) was added slowly. After complete addition, the reaction mixture was further stirred at room temperature for 6 h. After completion of reaction as per TLC, the reaction mass was passed through a tight celite bed, further ethanol (2x75 ml) was passed through the celite bed. Combined filtrate was evaporated using the rotary evaporator till its volume remained one-fourth to its original volume. Further, the reaction mass was acidified with 2N HCl, until its pH became neutral. Further, the reaction mass was taken in a separating funnel and extracted twice with ethyl acetate (2x150 ml). Combined ethyl acetate layer was first washed with water (300 ml) and then with brine (300 ml). Ethyl acetate layer was dried over anhydrous sodium sulphate and finally evaporated using rotary evaporator to afford the reduced intermediate compound **34** as crude oil. Crude **34** was purified by column chromatography using 5% ethyl acetate in hexane as mobile phase and silica (mesh size 100-200) as stationary phase, which afforded the pure compound **34**, as pale yellow oil with 87% yield [8].

Synthesis of 3-(6-methoxy-3,4-dihydroquinolin-1(*2H*)-yl) propanoic acid (36)

3-bromopropanoic acid **35** (1.80 ml, 21.4 mmol) was added portion wise to the stirring solution of 6-methoxy-1,2,3,4-tetrahydroquinoline **34** (3.5 g, 21.4 mmol) in acetonitrile, containing triethylamine (7.30 ml, 53.5 mmol) as a base and the catalytic amount of potassium iodide. The reaction mixture was refluxed and the progress of the reaction was monitored using TLC. After completion of reaction as per TLC (after 5h), acetonitrile was evaporated using rotary evaporator, 100 ml of water was added to reaction mixture and extracted with hexane (150 ml). Further, the aqueous layer was separated and neutralized

with 6 N HCl and twice extracted with ethyl acetate (2x250 ml). Combined ethyl acetate layer was first washed with water (250 ml) and then subsequently with brine (250 ml). Ethyl acetate layer was dried over anhydrous sodium sulphate and finally evaporated using rotary evaporator to afford IInd intermediate compound **36** as pale yellow semisolid with 73% yield.

General procedure for the synthesis of 3-(6-methoxy-3,4-dihydroquinolin-1(*2H*)-yl)-1-(4-phenylpiperazin-1-yl)propan-1-one derivatives (38a-o)

To the stirred solution of 3-(6-methoxy-3,4-dihydroquinolin-1(*2H*)-yl) propanoic acid **36** (0.235 g, 1 mmol) in dry DCM, HOBt (0.16 g, 1.2 mmol) and EDCI. HCl (0.23 g, 1.2 mmol), triethylamine (0.253 g, 2.5 mmol) were added and continued stirring for 30 min. at room temperature. Further, to the reaction mixture, corresponding piperazines (**37a-o**) were added and further stirred at room temperature for 6-8 h. After completion of reaction as per TLC, the reaction mass was taken in a separating funnel, to this 25 ml more DCM was added and the organic layer was washed with saturated sodium bicarbonate solution (50 ml). Organic layer was then washed with distilled water, followed by brine (50ml), separated and dried over anhydrous sodium sulphate and finally evaporated to afford the final compounds **38a-o** [9]. Preliminary characteristics data of compounds **38a-o** is shown in table no. **5.9.**

Table 5.9 Preliminary characteristics data of compounds **38a-o**

Comp. code	R_8	Mol. formula	Mol. Wt	% Yield	Melting point (˚C)
38a	Ph	$C_{23}H_{29}N_3O_2$	379.23	83	Semisolid
38b	2-Me-Ph	$C_{24}H_{31}N_3O_2$	393.24	88	Semisolid
38c	4-Me-Ph	$C_{24}H_{31}N_3O_2$	393.24	84	Semisolid
38d	2-MeO-Ph	$C_{24}H_{31}N_3O_3$	409.24	82	Semisolid
38e	3-MeO-Ph	$C_{24}H_{31}N_3O_3$	409.24	92	Semisolid
38f	4-MeO-Ph	$C_{24}H_{31}N_3O_3$	409.24	90	54-56
38g	2-F-Ph	$C_{23}H_{28}FN_3O_2$	397.22	74	Semisolid
38h	4-F-Ph	$C_{23}H_{28}FN_3O_2$	397.22	78	Semisolid
38i	2-Cl-Ph	$C_{23}H_{28}ClN_3O_2$	413.19	82	Semisolid
38j	3-Cl-Ph	$C_{23}H_{28}ClN_3O_2$	413.19	87	Semisolid
38k	4-Cl-Ph	$C_{23}H_{28}ClN_3O_2$	413.19	85	76-79
38l	4-NO_2-Ph	$C_{23}H_{28}N_4O_4$	424.21	76	62-66
38m	Benzyl	$C_{24}H_{31}N_3O_2$	393.24	86	Semisolid
38n	2-Pyridine	$C_{22}H_{28}N_4O_2$	380.22	74	Semisolid
38o	2,3-di-Cl-Ph	$C_{23}H_{27}Cl_2N_3O_2$	447.15	83	Semisolid

Spectral Characterization of compounds (38a-o)

Synthesized compounds of series (**38a-o**) were characterized by various spectral techniques like IR, ^{1}H NMR, ESI-MS and elemental analysis. The IR spectra of compounds **38a-o** showed the expected absorption bands, for example corresponding to stretching of amide carbonyl adjacent to piperazine (C=O) peak appeared at 1635-1690 cm^{-1}. Absorption band of C–O stretching corresponding to 6-methoxy group of THQ appeared at around 1230–1242 cm^{-1}. ^{1}H NMR spectrum of the reported compounds exhibited characteristic peak around δ 1.95-1.97 corresponding to the two protons at the 3rd position of THQ ring, while two protons at the fourth position displayed peaks (dd or mutliplet) near δ 2.64-2.65. Protons at the carbon adjacent to the keto group appeared as triplet (also multiplet in some compounds) near δ 2.74-2.76, while three protons of 6-methoxy group appeared as singlet at δ ~3.75. Furthermore, for remaining protons also their peak pattern as well as proton counting was found in accordance with the proposed structures. The calculated and observed elemental values of C H N were found within the acceptable range. ESI-MS of the synthesized compounds showed the corresponding M+1 peak. Spectral data of compounds **38a-o** are given below:

3-(6-methoxy-3,4-dihydroquinolin-1(2H)-yl)-1-(4-phenylpiperazin-1-yl)propan-1-one (38a)

Pale yellow semisolid; IR (KBr, v, cm^{-1}): 3412, 2904, 1664, 1504, 1444, 1269, 1230, 1203, 1155, 1033, 900; ^{1}H NMR (400 MHz, $CDCl_3$) δ 7.31 (d, *J* = 7.7 Hz, 2H), 6.96 – 6.90 (m, 3H), 6.69 (dd, *J* = 8.8, 3.0 Hz, 1H), 6.60 (dd, *J* = 11.3, 5.9 Hz, 2H), 3.83 – 3.79 (m, 2H), 3.75 (s, 3H), 3.71 – 3.65 (m, 2H), 3.62 – 3.56 (m, 2H), 3.30 – 3.24 (m, 2H), 3.20 – 3.09 (m, 4H), 2.76 (t, *J* = 6.4 Hz, 2H), 2.69 – 2.61 (m, 2H), 1.97 (dt, *J* = 12.6, 6.4 Hz, 2H); Anal. calculated for $C_{23}H_{29}N_3O_2$: C, 72.79; H, 7.70; N, 11.07. Found: C, 72.74; H, 7.72; N, 11.08; MS: m/z 380.3 (M+1).

3-(6-methoxy-3,4-dihydroquinolin-1(2H)-yl)-1-(4-o-tolylpiperazin-1-yl)propan-1-one (38b)

Pale yellow semisolid; IR (KBr, v, cm^{-1}): 3437, 3361, 2929, 2916, 1747, 1635, 1506, 1456, 1435, 1269, 1224, 1033, 761; ^{1}H NMR (400 MHz, $CDCl_3$) δ 7.28 (d, *J* = 1.7 Hz, 1H), 7.25 – 7.15 (m, 2H), 7.03 (t, *J* = 7.3 Hz, 1H), 6.96 (d, *J* = 7.9 Hz, 1H), 6.69 (d, *J* = 8.9 Hz, 1H), 6.61 (s, 1H), 3.79 (s, 2H), 3.75 (d, *J* = 1.7 Hz, 3H), 3.66 (s, 2H), 3.58 (d, *J* = 3.7 Hz, 2H), 3.33 – 3.19 (m, 2H), 2.91 – 2.79 (m, 4H), 2.79 – 2.73 (m, 2H), 2.68 – 2.62 (m, 2H), 2.33 (s, 3H), 2.00 – 1.94 (m, 2H); Anal. calculated for $C_{24}H_{31}N_3O_2$: C, 73.25; H, 7.94; N, 10.68. Found: C, 73.29; H, 7.96; N, 10.70; MS: m/z 394.3 (M+1).

3-(6-methoxy-3,4-dihydroquinolin-1(2H)-yl)-1-(4-p-tolylpiperazin-1-yl)propan-1-one (38c)

Pale yellow semisolid; IR (KBr, v, cm^{-1}): 3391, 2922, 2860, 1813, 1638, 1508, 1435, 1236, 1205, 1029, 812.03; ^{1}H NMR (400 MHz, $CDCl_3$) δ 7.11 (d, *J* = 8.1 Hz, 2H), 6.87 – 6.81 (m, 2H), 6.69 (dd, *J* = 8.8, 3.0 Hz, 1H), 6.59 (dd, *J* = 11.1, 5.9 Hz, 2H), 3.82 – 3.78 (m, 2H), 3.75 (s, 3H), 3.67 (dd, *J* = 7.9, 6.5 Hz, 2H), 3.61 – 3.55 (m, 2H), 3.30 – 3.23 (m, 2H), 3.12 – 3.08 (m, 2H), 3.08 – 3.04 (m, 2H), 2.76 (t, *J* = 6.4 Hz, 2H), 2.67 – 2.62 (m, 2H), 2.30 (s, 3H), 1.97 (dd, *J* = 7.5, 3.6 Hz, 2H); Anal. calculated for $C_{24}H_{31}N_3O_2$: C, 73.25; H, 7.94; N, 10.68. Found: C, 73.21; H, 7.95; N, 10.70; MS: m/z 394.3 (M+1).

3-(6-methoxy-3,4-dihydroquinolin-1(2H)-yl)-1-(4-(2-methoxyphenyl)piperazin-1-yl)propan-1-one (38d)

Pale yellow semisolid; IR (KBr, v, cm^{-1}): 3406, 3313, 2885, 1681, 1509, 1446, 1239, 1205, 1031, 9976; ^{1}H NMR (400 MHz, $CDCl_3$) δ 7.21 (t, *J* = 8.2 Hz, 1H), 6.69 (dd, *J* = 8.8, 3.0 Hz, 1H), 6.59 (dd, *J* = 11.8, 5.9 Hz, 2H), 6.56 – 6.51 (m, 1H), 6.50 – 6.45 (m, 2H), 3.81 (s, 3H), 3.78 (s, 2H), 3.75 (s, 3H), 3.67 (dd, *J* = 7.9, 6.5 Hz, 2H), 3.62 – 3.55 (m, 2H), 3.29 – 3.23 (m, 2H), 3.19 – 3.14 (m, 2H), 3.14 – 3.10 (m, 2H), 2.76 (t, *J* = 6.4 Hz, 2H), 2.65 (dd, *J* = 7.9, 6.5 Hz, 2H), 2.00 – 1.93 (m, 2H); Anal. calculated for $C_{24}H_{31}N_3O_3$: C, 70.39; H, 7.63; N, 10.26. Found: C, 70.42; H, 7.65; N, 10.24; MS: m/z 410.3 (M+1).

3-(6-methoxy-3,4-dihydroquinolin-1(2H)-yl)-1-(4-(3-methoxyphenyl)piperazin-1-yl)propan-1-one (38e)

Pale yellow semisolid; IR (KBr, v, cm^{-1}): 3406, 2897, 1739, 1656, 1504, 1436, 1240, 1203, 1037, 993, 958; ^{1}H NMR (400 MHz, $CDCl_3$) δ 7.21 (t, *J* = 8.1 Hz, 1H), 6.69 (dd, *J* = 8.8, 3.0 Hz, 1H), 6.60 (dd, *J* = 11.6, 5.9 Hz, 2H), 6.56 – 6.52 (m, 1H), 6.50 – 6.45 (m, 2H), 3.81 (s, 3H), 3.79 (d, *J* = 5.3 Hz, 2H), 3.75 (s, 3H), 3.67 (dd, *J* = 7.9, 6.5 Hz, 2H), 3.60 – 3.56 (m, 2H), 3.29 – 3.23 (m, 2H), 3.19 – 3.14 (m, 2H), 3.14 – 3.10 (m, 2H), 2.76 (t, *J* = 6.4 Hz, 2H), 2.65 (dd, *J* = 7.9, 6.5 Hz, 2H), 1.96 (dd, *J* = 6.1, 5.1 Hz, 2H); Anal. calculated for $C_{24}H_{31}N_3O_3$: C, 70.39; H, 7.63; N, 10.26. Found: C, 70.41; H, 7.65; N, 10.25; MS: m/z 410.3 (M+1).

3-(6-methoxy-3,4-dihydroquinolin-1(2H)-yl)-1-(4-(4-methoxyphenyl)piperazin-1-yl)propan-1-one (38f)

White solid; IR (KBr, v, cm^{-1}): 3412, 3319, 2889, 2540, 1716, 1683, 1506, 1456, 1242, 1203, 1033, 948; ^{1}H NMR (400 MHz, $CDCl_3$) δ 6.93 – 6.88 (m, 2H), 6.88 – 6.84 (m, 2H), 6.68 (dd, *J* = 8.8, 3.0 Hz, 1H), 6.59 (dd, *J* = 11.4, 5.9 Hz, 2H), 3.80 (d, *J* = 2.0 Hz, 5H), 3.75 (s, 3H), 3.69 – 3.64 (m, 2H), 3.60 – 3.56 (m, 2H), 3.29 – 3.23 (m, 2H), 3.06 – 2.96 (m, 4H), 2.76 (t, *J* = 6.4 Hz, 2H), 2.67 – 2.61 (m, 2H), 1.97 (dd, *J* = 7.6, 3.5 Hz, 2H); Anal. calculated for $C_{24}H_{31}N_3O_3$: C, 70.39; H, 7.63; N, 10.26. Found: C, 70.43; H, 7.64; N, 10.23; MS: m/z 410.3 (M+1).

1-(4-(2-fluorophenyl)piperazin-1-yl)-3-(6-methoxy-3,4-dihydroquinolin-1(2H)-yl)propan-1-one (38g)

Pale yellow semisolid; IR (KBr, v, cm^{-1}): 3412, 2926, 1633, 1593, 1504, 1444, 1238, 1203, 1151, 1035; ^{1}H NMR (400 MHz, $CDCl_3$) δ 7.28 (d, *J* = 1.3 Hz, 1H), 7.11 – 7.03 (m, 2H), 7.03 – 6.97 (m, 1H), 6.92 (t, *J* = 8.3 Hz, 1H), 6.68 (dd, *J* = 8.7, 2.6 Hz, 1H), 6.60 (d, *J* = 6.5 Hz, 1H), 3.85 – 3.80 (m, 2H), 3.75 (s, 3H), 3.70 – 3.64 (m, 2H), 3.63 – 3.57 (m, 2H), 3.31 – 3.22 (m, 2H), 3.08 – 2.97 (m, 4H), 2.76 (t, *J* = 6.3 Hz, 2H), 2.67 – 2.62 (m, 2H), 1.99 – 1.94 (m, 2H); Anal. calculated for $C_{23}H_{28}FN_3O_2$: C, 69.50; H, 7.10; N, 10.57. Found: C, 69.54; H, 7.08; N, 10.59; MS: m/z 398.3 (M+1).

1-(4-(4-fluorophenyl)piperazin-1-yl)-3-(6-methoxy-3,4-dihydroquinolin-1(2H)-yl)propan-1-one (38h)

Pale yellow semisolid; IR (KBr, v, cm^{-1}): 3386, 2922, 1651, 1504, 1444, 1435, 1269, 1232, 1153, 1033, 518; ^{1}H NMR (400 MHz, $CDCl_3$) δ 7.02 – 6.96 (m, 2H), 6.90 – 6.85 (m, 2H), 6.68 (dd, *J* = 8.8, 3.0 Hz, 1H), 6.59 (dd, *J* = 11.9, 5.9 Hz, 2H), 3.81 – 3.78 (m, 2H), 3.74 (s, 3H), 3.69 – 3.64 (m, 2H), 3.61 – 3.56 (m, 2H), 3.29 – 3.23 (m, 2H), 3.07 (d, *J* = 5.2 Hz, 2H), 3.04 – 3.00 (m, 2H), 2.76 (t, *J* = 6.4 Hz, 2H), 2.64 (dd, *J* = 7.9, 6.5 Hz, 2H), 1.96 (dd, *J* = 6.2, 5.0 Hz, 2H); Anal. calculated for $C_{23}H_{28}FN_3O_2$: C, 69.50; H, 7.10; N, 10.57. Found: C, 69.57; H, 7.09; N, 10.58; MS: m/z 398.3 (M+1).

1-(4-(2-chlorophenyl)piperazin-1-yl)-3-(6-methoxy-3,4-dihydroquinolin-1(2H)-yl)propan-1-one (38i)

Pale yellow semisolid; IR (KBr, v, cm^{-1}): 3458, 3400, 2927, 2827, 1685, 1593, 1506, 1435, 1354, 1228, 1203, 1037; ^{1}H NMR (400 MHz, $CDCl_3$) δ 7.39 (dd, *J* = 7.9, 1.5 Hz, 1H), 7.27 – 7.22 (m, 1H), 7.06 – 6.97 (m, 2H), 6.69 (dd, *J* = 8.8, 3.0 Hz, 1H), 6.60 (dd, *J* = 7.5, 6.0 Hz, 2H), 3.85 – 3.81 (m, 2H), 3.75 (s, 3H), 3.68 (dd, *J* = 8.0, 6.5 Hz, 2H), 3.65 – 3.59 (m, 2H), 3.30 – 3.22 (m, 2H), 3.04 – 2.94 (m, 4H), 2.76 (t, *J* = 6.4 Hz, 2H), 2.65 (dd, *J* = 8.0, 6.5 Hz, 2H), 1.99 – 1.94 (m, 2H); Anal. calculated for $C_{23}H_{28}ClN_3O_2$: C, 66.74; H, 6.82; N, 10.15. Found: C, 66.77; H, 6.81; N, 10.17; MS: m/z 414.2 (M+1), 416.2 (M+3).

1-(4-(3-chlorophenyl)piperazin-1-yl)-3-(6-methoxy-3,4-dihydroquinolin-1(2H)-yl)propan-1-one (38j)

Pale yellow semisolid; IR (KBr, v, cm^{-1}): 3376, 2924, 2864, 1653, 1506, 1435, 1269, 1234, 1163, 1033, 989, 947; ^{1}H NMR (400 MHz, $CDCl_3$) δ 7.20 (td, *J* = 8.3, 5.0 Hz, 2H), 6.92 – 6.85 (m, 3H), 6.83 – 6.78 (m, 1H), 6.59 (dd, *J* = 13.6, 5.9 Hz, 1H), 3.79 (d, *J* = 4.8 Hz, 2H), 3.75 (s, 3H), 3.68 (d, *J* = 7.0 Hz, 2H), 3.65 – 3.62 (m, 2H), 3.28 – 3.19 (m, 4H), 3.17 (d, *J* = 5.1 Hz, 2H), 2.78 – 2.73 (m, 2H), 2.64 (dd, *J* = 7.8, 6.5 Hz, 2H), 1.98 – 1.94 (m, 2H); Anal. calculated for $C_{23}H_{28}ClN_3O_2$: C, 66.74; H, 6.82; N, 10.15. Found: C, 66.78; H, 6.81; N, 10.17; MS: m/z 414.2 (M+1), 416.2 (M+3).

1-(4-(4-chlorophenyl)piperazin-1-yl)-3-(6-methoxy-3,4-dihydroquinolin-1(2H)-yl)propan-1-one (38k)

White solid, IR (KBr, v, cm^{-1}): 3385, 2816, 1678, 1506, 1448, 1236, 1157, 1058, 1029; ^1H NMR (400 MHz, $CDCl_3$) δ 7.20 (td, *J* = 8.3, 5.0 Hz, 2H), 6.92 – 6.85 (m, 3H), 6.83 – 6.78 (m, 1H), 6.59 (dd, *J* = 13.6, 5.9 Hz, 1H), 3.79 (d, *J* = 4.8 Hz, 2H), 3.75 (s, 3H), 3.68 (d, *J* = 7.0 Hz, 2H), 3.65 – 3.62 (m, 2H), 3.28 – 3.19 (m, 4H), 3.17 (d, *J* = 5.1 Hz, 2H), 2.78 – 2.73 (m, 2H), 2.64 (dd, *J* = 7.8, 6.5 Hz, 2H), 1.98 – 1.94 (m, 2H); Anal. calculated for $C_{23}H_{28}ClN_3O_2$: C, 66.74; H, 6.82; N, 10.15. Found: C, 66.78; H, 6.84; N, 10.17; MS: m/z 414.2 (M+1), 416.2 (M+3).

3-(6-methoxy-3,4-dihydroquinolin-1(2H)-yl)-1-(4-(4-nitrophenyl)piperazin-1-yl)propan-1-one (38l)

Pale yellow solid, IR (KBr, v, cm^{-1}): 3404, 2912, 2638, 2576, 1757, 1687, 1593, 1506, 1317, 1240, 1114, 1031, 677; ^1H NMR (400 MHz, $CDCl_3$) δ 8.16 (d, *J* = 9.4 Hz, 2H), 6.82 (d, *J* = 9.4 Hz, 2H), 6.68 (dd, *J* = 8.8, 3.0 Hz, 1H), 6.59 (dd, *J* = 13.1, 5.9 Hz, 2H), 3.85 – 3.81 (m, 2H), 3.75 (s, 3H), 3.70 – 3.66 (m, 2H), 3.65 – 3.60 (m, 2H), 3.47 – 3.42 (m, 2H), 3.42 – 3.37 (m, 2H), 3.29 – 3.23 (m, 2H), 2.75 (t, *J* = 6.4 Hz, 2H), 2.68 – 2.63 (m, 2H), 1.95 (dd, *J* = 11.4, 6.2 Hz, 2H); Anal. calculated for $C_{23}H_{28}N_4O_4$: C, 65.08; H, 6.65; N, 13.20. Found, C: 65.11; H, 6.63; N, 13.23; MS: m/z 425.3 (M+1).

1-(4-benzylpiperazin-1-yl)-3-(6-methoxy-3,4-dihydroquinolin-1(2H)-yl)propan-1-one (38m)

Pale yellow semisolid; IR (KBr, v, cm^{-1}): 3643, 2926, 2767, 1768, 1732, 1504, 1454, 1435, 1265, 1240, 1035, 999, 931; ^1H NMR (400 MHz, $CDCl_3$) δ 7.36 – 7.29 (m, 5H), 6.67 (dd, *J* = 8.8, 3.0 Hz, 1H), 6.58 (dd, *J* = 18.8, 5.9 Hz, 2H), 3.75 (s, 3H), 3.67 (s, 2H), 3.62 (d, *J* = 7.4 Hz, 2H), 3.53 (s, 2H), 3.49 – 3.41 (m, 2H), 3.29 – 3.20 (m, 2H), 2.75 (t, *J* = 6.4 Hz, 2H), 2.60 – 2.56 (m, 2H), 2.47 – 2.43 (m, 2H), 2.40 (d, *J* = 4.6 Hz, 2H), 1.97 – 1.92 (m, 2H); Anal. calculated for $C_{24}H_{31}N_3O_2$: C, 73.25; H, 7.94; N, 10.68. Found: C, 73.29; H, 7.92; N, 10.65; MS: m/z 394.3 (M+1).

3-(6-methoxy-3,4-dihydroquinolin-1(2H)-yl)-1-(4-(pyridin-2-yl)piperazin-1-yl)propan-1-one (38n)

Pale yellow semisolid; IR (KBr, v, cm^{-1}): 3464, 2927, 2858, 1653, 1635, 1506, 1435, 1267, 1240, 1165, 1035, 979; ^1H NMR (400 MHz, $CDCl_3$) δ 8.21 (ddd, *J* = 4.9, 1.9, 0.8 Hz, 1H), 7.55 – 7.50 (m, 1H), 6.72 – 6.63 (m, 3H), 6.59 (dd, *J* = 8.9, 5.9 Hz, 2H), 3.78 (d, *J* = 5.1 Hz, 2H), 3.75 (s, 3H), 3.67 (dd, *J* = 7.9, 6.5 Hz, 2H), 3.56 (s, 4H), 3.51 (dd, *J* = 9.7, 4.5 Hz, 2H), 3.30 – 3.23 (m, 2H), 2.75 (t, *J* = 6.4 Hz, 2H), 2.65 (dd, *J* = 7.9, 6.5 Hz, 2H), 1.98 – 1.94 (m, 2H); Anal. calculated for $C_{22}H_{28}N_4O_2$: C, 69.45; H, 7.42; N, 14.73. Found: C, 69.42; H, 7.44; N, 14.76; MS: m/z 381.3 (M+1).

1-(4-(2,3-dichlorophenyl)piperazin-1-yl)-3-(6-methoxy-3,4-dihydroquinolin-1(2H)-yl)propan-1-one (38o)

Pale yellow semisolid; IR (KBr, v, cm^{-1}): 3396, 1731, 1636, 1508, 1416, 1285, 1203, 1037, 951; ^{1}H NMR (400 MHz, $CDCl_3$) δ 7.22 – 7.14 (m, 2H), 6.90 (dd, *J* = 7.8, 1.7 Hz, 1H), 6.69 (dd, *J* = 8.8, 3.0 Hz, 1H), 6.60 (dd, *J* = 8.0, 5.9 Hz, 2H), 3.82 (d, *J* = 5.9 Hz, 2H), 3.75 (s, 3H), 3.70 – 3.65 (m, 2H), 3.64 – 3.59 (m, 2H), 3.31 – 3.23 (m, 2H), 3.02 – 2.98 (m, 2H), 2.97 – 2.93 (m, 2H), 2.76 (t, *J* = 6.4 Hz, 2H), 2.68 – 2.61 (m, 2H), 1.97 (dt, *J* = 11.5, 6.5 Hz, 2H); Anal. calculated for $C_{22}H_{28}N_4O_2$: C, 61.61; H, 6.07; N, 9.37. Found: C, 61.66; H, 6.05; N, 9.35; MS: m/z 448.2 (M+1), 450.2 (M+3).

5.2.9 Synthesis and characterization of *N*'-benzylidene-2-(quinolin-6 yloxy)propanehydrazide derivatives (43a-p)

The synthetic route and reaction conditions used for the designed compounds **43a-p,** is illustrated in scheme **9**. Synthesis of the target compounds involved sequence of reactions, the first step involved demethylation reaction of 6-methoxyquinoline (**33)** using aluminum trichloride in dry DCM, which afforded intermediate 6-hydroxyquinoline (**39)**. The reaction of intermediate **39** with ethyl 2-bromopropanoate (**19**) was first tried under b1 conditions, but condition b1 was not provided the complete conversion of **39** into **40** as per TLC, while under condition b2, the complete conversion took place (as per TLC) and afforded the intermediate compound **40.** In the further step, intermediate compound **40** was treated with hydrazine hydrate which resulted in replacement of ethoxy group with hydrazine and afforded the intermediate compound **41.** In the final step, intermediate **41** was condensed with different aldehydes (**42a-p**), which afforded schiff base compounds (**43a-p**) in good to excellent yield.

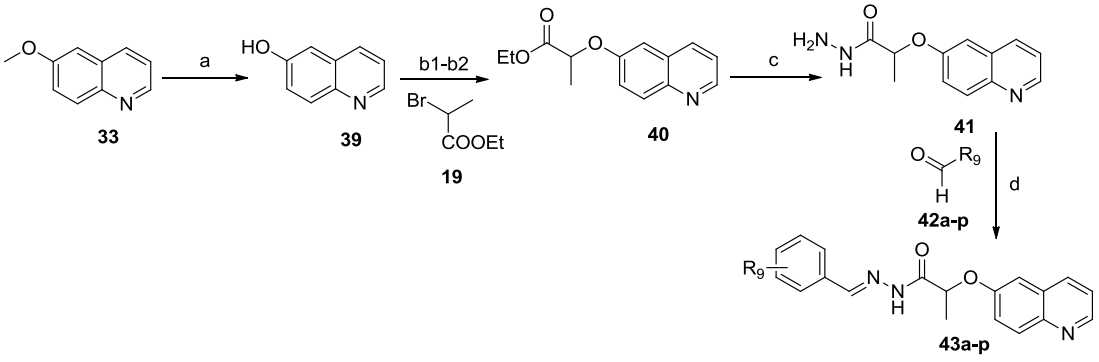

Scheme 9. Reagents and conditions: (a) $AlCl_3$, dry DCM, 24 h, rt (b1) ethyl 2-bromopropanoate, K_2CO_3, CH_3CN, reflux, 12 h (b2) ethyl 2-bromopropanoate, K_2CO_3, DMF, 100˚C, 10 h (c) NH_2-$NH_2.H_2O$, catalytic glacial AcOH, EtOH, reflux 8 h (d) EtOH, catalytic AcOH, reflux 2-3 h

Synthesis of quinolin-6-ol (**39**)

The commercially available compound, 6-methoxyquinoline **33** (7 g, 44 mmol) was added to stirred reaction mixture of aluminum trichloride (17.6 g, 132 mmol) in 200 ml dry DCM. Further, the reaction mass was allowed to stir at room temperature and the progress of the reaction was monitored by TLC. After completion of reaction as per TLC (after twenty four hours), the reaction mass was ice-cooled and 50 ml of cold water was added in order to quench the reaction and further stirred for twenty minutes. Then, the reaction mass was transferred into separating funnel, 150 ml more distilled water was added, organic and aqueous layers were separated. The aqueous portion was further twice extracted with DCM (2x150 ml), combined DCM portion was washed with brine (400 ml), dried over sodium sulphate and evaporated using rotary evaporator to afford the compound **39** [10].

Light brown solid; %Yield 85; M.P. 166-168 °C; IR (KBr, v, cm^{-1}): 3328, 3020, 2879, 1504, 1415, 1310, 1242, 1220, 921, 839; ^{1}H NMR (400 MHz, DMSO) δ 10.05 (s, 1H), 8.66 (dd, *J* = 4.1, 1.6 Hz, 1H), 8.14 (dd, *J* = 8.4, 0.9 Hz, 1H), 7.87 (d, *J* = 9.1 Hz, 1H), 7.40 (dd, *J* = 8.3, 4.2 Hz, 1H), 7.32 (dd, *J* = 9.1, 2.7 Hz, 1H), 7.15 (d, *J* = 2.7 Hz, 1H); MS: m/z 146.1 (M+1).

Synthesis of ethyl 2-(quinolin-6-yloxy)propanoate (40)

To the stirred reaction mixture of intermediate **39** (4.5 g, 31.02 mmol), potassium carbonate (10.7 g, 77.55 mmol) in 50 ml DMF, ethyl 2-bromopropanoate **19** (4.01 ml, 31.02 mmol) was added dropwise and the reaction mixture was stirred at 100˚C and progress was monitored by TLC. After completion of reaction as per TLC (after 10 h), 150 ml ice-cold water was added to the reaction mass. Further, the reaction mass was twice extracted with ethyl acetate (2x200 ml) using separating funnel. Combined organic layer was washed with brine (400 ml), dried over anhydrous sodium sulphate and evaporated using rotary evaporator, which afforded titled compound **40** [11].

White solid; %Yield 78; M.P. 128-130 °C; IR (KBr, v, cm^{-1}): 3116, 2991, 2756, 1747, 1504, 1435, 1199, 1095, 1041, 968, 850; ^{1}H NMR (400 MHz, $CDCl_3$) δ 8.82 (dd, *J* = 4.3, 1.6 Hz, 1H), 8.07 (d, *J* = 8.8 Hz, 2H), 7.48 – 7.38 (m, 2H), 7.02 (d, *J* = 2.8 Hz, 1H), 4.91 (q, *J* = 6.7 Hz, 1H), 4.35 – 4.16 (m, 2H), 1.72 (d, *J* = 6.8 Hz, 3H), 1.26 (t, *J* = 7.1 Hz, 3H); MS: m/z 246.2 (M+1).

Synthesis of 2-(quinolin-6-yloxy)propanehydrazide (41)

To the stirred solution of intermediate **40** (5.5 g, 22.44 mmol) in 80 ml ethanol, hydrazine hydrate (3.26 ml, 67.32 mmol) was added dropwise, followed by 1 drop of glacial acetic acid. The reaction mixture was refluxed and progress was monitored by TLC. After completion of reaction as per TLC (after 8 h refluxing), the reaction mass was concentrated under reduced

pressure, until it reduced to half of its original volume. Further, 100 ml of ice-cold water was added, which resulted the precipitation of white solid. Finally, the reaction mass was filtered using vacuum filtration, solid residues was thrice washed with distilled water (3x100 ml) and dried to afford the titled compound **41** [3].

White solid; %Yield 82; M.P. 118-120 °C; IR (KBr, v, cm^{-1}): 3471, 3055, 2983, 2904, 2873, 2785, 1681, 1514, 1505, 1237, 1334, 1178, 1097, 1041, 941; ^{1}H NMR (400 MHz, $CDCl_3$) δ 8.84 (s, 1H), 8.07 (d, *J* = 8.4 Hz, 2H), 7.67 (s, 1H), 7.46 – 7.36 (m, 2H), 7.09 (s, 1H), 4.96 (d, *J* = 6.6 Hz, 1H), 3.90 (s, 2H), 1.70 (d, *J* = 6.7 Hz, 3H); MS: m/z 232.1 (M+1).

General procedure for the synthesis of quinolin-6-yloxy)propanehydrazide derivatives (43a-p)

Intermediate hydrazide **41** (0.23 g, 1 mmol) was added to the stirring solution of corresponding aldehydes (**42a-p**, 1 mmol) in ethanol containing catalytic amount of glacial acetic acid. The reaction mixture was refluxed for 2 to 3 h, the progress of the reaction was monitored by TLC. After completion of reaction, ethanol was evaporated; ethyl acetate (20 ml) was added to the reaction mass. Ethyl acetate layer was twice washed with distilled water (2x20 ml) and then with brine water (20 ml). Organic layer was dried over anhydrous sodium sulphate and finally evaporated using rotary evaporator to afford the final derivatives **43a-p** [4]. Synthesized compounds were purified by washing with hexane and cold diethyl ether. Preliminary characteristics data of compounds **43a-p** is shown in table **5.10.**

Table 5.10 Preliminary characteristics data of compounds **43a-p**

Comp. code	R	Mol. formula	Mol. Wt	% Yield	Melting point (˚C)
43a	H	$C_{19}H_{17}N_3O_2$	319.13	82	176-178
43b	2-CH_3	$C_{20}H_{19}N_3O_2$	333.15	86	126-128
43c	3-OCH_3	$C_{20}H_{19}N_3O_3$	349.14	92	142-144
43d	4-OCH_3	$C_{20}H_{19}N_3O_3$	349.14	87	144-146
43e	2-F	$C_{19}H_{16}FN_3O_2$	337.12	87	148-150
43f	4-F	$C_{19}H_{16}FN_3O_2$	337.12	91	162-164
43g	2-Cl	$C_{19}H_{16}ClN_3O_2$	353.09	86	166-168
43h	4-Cl	$C_{19}H_{16}ClN_3O_2$	353.09	89	178-180
43i	3-Br	$C_{19}H_{16}BrN_3O_2$	397.04	94	108-110
43j	4-Br	$C_{19}H_{16}BrN_3O_2$	397.04	88	162-164
43k	2-NO_2	$C_{19}H_{16}N_4O_4$	364.12	91	158-160
43l	3-NO_2	$C_{19}H_{16}N_4O_4$	364.12	88	168-170
43m	4-NO_2	$C_{19}H_{16}N_4O_4$	364.12	92	134-136
43n	4-CN	$C_{20}H_{16}N_4O_2$	344.13	83	174-176
43o	3,4-di-Cl	$C_{19}H_{15}Cl_2N_3O_2$	387.05	78	170-172
43p	3,4,5-tri-MeO	$C_{22}H_{23}N_3O_5$	409.16	73	180-182

Spectral characterization of compounds 43a-p

All the synthesized compounds were characterized by spectral techniques like FTIR, ^{1}H NMR and Mass. Four representative compounds of the series (**43c, 43e, 43i** and **43k**) were also characterized by ^{13}C NMR and elemental analysis. FTIR spectrum of the tested compounds exhibited the expected absorption bands, for example, all compounds possessed hydrogen at carboxylic hydrazide bond (=N-N**H**-C=O), a corresponding stretching peak (broad, moderate intensity) appeared in IR spectrum at 3175–3210 cm^{-1}. Another discrete and characteristic peak (sharp, strong intensity), appeared at the region 1680-1703 cm^{-1} corresponding to the stretching of carbonyl group (-NH-**C=O**). The ^{1}H NMR spectrum of the compounds showed characteristic doublet around δ ~1.8 corresponding to the methyl group (attached at the carbon connecting carbonyl and oxygen), while single proton at the adjacent carbon appeared (quartet) at δ ~5. Further, proton at the 5th position of quinoline showed characteristic peak around δ ~7.15-7.20. Single proton attached at the imine carbon appeared in strong down field region (δ ~8.80-8.90). Hydrazide proton (=N-N**H**-C=O) shifted to most down field and appeared as singlet at δ ~9.30-10. Further, peak pattern and counting of NMR signals corresponding to other protons were also supported the proposed structure of compounds. ^{13}C NMR spectral data of compounds **43c, 43e, 43i** and **43k** was found in compliance with their corresponding structure and calculated and observed elemental values of C H N were also found within the acceptable range. Mass spectrum (ESI-MS) of the synthesized compounds exhibited the corresponding M+1 peak. Details of spectral data are given below;

N'-benzylidene-2-(quinolin-6-yloxy)propanehydrazide (43a)

White solid; IR (KBr, v, cm^{-1}): 3194, 3076, 3051, 2978, 2904, 1682, 1504, 1398, 1271, 1238, 1163, 1041; ^{1}H NMR (400 MHz, $CDCl_3$) δ 9.42 (s, 1H), 8.84 (d, *J* = 2.7 Hz, 1H), 8.11 – 8.02 (m, 2H), 7.54 – 7.46 (m, 3H), 7.41 (t, *J* = 7.5 Hz, 2H), 7.31 (dd, *J* = 7.5, 1.5 Hz, 2H) 7.14 (d, *J* = 2.8 Hz, 1H), 5.02 (q, *J* = 6.6 Hz, 1H), 1.78 (d, *J* = 6.9 Hz, 3H); MS: m/z 320.1 (M+1).

N'-(2-methylbenzylidene)-2-(quinolin-6-yloxy)propanehydrazide (43b)

White solid; IR (KBr, v, cm^{-1}): 3205, 3055, 2989, 2908, 1682, 1556, 1504, 1293, 1222, 1078, 981, 848; ^{1}H NMR (400 MHz, $CDCl_3$) δ 9.65 (d, *J* = 5.7 Hz, 1H), 8.83 (d, *J* = 2.9 Hz, 1H), 8.47 (s, 1H), 8.09 – 8.06 (m, 1H), 7.99 (t, *J* = 8.8 Hz, 2H), 7.43 – 7.30 (m, 3H), 7.22 (d, *J* = 7.3 Hz, 1H), 7.19 (d, *J* = 2.8 Hz, 1H), 7.15 (d, *J* = 7.5 Hz, 1H), 5.02 (d, *J* = 6.8 Hz, 1H), 2.41 (s, 3H), 1.81 (d, *J* = 5.4 Hz, 3H); MS: m/z 334.2 (M+1).

N'-(3-methoxybenzylidene)-2-(quinolin-6-yloxy)propanehydrazide (43c)

White solid; IR (KBr, v, cm^{-1}): 3182, 3084, 3062, 2983, 2891, 1681, 1500, 1452, 1396, 1273, 1228, 1136, 1099, 1039, 933, 829; ^{1}H NMR (400 MHz, $CDCl_3$) δ 9.32 (s, 1H), 8.84 (d, *J* =

2.7 Hz, 1H), 8.11 – 8.06 (m, 3H), 7.63 (d, *J* = 8.0 Hz, 2H), 7.46 (d, *J* = 9.4 Hz, 1H), 7.41 (dd, *J* = 8.3, 4.2 Hz, 1H), 7.21 (s, 1H), 7.19 (d, *J* = 2.8 Hz, 2H), 5.02 (q, *J* = 6.7 Hz, 1H), 2.38 (s, 3H), 1.79 (d, *J* = 6.8 Hz, 3H); ^{13}C NMR (100 MHz, $CDCl_3$) δ 168.06, 154.68, 149.73, 148.80, 141.28, 135.27, 134.98, 131.35, 130.29, 129.60, 129.43, 127.81, 127.28, 122.43, 122.14, 121.76, 107.91, 75.39, 70.80, 21.57; Anal. calculated for $C_{20}H_{19}N_3O_3$: C, 68.75; H, 5.48; N, 12.03. Found: C, 68.73; H, 5.43; N, 12.01; MS: m/z 350.1 (M+1).

N'-(4-methoxybenzylidene)-2-(quinolin-6-yloxy)propanehydrazide (43d)

White solid; IR (KBr, v, cm^{-1}): 3178, 3057, 2900, 2872, 2559, 1681, 1504, 1311, 1274, 1226, 1180, 798; ^{1}H NMR (400 MHz, $CDCl_3$) δ 9.30 (s, 1H), 8.84 (dd, *J* = 4.2, 1.6 Hz, 1H), 8.11 – 8.01 (m, 3H), 7.72 – 7.65 (m, 2H), 7.43 (ddd, *J* = 14.8, 8.7, 3.5 Hz, 2H), 7.18 (d, *J* = 2.8 Hz, 1H), 6.91 (d, *J* = 8.9 Hz, 2H), 5.01 (q, *J* = 6.7 Hz, 1H), 3.85 (s, 3H), 1.79 (d, *J* = 6.8 Hz, 3H); MS: m/z 350.1 (M+1).

N'-(2-fluorobenzylidene)-2-(quinolin-6-yloxy)propanehydrazide (43e)

White solid; IR (KBr, v, cm^{-1}): 3198, 3068, 2983, 2970, 2864, 1691, 1500, 1452, 1381, 1269, 1222, 1093, 1039, 972; ^{1}H NMR (400 MHz, $CDCl_3$) δ 9.57 (s, 1H), 8.84 (dd, *J* = 4.2, 1.5 Hz, 1H), 8.39 (s, 1H), 8.09 (ddd, *J* = 9.4, 5.6, 4.0 Hz, 3H), 7.47 – 7.36 (m, 3H), 7.21 – 7.15 (m, 2H), 7.09 – 7.04 (m, 1H), 5.03 (q, *J* = 6.8 Hz, 1H), 1.79 (d, *J* = 6.8 Hz, 3H); ^{13}C NMR (100 MHz, $CDCl_3$) δ 168.30, 161.49 (d, *J* = 252.5 Hz), 154.62, 148.83, 144.77, 142.61, 135.23, 132.36 (d, *J* = 8.5 Hz), 131.39, 129.09, 127.30, 124.47 (d, *J* = 3.5 Hz), 122.39, 122.11, 121.77, 115.64 (d, *J* = 20.9 Hz), 107.92, 75.32, 19.04; Anal. calculated for $C_{19}H_{16}FN_3O_2$: C, 67.65; H, 4.78; N, 12.46. Found: C, 67.67; H, 4.83; N, 12.47; MS: m/z 338.7 (M+1).

N'-(4-fluorobenzylidene)-2-(quinolin-6-yloxy)propanehydrazide (43f)

White solid; IR (KBr, v, cm^{-1}): 3188, 3076, 3057, 2987, 2962, 2781, 1681, 1504, 1454, 1404, 1273, 1232, 1159, 1096, 1039; ^{1}H NMR (400 MHz, $CDCl_3$) δ 9.49 (s, 1H), 8.89 – 8.80 (m, 1H), 8.15 (s, 1H), 8.09 – 8.03 (m, 2H), 7.72 (dd, *J* = 8.7, 5.4 Hz, 2H), 7.46 – 7.38 (m, 2H), 7.18 (d, *J* = 2.7 Hz, 1H), 7.08 (t, *J* = 8.7 Hz, 2H), 5.02 (q, *J* = 6.8 Hz, 1H), 1.79 (d, *J* = 6.8 Hz, 3H); MS: m/z 338.7 (M+1).

N'-(2-chlorobenzylidene)-2-(quinolin-6-yloxy)propanehydrazide (43g)

White solid; IR (KBr, v, cm^{-1}): 3196, 3055, 2989, 2937, 1686, 1552, 1504, 1469, 1284, 1234, 1130, 1049, 981, 927; ^{1}H NMR (400 MHz, $CDCl_3$) δ 9.47 (s, 1H), 8.80 (dd, *J* = 4.2, 1.5 Hz, 1H), 8.37 (s, 1H), 8.07 (ddd, *J* = 9.2, 5.4, 4.0 Hz, 3H), 7.43 – 7.31 (m, 3H), 7.19 – 7.13 (m, 2H), 7.07 – 7.01 (m, 1H), 5.02 (q, *J* = 6.8 Hz, 1H), 1.77 (d, *J* = 6.8 Hz, 3H); MS: m/z 354.2 (M+1).

N'-(4-chlorobenzylidene)-2-(quinolin-6-yloxy)propanehydrazide (43h)

White solid; IR (KBr, v, cm^{-1}): 3186, 3067, 3062, 2987, 2872, 2831, 2603, 1681, 1498, 1454, 1409, 1261, 1230, 1136, 1097, 1041; ^{1}H NMR (400 MHz, $CDCl_3$) δ 9.53 (s, 1H), 8.84 (d, *J* = 3.0 Hz, 1H), 8.15 (s, 1H), 8.05 (dd, *J* = 16.3, 6.8 Hz, 2H), 7.66 (d, *J* = 8.5 Hz, 2H), 7.43 – 7.34 (m, 4H), 7.17 (d, *J* = 2.7 Hz, 1H), 5.02 (q, *J* = 6.8 Hz, 1H), 1.79 (d, *J* = 6.8 Hz, 3H); MS: m/z 354.2 (M+1).

N'-(3-bromobenzylidene)-2-(quinolin-6-yloxy)propanehydrazide (43i)

White solid; IR (KBr, v, cm^{-1}): 3195, 3049, 2831, 2357, 1682, 1500, 1498, 1288, 1172, 1068, 784; ^{1}H NMR (400 MHz, $CDCl_3$) δ 9.56 (s, 1H), 8.85 (s, 1H), 8.13 (s, 1H), 8.07 (t, *J* = 9.9 Hz, 2H), 7.93 (s, 1H), 7.55 (dt, *J* = 17.1, 8.6 Hz, 3H), 7.46 – 7.35 (m, 2H), 7.18 (s, 1H), 5.02 (q, *J* = 6.6 Hz, 1H), 1.79 (d, *J* = 6.9 Hz, 3H); ^{13}C NMR (100MHz, $CDCl_3$) δ 168.19, 154.56, 147.84, 135.22, 133.67, 132.45, 131.54, 130.19, 130.25, 128.16, 126.50, 126.14, 122.97, 122.07, 119.71, 108.04, 107.30, 75.37, 18.99; Anal. calculated for $C_{19}H_{16}BrN_3O_2$: C, 57.30; H, 4.05; N, 10.55. Found: C, 57.32; H, 4.09; N, 10.57; MS: m/z 398.1 (M+1).

N'-(4-bromobenzylidene)-2-(quinolin-6-yloxy)propanehydrazide (43j)

White solid; IR (KBr, v, cm^{-1}): 3197, 3086, 2987, 2908, 2873, 2829, 2785, 2603, 1681, 1622, 1498, 1450, 1398, 1230, 1095, 754; ^{1}H NMR (400 MHz, $CDCl_3$) δ 9.55 (s, 1H), 8.84 (d, *J* = 3.0 Hz, 1H), 8.15 (s, 1H), 8.09 – 8.03 (m, 2H), 7.58 (d, *J* = 8.6 Hz, 2H), 7.53 – 7.50 (m, 2H), 7.43 – 7.37 (m, 2H), 7.17 (d, *J* = 2.8 Hz, 1H), 5.01 (q, *J* = 6.8 Hz, 1H), 1.78 (d, *J* = 6.7 Hz, 3H); MS: m/z 398.1 (M+1).

N'-(2-nitrobenzylidene)-2-(quinolin-6-yloxy)propanehydrazide (43k)

Pale yellow solid; IR (KBr, v, cm^{-1}): 3197, 3159, 3053, 2868, 1703, 1519, 1504, 1440, 1338, 1274, 1222, 1172, 1080, 979, 840, 754; ^{1}H NMR (400 MHz, $CDCl_3$) δ 10.04 (s, 1H), 8.83 (d, *J* = 4.0 Hz, 1H), 8.77 (s, 1H), 8.27 (d, *J* = 7.9 Hz, 1H), 8.08 (d, *J* = 8.3 Hz, 1H), 8.02 (dd, *J* = 13.9, 8.7 Hz, 2H), 7.66 (t, *J* = 7.8 Hz, 1H), 7.55 (t, *J* = 7.7 Hz, 1H), 7.41 (dd, *J* = 8.3, 4.2 Hz, 1H), 7.36 (dd, *J* = 9.2, 2.7 Hz, 1H), 7.19 (d, *J* = 2.6 Hz, 1H), 5.05 (q, *J* = 6.8 Hz, 1H), 1.80 (d, *J* = 6.7 Hz, 3H); ^{13}C NMR (100 MHz, $CDCl_3$) δ 168.54, 154.52, 148.89, 148.07, 144.82, 144.61, 135.23, 133.67, 131.51, 130.86, 129.28, 129.08, 128.30, 124.80, 122.09, 121.79, 108.07, 75.28, 18.92; Anal. calculated for $C_{19}H_{16}N_4O_4$: C, 62.63; H, 4.43; N, 15.38. Found: C, 62.61; H, 4.47; N, 15.39; MS: m/z 365.1 (M+1).

N'-(3-nitrobenzylidene)-2-(quinolin-6-yloxy)propanehydrazide (43l)

Pale yellow solid; IR (KBr, v, cm^{-1}): 3196, 3161, 3041, 3028, 1666, 1529, 1504, 1288, 1224, 1078, 981, 850; ^{1}H NMR (400 MHz, $CDCl_3$) δ 9.67 (s, 1H), 8.85 (dd, *J* = 4.2, 1.5 Hz, 1H), 8.50 (s, 1H), 8.38 (s, 1H), 8.26 (dd, *J* = 8.2, 1.3 Hz, 1H), 8.15 – 8.03 (m, 3H), 7.60 (t, *J* = 8.0 Hz, 1H), 7.42 (dt, *J* = 9.2, 3.4 Hz, 2H), 7.19 (d, *J* = 2.7 Hz, 1H), 5.05 (q, *J* = 6.8 Hz, 1H), 1.81 (d, *J* = 6.8 Hz, 3H); MS: m/z 365.1 (M+1).

N'-(4-nitrobenzylidene)-2-(quinolin-6-yloxy)propanehydrazide (43m)

Pale yellow solid; IR (KBr, v, cm^{-1}): 3213, 3032, 2983, 1683, 1681, 1517, 1504, 1338, 1224, 1089, 968; ^{1}H NMR (400 MHz, $CDCl_3$) δ 9.91 (s, 1H), 8.84 (d, *J* = 3.7 Hz, 1H), 8.36 (s, 1H), 8.23 (d, *J* = 8.2 Hz, 2H), 8.08 (d, *J* = 8.4 Hz, 1H), 7.99 (d, *J* = 9.2 Hz, 1H), 7.89 (t, *J* = 10.9 Hz, 2H), 7.42 (dd, *J* = 8.1, 4.0 Hz, 1H), 7.33 (d, *J* = 7.1 Hz, 1H), 7.17 (s, 1H), 5.04 (q, *J* = 6.6 Hz, 1H), 1.80 (d, *J* = 6.7 Hz, 3H); MS: m/z 365.1 (M+1).

N'-(4-cyanobenzylidene)-2-(quinolin-6-yloxy)propanehydrazide (43n)

White solid; IR (KBr, v, cm^{-1}): 3250, 3051, 3010, 2225, 1697, 1500, 1319, 1253, 1228, 1136, 936; ^{1}H NMR (400 MHz, $CDCl_3$) δ 9.81 (s, 1H), 8.84 (d, *J* = 2.9 Hz, 1H), 8.29 (s, 1H), 8.08 (d, *J* = 7.8 Hz, 1H), 7.99 (d, *J* = 9.2 Hz, 1H), 7.82 (d, *J* = 8.3 Hz, 2H), 7.67 (d, *J* = 8.4 Hz, 2H), 7.42 (dd, *J* = 8.3, 4.2 Hz, 1H), 7.34 (dd, *J* = 9.2, 2.8 Hz, 1H), 7.16 (d, *J* = 2.7 Hz, 1H), 5.03 (q, *J* = 6.8 Hz, 1H), 1.79 (d, *J* = 6.8 Hz, 3H); MS: m/z 345.3 (M+1).

N'-(3,4-dichlorobenzylidene)-2-(quinolin-6-yloxy)propanehydrazide (43o)

White solid; IR (KBr, v, cm^{-1}): 3176, 3024, 2993, 2902, 2829, 2600, 1693, 1554, 1498, 1471, 1377, 1325, 1222, 1128; ^{1}H NMR (400 MHz, $CDCl_3$) δ 9.67 (s, 1H), 8.84 (s, 1H), 8.16 (s, 1H), 8.07 (d, *J* = 8.3 Hz, 1H), 8.01 (d, *J* = 9.4 Hz, 1H), 7.83 (s, 1H), 7.56 – 7.43 (m, 3H), 7.39 – 7.33 (m, 1H), 7.17 (s, 1H), 5.02 (q, *J* = 6.4 Hz, 1H), 1.79 (d, *J* = 6.6 Hz, 3H); MS: m/z 388.2 (M+1).

2-(quinolin-6-yloxy)-N'-(3,4,5-trimethoxybenzylidene)propanehydrazide (43p)

White solid; IR (KBr, v, cm^{-1}): 3201, 3051, 2935, 2902, 2883, 2642, 1681, 1504, 1415, 1330, 1232, 1126, 1008, 943; ^{1}H NMR (400 MHz, $CDCl_3$) δ 9.49 (s, 1H), 8.90 – 8.80 (m, 1H), 8.11 – 8.02 (m, 3H), 7.45 – 7.37 (m, 2H), 7.17 (s, 1H), 6.92 (dd, *J* = 16.0, 1.7 Hz, 2H), 5.07 – 4.96 (m, 1H), 3.88 (d, *J* = 1.6 Hz, 9H), 1.79 (d, *J* = 6.8 Hz, 3H); MS: m/z 410.3 (M+1).

5.2.10 Synthesis and characterization of 2-(benzyl(4-chlorophenyl)amino)-1-(piperazin-1-yl)ethanone derivatives (51a-n)

Designed compounds (**51a-n)** were synthesized via four step synthetic route, details of the reaction conditions followed for the synthesis of target compounds are given below (Scheme **10)**. First step involved reaction of *p*-chloroaniline (**44**) with benzaldehyde (**45**) which afforded imine **46** as intermediate**,** which on subsequent reduction with sodium borohydride gave *N*-benzyl-4-chloroaniline (**47**). In next step, intermediate **47** was treated with bromo acetic acid (**48**) under reflux condition which afforded intermediate compound **49**. Further, coupling reaction of intermediate acid compound **49** with different substituted piperazines (**50a-n**) afforded target compounds **51a-n** in good to excellent yields.

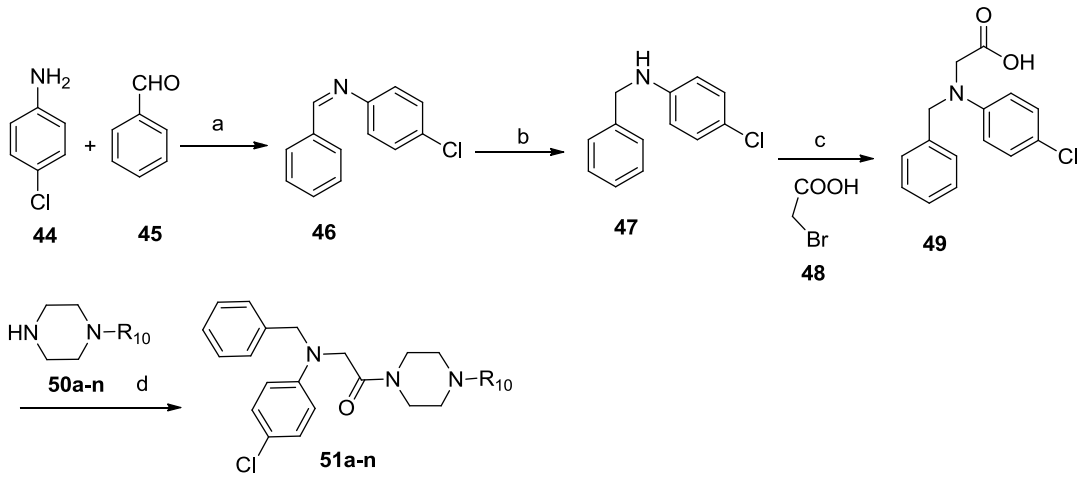

Scheme 10. Reagents and conditions: (a) EtOH, catalytic AcOH, 3h, reflux (b) MeOH, $NaBH_4$, 0˚C-rt, 2 h (c) ACN, Et_3N, reflux, 5 h (d) HOBT, EDC. HCl, Et_3N, DCM, rt, 6-8 h

Synthesis of *N*-benzylidene-4-chloroaniline (**46**)

Commercially available compound, 4-chloroaniline **(44)** (4.79 g, 37.6 mmol) was added to the stirred reaction mixture of benzaldehyde **(45)** (3.84 ml, 37.6 mmol) in 200 ml ethanol. Further, catalytic amount of acetic acid was added to the reaction mass and refluxed for 3 h. After completion of reaction as per TLC, ethanol was evaporated over rotary evaporator and 200 ml ethyl acetate was added. Further, the reaction mass was transferred into separating funnel, 200 ml distilled water was added, organic and aqueous layers were separated. Organic layer was further washed with brine water (200 ml), dried over sodium sulphate and evaporated using rotary evaporator to afford the intermediate compound **46** as pale yellow dense oil with 86 % yield [12].

Synthesis of *N*-benzyl-4-chloroaniline (47)

To the ice-cooled stirred solution of intermediate compound **46** (6.5 g, 30.02 mmol) in dry methanol (250 ml), sodium borohydride (3.40 g, 90.06 mmol) was added in portions. After complete addition of sodium borohydride, the reaction mass was stirred at room temperature and the progress of reaction was monitored by TLC. After completion of reaction as per TLC (after 2h), methanol was evaporated using rotary evaporator and 200 ml ice-cold water was added to the reaction mass. Further, the reaction mass was twice extracted with ethyl acetate (2x200 mL) using separating funnel. Combined organic layer was washed with brine (400 ml), dried over anhydrous sodium sulphate and evaporated using rotary evaporator, which afforded titled compound **47** as dense oil with 91% yield [13].

Synthesis of 2-(benzyl(4-chlorophenyl)amino)acetic acid (49)

To the stirred solution of intermediate **47** (5.5 g, 25.26 mmol) in 150 ml acetonitrile, triethylamine (10.3 ml, 75.7 mmol) was added with catalytic amount of potassium iodide,

reaction mixture was stirred at room temperature for 15 min. Further, temperature of reaction was reduced to 2-5 ˚C using ice water bath and bromoacetic acid **(48)** (1.81 ml, 25.26 mmol) was added dropwise. After complete addition, the reaction mass was refluxed and the progress of reaction was monitored by TLC. After completion of reaction as per TLC (after 5h refluxing), solvent acetonitrile was evaporated using rotary evaporator and 150 ml of ethyl acetate was added. The reaction mass was transferred to separating funnel and washed with 150 ml distilled water followed by brine water (150 ml). Organic layer was dried over anhydrous sodium sulphate and evaporated on rotary evaporator, which afforded crude intermediate acid **49.** Crude product **49** was washed with chilled diethyl ether (2x25 ml), dried in oven at 40 ˚C to afford the pure compound **49** [11].

Creamy solid; %Yield 78; M.P. 78-80 °C; IR (KBr, v, cm^{-1}): 3028 (broad), 3055, 2933, 2912, 2875, 1704, 1514, 1337, 1234, 1178, 1094, 941; ^{1}H NMR (400 MHz, $CDCl_3$) δ 9.55 (s, 1H), 7.39 – 7.33 (m, 2H), 7.30 – 7.27 (m, 3H), 7.18 – 7.11 (m, 2H), 6.63 – 6.55 (m, 2H), 4.63 (s, 2H), 4.14 (s, 2H); MS: m/z 276.1 (M+1).

General procedure for the synthesis of compounds (51a-n)

To the stirred solution of 2-(benzyl(4-chlorophenyl)amino)acetic acid (**49**, 0.275 g, 1 mmol) in dry DCM, HOBt (0.16 g, 1.2 mmol) and EDCI. HCl (0.23 g, 1.2 mmol), triethylamine (0.34 ml, 2.5 mmol) were added and stirring was continued for 30 min at room temperature. To the reaction mixture, corresponding piperazines (**50a-n**) were added and the reaction mixture was further stirred at room temperature for 6-8 h. After completion of reaction as per TLC, the reaction mass was taken in a separating funnel, to this 25 ml more DCM was added and organic layer was washed with saturated sodium bicarbonate solution (50 ml). Organic layer was then washed with distilled water (50ml), followed by brine water (50ml). DCM layer was separated and dried over anhydrous sodium sulphate and finally evaporated to afford the final compounds **51a-n** [9]. Preliminary characteristics data of compounds **51a-n is** summarized in table **5.11.**

Table 5.11 Preliminary characteristics data of compounds **51a-n**

Comp. code	R_{10}	Mol. formula	Mol. Wt	% Yield	Melting point (˚C)
51a	Ph	$C_{25}H_{26}ClN_3O$	419.18	81	118-121
51b	2-CH_3-Ph	$C_{26}H_{28}ClN_3O$	433.19	84	112-114
51c	4-CH_3-Ph	$C_{26}H_{28}ClN_3O$	433.19	85	114-116
51d	2-CH_3O-Ph	$C_{26}H_{28}ClN_3O_2$	449.19	82	116-118
51e	3-CH_3O-Ph	$C_{26}H_{28}ClN_3O_2$	449.19	92	88-89
51f	4-CH_3O-Ph	$C_{26}H_{28}ClN_3O_2$	449.19	90	118-120
51g	2-F-Ph	$C_{25}H_{25}ClFN_3O$	437.17	74	146-148
51h	4-F-Ph	$C_{25}H_{25}ClFN_3O$	437.17	78	126-129
51i	3-Cl-Ph	$C_{25}H_{25}Cl_2N_3O$	453.14	82	138-140
51j	4-Cl-Ph	$C_{25}H_{25}Cl_2N_3O$	453.14	87	128-130
51k	4-NO_2-Ph	$C_{25}H_{25}ClN_4O_3$	464.16	76	154-157
51l	Benzyl	$C_{26}H_{28}ClN_3O$	433.19	77	88-90
51m	2,3-DCl-Ph	$C_{25}H_{24}Cl_3N_3O$	487.10	83	122-125
51n	Benzhydryl	$C_{32}H_{32}ClN_3O$	509.22	77	154-156

Spectral data of compounds 51a-n

All synthesized compounds were characterized by spectral techniques like ^{1}H NMR, IR, ESI-MS and elemental analysis. IR spectra of the titled compounds exhibited expected absorption bands, for example, all compounds possessed amide linkage (-NH-**C=O**), a corresponding **C=O** stretching peak (with strong intensity) appeared at 1645–1661 cm^{-1}. The ^{1}H NMR spectrum of the compounds showed characteristic singlet around δ ~4.65 corresponding to two benzylic protons. Further, two hydrogen of methylene group (at carbon connecting carbonyl group and nitrogen) appeared as singlet (δ ~4.19). The position of eight piperazine protons in the proton spectra of series varied depending upon the nature of substitution. All compounds (except **51l**) displayed peaks between δ ~3.85 to 3.04 corresponding to eight hydrogen of piperazine moiety, as compounds **51l** possessed benzyl instead of phenyl ring, so its piperazine protons appeared in up-field region (δ ~3.66-2.47). Proton counting and peak pattern of NMR signals corresponding to other protons of compounds was observed in compliance with the proposed structure. The calculated and observed elemental values of C H N were found within the acceptable range. ESI-MS spectrum of the synthesized compounds exhibited the corresponding M+1 peak.

2-(benzyl(4-chlorophenyl)amino)-1-(4-phenylpiperazin-1-yl)ethanone (51a)

White solid; IR (KBr, v, cm^{-1}): 3116, 3020, 2812, 1658, 1568, 1504, 1396, 1230, 1024, 813, 734; ^{1}H NMR (400 MHz, $CDCl_3$) δ 7.34 (dd, *J* = 13.3, 4.0 Hz, 4H), 7.30 (d, *J* = 4.0 Hz, 3H), 7.17 – 7.13 (m, 2H), 6.99 – 6.93 (m, 3H), 6.64 – 6.59 (m, 2H), 4.65 (s, 2H), 4.19 (s, 2H), 3.82 (d, *J* = 4.6 Hz, 2H), 3.62 (s, 2H), 3.20 (d, *J* = 4.9 Hz, 4H); Anal. calculated for $C_{25}H_{26}ClN_3O$:

C, 71.50; H, 6.24; N, 10.01. Found: C, 71.54; H, 6.21; N, 10.04; MS: m/z 420.3 (M+1), 422.3 (M+3).

2-(benzyl(4-chlorophenyl)amino)-1-(4-(o-tolyl)piperazin-1-yl)ethanone (51b)

White solid; IR (KBr, v, cm^{-1}): 3055, 2951, 2908, 1651, 1597, 1504, 1454, 1379, 1226, 1029, 958, 812; ^1H NMR (400 MHz, $CDCl_3$) δ 7.37 (dd, *J* = 9.2, 5.3 Hz, 2H), 7.31 (d, *J* = 6.4 Hz, 3H), 7.23 (dd, *J* = 7.6, 2.4 Hz, 2H), 7.18 – 7.13 (m, 2H), 7.04 (ddd, *J* = 22.2, 11.1, 4.5 Hz, 2H), 6.66 – 6.59 (m, 2H), 4.66 (s, 2H), 4.20 (s, 2H), 3.81 (s, 2H), 3.65 – 3.54 (m, 2H), 2.98 – 2.85 (m, 4H), 2.35 (s, 3H); Anal. calculated for $C_{26}H_{28}ClN_3O$: C, 71.96; H, 6.50; N, 9.68. Found: C, 71.97; H, 6.54; N, 9.65; MS: m/z 434.3 (M+1), 436.3 (M+3).

2-(benzyl(4-chlorophenyl)amino)-1-(4-(p-tolyl)piperazin-1-yl)ethanone (51c)

White solid; IR (KBr, v, cm^{-1}): 3026, 2956, 2908, 2864, 1651, 1595, 1504, 1435, 1224, 1207, 956, 896, 806, 764; ^1H NMR (400 MHz, $CDCl_3$) δ 7.40 – 7.34 (m, 2H), 7.30 (d, *J* = 5.3 Hz, 3H), 7.14 (t, *J* = 8.8 Hz, 4H), 6.87 (d, *J* = 8.5 Hz, 2H), 6.65 – 6.59 (m, 2H), 4.65 (s, 2H), 4.19 (s, 2H), 3.86 – 3.76 (m, 2H), 3.65 – 3.56 (m, 2H), 3.14 (d, *J* = 4.8 Hz, 4H), 2.32 (s, 3H); Anal. calculated for $C_{26}H_{28}ClN_3O$: C, 71.96; H, 6.50; N, 9.68. Found: C, 71.94; H, 6.53; N, 9.66; MS: m/z 434.3 (M+1), 436.3 (M+3).

2-(benzyl(4-chlorophenyl)amino)-1-(4-(2-methoxyphenyl)piperazin-1-yl)ethanone (51d)

White solid; IR (KBr, v, cm^{-1}): 3046, 3007, 2812, 1651, 1504, 1240, 1031, 958, 898, 812, 738; ^1H NMR (400 MHz, $CDCl_3$) δ 7.36 (dd, *J* = 7.7, 6.8 Hz, 2H), 7.30 (d, *J* = 6.3 Hz, 3H), 7.19 – 7.12 (m, 2H), 7.11 – 7.05 (m, 1H), 6.99 – 6.90 (m, 3H), 6.65 – 6.59 (m, 2H), 4.66 (s, 2H), 4.19 (s, 2H), 3.91 (s, 3H), 3.87 – 3.82 (m, 2H), 3.67 – 3.60 (m, 2H), 3.08 (s, 4H); Anal. calculated for $C_{26}H_{28}ClN_3O_2$: C, 69.40; H, 6.27; N, 9.34. Found: C, 69.43; H, 6.31; N, 9.31; MS: m/z 450.3 (M+1), 452.3 (M+3).

2-(benzyl(4-chlorophenyl)amino)-1-(4-(3-methoxyphenyl)piperazin-1-yl)ethanone (51e)

White solid; IR (KBr, v, cm^{-1}): 3026, 2887, 2833, 1651, 1595, 1496, 1354, 1209, 1172, 1029, 962, 823, 734; ^1H NMR (400 MHz, $CDCl_3$) δ 7.37 (dd, *J* = 10.2, 4.3 Hz, 2H), 7.30 (t, *J* = 3.2 Hz, 3H), 7.23 (t, *J* = 8.1 Hz, 1H), 7.19 – 7.12 (m, 2H), 6.65 – 6.59 (m, 2H), 6.59 – 6.53 (m, 1H), 6.53 – 6.46 (m, 2H), 4.64 (s, 2H), 4.18 (s, 2H), 3.82 (s, 5H), 3.61 (s, 2H), 3.20 (d, *J* = 4.4 Hz, 4H); Anal. calculated for $C_{26}H_{28}ClN_3O_2$: C, 69.40; H, 6.27; N, 9.34. Found: C, 69.37; H, 6.29; N, 9.33; MS: m/z 450.3 (M+1), 452.3 (M+3).

2-(benzyl(4-chlorophenyl)amino)-1-(4-(4-methoxyphenyl)piperazin-1-yl)ethanone (51f)

White solid; IR (KBr, v, cm^{-1}): 3024, 2958, 2806, 1645, 1506, 1222, 1026, 956, 798, 777; ^1H NMR (400 MHz, $CDCl_3$) δ 7.40 – 7.29 (m, 5H), 7.15 (d, *J* = 9.1 Hz, 2H), 6.95 – 6.86 (m, 4H), 6.64 – 6.58 (m, 2H), 4.64 (s, 2H), 4.18 (s, 2H), 3.80 (s, 5H), 3.64 – 3.57 (m, 2H), 3.07 (d, *J* =

4.6 Hz, 4H); Anal. calculated for $C_{26}H_{28}ClN_3O_2$: C, 69.40; H, 6.27; N, 9.34. Found: C, 69.35; H, 6.30; N, 9.36; MS: m/z 450.3 (M+1), 452.3 (M+3).

2-(benzyl(4-chlorophenyl)amino)-1-(4-(2-fluorophenyl)piperazin-1-yl)ethanone (51g)

White solid; IR (KBr, v, cm^{-1}): 3057, 3028, 2814, 1656, 1597, 1552, 1450, 1238, 1172, 1038, 812, 758; ^1H NMR (400 MHz, $CDCl_3$) δ 7.39 – 7.34 (m, 2H), 7.30 (d, *J* = 5.6 Hz, 3H), 7.19 – 7.14 (m, 2H), 7.12 – 7.06 (m, 2H), 7.02 (ddd, *J* = 5.4, 4.3, 1.6 Hz, 1H), 6.99 – 6.92 (m, 1H), 6.65 – 6.59 (m, 2H), 4.65 (s, 2H), 4.19 (s, 2H), 3.87 – 3.78 (m, 2H), 3.66 – 3.58 (m, 2H), 3.09 (s, 4H); Anal. calculated for $C_{25}H_{25}ClFN_3O$: C, 68.56; H, 5.75; N, 9.60. Found: C, 68.57; H, 5.74; N, 9.63; MS: m/z 438.3 (M+1), 440.3 (M+3).

2-(benzyl(4-chlorophenyl)amino)-1-(4-(4-fluorophenyl)piperazin-1-yl)ethanone (51h)

White solid; IR (KBr, v, cm^{-1}): 3055, 2902, 2819, 1645, 1506, 1435, 1226, 1165, 1026, 960, 860, 813; ^1H NMR (400 MHz, $CDCl_3$) δ 7.37 (dd, *J* = 10.2, 4.3 Hz, 2H), 7.30 (t, *J* = 3.1 Hz, 3H), 7.17 – 7.13 (m, 2H), 7.01 (dd, *J* = 11.6, 5.7 Hz, 2H), 6.93 – 6.88 (m, 2H), 6.64 – 6.60 (m, 2H), 4.64 (s, 2H), 4.18 (s, 2H), 3.84 – 3.77 (m, 2H), 3.65 – 3.57 (m, 2H), 3.10 (d, *J* = 4.8 Hz, 4H); Anal. calculated for $C_{25}H_{25}ClFN_3O$: C, 68.56; H, 5.75; N, 9.60. Found: C, 68.52; H, 5.77; N, 9.58; MS: m/z 438.3 (M+1), 440.3 (M+3).

2-(benzyl(4-chlorophenyl)amino)-1-(4-(3-chlorophenyl)piperazin-1-yl)ethanone (51i)

White solid; IR (KBr, v, cm^{-1}): 3029, 2885, 2823, 1651, 1598, 1493, 1356, 1207, 1172, 959, 821, 737; ^1H NMR (400 MHz, $CDCl_3$) δ 7.74 (dd, *J* = 8.8, 4.3 Hz, 1H), 7.45 – 7.41 (m, 1H), 7.35 (d, *J* = 6.9 Hz, 2H), 7.30 (d, *J* = 5.9 Hz, 2H), 7.27 (s, 1H), 7.14 (d, *J* = 9.0 Hz, 2H), 6.90 (dd, *J* = 4.1, 1.9 Hz, 2H), 6.61 (d, *J* = 9.0 Hz, 2H), 4.63 (s, 2H), 4.18 (s, 2H), 3.83 – 3.76 (m, 2H), 3.63 – 3.57 (m, 2H), 3.20 (s, 4H); Anal. calculated for $C_{25}H_{25}Cl_2N_3O$: C, 66.08; H, 5.55; N, 9.25. Found: C, 66.13; H, 5.57; N, 9.21; MS: m/z 454.2 (M+1), 456.2 (M+3).

2-(benzyl(4-chlorophenyl)amino)-1-(4-(4-chlorophenyl)piperazin-1-yl)ethanone (51j)

White solid; IR (KBr, v, cm^{-1}): 3048, 2986, 2906, 2873, 1651, 1504, 1450, 1232, 1095, 754; ^1H NMR (400 MHz, $CDCl_3$) δ 7.46 – 7.39 (m, 2H), 7.28 – 7.24 (m, 2H), 7.21 (d, *J* = 5.2 Hz, 3H), 7.16 – 7.09 (m, 2H), 6.85 – 6.81 (m, 2H), 6.66 – 6.62 (m, 2H), 4.63 (s, 2H), 4.19 (s, 2H), 3.81 (d, *J* = 5.1 Hz, 2H), 3.63 (s, 2H), 3.27 – 3.18 (m, 4H); Anal. calculated for $C_{25}H_{25}Cl_2N_3O$: C, 66.08; H, 5.55; N, 9.25. Found: C, 66.03; H, 5.57; N, 9.21; MS: m/z 454.2 (M+1), 456.2 (M+3).

2-(benzyl(4-chlorophenyl)amino)-1-(4-(4-nitrophenyl)piperazin-1-yl)ethanone (51k)

Pale yellow solid; IR (KBr, v, cm^{-1}): 3062, 2902, 2843, 1657, 1597, 1489, 1325, 1232, 1020, 823, 752; ^1H NMR (400 MHz, $CDCl_3$) δ 8.20 – 8.16 (m, 2H), 7.40 – 7.34 (m, 2H), 7.31 (d, *J* = 5.2 Hz, 3H), 7.19 – 7.13 (m, 2H), 6.87 – 6.83 (m, 2H), 6.66 – 6.60 (m, 2H), 4.64 (s, 2H), 4.18 (s, 2H), 3.83 (d, *J* = 4.9 Hz, 2H), 3.65 (s, 2H), 3.50 – 3.45 (m, 4H); Anal. calculated for

$C_{25}H_{25}ClN_4O_3$: C, 64.58; H, 5.42; N, 12.05. Found: C, 64.54; H, 5.45; N, 12.07; MS: m/z 465.3 (M+1), 467.3 (M+3).

2-(benzyl(4-chlorophenyl)amino)-1-(4-benzylpiperazin-1-yl)ethanone (51l)

White solid; IR (KBr, v, cm^{-1}): 3046, 2933, 2814, 2767, 1651, 1595, 1504, 1440, 1278, 1226, 999, 817, 731; ^1H NMR (400 MHz, $CDCl_3$) δ 7.39 – 7.33 (m, 5H), 7.31 – 7.25 (m, 5H), 7.17 – 7.10 (m, 2H), 6.59 (dd, *J* = 7.4, 5.2 Hz, 2H), 4.63 (s, 2H), 4.13 (s, 2H), 3.66 (d, *J* = 4.4 Hz, 2H), 3.56 (s, 2H), 3.50 – 3.40 (m, 2H), 2.52 – 2.38 (m, 4H); Anal. calculated for $C_{26}H_{28}ClN_3O$: C, 71.96; H, 6.50; N, 9.68. Found: C, 71.92; H, 6.52; N, 9.65; MS: m/z 434.3 (M+1), 436.3 (M+3).

2-(benzyl(4-chlorophenyl)amino)-1-(4-(2,3-dichlorophenyl)piperazin-1-yl)ethanone (51m)

White solid; IR (KBr, v, cm^{-1}): 3061, 3018, 2902, 1651, 1504, 1433, 1504, 1433, 1232, 964, 808, 758 ; ^1H NMR (400 MHz, $CDCl_3$) δ 7.79 – 7.70 (m, 1H), 7.43 (dd, *J* = 6.4, 2.8 Hz, 1H), 7.35 (dd, *J* = 4.3, 2.6 Hz, 2H), 7.30 (d, *J* = 5.7 Hz, 2H), 7.23 – 7.21 (m, 1H), 7.16 – 7.13 (m, 2H), 6.94 (dd, *J* = 7.7, 1.7 Hz, 1H), 6.62 – 6.58 (m, 2H), 4.64 (s, 2H), 4.20 (s, 2H), 3.84 (s, 2H), 3.69 – 3.60 (m, 2H), 3.04 (d, *J* = 5.3 Hz, 4H); Anal. calculated for $C_{25}H_{24}Cl_3N_3O$: C, 61.42; H, 4.95; N, 8.60. Found: C, 61.41; H, 4.93; N, 8.58; MS: m/z 488.2 (M+1), 492.2 (M+5).

1-(4-benzhydrylpiperazin-1-yl)-2-(benzyl(4-chlorophenyl)amino)ethanone (51n)

White solid; IR (KBr, v, cm^{-1}): 3057, 2930, 2814, 1660, 1597, 1502, 1232, 964, 808; ^1H NMR (400 MHz, $CDCl_3$) δ 7.62 – 7.32 (m, 5H), 7.32 – 7.24 (m, 3H), 7.15 (dd, *J* = 8.6, 4.3 Hz, 1H), 6.66 – 6.54 (m, 1H), 4.59 (s, 1H), 4.09 (s, 1H), 3.66 (s, 1H), 3.47 (s, 1H), 2.43 (s, 2H); Anal. calculated for $C_{32}H_{32}ClN_3O$: C, 75.35; H, 6.32; N, 8.24. Found: C, 75.39; H, 6.33; N, 8.21; MS: m/z 510.3 (M+1), 512.3 (M+3).

5.2.11 Synthesis and characterization of 5-chloro-3-hydroxy-3-(2-oxo-2-phenylethyl)indolin-2-one derivatives (54a-k)

Different conditions were tried (a1-a3, Table **5.12**) for the synthesis of target compound **54a** using starting materials **52** and **53a.** Overall, condition a3 in which diethylamine and ethanol were used as base and solvent respectively, found to be appropriate and afforded compound **54a** in good yield. Further, rest of the compounds (**54b-k**) were synthesized by using the optimized reaction conditions (a3).

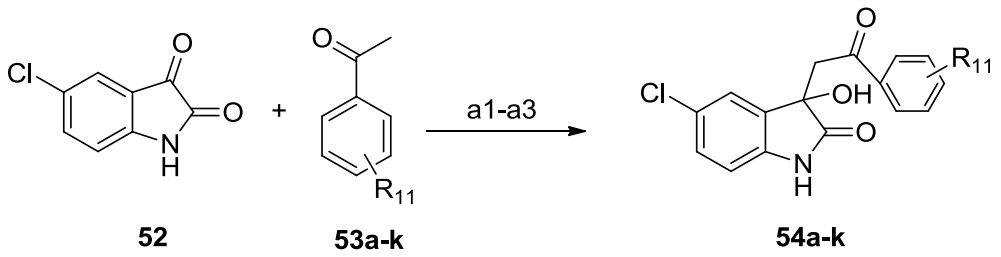

52 **53a-k** **54a-k**

Scheme 11. Reagents and conditions

Table 5.12. Optimization of the reaction conditions to obtain compound **54a**

S. No	Solvent	Base	Reaction condition	Inference
a1	DMF	K_2CO_3, (2 Eq.)	rt, 4 h	Multiple spots
a2	ACN	Et_3N, (2 Eq.)	heating, 80 C˚, 3 h	30% yield (was purified by column chromatography)
a3	EtOH	Et_2NH, (1.2 Eq.)	rt, 6 h	88% yield, single spot reaction

General procedure for the synthesis of compounds 54a-k using optimized reaction condition (a3)

Selected acetophenones (**53a-k**, 2 mmol) were stirred in ethanol (15 ml) containing diethylamine (2.4 mmol, 0.32 ml) for 20 minutes at room temperature, then starting material **52** (2 mmol, 0.362 g) was added slowly in portions. Further, the reaction mass was stirred at room temperature (5-9 h) till completion as per TLC. After completion of reaction, ethanol was evaporated on rotary evaporator to half of its original volume and 15 ml of ice cold water was added to the reaction mixture. Resulting precipitates were filtered using vacuum filtration and twice washed with cold ethanol (2x10 ml), followed by diethyl ether (10 ml) and finally dried in oven at 45 ˚C to get desired compounds **54a-k** [14]**.** Preliminary characteristics data of the synthesized compounds **54a-k** are summarized in table **5.13.**

Table 5.13. Preliminary characteristics data of compounds **54a-k**

Comp. code	R_{11}	Mol. formula	Mol. Wt	% Yield	Melting point (˚C)
54a	H	$C_{16}H_{12}ClNO$	301.05	88	188-190
54b	2-CH_3O	$C_{16}H_{11}ClNO_3$	331.06	91	174-175
54c	3-CH_3O	$C_{16}H_{11}ClNO_3$	331.06	93	178-179
54d	4-F	$C_{16}H_{11}ClFNO_3$	319.04	86	196-198
54e	2-Cl	$C_{16}H_{11}Cl_2NO_3$	335.01	83	198-201
54f	3-Cl	$C_{16}H_{11}Cl_2NO_3$	335.01	87	170-172
54g	3-Br	$C_{16}H_{11}BrClNO$	378.96	92	208-211
54h	3-NO_2	$C_{16}H_{11}ClN_2O_5$	346.04	78	186-188
54i	3,4-DiMeO	$C_{18}H1_6ClNO_5$	361.07	88	170-171
54j	3,4-DiCl	$C_{16}H_{10}Cl_3NO_3$	368.97	85	198-200
54k	2-Br, 4-CN	$C_{17}H_{10}BrClN_2O_3$	403.96	87	210-213

Spectral data of compounds 54a-k

Synthesized compounds were characterized by spectral techniques like ^{1}H NMR, IR, ESI-MS, while three compounds (**54a**, **54e** and **54g**) also characterized by ^{13}C NMR as representative of series. Titled compounds possessed secondary alcohol and amidic group, so corresponding to **O-H** and **N-H** stretching, a merged peak with broad range (3000-3650 cm^{-1}) appeared in the IR spectra, moreover, centre of this broad peak (point with minimum transmittance) lied between 3178-3196 cm^{-1}. Further, corresponding to the two carbonyl group, **C=O** stretching peaks were observed, for example, one prominent peak around 1703-1718 cm^{-1} and another around 1681-1698 cm^{-1} were observed certainly due to the keto and carbonyl of amidic bond, respectively.

In the ^{1}H NMR spectra of the tested compounds, a pair of methylene protons (at carbon adjacent to carbonyl group) displayed two distinct peaks (doublet) with significant difference in their δ values (at δ 3.57-3.83 and 3.98-4.37). Further, characteristic peak of hydroxyl proton (-O**H**) appeared as singlet at δ 6.15-6.33, while another distinct peak corresponding to the amidic proton (-CON**H**-) appeared between δ values 10.38-10.48. Further, proton counting as well as peak pattern of other aromatic protons was also found in accordance with their proposed structures. ^{13}C NMR spectra of three representative compounds (**54a**, **54e** and **54g**) showed two distinct peaks at δ around 196-199 and 178 due to presence of carbonyl and amidic carbonyl group, respectively. Furthermore, overall counting of carbons and their position in ^{13}C NMR spectra also confirm the titled compounds. ESI-MS spectra of synthesized compounds exhibited the corresponding M+1 and M+3 peaks. Details of spectral data for series **54a-k** are given below:

5-chloro-3-hydroxy-3-(2-oxo-2-phenylethyl) indolin-2-one (54a)

White solid; IR (KBr, v, cm^{-1}): 3180, 3145, 3061, 2814, 1712, 1698, 1620, 1473, 1350, 1338, 1220, 991, 825, 758; ^{1}H NMR (400 MHz, DMSO) δ 10.44 (s, 1H), 7.90 (d, *J* = 7.4 Hz, 2H), 7.64 (t, *J* = 7.4 Hz, 1H), 7.51 (t, *J* = 7.7 Hz, 2H), 7.41 (d, *J* = 2.1 Hz, 1H), 7.23 (dd, *J* = 8.2, 2.2 Hz, 1H), 6.84 (d, *J* = 8.2 Hz, 1H), 6.24 (s, 1H), 4.18 (d, *J* = 18.0 Hz, 1H), 3.65 (d, *J* = 17.9 Hz, 1H); ^{13}C NMR (100 MHz, DMSO) δ 197.03, 178.54, 142.36, 136.37, 134.42, 134.00, 129.20, 129.10, 128.39, 125.62, 124.42, 111.27, 73.50, 46.17; MS: m/z 302.2 (M+1), 304.2 (M+3).

5-chloro-3-hydroxy-3-(2-(2-methoxyphenyl)-2-oxoethyl)indolin-2-one (**54b**)

White solid; IR (KBr, v, cm^{-1}): 3196, 3061, 1712, 1697, 1658, 1622, 1435, 1338, 1244, 1064, 997, 833; ^{1}H NMR (400 MHz, DMSO) δ 10.38 (s, 1H), 7.57 – 7.51 (m, 1H), 7.37 (dd, *J* = 7.7, 1.8 Hz, 1H), 7.30 (d, *J* = 2.2 Hz, 1H), 7.21 (dd, *J* = 8.2, 2.2 Hz, 1H), 7.18 (d, *J* = 8.1 Hz, 1H), 6.96 (dd, *J* = 10.9, 4.0 Hz, 1H), 6.81 (d, *J* = 8.2 Hz, 1H), 6.15 (s, 1H), 3.98 (d, *J* = 18.2 Hz, 1H), 3.93 (s, 3H), 3.63 (d, *J* = 18.2 Hz, 1H); MS: m/z 332.2 (M+1), 334.2 (M+3).

5-chloro-3-hydroxy-3-(2-(3-methoxyphenyl)-2-oxoethyl)indolin-2-one (54c)

White solid; IR (KBr, v, cm^{-1}): 3178, 3142, 2947, 2827, 1711, 1697, 1681, 1487, 1338, 1263, 1222, 1043, 856, 725; ^{1}H NMR (400 MHz, DMSO) δ 10.43 (s, 1H), 7.52 (d, *J* = 7.7 Hz, 1H), 7.46 – 7.39 (m, 2H), 7.35 (s, 1H), 7.25 – 7.18 (m, 2H), 6.83 (d, *J* = 8.2 Hz, 1H), 6.22 (s, 1H), 4.17 (d, *J* = 18.0 Hz, 1H), 3.80 (s, 3H), 3.63 (d, *J* = 18.0 Hz, 1H); MS: m/z 332.2 (M+1), 334.2 (M+3).

5-chloro-3-(2-(4-fluorophenyl)-2-oxoethyl)-3-hydroxyindolin-2-one (54d)

White solid; IR (KBr, v, cm^{-1}): 3185, 3078, 1714, 1696, 1685, 1600, 1506, 1487, 1338, 1184, 1074, 989, 825; ^{1}H NMR (400 MHz, DMSO) δ 10.43 (s, 1H), 8.03 – 7.93 (m, 2H), 7.43 – 7.29 (m, 3H), 7.22 (dd, *J* = 8.2, 2.2 Hz, 1H), 6.82 (d, *J* = 8.2 Hz, 1H), 6.23 (s, 1H), 4.15 (d, *J* = 17.9 Hz, 1H), 3.62 (d, *J* = 17.9 Hz, 1H); MS: m/z 320.1 (M+1), 322.1 (M+3).

5-chloro-3-(2-(2-chlorophenyl)-2-oxoethyl)-3-hydroxyindolin-2-one (54e)

White solid; IR (KBr, v, cm^{-1}): 3176, 3112, 3062, 1708, 1681, 1471, 1436, 1319, 827, 759; ^{1}H NMR (400 MHz, DMSO) δ 10.48 (s, 1H), 7.65 – 7.59 (m, 1H), 7.55 – 7.48 (m, 2H), 7.43 (ddd, *J* = 6.6, 5.2, 2.8 Hz, 2H), 7.24 (dd, *J* = 8.2, 2.2 Hz, 1H), 6.83 (d, *J* = 8.2 Hz, 1H), 6.29 (s, 1H), 3.99 (d, *J* = 17.4 Hz, 1H), 3.57 (d, *J* = 17.4 Hz, 1H); ^{13}C NMR (101 MHz, DMSO) δ 199.02, 178.14, 142.15, 137.97, 133.75, 133.10, 131.04, 130.24, 129.93, 129.31, 127.82, 125.79, 124.71, 111.39, 73.54, 49.77; MS: m/z 336.1 (M+1), 338.1 (M+3).

5-chloro-3-(2-(3-chlorophenyl)-2-oxoethyl)-3-hydroxyindolin-2-one (54f)

White solid; IR (KBr, v, cm^{-1}): 3196, 3012, 1716, 1698, 1658, 1435, 1244, 1064, 997, 83; ^{1}H NMR (400 MHz, DMSO) δ 10.42 (s, 1H), 7.73 – 7.65 (m, 2H), 7.47 – 7.35 (m, 3H), 7.22 (dd,

J = 8.2, 2.2 Hz, 1H), 6.82 (d, *J* = 8.2 Hz, 1H), 6.20 (s, 1H), 4.14 (d, *J* = 17.9 Hz, 1H), 3.61 (d, *J* = 17.9 Hz, 1H); MS: m/z 336.10 (M+1), 338.1 (M+3).

3-(2-(3-bromophenyl)-2-oxoethyl)-5-chloro-3-hydroxyindolin-2-one (54g)

White solid; IR (KBr, v, cm^{-1}): 3174, 3138, 2895, 1791, 1707, 1697, 1471, 1421, 1338, 1209, 1070, 1008, 898, 779; ^{1}H NMR (400 MHz, DMSO) δ 10.46 (s, 1H), 8.02 (s, 1H), 7.87 (dd, *J* = 24.1, 7.9 Hz, 2H), 7.48 (t, *J* = 7.9 Hz, 1H), 7.41 (d, *J* = 2.0 Hz, 1H), 7.23 (dd, *J* = 8.2, 2.1 Hz, 1H), 6.83 (d, *J* = 8.2 Hz, 1H), 6.26 (s, 1H), 4.19 (d, *J* = 18.0 Hz, 1H), 3.63 (d, *J* = 17.9 Hz, 1H); ^{13}C NMR (101 MHz, DMSO) δ 196.06, 178.40, 142.27, 138.35, 136.57, 134.19, 131.44, 131.03, 129.18, 127.48, 125.67, 124.55, 122.60, 111.31, 73.47, 46.23; MS: m/z 380.0 (M+1), 382.0 (M+3).

5-chloro-3-hydroxy-3-(2-(3-nitrophenyl)-2-oxoethyl)indolin-2-one (54h)

Pale yellow solid; IR (KBr, v, cm^{-1}): 3194, 3088, 2902, 2825, 1712, 1693, 1614, 1531, 1475, 1344, 1217, 1184, 1001, 829, 734; ^{1}H NMR (400 MHz, DMSO) δ 10.48 (s, 1H), 8.57 (d, *J* = 1.7 Hz, 1H), 8.46 (dd, *J* = 8.2, 1.5 Hz, 1H), 8.33 (d, *J* = 7.8 Hz, 1H), 7.81 (t, *J* = 8.0 Hz, 1H), 7.41 (d, *J* = 2.1 Hz, 1H), 7.23 (dd, *J* = 8.3, 2.2 Hz, 1H), 6.83 (d, *J* = 8.3 Hz, 1H), 6.30 (s, 1H), 4.28 (d, *J* = 17.9 Hz, 1H), 3.70 (d, *J* = 17.9 Hz, 1H); MS: m/z 347.1 (M+1), 349.1 (M+3).

5-chloro-3-(2-(3,4-dimethoxyphenyl)-2-oxoethyl)-3-hydroxyindolin-2-one (54i)

White solid; IR (KBr, v, cm^{-1}): 3182, 3142, 2900, 2839, 1703, 1691, 1517, 1338, 1271, 1026, 808, 719; ^{1}H NMR (400 MHz, DMSO) δ 10.40 (s, 1H), 7.62 (dd, *J* = 8.4, 1.8 Hz, 1H), 7.38 (d, *J* = 2.1 Hz, 1H), 7.32 (d, *J* = 1.8 Hz, 1H), 7.22 (dd, *J* = 8.2, 2.2 Hz, 1H), 7.06 (d, *J* = 8.5 Hz, 1H), 6.82 (d, *J* = 8.2 Hz, 1H), 6.19 (s, 1H), 4.12 (d, *J* = 17.8 Hz, 1H), 3.84 (s, 3H), 3.77 (s, 3H), 3.59 (d, *J* = 17.8 Hz, 1H); MS: m/z 362.2 (M+1), 364.2 (M+3).

5-chloro-3-(2-(3,4-dichlorophenyl)-2-oxoethyl)-3-hydroxyindolin-2-one (54j)

White solid; IR (KBr, v, cm^{-1}): 3183, 3145, 2818, 1712, 1695, 1622, 1487, 1392, 1338, 1224, 1205, 1072, 823, 731; ^{1}H NMR (400 MHz, DMSO) δ 10.46 (s, 1H), 8.10 (s, 1H), 7.82 (dd, *J* = 21.7, 8.4 Hz, 2H), 7.39 (s, 1H), 7.27 – 7.16 (m, 1H), 6.82 (d, *J* = 8.2 Hz, 1H), 6.26 (s, 1H), 4.17 (d, *J* = 18.0 Hz, 1H), 3.63 (d, *J* = 17.9 Hz, 1H); MS: m/z 370.1 (M+1), 372.1 (M+3).

3-bromo-4-(2-(5-chloro-3-hydroxy-2-oxoindolin-3-yl)acetyl)benzonitrile (54k)

White solid; IR (KBr, v, cm^{-1}): 3193, 3091, 3018, 2253, 1718, 1698, 1622, 1483, 1446, 1296, 1222, 933, 837, 775; ^{1}H NMR (400 MHz, DMSO) δ 10.51 (s, 1H), 8.57 (d, *J* = 1.7 Hz, 1H), 7.53 (s, 1H), 7.83 (t, *J* = 8.0 Hz, 1H), 7.49 (d, *J* = 2.1 Hz, 1H), 7.31 (dd, *J* = 8.1, 2.1 Hz, 1H), 6.91 (d, *J* = 8.1 Hz, 1H), 6.33 (s, 1H), 4.37 (d, *J* = 17.9 Hz, 1H), 3.83 (d, *J* = 17.9 Hz, 1H); MS: m/z 305.1 (M+1), 307.1 (M+3).

5.3 References

1. S. Murugesan, S. Ganguly, G, Maga, Synthesis, evaluation and molecular modeling studies of some novel tetrahydroisoquinoline derivatives targeted at the HIV-1 reverse Transcriptase. Der Pharmacia Lettre, 3 (2011) 317-332.
2. S. Murugesan, S. Ganguly G. Maga, Synthesis, evaluation and molecular modeling studies of some novel 3-(3,4-dihydroisoquinolin-2(*1H*)-*N*-substituted-phenyl)propanamides as HIV-1 non-nucleoside Reverse Transcriptase inhibitors. Journal of Chemical Sciences, 122 (2010) 169-176.
3. A. Rathore, M.U. Rahman, A.A. Siddiqui, A. Ali. M. Shaharyar, Design and synthesis of benzimidazole analogs endowed with oxadiazole as selective COX-2 inhibitor. Archiv der Pharmazie, 347 (2014) 923-935.
4. F. Zhang, X.L. Wang, J. Shi, S.F. Wang, Y. Yin, Y.S. Yang, W.M. Zhang, Synthesis, molecular modeling and biological evaluation of N-benzylidene-2-((5-(pyridin-4-yl)-1,3,4-oxadiazol-2-yl)thio)acetohydrazide derivatives as potential anticancer agents. Bioorganic & Medicinal Chemistry, 22 (2014) 468-477.
5. S. Chander, A. Penta, R. Singh, P.N. Jha, and S. Murugesan, A rapid, green, efficient microwave-assisted synthesis and antimicrobial activity of novel glycinamide of 6,7-dimethoxy-1, 2, 3, 4-tetrahydroisoquinolines. Current Microwave Chemistry, 2 (2015) 44-52.
6. T. Chandrasekhar, V. Kumar, A.B Reddy, P.J. Naik, G.N. Swamy, Synthesis and biological evaluation of some new Aryl acid N'-(1H-indazole-3-carbonyl)-hydrazide derivatives: Journal of Chemical and Pharmaceutical Research, 4 (2012) 2795-2802.
7. D. Kupfer, Altered selectivity of reduction of steroidal carbonyls. Tetrahedron, 15 (1961) 193-196.
8. K.K. Roy, S. Tota, T. Tripathi, S. Chander, C. Nath, A.K. Saxena, Lead optimization studies towards the discovery of novel carbamates as potent AChE inhibitors for the potential treatment of Alzheimer's disease. Bioorganic & Medicinal Chemistry, 20 (2012) 6313-6320.
9. P. Ashok, S. Chander, J. Balzarini, C. Pannecouque, S. Murugesan, Design, synthesis of new β-carboline derivatives and their selective anti-HIV-2 activity, Bioorganic & Medicinal Chemistry Letters, 25 (2015) 1232-1235.
10. A.S. Negi, S.K. Chattopadhyay S. Srivastava, A.K. Bhattacharya, A Simple regioselective demethylation of p-Aryl methyl ethers using aluminium chloride-dichloromethane system. Synthetic Communications, 35 (2005) 15-21.

11. M.G. Perrone, E. Santandrea, L. Bleve, P. Vitale, N.A. Colabufo, R. Jockers, F.M. Milazzo, Stereospecific synthesis and bio-activity of novel β3-adrenoceptor agonists and inverse agonists. Bioorganic & Medicinal Chemistry, 16 (2008) 2473-2488.
12. M. De Rosa, G. Vigliotta, G. Palma, C. Saturnino, A. Soriente, Novel penicillin-type analogues bearing a variable substituted 2-azetidinone ring at position 6: Synthesis and biological evaluation. Molecules, 20 (2015) 22044-22057.
13. A.F. Abdel-Magid, K.G. Carson, B.D. Harris, C.A. Maryanoff, R.D. Shah, Reductive amination of aldehydes and ketones with sodium triacetoxyborohydride. Studies on direct and indirect reductive amination procedures. Journal of Organic Chemistry, 61 (1996) 3849-3862.
14. A.K. Gupta, S. Kalpana, J.K. Malik, Synthesis and in vitro antioxidant activity of new 3-substituted-2-oxindole derivatives. Indian Journal of Pharmaceutical Sciences, 74 (2012) 481-486.

CHAPTER 6

Biological Evaluation

All the synthesized compounds were *in-vitro* evaluated for HIV-1 RT inhibitory activity via colorimetric ELISA based assay. Among the compounds screened against HIV-1 RT, some compounds of series (**28a-l, 38a-o, 51a-n** and **54a-k**) displayed encouraging RT inhibition; among which few top active compounds were selected from each series and evaluated for anti-HIV-1 activity (HIV-1_{IIIB} strain) and cytotoxicity against T cell lines (C8166). The anti-tubercular activity of the synthesized compounds was evaluated against *Mycobacterium tuberculosis* (H37Rv/a strain). Further, all the synthesized compounds were also evaluated *in-vitro* for antibacterial activity against two Gram (-)ve (*Escherichia coli, Pseudomonas putida*) and two Gram (+)ve (*Staphylococcus aureus* and *Bacillus cereus*) strains. The *in-vitro* anti-fungal activity of all the compounds was evaluated against *Candida albicans* and *Aspergillus niger*.

6.1 *In-vitro* HIV-1 RT assay

6.1.1 Experimental and Methodology

All the synthesized compounds were evaluated for *in-vitro* HIV-1 RT inhibitory activity using colorimetric assay (Roche diagnostics), in accordance with the kit protocol. Marketed drug efavirenz (kindly donated by Ranbaxy Laboratories, Gurgaon) was used as reference positive control during the study, while 5% DMSO as solvent. The test is based upon the colorimetric enzyme immunoassay, which quantitatively determines the retroviral reverse transcriptase activity. Briefly, the reaction mixture was set with template primer complex, RT enzyme and dNTPs in the lysis buffer with or without inhibitors. The reaction mixture was incubated at 37 ˚C for 1h and then transferred to streptavidin coated microtiter plate (MTP). The biotin-labeled dNTPs that are incorporated in the template due to the activity of RT were bound to streptavidin. The unbound dNTPs were washed using wash buffer and anti-DIG-POD was added to the MTP. The DIG-labeled dNTPs incorporated in the template were bound to anti-DIG-POD antibody. The unbound anti-DIG-POD was washed using wash buffer and the peroxide substrate (ABST) was added to the MTP. A colored reaction product was produced during the cleavage of the substrate catalyzed by a peroxide enzyme. The activity of RT in the presence of 5% DMSO in lysis buffer (without inhibitor) was considered as fullest activity (100%). The intensity of color produced was measured as optical density (OD) at 405 nm using microtiter plate ELISA reader [1].

The % inhibition of HIV-1 RT was calculated using the following formula;

$$\%\ \text{inhibition} = 100 - \left(\frac{\text{OD at 405 nm with inhibitor}}{\text{OD at 405 nm without inhibitor}} \times 100\right)$$

Initially, all the synthesized compounds were *in-vitro* screened at 100 µM concentration, and HIV-1 RT inhibitory activity of the test compounds was expressed in terms of % inhibition of RT enzyme, taken as the average of duplicate value. Compounds of series **28a-l, 38a-o,**

51a-n and **54a-k** displayed overall superior inhibition of HIV-1 RT compared to the compounds of other series. Moreover, several compounds of these series exhibited more than 75% inhibition of HIV-RT at the tested concentration (100µM). So, IC_{50} was calculated for the compounds of series **28a-l, 38a-o, 51a-n** and **54a-k.** Reference drug efavirenz displayed promising activity with average 98.87% inhibition of HIV-RT and IC_{50} of efavirenz was determined which was found to be 0.057 µM.

6.1.2 Outcome of *in-vitro* HIV-1 RT assay

6.1.2.1 *In-vitro* HIV-1 RT inhibition activity of series 5a-o

In-vitro HIV-1 RT inhibition activity of 2-(6,7-dimethoxy-3,4-dihydroisoquinolin-2(1*H*)-yl)-*N*-phenylacetamide derivatives (**5a-o)** is shown in Table **6.1**. Based upon the RT inhibition activity, compounds are classified as significantly active (≥ 50% inhibition), moderately active (% inhibition between <50 to ≥35) and weakly active (<35% inhibition). Among the series, compounds **5d, 5f, 5h, 5n** and **5o** exhibited significant activity, compounds **5b, 5c, 5e, 5i, 5k** and **5m** exhibited moderate, while compounds **5a, 5g, 5j** and **5l** exhibited weak activity against HIV-1 RT (Table **6.1**). Un-substituted prototype compound **5a** of series displayed weak activity with 34.32% inhibition of HIV-1 RT. As shown in Table **6.1**, substitutions on phenyl ring displayed significant effect on the HIV-1 RT inhibition activity. Among the mono substituted compounds, substitution with electron donating groups like methyl and methoxy especially at the *para* position of the phenyl ring (compounds **5d** and **5f**) enhanced the potency against HIV-1 RT, exhibited 52.46 and 56.23% inhibition of HIV-1 RT, respectively.

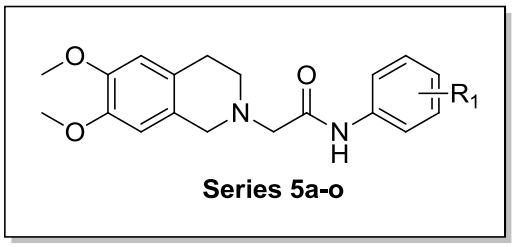

Series 5a-o

Substitution of phenyl ring with electron withdrawing group also altered the inhibition potency against HIV-1 RT, for example, chloro substituted compounds (**5h, 5i** and **5j**) followed the decreasing order of potency *ortho*>*meta*>*para*. Furthermore, compound **5g** having *p*-fluoro substitution decreased the potency, while substitution of phenyl ring with *p*-nitro group (**5k**) slightly enhanced the potency. Compound **5l** with strong electron withdrawing group (*m*-trifluoromethyl) also showed less potency against HIV-1 RT. Upon di-substitution at phenyl ring, good enhancement in the potency was observed (compounds **5m, 5n** and **5o**). Moreover, compound **5n** (3,4-dimethyl substitution) showed the highest potency (58.12% inhibition) among the tested **5a-o** series of compounds.

Table 6.1 Result of HIV-1 RT inhibition activity of series **5a-o**

Comp. code	R_1	% HIV-1 RT Inhibition[a]
5a	H	34.32
5b	2-CH_3	36.23
5c	3-CH_3	39.51
5d	**4-CH_3**	**52.46**
5e	3-OCH_3	44.21
5f	**4-OCH_3**	**56.23**
5g	4-F	28.45
5h	**2-Cl**	**52.34**
5i	3-Cl	37.26
5j	4-Cl	33.65
5k	4-NO_2	42.78
5l	3-CF_3	30.64
5m	2,6-di-Me	48.36
5n	**3,4-di-Me**	**58.12**
5o	**2-Me,5-Cl**	**53.76**
Efavirenz		**98.87**

[a]Value is average of at least two independent experiment, standard deviation (SD) was found within ±10%.

6.1.2.2 *In-vitro* HIV-1 RT inhibition activity of series 9a-o

The result of *in-vitro* evaluation of compounds **9a-o** against HIV-1 RT (Table **6.2**), revealed that five compounds (**9f, 9h, 9i, 9k, 9n**) showed significant RT inhibition. Further, seven compounds (**9b**, **9d**, **9e, 9j, 9l, 9m**, **9o**) exhibited moderate while three compounds (**9a, 9c, 9g**) showed weak inhibitory activity against HIV-1 RT. SAR studies of the test compounds revealed that substitutions with electron donating groups especially at the *para* position of the phenyl ring enhanced the potency against HIV-1 RT, for example *p*-methoxy substituted compound **9f** (52.28% inhibition) exhibited nearly twice potency as compared to un-substituted compound **9a** (28.24% inhibition). Substitution with halogens also altered the potency, among the chloro substituted compounds (**9h, 9i** and **9j**), *ortho* substituted compound **9h** showed better activity (61.42% inhibition) as compared to the compounds **9i** and **9j** (52.68 and 41.75% inhibition, respectively) having *meta* and *para* substitution, respectively.

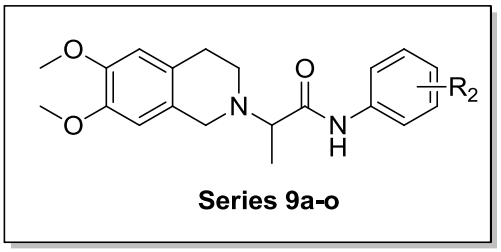

Series 9a-o

Compounds **9g** and **9m** with *p*-fluoro and *p*-nitro substitution also exhibited less potency (34.31 and 36.74% inhibition, respectively). Compound **9k,** having substitution with strong electron withdrawing group at the *ortho* position of phenyl ring (*o*-trifluoromethyl) also exhibited significant inhibition of HIV-1 RT (52.16% inhibition). Di-substitution of phenyl ring

with methyl groups (**9n** and **9o**) increased the potency against HIV-1 RT as compared to the mono methyl substituted compounds. So, overall compound **9h** (*o*-chloro substitution) showed highest potency (61.42% inhibition) and un-substituted compound **9a** showed lowest potency (28.24% inhibition) against HIV-1 RT among the series.

Table 6.2 Result of HIV-1 RT inhibition activity of series **9a-o**

Comd. code	R_2	% HIV-1 RT Inhibition[a]
9a	H	28.24
9b	2-CH_3	36.34
9c	3-CH_3	31.75
9d	4-CH_3	38.86
9e	3-OCH_3	42.43
9f	**4-OCH_3**	**54.28**
9g	4-F	34.31
9h	**2-Cl**	**61.42**
9i	**3-Cl**	**52.68**
9j	4-Cl	41.75
9k	**2-CF_3**	**52.16**
9l	3-CF_3	38.34
9m	4-NO_2	36.74
9n	**2,4-di-Me**	**54.21**
9o	3,4-di-Me	47.53
Efavirenz		**98.87**

[a]Value is average of at least two independent experiment, standard deviation (SD) was found within ±10%.

6.1.2.3 *In-vitro* HIV-1 RT inhibition activity of series 14a-k

Compounds of series *N*'-benzylidene-2-(6,7-dimethoxy-3,4-dihydroisoquinolin-2(1*H*)-yl)acetohydrazide (**14a-k)**, showed weak activity (% inhibition <35) against the HIV-1 RT (Table **6.3**). In this series, potency of compounds did not alter significantly with nature and position of substitution. In the series, compound **14b** showed least potency (17.24% inhibition) while compound **14j** displayed highest potency (32.82% inhibition) among the series.

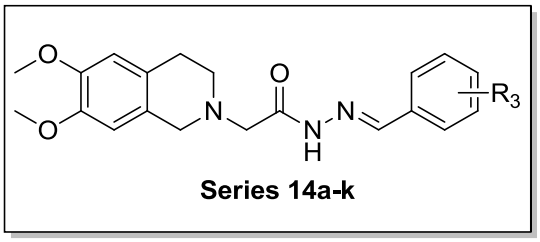

Series 14a-k

Table 6.3 Result of HIV-1 RT inhibition activity of series **14a-k**

Comp. code	R_3	% HIV-1 RT Inhibition[a]
14a	2-CH_3	24.23
14b	3-OCH_3	17.24
14c	4-OCH_3	23.73
14d	4-F	27.24
14e	2-Cl	22.21
14f	4-Cl	25.64
14g	3-Br	31.25
14h	4-Br	26.34
14i	4-NO_2	24.58
14j	4-CN	32.82
14k	3,4,5-tri-MeO	25.47
Efavirenz		**98.87**

[a]Value is average of at least two independent experiment, standard deviation (SD) was found within ±10%.

6.1.2.4 *In-vitro* HIV-1 RT inhibition activity of series 17a-o

The majority of compounds in **17a-o** series displayed significant inhibition of HIV-1 RT (Table **6.4**) except compounds **17a** and **17d** which exhibited moderate inhibition. Among the compounds containing methoxy group at phenyl ring (**17a, 17b** and **17c**) potency against HIV-1 RT changed with substitution in the order *ortho* <*meta* <*para.* So, *p*-methoxy substituted compound **17c** displayed more potency (57.45% inhibition) as compared to *ortho* and *para* substituted compounds (**17a** and **17b**), which exhibited 45.31 and 51.32% inhibition of HIV-1 RT respectively. Compounds substituted with electron withdrawing fluoro group (**17d** and **17e**) did not show much difference in their potency. However, compounds having substitution with other electron withdrawing groups like chloro, bromo, nitro, nitrile, aceto and trifluromethyl (**17f, 17g, 17h, 17i, 17jk, 17k, 17l, 17m** and **17n**) displayed significant inhibition of HIV-1 RT.

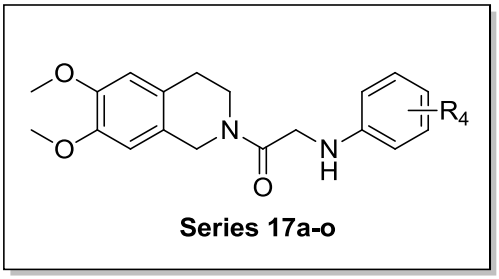

Series 17a-o

Compounds having chloro substitution at the *ortho* and *meta* position (**17f** and **17g**) did not show any significant difference in potency, but substitution at *para* position (**17h**) significantly enhanced the potency (74.82% inhibition). Moreover, *para* bromo substituted compound also showed better activity compared to compounds with *ortho* and *meta* substitution. Further, substitution with cyano, a strong electron withdrawing group at *para* position (**17l**) significantly increased the potency (72.58% inhibition), also compounds **17m** and **17n** having aceto and trifluoromethyl group at *meta* position showed significant potency (54.75 and 66.74% inhibition, respectively) against HIV-1 RT. Further, dimethyl substituted

compound **17o** displayed better activity compared to the single methoxy substituted compounds (**17a, 17b** and **17c)**. Overall, among the tested compounds **17a-o**, compound **17h** (*p*-chloro substitution) exhibited the highest potency (74.82% inhibition of HIV-1 RT).

Table 6.4 Result of HIV-1 RT inhibition activity of series **17a-o**

Comp. code	R_4	% HIV-1 RT Inhibition[a]
17a	2-OCH_3	45.31
17b	**3-OCH_3**	**51.32**
17c	**4-OCH_3**	**57.45**
17d	3-F	48.37
17e	**4-F**	**53.93**
17f	**2-Cl**	**61.38**
17g	**3-Cl**	**63.74**
17h	**4-Cl**	**74.82**
17i	**2-Br**	**63.38**
17j	**3-Br**	**60.46**
17k	**4-Br**	**68.63**
17l	**4-CN**	**72.58**
17m	**3-$COCH_3$**	**54.75**
17n	**3-CF_3**	**66.74**
17o	**2,5-di-Me**	**63.64**
Efavirenz		**98.87**

[a]Value is average of at least two independent experiment, standard deviation (SD) was found within ±10%.

6.1.2.5 *In-vitro* HIV-1 RT inhibition activity of series 23a-o

The result of *in-vitro* evaluation of compounds **23a-o** against HIV-1 RT revealed that three compounds **23d, 23f** and **23o** displayed moderate inhibition while rest of twelve compounds (**23a, 23b, 23c, 23e, 23g, 23h, 23i, 23j, 23k, 23l, 23m** and **23n**) exhibited weak inhibition (Table **6.5**). Further, it was observed that change in the potency of these compounds against RT was less dependent on the type of substitution. Unsubstituted prototype compound **23a** showed weak potency against HIV-1 RT (24.34% inhibition). Among the compounds substituted with methoxy an electron donating group, substitution at the *ortho* and *para* position (**23b** and **23d**) slightly enhanced the potency (32.27 and 36.24% inhibition, respectively) compared to unsubstituted one. However, the potency of *meta* substituted compound **23c** remained almost unaltered.

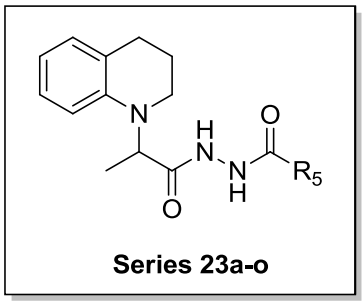

Series 23a-o

Substitution with fluoro group enhanced the potency especially at *meta* position (**23f**). Furthermore, nitro group at *ortho* and *para* position (**23h** and **23j**) slightly increased the

potency, but at *meta* position (**23i**) it resulted in the reduction of activity. Among the compounds having more than one substitution like dichloro (**23l**) showed slightly enhanced potency while substitution with dimethoxy (compound **23k**) did not alter the potency significantly. Further, trisubstitution with methoxy group (compound **23m**) further reduced the potency. The compound in which phenyl ring was replaced by styrene moiety (compound **23n**), slight enhancement of potency (34.36% inhibition) was observed. Further, substitution of styrene with nitro group at *meta* position further enhanced the potency (41.76% inhibition).

Table 6.5 Result of HIV-1 RT inhibition activity of series **23a-o**

Comp code	R_5	% HIV-1 RT Inhibition[a]
23a	Ph	24.34
23b	2-MeO-Ph	32.27
23c	3-MeO-Ph	27.24
23d	4-MeO-Ph	36.24
23e	2-F-Ph	33.46
23f	3-F-Ph	38.26
23g	4-F-Ph	28.64
23h	2-NO_2-Ph	30.71
23i	3-NO_2-Ph	16.52
23j	4-NO_2-Ph	31.75
23k	3,4-DMeO-Ph	24.85
23l	2,4-DCl-Ph	34.60
23m	3,4,5-tri-MeO-Ph	17.86
23n	Styrene	34.36
23o	Styrene-3-NO_2	41.76
Efavirenz		**98.87**

[a]Value is average of at least two independent experiment, standard deviation (SD) was found within ±10%.

6.1.2.6 *In-vitro* HIV-1 RT inhibition activity of series 28a-l

In the preliminary screening of compounds **28a-l** at 100 µM concentration, several compounds displayed encouraging activity against HIV-1 RT (>75 % inhibition), so IC_{50} was calculated for the whole series of compounds (**28a-l**). Among the series, compounds **28b, 28h, 28i, 28j** and **28l** exhibited relatively good potency with IC_{50} ≤25 µM (highlighted in bold font in Table **6.6**). Further, compounds **28a**, **28g** and **28k** displayed moderate (IC_{50}>25 to≤50 µM), while rest of compounds exhibited poor potency against the tested RT strain. SAR studies of tested compounds revealed that compound **28a** (with un-substituted phenyl) displayed moderate inhibition of RT activity (IC_{50} 36.98 µM). Further, substitution of phenyl with methyl group at *ortho* position markedly increased the potency against HIV-1 RT (IC_{50} 8.12 µM), while methyl substitution at *meta* and *para* position decreased the potency (IC_{50} 68.26 and 83.60, respectively).

Among the compounds containing fluoro substitution at phenyl ring (**28e, 28f** and **28g),** potency against RT varied in the order *ortho* <*meta* <*para.* Substitution with electron withdrawing chloro group at the *para* position of phenyl (compound **28h**) resulted in enhancement of RT inhibition activity (IC_{50} 23.76 µM) compared to compound **28a.** Furthermore, substitution with nitro group at the *para* position of phenyl ring (compound **28i**) markedly increased the potency (IC_{50} 5.42 µM), while nitro group at *meta* position slightly reduced the potency (IC_{50} 14.87 µM). Compound **28k** substituted with ethyl carboxylate group at *ortho* position of phenyl ring retained the medium potency (IC_{50} 38.97 µM), but interestingly substitution with the same group at *para* position (compound **28l)** markedly enhanced the potency (IC_{50} 12.34 µM) against RT. So, SAR studies revealed that methyl group at *ortho* position and electron withdrawing groups of moderate size at *para* position of phenyl ring resulted in enhancement of potency against HIV-1 RT.

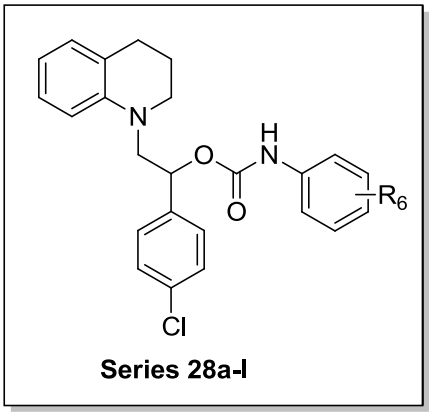

Series 28a-l

Table 6.6 Result of HIV-1 RT inhibition activity of series **28a-l**

Comp. Code	R_6	HIV-1 RT inhibition IC_{50} (µM)[a]
28a	H	36.98
28b	**2-CH_3**	**8.12**
28c	3-CH_3	68.26
28d	4-CH_3	83.60
28e	2-F	90.30
28f	3-F	72.14
28g	4-F	48.57
28h	**4-Cl**	**23.76**
28i	**3-NO_2**	**14.87**
28j	**4-NO_2**	**5.42**
28k	2-COOEt	38.97
28l	**4-COOEt**	**12.34**
Efavirenz		**0.057**

[a]Value is average of at least two independent experiment, standard deviation (SD) was found within ±10%.

6.1.2.7 *In-vitro* HIV-1 RT inhibition activity of series 32a-n

Among the series of 2-(1-(4-chlorophenyl)-2-(3,4-dihydroquinolin-1(*2H*)-yl)ethoxy)-*N*-phenylacetamide derivative **32a-n**, compound **32m** exhibited significant, compounds **32a**, **32b**, **32e**, **32h**, **32i**, **32k**, **32l** exhibited moderate while rest of compounds showed weak inhibition of HIV-1 RT (Table **6.7**). Unsubstituted phenyl derivative (**32a**) exhibited moderate

inhibition (40.78%) of HIV-1 RT, further substitution with methyl group at *ortho* position slightly increased the activity (47.34% inhibition), while at *meta* and *para* position it declined the RT inhibition activity (29.45 and 31.58% inhibition, respectively). Further, RT inhibition activity remains almost unchanged (38.64%) upon substitution with methoxy group (**32e**) at *ortho* position, but at *meta* and especially *para* substitution (**32f** and **32g**) declined the activity (26.68 and 17.86% inhibition respectively).

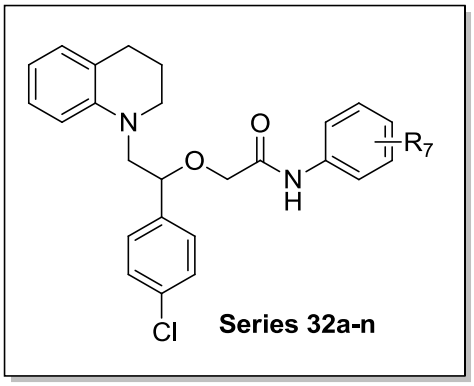

Series 32a-n

Fluoro substitution at *para* position of phenyl (compound **32h**) slightly enhanced the RT inhibition activity (46.86%), while chloro at *meta* and *para* position (compound **32i** and **32j**) reduced the activity (36.47 and 32.65% inhibition, respectively). Bromo substitution at *para* position (compound **32l**) not significantly altered the activity (39.46% inhibition), while at *meta* position (compound **32k**), it slightly enhanced the activity (46.36% inhibition). Interestingly, nitro substitution at *meta* position (compound **32m**) significantly increased the activity (57.34% inhibition), while di-substituted compound **32n** showed weak activity (18.87% inhibition) against HIV-1 RT.

Table 6.7 Result of HIV-1 RT inhibition activity of series **32a-n**

Comp. Code	R_7	% HIV-1 RT Inhibition[a]
32a	H	40.78
32b	2-CH_3	47.34
32c	3-CH_3	29.45
32d	4-CH_3	31.58
32e	2-OCH_3	38.64
32f	3-OCH_3	26.68
32g	4-OCH_3	17.86
32h	4-F	46.86
32i	3-Cl	36.47
32j	4-Cl	32.65
32k	3-Br	46.36
32l	4-Br	39.46
32m	**4-NO_2**	**57.34**
32n	2,4-di-Me	18.87
Efavirenz		**98.87**

[a]Value is average of at least two independent experiment, standard deviation (SD) was found within ±10%.

6.1.2.8 *In-vitro* HIV-1 RT inhibition activity of series 38a-o

Several compounds of series (**38a-o**) showed good inhibitory activity against HIV-1 RT (>75 % inhibition) at initial tested 100 µM concentration, so IC_{50} was calculated for the whole series of compounds. Among the series **38a-o**, compounds **38a, 38b, 38j, 38k** and **38o** exhibited IC_{50} ≤25 µM (highlighted in bold font in Table **6.8**). Furthermore, compounds **38c**, **38g**, **38i** and **38n** displayed comparatively moderate activity (IC_{50}>25 to ≤50µM), while rest of compounds exhibited weak to least activity (IC_{50} >50µM). Compound with un-substituted phenyl ring (compound **38a**) displayed good inhibitory potential against RT (IC_{50} 24.26 µM). Further, substitution with methyl group at *ortho* position increased the potency against RT (IC_{50} 12.48µM), while at *para* position, potency was decreased (IC_{50} 28.46 µM). Further, substitution with more electron releasing group like methoxy (compound **38d, 38e** and **38f**) decreased the potency against RT at all positions. Moreover, *ortho* and *meta* substituted compounds, **38d** and **38e** did not show the significant difference in their potency, however, substitution at *para* position of phenyl ring (compound **38f**) markedly decreased the potency. Fluoro substituted compounds at *ortho* and *meta* position (compound **38g** and **38h**) exhibited moderate to weak inhibition of HIV-1 RT (IC_{50} 47.45 and 78.48µM respectively).

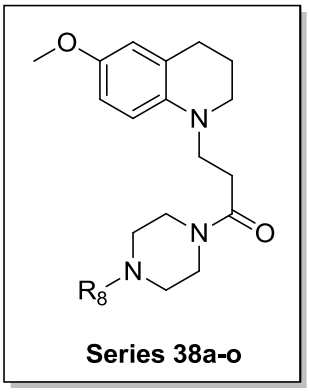

Series 38a-o

Chloro substitution at *meta* and *para* position found to be favourable for RT inhibition (compounds **38j** and **38k**) with IC_{50} <25 µM, while *para* nitro substitution markedly reduced the potency (IC_{50} 82.68µM). The compound in which phenyl ring was replaced with benzyl (compound **38m**) and 2-pyridine (compound **38n**) exhibited least and moderate inhibition of HIV-1 RT (>100 and 48.62 µM, respectively). Compounds having di-substitution with chloro at *ortho* and *meta* position of phenyl ring also displayed improved inhibition of HIV-1 RT (IC_{50} 14.46 µM). So, overall methyl group at *ortho* position, chloro at *meta* as well as *para* and at dual positions (*ortho* and *meta*) significantly favoured RT inhibitory activity.

Table 6.8 Result of HIV-1 RT inhibition activity of series **38a-o**

Comp. Code	R_8	HIV-1 RT inhibition (IC_{50} µM)[a]
38a	**Ph**	**24.26**
38b	**2-Me-Ph**	**12.48**
38c	4-Me-Ph	28.46
38d	2-MeO-Ph	52.84
38e	3-MeO-Ph	58.24
38f	4-MeO-Ph	>100
38g	2-F-Ph	47.45
38h	4-F-Ph	78.48
38i	2-Cl-Ph	32.86
38j	**3-Cl-Ph**	**18.58**
38k	**4-Cl-Ph**	**24.91**
38l	4-NO_2-Ph	82.68
38m	Benzyl	>100
38n	2-Pyridine	48.62
38o	**2,3-di-Cl-Ph**	**14.46**
Efavirenz		**0.057**

[a]Value is average of at least two independent experiment, standard deviation (SD) was found within ±10%.

6.1.2.9 *In-vitro* HIV-1 RT inhibition activity of series 43a-p

All synthesized derivatives **43a-p** were *in vitro* evaluated for HIV-1 RT inhibitory activity at 100 µM concentration. Several compounds like **43a, 43c, 43d, 43g, 43j, 43k, 43l, 43m** and **43o** displayed significant inhibitory activity (>50% inhibition) against HIV-1 RT at the tested concentration (Table **6.9**). Furthermore, compound **43e** and **43f** showed weak inhibition**,** while rest of the compounds displayed moderate inhibition of RT. In order to explore the effects of different substitutions of phenyl ring over their RT inhibitory activity, SAR studies were performed. The compound having no substitution at phenyl ring (compound **43a**) displayed significant inhibition of HIV-1 RT (52.24 % inhibition). Further, substitution with electron donating methyl group at *ortho* position (compound **43b**) resulted slightly decrease in RT inhibitory activity. Substitution with methoxy group at *meta* position (compound **43c**) enhanced the activity against RT, while at *para* position (compound **43d**) activity remained almost unaltered.

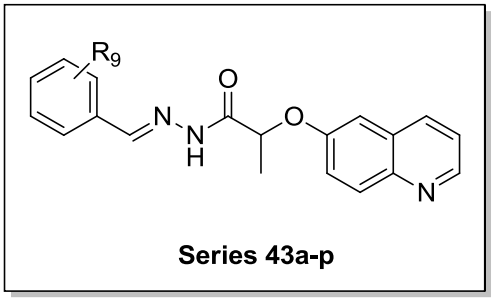

Series 43a-p

Fluoro, a strong electron withdrawing group at *ortho* position (compound **43e**) moderately decreased the potency, while at *para* position (compound **43f**) marked reduction in RT

inhibition potential was observed. Chloro substitution at *ortho* and para positions (compounds **43g** and **43h**, respectively) did not make significant impact on activity compared to compound **43a**. Further, bromo group at *meta* position (compound **43i**) displayed slightly reduced activity, while at *para* position (compound **43j**) little improvement in potency was observed against RT. Nitro group did not change the activity significantly at *ortho* and *meta* positions (compound **43k** and **43l**), while nitro at *para* position significantly enhanced the potency (compound **43m**). Moreover, compound **43m** displayed highest potency against HIV-1 RT (64.74 % inhibition) among the series. Substitution with another strong electron withdrawing group cyano at *para* position of phenyl ring (compound **43n**) unexpectedly decreased the RT inhibitory potency. The compound having dichloro substitutions at phenyl ring (compound **43o**) has not displayed any significant difference in potency, while trimethoxy substitution on phenyl resulted slightly decreased in potency against RT (compound **43p**). Overall, methoxy group at *meta* position and nitro group at *para* position significantly favored the RT inhibitory potency, while fluoro substitution at *ortho* as well as *para* position markedly reduced the RT inhibitory activity.

Table 6.9 Result of HIV-1 RT inhibition activity of series **43a-p**

Comp. Code	R_9	% HIV-1 RT Inhibition[a]
43a	**H**	**52.24**
43b	2-CH_3	48.74
43c	**3-OCH_3**	**61.87**
43d	**4-OCH_3**	**52.32**
43e	2-F	32.86
43f	4-F	18.26
43g	**2-Cl**	**51.34**
43h	4-Cl	48.16
43i	3-Br	41.68
43j	**4-Br**	**57.23**
43k	**2-NO_2**	**56.42**
43l	**3-NO_2**	**50.28**
43m	**4-NO_2**	**64.74**
43n	4-CN	40.52
43o	**3,4-di-Cl**	**55.41**
43p	3,4,5-tri-MeO	46.27
Efavirenz		**98.87**

[a]Value is average of at least two independent experiment, standard deviation (SD) was found within ±10 %.

6.1.2.10 *In-vitro* HIV-1 RT inhibition activity of series 51a-n

Several compounds of series (**51a-n**) displayed encouraging RT inhibitory potential (>75% RT inhibition) during the initial screening at 100 µM concentration, so IC_{50} was determined for the whole series (**51a-n**). The result of the study revealed that six compounds (**51a, 51b, 51d, 51k, 51l** and **51m**) exhibited good potency and inhibited HIV-1 RT with IC_{50} ≤25 µM.

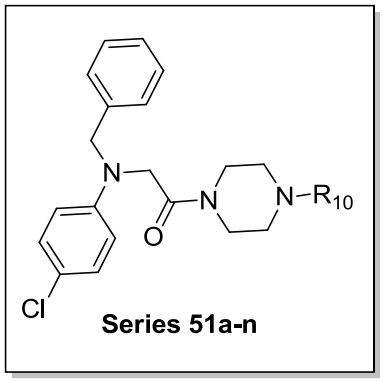

Series 51a-n

Further, compounds **51c, 51e, 51g** and **51j** displayed moderate potency (IC_{50} >25 to ≤50 µM), while rest of the compounds displayed weak to least RT inhibitory activity. Compound **51a** having un-substituted phenyl ring showed good potency against HIV-1 RT (IC_{50} 20.56 µM). Substitution of phenyl ring with methyl group at *ortho* and *para* position (**51b** and **51c**) slightly decreased their potency (IC_{50} 23.47 and 28.14 µM, respectively). Further, substitution with methoxy group slightly increased the potency at *ortho* position, while it decreased at *meta* and *para* position, so for methoxy substituted compounds (**51d**, **51e** and **51f**), potency against RT varied in the order *ortho* >*meta* > *para.*

Compounds having fluoro substitution at *ortho* position (compound **51g**) exhibited medium while at *para* position (compound **51h**) it showed weak potency. Furthermore, *meta* chloro substituted compound (compound **51i**) exhibited weak potency against RT, while chloro at *para* position (compound **51j**) improved the potency compared to compound **51i**. Interestingly, *para* nitro substitution at phenyl ring (compound **51k**) found to be favourable for HIV-1 RT inhibition (IC_{50} 14.18 µM) and replacement of phenyl ring with benzyl (compound **51l**) slightly reduced the potency (21.51µM). Further, upon di-substitution of phenyl ring with chloro (compound **51m**) resulted in enhancement of RT inhibitory activity, moreover compound **51m** exhibited highest potency (IC_{50} 12.26 µM) against RT among the tested series. Replacement of phenyl ring with benzhydryl, a more bulky entity (compound **51n**) markedly decreases the potency against RT. Overall, compounds having un-substituted phenyl ring (compound **51a**), electron donating group like methyl, methoxy at *ortho* position (compound **51b** and **51d**) and strong electron withdrawing nitro group at *para* position (compound **51k**) exhibited significant RT inhibitory potency. Moreover, replacement of phenyl with benzyl (compound **51l**) as well as chloro di-substitution at phenyl ring (compound **51m**) were also found to be favourable for RT inhibitory activity.

Table 6.10 Result of HIV-1 RT inhibition activity of series **51a-n**

Comp. code	R_{10}	HIV-1 RT inhibition (IC_{50} µM)[a]
51a	**Ph**	**20.56**
51b	**2-CH_3-Ph**	**23.47**
51c	4-CH_3-Ph	28.14
51d	**2-CH_3O-Ph**	**16.27**
51e	3-CH_3O-Ph	34.32
51f	4-CH_3O-Ph	77.53
51g	2-F-Ph	38.41
51h	4-F-Ph	56.24
51i	3-Cl-Ph	61.83
51j	4-Cl-Ph	31.48
51k	**4-NO_2-Ph**	**14.18**
51l	**Benzyl**	**21.51**
51m	**2,3-di-Cl-Ph**	**12.26**
51n	Benzhydryl	**>100**
Efavirenz		**0.057**

[a]Value is average of at least two independent experiment, standard deviation (SD) was found within ±10 %.

6.1.2.11 *In-vitro* HIV-1 RT inhibition activity of series 54a-k

Anti-HIV-1 RT activity of compounds **(54a-k)** is summarized in Table **6.11.** Several compounds of this series showed excellent inhibitory activity against HIV-1 RT (>75 % inhibition) at initial tested 100 µM concentration, so IC_{50} was calculated for the whole series of compounds. Among the series, top active compounds **54b, 54d, 54e** and **54k** displayed good to excellent inhibition of RT with IC_{50} <10 µM (highlighted by bond font in the table **6.11**). Furthermore, compounds **54a** and **54f** displayed moderate potency against RT (IC_{50}>25 to ≤50 µM), while rest of the compounds were found to be weak inhibitor of HIV-1 RT. SAR study of compounds revealed that un-substituted compound **54a** displayed moderate potency against HIV-1 RT (27.26µM) compared to the overall compounds in the series. Substitution of phenyl ring with electron donating methoxy group (compound **54b**) at *ortho* position markedly increases the potency, while methoxy group at *meta* position significantly decreased the activity. Moreover, compound **54b** displayed highest potency against HIV-1 RT among the all series of compounds (IC_{50}0.27 µM). Substitution with smaller size halogen, fluoro at *para* position of phenyl ring (compound **54d**) resulted increase in the RT inhibitory potency.

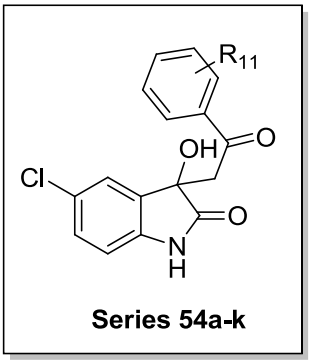

Series 54a-k

Further, moderate size halogen, chloro at *ortho* position (compound **54e**) significantly enhanced the potency while *meta* chloro substituted compound (compound **54f**) showed

markedly reduced potency. Substitution with *meta* bromo (compound **54g**) and *meta* nitro group (compound **54h**), reduced the RT inhibitory potency. Di-substitution of phenyl ring with methoxy and chloro group markedly decreases the RT inhibitory activity (compound **54i** and **54j**), interestingly compound **54k** substituted with bromo and cyano at *ortho* and *para* position of phenyl respectively, exhibited significant inhibition of RT activity (IC_{50} 9.16 µM). Overall, among the series of **54a-k** compounds, substitution with methoxy and chloro groups at *ortho* position, fluoro at *para* position and di-substitution with bromo and cyano (at *ortho* and *para* position) of phenyl ring favored RT inhibition activity.

Table 6.11 Result of HIV-1 RT inhibition activity of series **54a-k**

Comp. code	R_{11}	HIV-1 RT inhibition (IC_{50} µM)[a]
54a	H	27.26
54b	**2-CH_3O**	**0.27**
54c	3-CH_3O	51.31
54d	**4-F**	**5.92**
54e	**2-Cl**	**0.76**
54f	3-Cl	34.25
54g	3-Br	62.14
54h	3-NO_2	58.51
54i	3,4-di-MeO	73.08
54j	3,4-di-Cl	68.86
54k	**2-Br, 4-CN**	**9.16**
Efavirenz		**0.057**

[a]Value is average of at least two independent experiment, standard deviation (SD) was found within ±10%.

6.1.3 Key findings from HIV-1 RT inhibitory assay

Overall, all the compounds of series **5a-o, 9a-o, 14a-k, 17a-o, 23a-o, 28a-l, 32a-n, 38a-o, 43a-p, 51a-n** and **54a-k** were screened for HIV-RT inhibitory activity using ELISA based *in-vitro* assay. During the preliminary screening studies (at 100 µM concentration), none of the compounds of series **14a-k** and **23a-o** displayed significant activity (% inhibition of RT remained <50)**,** while only one compound of series **32a-n** found to be significantly active. From the series **5a-o, 9a-o, 17a-o,** and **43a-p,** five, five, thirteen and nine compounds, respectively displayed significant inhibition of RT. Although, several compounds of the above series were found to be significantly active, but none of the compounds exhibited much encouraging results compared to the reference drugs, moreover their RT inhibitory ability remained <75 % at the tested concentration (100 µM)**.**

Several compounds of series **28a-l, 38a-o, 51a-n** and **54a-k** displayed overall superior inhibition (>75% inhibition) of HIV-1 RT at 100 µM concentration. Therefore, IC_{50} was

calculated for all the compounds of above four series, which revealed that twenty compounds (**28b, 28h, 28i, 28j, 28l, 38a, 38b, 38j, 38k 38o, 51a, 51b, 51d, 51k, 51l**, **51m, 54b, 54d, 54e** and **54k**) collectively from the above four series displayed IC_{50} ≤25 µM. Further, segregation of above compounds based on their RT inhibitory potency demonstrated that two compounds (**28b** and **28j**) of series **28a-l** and four compounds (**54b, 54d, 54e, 54k**) of series **54a-k** displayed excellent potency against RT with IC_{50} ≤ 10 µM. Moreover, two compounds (**54b** and **54e**) of series **54a-k,** showed sub-micromolar potency (IC_{50} 0.27 and 0.76, respectively) against HIV-1 RT and can be considered potent searched hit against the selected target. Conclusively, series **54a-k,** which was designed based on the virtual screening studies, found to be most fruitful and afforded two potent hit against RT. Reference drug efavirenz displayed promising activity with average 98.87% inhibition of HIV-RT at 100 µM concentration and IC_{50} of efavirenz was determined which was found to be 0.057 µM.

6.2 Anti-HIV-1 activity and cytotoxicity studies of selected compounds

Overall several compounds from the series **28a-l, 38a-o, 51a-n** and **54a-k** displayed encouraging inhibition of HIV-1 RT. Some compounds from the above series having good/excellent inhibition potency of HIV-1 RT were selected for anti-HIV-1 activity (against HIV-1_{IIIB} strain). Selected compounds were also evaluated for cytotoxicity upon $CD4^+$ bearing T cells by MTT colorimetric assay. Marketed drug zidovudine was used as reference compound for anti-HIV-1 activity and cytotoxicity studies.

6.2.1 Experimental and Methodology

All samples were dissolved in DMSO. AZT was purchased from USP and dissolved in serum-free RPMI-1640 medium. HEPES (N-2 (2-Hydroxyothyl)-piperazine-*N*'-(2-ethanesufonic acid), MTT (3,(4,5-dimethylthiazol-2-yl)-2,5-diphenyl tetrazolium bromide), DMF (N,N'-Dimethylformamide), Penicillin, Streptomycin sulfate, Glutamine were purchased from Sigma; 2-ME (2-Mercaptoethanol) was purchased from Bio-Rad. RPMI-1640 and fetal bovine serum (FBS) were purchased from Gibco. C8166 cell and HIV-1_{IIIB} were kindly donated by Medical Research Council, AIDS Regent Project. The cells were maintained at 37℃ in 5% CO_2 in RPMI-1640 medium supplemented with 10% heat-inactivating FBS (Gibco). HIV-1_{IIIB} was prepared from the supernatants of H9/HIV-1_{IIIB} cells. The 50% HIV-1 tissue culture infectious dose ($TCID_{50}$) in C8166 cells was determined and calculated by Reed and Muench method. Virus stocks were stored in small aliquots at -80℃. The titer of virus stock was 1.0×10^8 $TCID_{50}$ per ml.

6.2.1.1 Procedure for anti-HIV assay (Inhibition of syncytia formation)

The inhibitory effect of samples on acute HIV-1_{IIIB} infection was measured by syncytia formation assay. In the presence or absence of various concentrations of samples, 4×10^4 C8166 cells were infected with HIV-1 at a multiplicity of infection (MOI) of 0.04 and cultured in 96-well plates at 37℃ in 5% CO_2 for 3 days. AZT was used as a positive control. At 3 days post-infection, the cytopathic effect (CPE) was measured by counting the number of syncytia (multinucleated giant cell) in each well of 96-well plates under an inverted microscope (100×). The inhibitory percentage of syncytia formation was calculated by the percentage of syncytia number in sample treated culture compared to that in infected control culture. Effective concentration (EC_{50}) was determined from dose-response curve; final value is the mean of three independent experiments and SD was found within ±10 from mean [2].

Formula:

$$\text{CPE inhibition (\%)} = (1\text{-}CPE_{test}/CPE_{ctrl})\times100$$

6.2.1.2 Procedure for evaluation of cytotoxicity

The cellular toxicity of compounds on C8166 was assessed by MTT colorimetric assay. Briefly, 100 µl of 4×10^5 cells were plated into 96-well plates, 100 µl of various concentration of compounds was added and incubated at 37℃ in a humidified atmosphere of 5% CO_2 for 72 h. MTT reagent was added and incubated for 4 h, 100 µl supernatant was discarded and 100 µl 50% DMF-15% SDS was added. After the formazan was dissolved completely, the plates were analyzed by a Bio-Tek ELx800 ELISA reader at 570 nm/630 nm. 50% cytotoxicity concentration (CC_{50}) was determined from dose-response curve, final value of CC_{50} is the mean of three independent experiments, and SD was found within ±10% from mean [3]. Therapeutic index (TI) of anti-HIV activity is CC_{50}/EC_{50}.

Formula:

$$\text{Cell viability (\% of control)} = (OD_{test}-OD_{blk})/(OD_{ctrl}-OD_{blk})\times100$$

6.2.2 Outcome of anti-HIV-1 activity and cytotoxicity studies

Three to four top active HIV-1 RT inhibitors (collectively fifteen compounds) from each of the series **28a-l, 38a-o, 51a-n** and **54a-k** were evaluated for anti-HIV-1 activity and cytotoxicity, the result of the both studies are summarized in Table **6.12.** In order to study the comparative potencies of selected compounds against HIV-1RT and HIV-1, RT inhibitory activity (in µM as well as µg/mL) of the selected compounds are also included in the Table **6.12**. The result of the study revealed that out of fifteen compounds, eight compounds (**28j, 38b, 51a, 51k, 51m, 54b, 54e** and **54k**) displayed good to excellent potency (EC_{50} <10 µg/mL) against HIV-1 cells, further except compound **51d** rest of the compounds (**28b**, **28l**, **38a**, **38j**, **38o** and **54d**) can be considered as moderately active against HIV-1 (EC_{50} ≥10 to<20 µg/mL). Compounds **51d** and **54d** displayed poor correlation between the RT inhibitory potency and anti-HIV-1 activity, while rest of compound showed moderate to excellent correlation between the both type of activity.

Overall, compounds **28j, 38b, 51a, 51k, 51m, 54b, 54e** and **54k** (highlighted by bold font in Table **6.12**) displayed good to excellent potency against HIV-1 RT as well as HIV-1 with IC_{50} and EC_{50} <10 µg/mL, in which except compounds **28j** and **54k** rest of compounds displayed superior safety index >20. Interestingly, most potent compounds (**54b** and **54e**) among all series displayed sub-micromolar potency against RT and both the compounds were also found to be active against HIV-1 with EC_{50} 0.030 µg/mL and EC_{50} 0.59 µg/mL, respectively, Furthermore, both the compounds **54b** and **54e** displayed admirable safety index (6200 and >338.9, respectively). Reference compounds zidovudine displayed promising potency (0.0034 µg/mL) against HIV-1 with remarkable safety index (460505.88). So, overall from RT

inhibitory, anti-HIV-1 and cytotoxicity studies, we got two potential hit (**54b** and **54e**) having potent RT inhibitory as well as anti-HIV-1 activity with good safety index.

Table 6.12 Result of anti-HIV-1 activity and cytotoxicity studies

Comp. code	HIV-1 RT activity (IC_{50} in µM)	HIV-1 RT activity (IC_{50} in µg/mL)	Anti-HIV-1 activity (EC_{50} in µg/mL)	Cytotoxicity (CC_{50} µg/mL)	Safety index (EC_{50}/CC_{50})
28b	8.12	3.41	11.10	108.73	9.8
28j	**5.42**	**2.45**	**2.76**	**18.95**	**6.9**
28l	12.34	5.90	12.62	74.86	5.93
38a	24.26	9.20	14.21	83.21	5.9
38b	**12.48**	**4.91**	**4.72**	**114.33**	**24.2**
38j	18.58	7.68	18.38	97.51	5.3
38o	14.46	6.47	17.40	104.10	6
51a	**20.56**	**8.62**	**4.24**	**>400**	**>94.4**
51d	16.27	7.31	46.03	102.56	2.2
51k	**14.18**	**6.58**	**9.85**	**>200**	**>20.3**
51m	**12.26**	**5.97**	**5.61**	**>200**	**>35**
54b	**0.27**	**0.089**	**0.030**	**186.00**	**6200**
54d	5.92	1.88	19.00	39.68	2.08
54e	**0.76**	**0.25**	**0.59**	**>200**	**>338.9**
54k	**9.16**	**3.70**	**0.92**	**8.75**	**9.51**
Zidovudine			0.0034	1565.72	460505.88

6.3 *In-vitro* anti-bacterial activity of the synthesized compounds

All the synthesized compounds were evaluated for *in-vitro* anti-bacterial activity against two Gram (-)ve bacterial strains; *E. coli* (MTCC 1652) *and P. putida* (MTCC 102) and two Gram (+)ve bacterial strains; *S. aureus* (ATCC 25923) and *B. cereus* (MTCC 2445). Anti-bacterial activity of the test compounds was expressed in terms of Zone of Inhibition (ZOI) and Minimum Inhibitory Concentration (MIC). Chloramphenicol was taken as a reference drug for the study and 5% DMSO was used as a negative control.

6.3.1 Experimental and Methodology

Procedure followed is described briefly**,** autoclaved Muller-Hilton (Himedia, India) agar medium was poured into autoclaved Petri plates and the agar plates were swabbed with 100µl inocula of each test organism (10^6 CFU/ml) under aseptic condition. After adsorption of inocula, wells size of 6 mm diameter were made by the sterile metallic borer and the solution (20 µL) of test compounds in 5% DMSO was poured into the wells. The plates were incubated at 37℃ for 24 h and ZOI was calculated as mean of duplicate values. [4]. MIC was determined for the tested compounds using broth double dilution method. In order to ensure the robustness of method, MIC tests were also performed in duplicates and finally minimum concentration which inhibited the visible growth of test organism with reproducible results in duplicates was taken as MIC. In procedure, a set of tubes containing Muller Hilton broth medium with different concentrations of test compound were prepared. The tubes were inoculated with 100 µl bacterial cultures (10^6 CFU/ml) and incubated on a rotary shaker (180 rpm) at 37℃ for 24 h under dark conditions and the lowest concentration of compound which prevented the visible growth of bacteria after the incubation period was determined [5].

6.3.2 Outcome of *in-vitro* anti-bacterial activity

The result of anti-bacterial screening of all screened compounds is expressed in terms of ZOI and MIC (Table **6.13-6.23**). Based upon the values of ZOI in mm, compounds are classified into; significantly active (ZOI ≥15 mm, highlighted by bold font in Tables), moderately active (ZOI 13 to 14 mm), weakly active (ZOI 10 to 12 mm) and least active (ZOI less than 10 mm). MIC was not calculated for compounds which showed ZOI less than 10 mm.

6.3.2.1 *In-vitro* anti-bacterial activity of series 5a-o

Among the series of compounds **5a-o,** nine compounds possessed moderate to significant anti-bacterial activity against *E. coli,* while six compounds showed weak to least activity (Table **6.13**). Among the former nine compounds, seven compounds **(5d, 5f, 5h, 5j, 5k, 5n** and **5o)** showed significant while two compounds (**5c** and **5i**) showed moderate activity.

Against, *S. aureus*, ten compounds displayed noticeable anti-bacterial activity, in which four compounds (**5f, 5j, 5k** and **5o**) showed significant, three compounds (**5a, 5d** and **38e**) showed moderate and rest showed weak or least activity. Furthermore, eight compound (**5b, 5d, 5f, 5g, 5i, 5j, 5k** and **5n**) showed significant, three (**5a, 5h** and **5m**) showed moderate, while rest of the compounds exhibited weak to least inhibitory potential against *P. putida*.

Against the second G (+)ve strain (*B. cereus)* four compounds (**5f, 5i, 5j** and **5k)** showed significant, four compounds (**5b, 5e, 5g** and **5o)** showed moderate while rest of the compounds showed weak to least anti-bacterial activity. Overall, compounds of series **5a-o** exhibited relatively better potency against both G (-)ve bacterial strains (*E. coli* and *P. putida*) compared to G (+)ve strains (*S. aureus* and *B. cereus*). Reference drug chloramphenicol exhibited potent activity against all tested bacterial strains with ZOI 21-23 mm and MIC 16 µg/mL. Further, it's worthy to note that three compounds (**5f, 5j** and **5k**) exhibited significant growth inhibition of all four tested bacterial strains.

Table 6.13 Result of *in-vitro* anti-bacterial activity of compounds **5a-o**

Comp. Code	*E. coli*		*S. aureus*		*P. putida*		*B. cereus*	
	ZOI (mm)	**MIC (µg/mL)**	**ZOI (mm)**	**MIC (µg/mL)**	**ZOI (mm)**	**MIC (µg/mL)**	**ZOI (mm)**	**MIC (µg/mL)**
5a	-	-	14	128	13	>64	-	-
5b	10	>128	10	>128	**15**	**128**	14	>128
5c	14	>128	-	-	11	>64	-	-
5d	**15**	**128**	13	>128	**17**	**>32**	11	>128
5e	12	>64	14	>64	-	-	13	> 64
5f	**16**	**>64**	**15**	**>64**	**16**	**>64**	**15**	**64**
5g	-	-	-	-	**17**	**64**	13	>128
5h	**15**	**>128**	12	128	13	>128	-	-
5i	14	>64	-	-	**15**	**>64**	**15**	**>64**
5j	**16**	**>32**	**16**	**>32**	**16**	**64**	**16**	**>64**
5k	**16**	**>64**	**15**	**64**	**15**	**64**	**17**	**>32**
5l	-	-	12	>128	10	>128	-	-
5m	11	>128	-	-	14	>128	-	-
5n	**15**	**128**	-	-	**16**	**64**	10	>128
5o	**16**	**64**	**15**	**64**	-	-	14	>128
Chlor.	**22**	**16**	**22**	**16**	**23**	**16**	**21**	**16**

6.3.2.2 *In-vitro* anti-bacterial activity of series 9a-o

Results of anti-bacterial activity of the synthesized compounds **9a-o** (Table **6.14**) revealed that ten compounds exhibited noticeable inhibitory potential against *E. coli*. Among these, four compounds (**9f, 9i, 9j** and **9n**) showed significant, five compounds (**9d, 9e, 9h, 9k** and **9o**) exhibited moderate while one compound (**9b**) possessed weak anti-bacterial activity.

Further, except two compounds (**9k** and **9l**) rest of compounds inhibited the growth of *S. aureus*, in which three compounds (**9c, 9g** and **9m**) showed moderate, while ten compounds (**9a, 9b, 9d, 9e, 9f, 9h, 9i, 9j, 9n** and **9o**) showed significant growth inhibition. Against the G (-)ve strain *P. putida*, five compounds (**9d, 9e, 9f, 9j** and **5o**) showed significant and also five compounds showed moderate (**9a, 9c, 9i, 9k** and **9n**), while rest of the compounds possessed least growth inhibitory potential.

Furthermore, compound **9f** showed significant, five compounds (**9d, 9e, 9i, 9j** and **9k**) exhibited moderate while rest of the compounds showed weak to least inhibitory potential against *B. cereus.* Overall, compound **9f** significantly inhibited the growth of all the tested G (+)ve and G (-)ve bacterial strains. Among the individual strains, *S. aureus* was found to be most sensitive while *B. cereus* exhibited least sensitivity to the tested compounds.

Table 6.14 Result of *in-vitro* anti-bacterial activity of compounds **9a-o**

Comp. code	*E. coli*		*S. aureus*		*P. putida*		*B. cereus*	
	ZOI (mm)	**MIC (µg/mL)**	**ZOI (mm)**	**MIC (µg/mL)**	**ZOI (mm)**	**MIC (µg/mL)**	**ZOI (mm)**	**MIC (µg/mL)**
9a	-	-	**16**	**128**	14	>128	-	-
9b	11	>128	**15**	**>128**	-	-	-	-
9c	-	-	14	>64	13	>128	12	>128
9d	14	>128	**16**	**>64**	**15**	**>128**	13	>128
9e	13	>64	**17**	**64**	**16**	**>32**	14	128
9f	**15**	**>64**	**18**	**32**	**15**	**>64**	**15**	**>64**
9g	-	-	14	>64	-	-	-	-
9h	14	>128	**15**	**>128**	-	-	-	-
9i	**15**	**>64**	**15**	**>64**	14	>128	13	>128
9j	**16**	**64**	**16**	**64**	**15**	**>128**	14	128
9k	14	>128	-	-	14	64	14	>128
9l	-	-	-	-	-	-	-	-
9m	-	-	13	>128	-	-	11	>128
9n	**15**	**128**	**16**	**64**	14	>64	10	>128
9o	14	>128	**16**	**>64**	**16**	**64**	-	-
Chlor.	**22**	**16**	**22**	**16**	**23**	**16**	**21**	**16**

6.3.2.3 *In-vitro* anti-bacterial activity of series 14a-k

Among the eleven compounds of series **14a-k**, only two compounds **14c** and **14k** inhibited the growth of *E. coli*, but in this series none of the compound showed inhibitory activity against *S. aureus* (Table **6.15**). Most of the compounds in this series showed, significant to weak inhibitory activity against *P. putida* (except compound **14d** and **14j**), in which three compounds (**14f, 14h** and **14k**) showed significant, while four (**14a, 14c, 14e** and **14g**) exhibited moderate anti-bacterial activity. Only three compounds in this series (**14b, 14f** and

14k) showed inhibitory potency against *B. cereus*, in which compound **14k** showed moderate while compounds **14b** and **14f** showed weak inhibition. Overall, compound **14k** exhibited significant inhibitory activity against both G (-)ve bacterial strains (*E. coli* and *P. putida*).

Table 6.15 Result of *in-vitro* anti-bacterial activity of compounds **14a-k**

Comp. Code	*E. coli*		*S. aureus*		*P. putida*		*B. cereus*	
	ZOI (mm)	**MIC (µg/mL)**	**ZOI (mm)**	**MIC (µg/mL)**	**ZOI (mm)**	**MIC (µg/mL)**	**ZOI (mm)**	**MIC (µg/mL)**
14a	-	-	-	-	13	>128	-	-
14b	-	-	-	-	11	>128	11	>128
14c	12	>128	-	-	14	64	-	-
14d	-		-	-	-	-	-	-
14e	-		-	-	13	>128	-	-
14f	-		-	-	**15**	**64**	12	>128
14g	-		-	-	14	>128	-	-
14h	-		-	-	**15**	**128**	-	-
14i	-		-	-	12	>64	-	-
14j	-	-	-	-	-	-	-	-
14k	**15**	**>64**	-	-	**16**	**>64**	14	>128
Chlor.	**22**	**16**	**22**	**16**	**23**	**16**	**21**	**16**

6.3.2.4 *In-vitro* anti-bacterial activity of series 17a-o

Among the fifteen compounds of series **17a-o**, thirteen compounds (except compound **17l** and **17m**) showed moderate to significant inhibitory activity against *E. coli* (Table **6.16**). Among these thirteen compounds, five compounds **(17a, 17c, 17i, 17k** and **17n)** showed moderate while remaining compounds showed significant growth inhibition of *E. coli.* In this series, except three compounds (**17g, 17h** and **17l**) remaining twelve compounds showed moderate to significant inhibition of *S. aureus.* Further, except compounds **17e** and **17o** which did not show noticeable activity, rest of thirteen compounds exhibited moderate to significant growth inhibition of *P. putida*. Majority of compounds of this series (except compound **17n**) showed inhibitory potential against *B. cereus*, in which six compounds (**17a, 17d, 17f, 17i, 17j** and **17k**) showed significant, four compounds (**17b, 17g, 17h** and **17l**) showed moderate, while others showed weak to least activity. Overall, compounds of **17a-o** series exhibited encouraging anti-bacterial activity against the all bacterial strains, moreover three compounds (**17d, 17f** and **17j**) possessed significant anti-bacterial potency against all four tested strains.

Table 6.16 Result of *in-vitro* anti-bacterial activity of compounds **17a-o**

Comp. code	*E. coli*		*S. aureus*		*P. putida*		*B. cereus*	
	ZOI (mm)	**MIC (µg/mL)**	**ZOI (mm)**	**MIC (µg/mL)**	**ZOI (mm)**	**MIC (µg/mL)**	**ZOI (mm)**	**MIC (µg/mL)**
17a	14	64	**16**	**128**	14	64	**15**	**64**
17b	**15**	**>128**	14	>64	14	>128	13	>64
17c	14	64	**15**	**64**	14	>64	11	>128
17d	**16**	**>64**	**17**	**64**	**18**	**128**	**16**	**64**
17e	**15**	**128**	**16**	**>64**	-	-	12	>128
17f	**17**	**>32**	**17**	**64**	**18**	**>32**	**16**	**64**
17g	**17**	**>64**	-	-	**18**	**64**	13	>128
17h	**18**	**64**	-	-	**15**	**128**	14	>128
17i	14	>64	**16**	**64**	14	>64	**17**	**32**
17j	**15**	**>64**	**17**	**64**	**16**	**128**	**15**	**>64**
17k	14	128	14	64	**15**	**>64**	**15**	**>64**
17l	-	-	-	-	14	>128	13	128
17m	-	-	**16**	**64**	14	>128	11	>128
17n	13	>64	**15**	**>128**	**15**	**64**	-	-
17o	**17**	**128**	**16**	**64**	-	-	12	>128
Chlor.	**22**	**16**	**22**	**16**	**23**	**16**	**21**	**16**

6.3.2.5 *In-vitro* anti-bacterial activity of series 23a-o

Majority of compounds of series **23a-o** showed moderate to least anti-bacterial activity against the four tested bacterial strains (Table **6.17**). Among series **23a-o**, compound **23j** showed significant, compound **23i** and **23o** exhibited moderate, while other showed weak to least growth inhibition of *E. coli.* Further, nine compounds of this series showed noticeable inhibitory potential against G (+)ve bacteria *S. aureus,* in which **23m** showed significant, four compounds (**23e, 23k, 23n** and **23o**) exhibited moderate while others showed least to weak inhibition. Furthermore, against *P. putida* compounds **23d, 23i** and **23j** showed moderate while rest four (**23c, 23h, 23m** and **23o**) exhibited weak activity. Compounds of this series showed least activity against *B. cereus* among the four tested bacterial strains, only three compounds (**23b**, **23j** and **23o**) of this series showed weak inhibition against this strain.

Table 6.17 Result of *in-vitro* anti-bacterial activity of compounds **23a-o**

Comp. code	*E. coli*		*S. aureus*		*P. putida*		*B. cereus*	
	ZOI (mm)	**MIC (µg/mL)**	**ZOI (mm)**	**MIC (µg/mL)**	**ZOI (mm)**	**MIC (µg/mL)**	**ZOI (mm)**	**MIC (µg/mL)**
23a	-	-	-	-	-	-	-	-
23b	-	-	-	-	-	-	10	>128
23c	11	>128	-	-	12	>128	-	-
23d	-	-	12	>128	13	>128	-	-
23e	12	>128	14	>128	-	-	-	-
23f	-	-	11	>128	-	-	-	-
23g	-	-	-	-	-	-	-	-
23h	12	>128	-	-	11	>128	-	-
23i	14	>128	-	-	13	>128	-	-
23j	**15**	**64**	12	>128	14	>128	12	>128
23k	-	-	13	>128	-	-	-	-
23l	-	-	12	>128	-	-	-	-
23m	-	-	**15**	**64**	10	>128	-	-
23n	-	-	13	>128	-	-	-	-
23o	13	>128	14	>128	12	>128	12	>128
Chlor.	**22**	**16**	**22**	**16**	**23**	**16**	**21**	**16**

6.3.2.6 *In-vitro* anti-bacterial activity of series 28a-l

Among the twelve compounds of series **28a-l**, except two compounds (**28c** and **28e**), rest of ten compounds inhibited the growth of *E. coli*, in which five compounds (**28d, 28h, 28j, 28k** and **28l**) showed significant inhibition while rest of the compounds showed moderate inhibition (Table **6.18**). Further, four compounds **(28h, 28j, 28k** and **28l**) exhibited significant, two moderate (**28d** and **28i**) while others showed weak or least inhibition of *S. aureus.* Interestingly, except one compound **28e**, rest of the compounds exhibited the growth inhibition of *P. putida,* in which four compounds **(28i, 28j, 28k** and **28l**) displayed significant inhibition. Furthermore, against G (+)ve bacteria *B. cereus* also, four compounds (**28d, 28j, 28k** and **28l**) showed significant inhibitory activity while others showed moderate to least activity. Three compounds of this series (**28j, 28k** and **28l**) significantly inhibited the growth of all four tested strains of bacteria.

Table 6.18 Result of *in-vitro* anti-bacterial activity of compounds **28a-l**

Comp. code	*E. coli*		*S. aureus*		*P. putida*		*B. cereus*	
	ZOI (mm)	**MIC (µg/mL)**	**ZOI (mm)**	**MIC (µg/mL)**	**ZOI (mm)**	**MIC (µg/mL)**	**ZOI (mm)**	**MIC (µg/mL)**
28a	13	>128	12	>128	14	>64	-	-
28b	14	>128	-	-	12	>128	12	>128
28c	-	-	-	-	14	>128	-	-

28d	**15**	**>128**	14	>128	14	>128	**16**	**>64**
28e	-	-	12	>128	-	-	13	>128
28f	14	>128	-	-	12	>128	12	>64
28g	14	>128	-	-	12	>128	-	-
28h	**16**	**>32**	**15**	**>64**	13	>128	13	>128
28i	14	>128	13	>128	**16**	**>64**	14	**>**64
28j	**16**	**>64**	**16**	**>64**	**15**	**>64**	**15**	**>64**
28k	**18**	**>32**	**16**	**>64**	**17**	**>32**	**16**	**>64**
28l	**17**	**>64**	**15**	**>64**	**16**	**>64**	**17**	**>64**
Chlor.	**22**	**16**	**22**	**16**	**23**	**16**	**21**	**16**

6.3.2.7 *In-vitro* anti-bacterial activity of series 32a-n

Compounds of series **32a-n** overall showed poor anti-microbial activity against all the tested bacterial strains (Table **6.19**). For example, only two compounds **32j** and **32m** showed moderate and weak inhibitory potential respectively against *E. coli.* Similarly, compounds **32f** and **32m** showed weak and moderate growth inhibition of *S. aureus* and *P. pudida* respectively. Furthermore, against *B. cereus* compound **32e** showed weak growth inhibition, while rest of compounds did not show noticeable activity.

Table 6.19 Result of *in-vitro* anti-bacterial activity of compounds **32a-n**

Comp. code	***E. coli***		***S. aureus***		***P. putida***		***B. cereus***	
	ZOI (mm)	**MIC (µg/mL)**	**ZOI (mm)**	**MIC (µg/mL)**	**ZOI (mm)**	**MIC (µg/mL)**	**ZOI (mm)**	**MIC (µg/mL)**
32a	-	-	-	-	-	-	-	-
32b								
32c	-	-	-	-	-	-	-	-
32d	-	-	-	-	-	-	-	-
32e	-	-	-	-	-		11	>128
32f	-	-	11	>128	-	-	-	-
32g	-	-	-	-	-	-	-	-
32h	-	-	-	-	-	-	-	-
32i	-	-	-	-	-	-	-	-
32j	13	128	-	-	-	-	-	-
32k	-	-	-	-	-	-	-	-
32l	-	-	-	-	-	-	-	-
32m	12	>128	-	-	13	>64	-	-
32n	-	-	-	-	-	-	-	-
Chlor.	**22**	**16**	**22**	**16**	**23**	**16**	**21**	**16**

6.3.2.8 *In-vitro* anti-bacterial activity of series 38a-o

Among the series **38a-o,** twelve compounds showed moderate to significant inhibitory activity against *E. coli,* among these, eight compounds **(38a, 38c, 38e, 38g, 38i, 38j, 38k** and **38o)** showed moderate while four (**38d, 38f, 38l** and **38n**) showed significant inhibitory potential (Table **6.20**). Also, eight compounds exhibited inhibitory potential against the growth of *S. aureus*, in which two compounds (**38k** and **38n**) showed significant, five compounds (**38a, 38b, 38e, 38f** and **38i**) exhibited moderate and one compound (**38g**) showed weak inhibition. Further, one compound **38n** showed significant, seven compounds (**38b, 38e, 38d, 38f, 38h, 38i** and **38l**) showed moderate, while rest of the compounds exhibited weak to least inhibition against *P. putida*. Against *B. cereus*, five compounds (**38a, 38d, 38f, 38l** and **38n**) showed significant, six compounds (**38b, 38c, 38e, 38i, 38j** and **38m**) showed moderate while rest of the compounds showed weak to least activity. Interestingly, three compounds (**38d, 38f** and **38l**) exhibited significant growth inhibition of G (-)ve bacteria *E. coli* as well as G (+)ve *B. cereus*, while compound **38n** significantly inhibited the growth of all tested bacterial strains.

Table 6.20 Result of *in-vitro* anti-bacterial activity of compounds **38a-o**

Comp. code	*E. coli*		*S. aureus*		*P. putida*		*B. cereus*	
	ZOI (mm)	MIC (µg/mL)	ZOI (mm)	MIC (µg/mL)	ZOI (mm)	MIC (µg/mL)	ZOI (mm)	MIC (µg/mL)
38a	14	>128	13	>128	12	>128	**15**	**>64**
38b	-	-	14	>64	14	>128	14	>64
38c	13	>64	-	-	12	>128	13	>128
38d	**15**	**>64**	-	-	13	>128	**15**	**64**
38e	14	>128	14	>128	14	>64	13	>128
38f	**17**	**>32**	14	>128	14	>64	**16**	**64**
38g	13	>128	12	>128	-	-	-	-
38h	-	-	-	-	13	>128	12	>128
38i	14	>128	13	>128	13	>128	13	>128
38j	14	>128	-	-	-	-	14	>64
38k	13	>128	**15**	**>64**	11	>128	-	-
38l	**15**	**>64**	-	-	14	>128	**15**	**>64**
38m	-	-	-	-	12	>128	13	>128
38n	**18**	**32**	**15**	**>128**	**16**	**64**	**15**	**>128**
38o	13	>128	-	-	12	>128	11	>128
Chlor.	**22**	**16**	**22**	**16**	**23**	**16**	**21**	**16**

6.3.2.9 *In-vitro* anti-bacterial activity of series 43a-p

Among the series of compounds **43a-p,** compounds **43j** and **43p** displayed significant anti-bacterial potency, compounds **43e, 43g, 43i, 43l** and **43o** possessed moderate, while rest of

the compounds exhibited weak to least activity against *E coli*. Further, against G (+)ve *S. aureus,* compounds **43g, 43k** and **43p** exhibited significant, also three compounds **43e, 43l** and **43o** showed moderate, while others showed weak to least growth inhibitory activity. Furthermore, compounds displayed slightly improved activity against second G (-)ve strain (*P. putida*), in which four compounds (**43d, 43e, 43g** and **43o**) possessed significant, also four compounds (**43a, 43b, 43k** and **43p**) exhibited moderate activity. Fourth tested strain (*B. cereus*) found to be least sensitive towards the compounds of series **43a-p** and none of the compounds showed significant activity against this strain, although three compounds **43d, 43g** and **43k** showed moderate activity, but rest possessed weak to least anti-bacterial activity.

Table 6.21 Result of *in-vitro* anti-bacterial activity of compounds **43a-p**

Comp. code	*E. coli*		*S. aureus*		*P. putida*		*B. cereus*	
	ZOI (mm)	**MIC (µg/mL)**	**ZOI (mm)**	**MIC (µg/mL)**	**ZOI (mm)**	**MIC (µg/mL)**	**ZOI (mm)**	**MIC (µg/mL)**
43a	-	-	11	>128	14	>128	-	-
43b	11	>128	-	-	13	>128		
43c	-	-	-	-	-	-	10	>128
43d	-	-	11	>128	**15**	**>64**	13	>128
43e	13	>64	14	>64	**16**	**64**	12	>128
43f	10	>128	-	-	12	>64	-	-
43g	14	>64	**15**	**>64**	**16**	**>32**	14	>64
43h	-	-	-	-	12	>128	-	-
43i	13	>128	-	-	-	-	-	-
43j	**15**	**>64**	12	>128	12	>64	10	>128
43k	-	-	**15**	**>128**	14	>64	13	128
43l	13	>128	14	64	-	-	11	>128
43m	-	-	-	-	-	-	-	-
43n	-	-	-	-	12	>128	-	-
43o	13	>128	14	>64	**15**	**64**	-	-
43p	**15**	**>32**	**15**	**64**	14	>64	11	>128
Chlor.	**22**	**16**	**22**	**16**	**23**	**16**	**21**	**16**

6.3.2.10 *In-vitro* anti-bacterial activity of series 51a-n

Overall, compounds of series **51a-n** exhibited all spectrum of activity (significant to least) against three strains, except *S. aureus* against which none of the compounds exhibited the significant activity. Further exploration of results revealed that compounds **51g, 51k** and **51n** possessed significant, compounds **51c** and **51m** showed moderate, while other displayed either weak or least anti-bacterial activity against *E. coli.* As earlier discussed, none of the compound displayed significant activity against *S. aureus* although, compounds like **51a, 51h** and **51k** showed moderate anti-bacterial activity. Compounds **51b** and **51n** displayed

significant, also couple of compounds (**51c** and **51m**) exhibited moderate anti-bacterial activity against *P. putida*, while rest of the compounds possessed weak or least activity. Furthermore, two compounds (**51g** and **51m**) showed excellent, four compounds (**51h, 51k, 51k** and **51n**) possessed moderate, while rest of the compounds possessed weak to least anti-bacterial activity against *B. cereus.* Compound **51n** significantly inhibited the growth of both tested G (-)ve bacterial strains (*E. coli* and *P. putida*).

Table 6.22 Result of i*n-vitro* anti-bacterial activity of compounds **51a-n**

Comp. code	*E. coli*		*S. aureus*		*P. putida*		*B. cereus*	
	ZOI (mm)	**MIC (µg/mL)**	**ZOI (mm)**	**MIC (µg/mL)**	**ZOI (mm)**	**MIC (µg/mL)**	**ZOI (mm)**	**MIC (µg/mL)**
51a	12	>128	13	>64	12	>64	-	-
51b	10	>128	-	-	**15**	**>32**	12	>64
51c	13	>64	12	>128	13	>128	11	>128
51d	11	>128	-	-	11	>64	-	-
51e	-	-	-	-	-	-	-	-
51f	-	-	-	-	10	>128	12	>128
51g	**15**	**64**	12	>64	12	64	**16**	**64**
51h	-	-	14	64	-	-	14	>128
51i	12	>128	11	>128	12	>64	-	-
51j	11	>128	-	-	11	>128	13	>64
51k	**16**	**>32**	13	>64	12	>64	14	>128
51l	12	>64	-	-	12	>128	-	-
51m	14	>64	10	>128	14	>64	**16**	**>32**
51n	**15**	**>64**	11	>128	**16**	**64**	13	>64
Chlor.	**22**	**16**	**22**	**16**	**23**	**16**	**21**	**16**

6.3.2.11 *In-vitro* anti-bacterial activity of series 54a-k

Compounds of series **54a-k** displayed all spectrum of activity varied from least to significant against the four tested bacterial strains. Further, analysis on individual strain revealed that five compounds (**54d, 54f, 54h, 54j** and **54k**) displayed significant (ZOI ≥ 15mm) and three compounds (**54c, 54e** and **54h)** moderately inhibited the growth of *E. coli.* Compounds **54a-k,** possessed comparatively reduced anti-bacterial activity against *S. aureus* compared to *E. coli,* for example pair of compounds (**54f** and **54j**) showed significant, compounds **54e, 54g** and **54k** displayed moderate while rest of the compounds possessed weak to least activity. Against *P. putida*, except two compounds (**54b** and **54g**), rest all other compounds showed noticeable anti-bacterial activity in which compounds **54d, 54j** and **54k** displayed significant, compounds **54c, 54e** and **54h** showed moderate while rest of compounds showed weak or least activity. Furthermore, six compounds showed noticeable activity against the growth of *B. cereus,* in which three compounds possessed significant (**54e, 54j** and **54k**), two

moderate (**54f** and **54i**) and one compound showed weak activity (**54c**). Overall, compounds **54j** showed significant growth inhibition of all tested bacterial strains and compound **54k** displayed moderate activity against *S. aureus* and significant activity against rest of three bacterial strains.

Table 6.23 Result of *in-vitro* anti-bacterial activity of compounds **54a-k**

Comp. code	*E. coli*		*S. aureus*		*P. putida*		*B. cereus*	
	ZOI (mm)	**MIC (µg/mL)**	**ZOI (mm)**	**MIC (µg/mL)**	**ZOI (mm)**	**MIC (µg/mL)**	**ZOI (mm)**	**MIC (µg/mL)**
54a	10	>128	-	-	11	>128	-	-
54b	-	-	-	-	-	-	-	-
54c	13	>128	-	-	14	>128	12	>128
54d	**16**	**>32**	12	>128	**15**	**>64**	-	-
54e	14	>128	13	>128	14	>64	**15**	**>64**
54f	**16**	**>64**	**16**	**>64**	11	>64	13	>64
54g	13	>128	13	>128	-	-	-	-
54h	**17**	**32**	11	>128	14	>128	-	-
54i	-	-	-	-	12	>128	13	>128
54j	**15**	**>64**	**17**	**>32**	**15**	**>64**	**16**	**64**
54k	**17**	**32**	14	>64	**18**	**32**	**16**	**>32**
Chlor.	**22**	**16**	**22**	**16**	**23**	**16**	**21**	**16**

6.3.2.3 Key finding from anti-bacterial activity

In-vitro screening of tested compounds against the four bacterial strains revealed that sensitivity of strains varied significantly towards tested compounds. Moreover, compounds from the same series also exhibited much diversity in anti-bacterial potential depending upon their substitution pattern. Analysis against the individual strain demonstrated that out of one fifty three total tested compounds, forty, thirty five, thirty seven and twenty five compounds possessed significant anti-bacterial activity (ZOI ≥15) against *E. coli, S. aureus, P. putida,* and *B. cereus,* respectively. Out of all four tested bacterial strains, G (-)ve strain *E. coli* was found to be most sensitive to the tested compounds while G (+)ve strain *B. cereus* exhibited least susceptibility. Compounds of series **17a-o,** followed by **5a-o** showed overall better activity against the tested four bacterial strains, while majority of compounds of series **32a-n** and **23a-o** possessed weak to least activity against the tested strains.

Furthermore, compounds of series **14a-k** showed weak to significant activity against *P. putida*, while against the other three strains with few exceptions, all compounds possessed weak to least activity. Among the all tested compounds, twelve compounds (**5f, 5j, 5k**, **9f, 17d, 17f, 17j**, **28j, 28k, 28l, 38n** and **54j**) showed significant anti-bacterial activity with ZOI ≥ 15 mm against all four tested bacterial strains. Nine compounds (**5f, 5j, 5k**, **17d, 17f, 17j,**

28j, 28k and **28l**) out of above mentioned twelve compounds belonged to three series **5a-o, 17a-o** and **28a-l**. Structurally, scaffolds **5a-o** and **17a-o** are based on 6,7-dimethoxy tetrahydroisoquinoline connected via glycinamide linker to substituted phenyl ring, while series **28a-l** is basically tetrahydroquinoline based scaffold containing carbamate linker. Overall, all three scaffolds can be considered of interest regarding their anti-bacterial potency.

Apart from the above mentioned twelve compounds, nine compounds (**5d, 5n, 9j, 14k, 17g, 17h, 51n, 54d** and **54k**) possessed significant growth inhibition of both G (-)ve bacterial strains (*E. coli* and *P. putida*), while compounds **17a** and **17i** exhibited significant anti-bacterial activity against both G (+)ve strains (*S. aureus* and *B. cereus*). Reference compound chloramphenicol displayed potent activity against the all tested bacterial strains with ZOI ranges from 21-23 mm and MIC 16 µg/mL.

6.4 *In-vitro* anti-fungal activity of the synthesized compounds

All the synthesized compounds were screened *in-vitro* for anti-fungal activity against two fungal strains *Candida albicans* (MTCC 3958) and *Aspergillus niger* (MTCC 9933). Anti-fungal activity of the tested compounds is expressed in terms of ZOI (Zone of inhibition) and MIC (Minimum inhibitory concentration). Fluconazole was used as reference drug and 5% DMSO was used as negative control during the study.

6.4.1 Experimental and Methodology

The procedure followed is described briefly; autoclaved suitable growth medium; Malt Yeast Agar (HiMedia, India) for *Candida albicans* and Czapek Yeast Extract Agar-CYA (HiMedia, India) for *Aspergillus niger* was poured into autoclaved Petri plates. Further, the agar plates were swabbed with 100 µl inocula of each test organisms under aseptic condition. After adsorption, wells of 6 mm diameter were made by the sterile metallic borer and the solution (in 5% DMSO) of test the compound was poured into the wells. The plates were incubated at 28℃ for 48 h and ZOI was calculated. Further, MIC (Minimum concentration which inhibited the visible growth of fungal strain) value was determined using broth double dilution method for each compound, taking 100 µl inocula of each fungal culture, after incubation at 28℃ for 48 h [6]. All tests were performed in duplicate to ensure the reproducibility.

6.4.2 Outcome of *in-vitro* anti-fungal activity

The result of anti-fungal screening of all the synthesized compounds is expressed in terms of ZOI and MIC (Tables **6.24** to **6.26**). Compounds having ZOI value 15 mm or above were considered as significantly active (highlighted in bold font), ZOI 13 to 14 mm were considered as moderately active. Further, compounds having ZOI value 10 to 12 mm were considered as weakly active and ZOI value less than 10 mm were considered as least active (represented by -mark) and MIC was not determined for such compounds. Reference drug fluconazole exhibited potent fungicidal activity, with ZOI 21 and 22 mm against *C. albicans* and *A. niger,* respectively and MIC 8 µg/mL against each strain.

6.4.2.1 Anti-fungal activity of compounds 5a-o

Anti-fungal activity of compounds **5a-o** against *Candida albicans* and *Aspergillus niger* strains are summarized in Table **6.24,** which revealed that all the tested compounds displayed varied response against both the tested fungal strains. Among the series, compound **5f** exhibited significant anti-fungal activity (ZOI 16 mm) against *C. albicans,* while compounds **5d, 5e, 5h, 5k** and **5o** displayed moderate activity (ZOI 13-14 mm), while rest of the compounds possessed weak to least fungicidal activity against this strain. Further, in contrast to *C. albicans,* strain *A. niger* was found to be more sensitive towards tested strain,

for example, four compounds **5e, 5h, 5i** and **5k** possessed significant anti-fungal activity against *A. niger*, while compounds **5f, 5j** and **5o** displayed moderate and rest of the compounds possessed weak to least activity. Overall, compound **5i** displayed encouraging anti-fungal activity against *A. niger* with ZOI 16 mm and MIC 32 µg/mL.

6.4.2.2 Anti-fungal activity of compounds 9a-o

Among all compounds **9a-o** screened for anti-fungal activity, compound **9m** showed significant, three compounds (**9d, 9e** and **9o)** exhibited moderate, while rest of the compounds possessed weak to least inhibitory potential against the growth of *C. albicans* (Table **6.24**). Against *A. niger,* four compounds (**9e, 9f, 9i** and **9m**) exhibited significant, five compounds showed moderate (**9c, 9d, 9g, 9h** and **9j**) and rest of the compounds displayed weak to least inhibitory potential. Compound **9m** significantly inhibited the growth of both fungal strains, moreover, it showed promising anti-fungal activity against *A. niger* with ZOI 18 mm and MIC 16 µg/mL. Overall, *A. niger* was found to be more susceptible compared to *C. albicans* towards the tested compounds **9a-o**.

6.4.2.3 Anti-fungal activity of compounds 14a-k

In the tested compounds **14a-k**, seven compounds possessed anti-fungal activity against *C. albicans*, in which single compound **14i** displayed significant activity (ZOI 15 mm), compound **14g** displayed moderate and rest of the compounds possessed least or weak activity. Further, anti-fungal study against *A. niger* revealed the significant activity of compound **14h** with ZOI 16 mm and MIC 32 µg/mL. Furthermore, compounds **14c, 14f, 14g, 14i** and **14k** displayed moderate while rest of the compounds exhibited weak to least potency against *A. niger.* Overall, like the previous two series (**5a-o** and **9a-o**), compounds of **14a-k** also displayed noticeable anti-fungal potency against *A. niger* compared to *C. albicans.*

6.4.2.4 Anti-fungal activity of compounds 17a-o

Compounds of **17a-o** series also displayed varying anti-fungal activity against both the tested fungal strains. Against the fungal strain *C. albicans,* compounds **17b, 17j** and **17k** displayed significant and compounds **17c, 17f** and **17i** exhibited moderate while rest of the compounds displayed weak to least potency**.** In contemporary*,* six compounds (**17c, 17h, 17j, 17k, 17l** and **17o**) showed significant anti-fungal activity against *A. niger.* Furthermore, compounds **17b, 17g** and **17n** showed moderate fungicidal activity against *A. niger* while rest of the compounds showed weak to least potency. Overall, compounds **17a-o** also possessed preferred anti-fungal activity against *A. niger.* Interestingly, compounds **17j** and **17k** displayed significant potency against both the tested fungal strains with ZOI 16-18 mm and MIC 16-32 µg/mL.

Table 6.24 Result of *in-vitro* anti-fungal activity of compounds **5a-o, 9a-o, 14a-k** and **17a-o**

Comp. Code	*Candida albicans*		*Aspergillus niger*		Comp. Code	*Candida albicans*		*Aspergillus niger*	
	ZOI (mm)	**MIC (µg/mL)**	**ZOI (mm)**	**MIC (µg/mL)**		**ZOI (mm)**	**MIC (µg/mL)**	**ZOI (mm)**	**MIC (µg/mL)**
5a	10	>128	12	128	**9n**	11	>128	-	-
5b	-	-	10	>128	**9o**	13	128	10	>128
5c	-	-	-	-	**14a**	12	128	12	128
5d	13	128	-	-	**14b**	-	-	-	-
5e	14	>64	**15**	**64**	**14c**	-	-	14	128
5f	**16**	**64**	14	128	**14d**	10	>128	-	-
5g	-	-	11	>128	**14e**	-	-	11	>128
5h	14	64	**15**	**64**	**14f**	11	128	13	128
5i	12	128	**16**	**32**	**14g**	13	>32	14	64
5j	-	-	14	128	**14h**	12	64	**16**	**32**
5k	14	64	**16**	**64**	**14i**	**15**	>32	14	128
5l	-	-	11	>128	**14j**	-	-	12	>128
5m	-	-	12	64	**14k**	10	>128	14	64
5n	10	>128	-	-	**17a**	12	128	-	-
5o	14	128	13	64	**17b**	**16**	**64**	14	64
9a	-	-	11	>128	**17c**	13	>64	**15**	**64**
9b	10	>128	10	>128	**17d**	10	256	10	256
9c	-	-	13	> 64	**17e**	-	-	12	128
9d	13	128	14	64	**17f**	13	128	-	-
9e	14	>64	**16**	**64**	**17g**	-	-	13	128
9f	-	-	**18**	**32**	**17h**	12	128	**15**	**>32**
9g	12	128	14	128	**17i**	13	128	12	64
9h	10	>128	13	128	**17j**	**16**	**32**	**17**	**>16**
9i	-	-	**17**	**32**	**17k**	**17**	**>16**	**18**	**16**
9j	11	>128	13	128	**17l**	12	128	**15**	**>32**
9k	12	128	-	-	**17m**	-	-	11	128
9l	-	-	12	128	**17n**	10	256	14	64
9m	**15**	**>64**	**18**	**16**	**17o**	12	128	**16**	**32**
					Flu.	**21**	**8**	**22**	**8**

6.4.2.5 Anti-fungal activity of compounds 23a-o

Five compounds (**23f, 23i, 23j, 23n** and **23o**) of series **23a-o** possessed significant anti-fungal activity with ZOI 15-18 mm and MIC 32-64 µg/mL against *C. albicans* (Table **6.25**). Further, compounds **23a, 23e, 23g** and **23h** displayed moderate while rest of the compounds exhibited weak to least potency against *C. albicans.* Against *A. niger*, three compounds (**23i, 23j** and **23k)** showed significant activity, also three compounds (**23f, 23g** and **23n**) displayed moderate while other compounds of **23a-o** possessed weak to least anti-

fungal activity. Furthermore, unlike the previously reported series, compounds of **23a-o** proven more effective inhibitor of *C. albicans* compared to the *A. niger*. Compounds **23i** and **23j** significantly inhibited both the tested fungal strains.

6.4.2.6 Anti-fungal activity of compounds 28a-l

Among the compounds (**28a-l**) screened for anti-fungal activity, seven compounds (**28e, 28f, 28g, 28h, 28i, 28k** and **28l**) showed significant and three compounds (**28a, 28d** and **28j)** exhibited moderate activity against the growth of *C. albicans* (Table **6.25**). Against *A. niger,* six compounds (**28d, 28e, 28f, 28g, 28h** and **28l)** exhibited significant, two compounds (**28a** and **28j)** showed moderate**,** while other compounds displayed weak to least inhibitory potential. Further, it's worthy to note that five compounds (**28e, 28f, 28g, 28h** and **28l**) significantly inhibited the growth of both the tested fungal strains. Moreover, compounds **28g, 28h, 28i** and **28l** showed promising anti-fungal activity against *C. albicans,* in which compound **28h** showed anti-fungal activity almost comparable to reference drug fluconazole with ZOI 20 mm and MIC 8 µg/mL. Overall, *C. albicans* was found to be more sensitive compared to *A. niger* against the tested compounds.

6.4.2.7 Anti-fungal activity of compounds 32a-n

Compounds of series **32a-n** showed weak to moderate activity against the both tested fungal strains. Two compounds (**32k** and **32m**) of series moderately inhibited the growth of *C. albicans*, while rest of the compounds possessed weak to least potency. Further, compounds **32a-n** showed somewhat improved potency against *A. niger*, overall four compounds (**32a, 32c, 32h** and **32m**) were found to be moderately active while others showed weak to least activity.

6.4.2.8 Anti-fungal activity of compounds 38a-o

Compounds of series **38a-o** possessed encouraging anti-fungal activity against the both tested strains, in which seven compounds (**38a, 38c, 38e, 38f, 38h, 38l** and **38n**) showed significant and one compound **38i** exhibited moderate anti-fungal activity against *C. albicans* (Table **6.25**). Against the second fungal strain (*A. niger*), also seven compounds (**38b**, **38d, 38f, 38j, 38k, 38l** and **38n)** exhibited significant, five compounds (**38a, 38c, 38e, 38h** and **38m)** showed moderate**,** while rest of the compounds displayed weak to least inhibitory potential. Furthermore, compounds **38f, 38l** and **38n** significantly inhibited the growth of both the tested fungal strains. Moreover, compound **38n** showed promising anti-fungal activity against *C. albicans* and *A. niger* with ZOI 19, 20 mm and MIC 32, 16 µg/mL, respectively.

Table 6.25 Result of *in-vitro* anti-fungal activity of compounds **23a-o, 28a-l, 32a-n** and **38a-o**

Comp. Code	*Candida albicans*		*Aspergillus niger*		Comp. Code	*Candida albicans*		*Aspergillus niger*	
	ZOI (mm)	MIC (µg/mL)	ZOI (mm)	MIC (µg/mL)		ZOI (mm)	MIC (µg/mL)	ZOI (mm)	MIC (µg/mL)
23a	14	64	11	128	**32b**	-	-	-	-
23b	12	128	-	-	**32c**	-	-	13	>64
23c	-	-	-	-	**32d**	-	-	-	
23d	-	-	10	>128	**32e**	11	>128	11	128
23e	13	64	12	128	**32f**	10	>128	10	>128
23f	**18**	**32**	14	64	**32g**	-	-	-	-
23g	14	64	13	64	**32h**	12	128	14	128
23h	14	128	-	-	**32i**	-		-	-
23i	**15**	**>32**	**15**	**>32**	**32j**	-		-	-
23j	**17**	**32**	**16**	**32**	**32k**	13	128	-	-
23k	-	-	**15**	**64**	**32l**	10	>128	12	128
23l	10	>128	-	-	**32m**	13	64	14	64
23m	-	-	-	-	**32n**	-		-	-
23n	**17**	**>32**	14	128	**38a**	**16**	**64**	13	128
23o	**16**	**>32**	-	-	**38b**	12	>128	**15**	**64**
28a	13	64	13	128	**38c**	**15**	**128**	14	>64
28b	10	128	-	-	**38d**	-	-	**18**	**32**
28c	-	-	10	128	**38e**	**16**	**64**	14	>64
28d	14	64	**16**	**64**	**38f**	**19**	**>32**	**17**	**32**
28e	**16**	**64**	**18**	**64**	**38g**	-	-	11	>128
28f	**18**	**>16**	**16**	**>32**	**38h**	**16**	**64**	14	64
28g	**19**	**16**	**18**	**32**	**38i**	14	128	-	-
28h	**20**	**8**	**17**	**64**	**38j**	-	-	**15**	**64**
28i	**19**	**32**	12	128	**38k**	12	>128	**16**	**>64**
28j	14	128	14	64	**38l**	**18**	**>32**	**17**	**32**
28k	**16**	**>32**	-	-	**38m**	-	-	14	>64
28l	**20**	**16**	**18**	**>32**	**38n**	**19**	**32**	**20**	**16**
32a	11	>128	13	128	**38o**	11	>128	-	-
					Flu.	**21**	**8**	**22**	**8**

6.4.2.9 Anti-fungal activity of compounds 43a-p

Compounds of series **43a-p** did not displayed significant fungicidal activity against *C. albicans*, among the series, compound **43g** showed moderate potency, while rest of the compounds were found to be weak to least active against the tested strains. Furthermore, tested series **43a-p** compounds possessed relatively better potency against *A. niger* compared to *C. albicans*. Among the series, two compounds (**43i** and **43m**) exhibited significant, four compounds (**43a**, **43c, 43g** and **43k**) displayed moderate, while rest of the compounds showed weak to least activity.

6.4.2.10 Anti-fungal activity of compounds 51a-n

Compounds of series **51a-n**, displayed moderate to least inhibitory activity against the growth of *C. albicans* and none of the compounds possessed encouraging activity, for example, three compound **51b, 51h** and **51k** possessed moderate activity while rest of the compounds exhibited weak to least anti-fungal activity. Against *A. niger,* compounds of series **51a-n,** possessed comparatively better potency than *C. albicans*, in which four compounds (**51a, 51e, 51g** and **51h**) possessed significant, also four compounds showed moderate (**51b, 51f, 5i** and **51j**), while rest of the compounds displayed weak to least activity.

6.4.2.11 Anti-fungal activity of compounds 54a-k

Compounds of series **54a-k** exhibited varied potency against the two tested fungal strains, but interestingly unlike most of the other series, compounds of **54a-k** inhibited the growth of *C. albicans* more effectively compared to *A. niger.* Moreover, five compounds (**54d, 54f, 54g, 54h** and **54k**) of this series displayed significant growth inhibition of *C. albicans,* one compound (**54c**) exhibited moderate, while others showed either weak or least anti-fungal activity. In contemporarily, only two compounds (**54g** and **54h**) of series **54a-k** significantly inhibited the growth of *A. niger,* while five compounds (**54a, 54d, 54f, 54j** and **54k)** showed moderate activity**.** Overall, two compounds (**54g** and **54h**) significantly inhibited the growth of both the tested fungal strains. Moreover, both of these two compounds exhibited potent activity against *C. albicans* with ZOI 17, 18 mm and MIC16 µg/mL.

Table 6.26 Result of *in-vitro* anti-fungal activity of compounds **43a-p, 51a-n** and **54a-k**

Comp. Code	*Candida albicans*		*Aspergillus niger*		Comp. Code	*Candida albicans*		*Aspergillus niger*	
	ZOI (mm)	MIC (µg/mL)	ZOI (mm)	MIC (µg/mL)		ZOI (mm)	MIC (µg/mL)	ZOI (mm)	MIC (µg/mL)
43a	12	128	14	>64	**51f**	-	-	14	64
43b	-	-	-	-	**51g**	11	>64	**17**	**32**
43c	-	-	14	64	**51h**	13	64	**16**	**>32**
43d	10	>128	12	>64	**51i**	-	-	13	>64
43e	-	-	-	-	**51j**	-	-	14	64
43f	-	-	10	>128	**51k**	13	64	12	>64
43g	13	>64	13	128	**51l**	-	-	-	-
43h	12	64	-	-	**51m**	-	-	-	-
43i	-	-	**15**	**64**	**51n**	-	-	12	128
43j	11	>128	-	-	**54a**	11	>128	14	64
43k	-	-	13	>128	**54b**	-	-	10	>128
43l	-	-	-	-	**54c**	14	>128	-	-
43m	10	128	**16**	**64**	**54d**	**15**	**64**	13	128

43n	-	-	-	-	**54e**	10	>128	-	
43o	-	-	10	>128	**54f**	**16**	**32**	14	>64
43p	-	-	-	-	**54g**	**17**	**16**	**16**	**64**
51a	12	128	**16**	**32**	**54h**	**18**	**16**	**15**	**>32**
51b	14	64	14	64	**54i**	10	>128	12	>128
51c	-	-	-	-	**54j**	-	-	13	128
51d	-	-	12	128	**54k**	**16**	**64**	14	>64
51e	12	>128	**15**	**>32**	**Flu.**	**21**	**8**	**22**	**8**

6.4.3 Key findings from anti-fungal activity

In-vitro screening result of the synthesized compounds against two fungal strains revealed that susceptibility of both strains varied significantly towards tested compounds. Further, out of all tested compounds, thirty and thirty nine compounds significantly inhibited (ZOI ≥ 15 mm) the growth of *C. albicans* and *A. niger,* respectively. So, fungal strain *A. niger* showed comparatively more sensitivity towards the tested compounds compared to *C. albicans*. Further, two series of compounds **28a-l** and **38a-o** possessed better growth inhibitory activity against the tested fungal strains, for example in series **28a-l**, seven and six compounds showed significant activity against *C. albicans* and *A. niger* respectively, while in series **38a-o,** seven compound showed similar activity against the both tested strains. Collectively, fifteen compounds (**9m, 17j, 17k, 23i, 23j, 28e, 28f, 28g, 28h, 28l, 38f, 38l, 38n, 54g** and **54h**) exhibited significant growth inhibition of both the tested fungal strains. Out of above compounds, eight (**28e, 28f, 28g, 28h, 28l, 38f, 38l** and **38n**) belongs to two series **28a-l** and **38a-o.** Therefore, scaffolds containing tetrahydroquinoline moiety with carbamate linker **(28a-l)** and tetrahydroquinoline based compounds attached with phenylpiperazine entity (**38a-o**) possessed potential anti-fungal activity.

Compounds of series **32a-n** possessed comparatively weak anti-fungal activity and none of the compounds showed significant activity against either of the tested fungal strains. Furthermore, series **43a-p** and **51a-n** exhibited moderate to least activity against *C. albicans,* however, few compounds of the above series also showed significant inhibition of *A. niger*. Reference compound fluconazole displayed potent activity against *C. albicans* and *A. niger* strains with ZOI 21, 22 mm respectively and MIC 8 µg/mL against each strain. Moreover, among the tested compounds also few compounds possessed potent fungal inhibitory activity, for example, compounds **9m**, **17k**, **38n** exhibited ZOI 18, 18, 20 mm, respectively and MIC 16 µg/mL against *A. niger*. Whereas, against *C. albicans* compounds **28g, 28h, 28l, 54g, 54h** showed potent anti-fungal activity with ZOI 19, 20, 20, 17, 18 mm, respectively and MIC was found to be 16 µg/mL for compounds **28g, 28l, 54g, 54h**, while **28h** exhibited MIC 8 µg/mL, comparable to the reference compound fluconazole.

6.5 Anti-mycobacterial activity

All the synthesized compounds were evaluated for anti-mycobacterial activity against *M. tuberculosis* (*Mtb*). Inhibitory activity of compounds against *Mtb* was expressed in terms of MIC (minimum concentration which inhibited the growth of *M. tuberculosis).* Compounds of two series (**23a-o** and **43a-p**) displayed encouraging anti-*Mtb* activity, so all compounds of these two series were evaluated for cytotoxicity studies against human lung fibroblast cell (MRC-5).

6.5.1 Anti-mycobacterial activity of series 5a-o, 9a-o, 14a-k, **51a-n** and **54a-k**

6.5.1.1 Experimental and Methodology

Titled compounds were screened against *M. tuberculosis* $H_{37}Rv$ (ATCC 27294; Manassas, VA, USA) and MIC_{90} was determined by broth dilution method. The bacterial strains were grown for 10 to 15 days in Middlebrook 7H9 broth (Difco Laboratories, Detroit, MI, USA) supplemented with 0.5% (v/v) glycerol, 0.25% (v/v) Tween 80 (Himedia, Mumbai, India) and 10% ADC (albumin dextrose catalase, Becton Dickinson, Sparks, MD, USA) under shaking conditions at 37 °C in 5% CO_2 to facilitate exponential-phase growth of the organism. A bacterial suspension was prepared by suspending the *M. tuberculosis* growth in normal saline containing 0.5% Tween 80 and turbidity was adjusted to 1 McFarland (McF) standard, which is equivalent to 1.0×10^7 CFU/ml. The 2-fold serial dilutions of compounds were prepared in Middle brook 7H9 (Difco laboratories) for *M. tuberculosis* in 100 µl per well in 96-well U bottom microtiter plates (Tarson, Mumbai, India). The above-mentioned bacterial suspension was further diluted 1 : 10 in the growth media and 100 µl volume of this diluted inoculum was added to each well of the plate, resulting in a final inoculum of 1.0×10^6 CFU/ml in the well and the final concentration of compounds ranging from 8 µg/ml to 128 µg/ml. The plates were incubated at 37 °C for seven days in 5% CO_2. For evaluation of the results, the Resazurin Microtiter Assay (REMA) method was used. After incubation, 15 µl of 0.04% resazurin and 12.5 µl of 20% Tween 80 were added to each well of the plate including in the media and growth controls. After 48 h of incubation, the plates were read visually and the minimum concentration of the compound showing no change of colour was recorded as MIC [7].

6.5.1.2 Results and Discussion

Anti-*Mtb* results of series **5a-o, 9a-o, 14a-k**, **51a-n** and **54a-k** are summarized in Table **6.27**, which revealed that among the series **5a-o,** four compounds **5c, 5h, 5k** and **5l** displayed weak potency against the growth of *Mtb* (MIC 128 µg/mL) while rest of the compounds not inhibited the growth of *Mtb* at the highest tested concentration (128 µg/mL). Further, in the series **9a-o** also four compounds (**9c, 9i, 9l** and **9m**) displayed weak potency (MIC 64-128 µg/mL), while rest of the compounds not exhibited noticeable anti-*Mtb* activity. Furthermore, compounds of series **14a-k** comparatively possessed better activity, among the series, compound **14j** showed significant (MIC 16 µg/mL) and compound **14i** showed moderate activity (MIC 32 µg/mL) against the tested strain of *Mtb*. Further, six compounds (**14a, 14c, 14d, 14f, 14g** and **14h**) displayed weak potency (MIC 64-128 µg/mL), while rest of compounds displayed least or no activity. Compounds of series **51a-n** and **54a-k** also not displayed encouraging anti-*Mtb* activity, for example seven compounds (**51c, 51f, 51h, 51j, 51k, 51l** and **51n**) of series **51a-n** and six compounds (**54d, 54e, 54h, 54i, 54j** and **54k**) of **54a-k** possessed anti-*Mtb* activity but with weak potency (MIC 64-128 µg/mL).

Table 6.27 Result of *in-vitro* anti-*Mtb* evaluation of series **5a-o, 9a-o, 14a-k**, **51a-n** and **54a-k**

Comp. code	Substitution	MIC (µg/mL)	Comp. code	Substitution	MIC (µg/mL)
5a	H	-	**14d**	4-F	>64
5b	2-CH_3	-	**14e**	2-Cl	-
5c	3-CH_3	128	**14f**	4-Cl	64
5d	4-CH_3	-	**14g**	3-Br	128
5e	3-OCH_3	-	**14h**	4-Br	64
5f	4-OCH_3	-	**14i**	4-NO_2	32
5g	4-F	-	**14j**	**4-CN**	**16**
5h	2-Cl	128	**14k**	3,4,5-tri-MeO	-
5i	3-Cl	-	**51a**	Ph	-
5j	4-Cl	-	**51b**	2-CH_3-Ph	-
5k	4-NO_2	>64	**51c**	4-CH_3-Ph	>64
5l	3-CF3	128	**51d**	2-CH_3O-Ph	-
5m	2,6-di-Me	-	**51e**	3-CH_3O-Ph	-
5n	3,4-di-Me	-	**51f**	4-CH_3O-Ph	>64
5o	2-Me,5-Cl	-	**51g**	2-F-Ph	-
9a	H	-	**51h**	4-F-Ph	64
9b	2-CH_3	-	**51i**	3-Cl-Ph	-
9c	3-CH_3	128	**51j**	4-Cl-Ph	>64
9d	4-CH_3	-	**51k**	4-NO_2-Ph	>64
9e	3-OCH_3	-	**51l**	Benzyl	64
9f	4-OCH_3	-	**51m**	2,3-DCl-Ph	-
9g	4-F	-	**51n**	Benzhydryl	64
9h	2-Cl	-	**54a**	H	-

9i	3-Cl	>64	**54b**	2-CH_3O	-
9j	4-Cl	-	**54c**	3-CH_3O	-
9k	2-CF_3	-	**54d**	4-F	128
9l	3-CF_3	>64	**54e**	2-Cl	64
9m	4-NO_2	64	**54f**	3-Cl	-
9n	2,4-di-Me	-	**54g**	3-Br	-
9o	3,4-di-Me	-	**54h**	3-NO_2	64
14a	2-CH_3	>64	**54i**	3,4-di-MeO	>64
14b	3-OCH_3	-	**54j**	3,4-di-Cl	64
14c	4-OCH_3	128	**54k**	2-Br, 4-CN	128
			Rifampicin		0.091

6.5.2 Anti-mycobacterial activity and cytotoxicity studies of series 23a-o and 43a-p

6.5.2.1 Experimental and Methodology

6.5.2.1.1 Anti-mycobacterial activity

The Minimal Inhibitory Concentration (MIC) against mycobacteria of all the synthesized compounds was evaluated by serial dilution method. The *in-vitro* assay was based on a method in which a luminescent *Mycobacterium tuberculosis* H37Ra strain Lehmann & Neumann (ATCC® 25177™) transformed with pSMT1 luciferase reporter plasmid is used. The tested compounds were solublized in DMSO (Sigma-Aldrich) at the stock concentration of 10 mM. Serial dilutions of each compounds was made in the liquid 7H9 medium [Middlebrook 7H9 broth based (Difco)] with 10% oleic acid, albumin, dextrose, catalase (OADC) enrichment. The volume of 20 µl of the serial dilutions was added in triplicate to 96 well, flat-bottomed microwell plates. The bacterial suspension was made by thawing and dissolving a frozen Mycobacteria pellet in 7H9 broth supplemented with 10% OADC (7H9-10% OADC).

The dissolved pellet was passed through a 5.0 µM filter (Millipore) to eliminate clumps and left for 1 hour to recover at 37 °C, 5% CO_2. Next, the bacterial suspension was diluted in 7H9-10% OADC to obtain 50,000 Relative Light Units (RLU)/ml and a volume of 180 µl of bacteria was added to each well. A bacterial replication was analyzed by luminometry after 6 days of incubation. The bacterial suspension from each well was collected and transferred to a black of 96-well plates to evade cross luminescence between wells. The luminescent signal was evoked by addition of substrate for the bacterial luciferase, 1 % n-decanal in ethanol to each well by discover multi-plate reader from Promega and the light emission in each well was measured [8].

6.5.2.1.2 Cytotoxicity studies

Cytotoxic effect on the MRC-5 human lung fibroblast cell (ATCC® CCL-171™) was determined for the titled compounds by neutral red uptake assay. The neutral red uptake assay relies on the ability of viable cells to bind and incorporate the neutral red dye (toluylene red). The acute toxic concentration (IC_{50}) of a compound is defined as the concentration at which the uptake of the neutral red dye by the cells is reduced by 50%. The MRC-5 cells were grown in Dulbecco's Modified Eagle's Medium (DMEM) with 10% Foetal Calf Serum (FCS) until a semi-confluent layer of cells was obtained. The cells were trypsinized, washed and 40000 cells were seeded per well of a 96-well plate and left for recovery at 37°C, 5% CO_2. The following days, the compounds were solublized in DMSO to stock concentrations of 10 µM. A serial dilution of each compound was made in DMEM with 10% FCS. The MRC-5 cells were washed and exposed to the derivatives by adding the serial dilutions of the compounds to the wells. The plates were left for incubation at 37°C, 5% CO_2 for 24 h. After exposure, the cells were washed with 200 µL of PBS and 200 µL of neutral red working solution (Sigma) was added to each well. Subsequently, the plates were incubated for 3 h at 37°C, 5% CO_2. The wells were washed with 200 µL of PBS and 200 µL of ethanol/acetic acid (50%) mixture. The plates were left on the shaker until the color became homogeneous purple and the optical density was measured at 530 nm (NR max) and 620 nm (reference wavelength) with the paradigm detection platform [9].

6.5.2.2 Results and Discussion

Synthesized compounds **23a-o** and **43a-p** were evaluated for anti-tubercular activity against *M. Tuberculosis* (H37Ra strain) using luminometry method using rifampicin as the standard positive control. The minimum inhibitory concentration (MIC) values of the tested compounds along with positive control standard drug are shown in Table **6.28.** Among the series **23a-o**, two compounds (**23h** and **23o**) displayed significant anti-*Mtb* activity with MIC ≤25 µg/mL (highlighted by bold font in Table **6.28**), two compounds (**23a** and **23l**) exhibited moderate activity (MIC >25 to ≤50 µg/mL), while rest of the compounds exhibited weak to least activity. Furthermore, we investigated the effect of different substitution on anti-tubercular potency of compounds. Compound with un-substituted phenyl ring showed moderate anti-*Mtb* activity (MIC 47.76 µg/mL). Further, substitution of phenyl ring with electron donating methoxy group (**23b, 23c** and **23d**) decreased the anti-tubercular potency at all position of phenyl ring. Substitution with fluoro group at *ortho* position (**23e**) did not significantly alter the anti-*Mtb* potency, while at *meta* and *para* positions (**23f** and **23g**), it significantly decreased the potency (MIC 106.82 and 145.60 µg/mL, respectively). Interestingly, nitro substitution at *ortho* position of phenyl ring (**23h**) significantly increased the anti-*Mtb* potency (MIC 18.97 µg/mL), while substitution at the *meta* and *para* positions (**23i** and **23j**) resulted in reduction

of potency. Overall, anti-*Mtb* potency of nitro substituted compounds changed in the order *ortho>meta>para.*

Furthermore, making di or tri-substitution with methoxy group at phenyl ring (**23k** and **23m**) decreased the anti-*Mtb* potency (MIC70.78 and 63.80 µg/mL), while di-substitution with chloro (**23k**) group not significantly altered the potency (MIC 49.70 µg/mL). Further, replacement of phenyl with unsubstituted styrene moiety significantly decreased the potency, interestingly compounds containing 3-nitro substituted styrene (**23o**) exhibited significant anti-*Mtb* potency (MIC 19.09 µg/mL). Interestingly, none of the compounds exhibited cytotoxicity against MRC-5 at the tested concentration of 512 µM. Overall SAR study revealed that substitution with methoxy group at all positions of phenyl ring was found to be un-favourable, while substitution with nitro group specially at the *ortho* position of phenyl and *meta* position of styrene were found favourable for the anti-*Mtb* potency with good safety index.

Among the tested compounds of **43a-p** series, four compounds (**43h**, **43j**, **43l** and **43m**) displayed significant anti-*Mtb* activity with MIC <25 µg/mL (highlighted by the bold font in Table **6.28**). Further, we investigated the effect of different substitution pattern of phenyl ring on the anti-tubercular potency of compounds. Prototype compound **43a** containing un-substituted phenyl ring exhibited weak anti-*Mtb* activity. Further, substitution of phenyl ring with electron donating groups such as methyl and methoxy at *ortho* and *meta* position, respectively, further decreased their anti-tubercular potency. Whereas, methoxy group at the *para* position (**43d**) slightly enhanced the potency (MIC 38.51 µg/mL). Further, substitution with strong electron withdrawing fluoro group at *ortho* and *para* position (compound **43e** and **43f**) also result decreased in anti-tubercular potency (84.75 and 60.74 µg/mL, respectively). Interestingly, chloro substitution at *ortho* position of phenyl ring (**43g**) markedly decreased the potency (>180.78 µg/mL), while chloro at the *para* position (**43h**) considerably increased the potency against *Mtb* (MIC11.58 µg/mL). Substitution with bromo at *meta* position (**43i**) not significantly changed the anti-tubercular potency, while *para* substituted compound (**43j**) exhibited seven times more potency (MIC 7.70 µg/mL) as compared to the unsubstituted one.

Among the nitro substituted compounds (**43k, 43l** and **43m**)**,** compound **43k** exhibited moderate while compounds **43l** and **43m** showed significant anti-tubercular potency. Overall, the anti-*Mtb* potency of nitro substituted compounds changed in the order *ortho<meta<para* (MIC 38.33, 14.27 and 7.13 µg/mL, respectively). Further, 4-cyano substituted compound **43n** exhibited moderate potency while di-chloro and tri-methoxy substituted compounds (**43o** and **43p**) exhibited very weak anti-*Mtb* potency. Reference drug rifampicin showed promising anti-*Mtb* activity with MIC 0.14 µg/mL. All compounds of series **43a-p** were found

to be non-toxic at the tested concentration of 512 µM. Overall SAR study of the tested compounds revealed that anti-tubercular potency changed significantly with change in the position as well as nature of the substituent. Compounds with electron releasing groups (like methyl and methoxy) were found to be unfavorable for anti-*Mtb* activity, while electron withdrawing group of moderate to large size (like chloro, bromo, and nitro) at the *para* position of phenyl ring favoured anti-*Mtb* activity.

Table 6.28 Result of *in-vitro* anti-*Mtb* evaluation of series **23a-o** and **43a-p**

Comp. code	Substitution	MIC (µM)	MIC (µg/mL)	CC_{50} MRC5 (µM)	Selectivity ratio
23a	Ph	147.7	47.76	>512	>3.46
23b	2-MeO-Ph	314.5	111.15	>512	>1.62
23c	3-MeO-Ph	406.2	143.56	>512	>1.26
23d	4-MeO-Ph	480.1	169.67	>512	>1.06
23e	2-F-Ph	163.7	55.88	>512	>3.12
23f	3-F-Ph	312.9	106.82	>512	>4.79
23g	4-F-Ph	426.8	145.60	>512	>1.19
23h	2-NO_2-Ph	**51.5**	**18.97**	**>512**	**>9.94**
23i	3-NO_2-Ph	182.1	67.08	>512	>2.81
23j	4-NO_2-Ph	225.3	83.00	>512	>2.27
23k	3,4-DMeO-Ph	184.6	70.78	>512	>2.77
23l	2,4-DCl-Ph	126.7	49.70	>512	>4.04
23m	3,4,5-tri-MeO-Ph	154.3	63.80	>512	>3.31
23n	Styrene	536.7	187.54	>512	>0.95
23o	Styrene-3-NO_2	**48.4**	**19.09**	**>512**	**>10.57**
43a	H	162.30	51.79	>512	>3.15
43b	2-CH_3	234.60	78.15	>512	>2.18
43c	3-OCH_3	258.40	90.21	>512	>1.98
43d	4-OCH_3	110.30	38.51	>512	>4.64
43e	2-F	251.40	84.75	>512	>2.03
43f	4-F	180.20	60.74	>512	>2.84
43g	2-Cl	>512	>180.78	>512	-
43h	4-Cl	**32.80**	**11.58**	**>512**	**>15.60**
43i	3-Br	141.30	56.10	>512	>3.62
43j	4-Br	**19.40**	**7.70**	**>512**	**>26.39**
43k	2-NO_2	105.20	38.30	>512	>4.86
43l	3-NO_2	**39.20**	**14.27**	**>512**	**>13.06**
43m	4-NO_2	**19.60**	**7.13**	**>512**	**>26.12**
43n	4-CN	87.90	30.24	>512	>5.82
43o	3,4-di-Cl	407.60	157.76	>512	>1.25
43p	3,4,5-tri-MeO	422.70	172.95	>512	>1.21
Rifampicin		0.18	0.14		

6.5.3 Anti-mycobacterial activity of series 17a-o, 28a-l, 32a-n and 38a-o

6.5.3.1 Experimental and Methodology

The anti-microbial activity of compounds against *M. tuberculosis (*H37Rv) grown under aerobic conditions is assessed by determining the MIC. The assay is based on measurement of growth in the liquid medium of a fluorescent reporter strain of H37Rv where the readout is either optical density (OD) or fluorescence. The use of two readouts minimizes the problem caused by compound precipitation or auto fluorescence. A linear relationship between OD and fluorescence readout was established justifying the use of fluorescence as a measure of bacterial growth. The MIC of the compounds was determined by measuring the bacterial growth after 5 days in the presence of test compounds. Compounds were prepared in two-fold serial dilutions in DMSO (Fisher) and diluted into 7H9-Tw-OADC medium (VWR) in 96-well plates with a final DMSO concentration of 2%. Each plate included assay controls for background (medium/DMSO only, no bacterial cells), zero growth (100 µM rifampicin) and maximum growth (2% DMSO only), as well as rifampicin dose response curve. Plates were inoculated with *M. tuberculosis* and incubated for 5 days: growth was measured by OD_{590} and fluorescence (Ex 560/Em 590). Growth was calculated separately for OD_{590} and RFU. Finally, the concentration that resulted in 90% inhibition of growth (MIC_{90}) was determined [10, 11].

6.5.3.2 Results and Discussion

Anti-*Mtb* activity of compounds **17a-o**, **28a-l, 32a-n** and **38a-o** is summarized in Table **6.29**. Unfortunately, none of the compound exhibited significant potency against the selected strain. Among the series **17a-o**, four compounds (**17b, 17f, 17k** and **17n**) exhibited weak, while rest of the compounds not exhibited noticeable activity. Further, among the compounds **28a-l,** compound **28j** exhibited moderate potency (MIC 40 µg/mL), two compounds (**28k** and **28l**) exhibited weak while rest of the compounds showed least or no anti-*Mtb* activity. Furthermore, among the compounds **32a-n** and **38a-o,** none of the compounds exhibited significant or moderate activity, few compounds like **32g, 32m, 38b, 38c** and **38g** possessed weak potency (MIC 80-160 µg/mL), while rest of the compounds possessed either least or no activity.

Table 6.29 Result of *in-vitro* anti-*Mtb* evaluation of series **17a-o**, **28a-l, 32a-n** and **38a-o**

Comp. code	Substitution (-R)	MIC (µg/mL)	Comp. code	Substitution (-R)	MIC (µg/mL)
17a	2-OCH_3	-	**32b**	2-CH_3	-
17b	3-OCH_3	160	**32c**	3-CH_3	-
17c	4-OCH_3	-	**32d**	4-CH_3	-
17d	3-F	-	**32e**	2-OCH_3	-
17e	4-F	-	**32f**	3-OCH_3	-
17f	2-Cl	>80	**32g**	4-OCH_3	>80
17g	3-Cl	-	**32h**	4-F	-
17h	4-Cl	-	**32i**	3-Cl	-
17i	2-Br	-	**32j**	4-Cl	-
17j	3-Br	-	**32k**	3-Br	-
17k	4-Br	160	**32l**	4-Br	-
17l	4-CN	-	**32m**	4-NO_2	80
17m	3-$COCH_3$	-	**32n**	2,4-di-Me	-
17n	3-CF_3	>80	**38a**	Ph	-
17o	2,5-di-Me	-	**38b**	2-Me-Ph	>80
28a	H	-	**38c**	4-Me-Ph	80
28b	2-CH_3	-	**38d**	2-MeO-Ph	-
28c	3-CH_3	-	**38e**	3-MeO-Ph	-
28d	4-CH_3	-	**38f**	4-MeO-Ph	-
28e	2-F	-	**38g**	2-F-Ph	160
28f	3-F	-	**38h**	4-F-Ph	-
28g	4-F	-	**38i**	2-Cl-Ph	-
28h	4-Cl	-	**38j**	3-Cl-Ph	-
28i	3-NO_2	-	**38k**	4-Cl-Ph	-
28j	4-NO_2	40	**38l**	4-NO_2-Ph	-
28k	2-COOEt	>40	**38m**	Benzyl	-
28l	4-COOEt	80	**38n**	2-Pyridine	-
32a	H	-	**38o**	2,3-di-Cl-Ph	-
			Rifampicin		0.11

6.5.4 Key findings from Anti-*Mtb* activity

Overall, with few exceptions, majority of the tested compounds not showed encouraging potency against *Mbt* growth. Among the all tested compounds, seven compounds (**14j, 23h**, **23o, 43h**, **43j**, **43l** and **43m**) exhibited significant potency (MIC ≤25 µg/mL), also seven compounds (**14i, 23a, 23l**, **28j, 43d, 43k** and **43n**) showed moderate potency (MIC between >25 to ≤50 µg/mL), while rest of the compounds possessed weak or no activity against *Mtb*. One interesting thing worthy to note is that all seven significantly active compounds and majority of moderately active compounds (except **28j**) belongs to three series **14a-k, 23a-o** and **43a-p.** Compounds of these three series possessed carboxylic hydrazide as common entity, which is very well known for anti-tubercular activity also present in the blockbuster

drug isoniazid. In recent studies, several carbohydrazide bearing heterocyclic moieties are reported as potent inhibitor of pantothenate synthetase enzyme of *M. tuberculosis* [12, 13]. Moreover, our reported compounds also exhibit similar pharmacophoric features, so they may share the similar mechanism of action, but further studies are required to know the exact mechanism of action.

Overall, compounds of series **43a-p** exhibited relatively better anti-*Mtb* activity than all other tested series, four compounds of series **43a-p** showed significant potency (MIC ≤25 µg/mL), in which compounds **43j** and **43m** showed MIC <10 µg/mL with safety index of more than twenty six. So, anti-*Mtb* evaluation studies afforded two hits **43j** and **43m** with good anti-*Mtb* potency and safety index which can be used for further lead optimization studies or in designing of novel anti-*Mtb* agents.

6.6 References

1. J. Eberle, C.W. Knopf, Non-isotopic assays of viral polymerases and related proteins. Methods in Enzymology, 275 (1996) 257–276.
2. R.R. Wang, Q. Gu, Y.H. Wang, X.M. Zhang, L.M. Yang, J. Zhou, J.J. Chen, Anti-HIV-1 activities of compounds isolated from the medicinal plant Rhus chinensis. Journal of Ethnopharmacology, 117 (2008) 249-256.
3. G.H. Zhang, Q. Wang, J.J. Chen, X.M. Zhang, S.C. Tam, Y.T. Zheng, The anti-HIV-1 effect of scutellarin. Biochemical and Biophysical Research Communications, 334 (2005) 812-816.
4. P.A. Wayne, Methods for dilution of antimicrobial susceptibility tests for bacteria that grow aerobically: approved standard, M7-A7, (2006) 7th edn., Clinical and Laboratory Standards Institute.
5. J.M. Andrews, Determination of minimum inhibitory concentrations. Journal of Antimicrobial Chemotherapy, 48 (2001) 5-16.
6. S. Magaldi, S. Mata-Essayag, C. Hartung de Capriles, C. Perez, M.T. Colella, C. Olaizola, Y. Ontiveros, Well diffusion for antifungal susceptibility testing. International Journal of Infectious Diseases, 8 (2004) 39-45.
7. G. Munagala, K.R. Yempalla, S. Singh, S. Sharma, N.P. Kalia, V.S. Rajput, S. Kumar, Synthesis of new generation triazolyl and isoxazolyl-containing 6-nitro-2,3-dihydroimidazooxazoles as anti-TB agents: In vitro, structure-activity relationship, pharmacokinetics and in vivo evaluation. Organic & Biomolecular Chemistry, 13 (2015) 3610-3624.

8. V.A. Snewin, M.P. Gares, P.O. Gaora, Z. Hasan, I.N. Brown, D.B. Young, Assessment of immunity to mycobacterial infection with luciferase reporter constructs. Infection and Immunity, 67 (1999) 4586-4593.
9. P.A. Jones, A.V. King, High throughput screening (HTS) for phototoxicity hazard using the in vitro 3T3 neutral red uptake assay. Toxicology In Vitro, 17 (2003) 703-708.
10. J. Ollinger, M.A. Bailey, G.C. Moraski, A. Casey, S. Florio, T. Alling, M.J. Miller, A dual read-out assay to evaluate the potency of compounds active against Mycobacterium tuberculosis. PLOS One, 8 (2013) e60531.
11. A. Zelmer, P. Carroll, N. Andreu, K. Hagens, J. Mahlo, N. Redinger, B.D. Robertson. A new in vivo model to test anti-tuberculosis drugs using fluorescent imaging. Journal of Antimicrobial Chemotherapy, 67 (2012) 1948-1960.
12. G. Samala, R. Nallangi, P.B. Devi, S. Saxena, R. Yadav, J.P. Sridevi, P. Yogeeswari, Identification and development of 2-methylimidazo [1,2-a]pyridine-3-carboxamides as Mycobacterium tuberculosis pantothenate synthetase inhibitors. Bioorganic & Medicinal Chemistry, 22 (2014) 4223-4232.
13. G. Samala, P.B. Devi, S. Saxena, N. Meda, P. Yogeeswari, D. Sriram, Design, synthesis and biological evaluation of imidazo[2,1-b]thiazole and benzo[d]imidazo[2,1-b]thiazole derivatives as Mycobacterium tuberculosis pantothenate synthetase inhibitors. Bioorganic & Medicinal Chemistry, 24 (2016) 1298-1307.

CHAPTER 7

Docked Pose Analysis of Selected Compounds

Docked pose analysis of selected compounds against wild HIV-1 RT

In order to study the putative binding modes of compounds with HIV- RT, docking studies were performed using Glide module of Schrödinger suite [1]. Further, for the docking studies, best and least active compounds from each series were selected (based upon *in-vitro* results against wild HIV-1 RT). For the docking studies also wild HIV-1 RT strain was chosen (PDB ID: 3MEE), which possessed no mutations at the NNRTI binding site [2]. The detailed experimental protocol and validation part is already explained in chapter **4**, section **4.1.4.**

7.1 Results and Discussion

In order to perform comparative studies, two blockbuster drugs efavirenz and rilpivirine were made to dock with selected RT protein using the same protocol as followed for the selected compounds. Moreover, rilpivirine is also a co-crystallized ligand in the selected protein 3MEE. Docked pose of the reference drug efavirenz is shown in Fig. **7.1,** which revealed that its cyclopropyl ring extended towards deep hydrophobic pocket and exhibited hydrophobic interactions with residues like Tyr-188, Tyr-181, Leu-100 and Trp-229. Further, chlorophenyl ring of efavirenz displayed similar interactions with Tyr-318 and Val-106 residues. Apart from hydrophobic interactions, N-H and C=O of efavirenz formed hydrogen bonding interaction with C=O and N-H of Lys-101, respectively. Overall, strong hydrophobic and hydrophilic interactions of efavirenz with amino acid residues of receptor may be accounted for its enhanced stability inside the NNIBP and consequently for the potent *in-vitro* RT inhibitory activity.

Docked pose of reference compound rilpivirine inside the NNIBP of 3MEE (Fig. **7.2**) revealed the similar binding orientation as reported in the X-ray pose [3]. Dimethyl substituted phenyl moiety of rilpivirine exhibited hydrophobic interaction with amino acids like Tyr-188, Tyr-181, Phe-227, moreover, it also displayed *pi-pi* stacking interaction with Tyr-188. Another hydrophobic wing of rilpivirine (benzonitrile) showed hydrophobic interactions with Tyr-318 and Trp-229. Furthermore, the nitrogen of pyrimidine ring as well as hydrogen of adjacent NH linker, exhibited hydrogen bonding interaction with Lys-101, which additionally enhanced its binding affinity with the receptor. Overall, prominent hydrogen bonding, hydrophobic and *pi-pi* stacking interactions of rilpivirine may be responsible for its strong binding affinity as well as high potency against RT.

7.1.1 Docked pose analysis of best (5n) and least active (5l) compounds from series 5a-o

The best docked pose of compound **5n** revealed prominent hydrophobic interactions of THIQ moiety with Tyr-181 and Trp-229 residues, also similar interactions but of weak intensity with

Tyr-188 and Val-106 (Fig. **7.3**). Further, methylene moiety of glycinamide linker also displayed hydrophobic interaction with Trp-229 and Phe-227. Dimethylphenyl moiety of **5n** displayed similar interactions with Val-108 and Phe-227 of moderate intensity.

In contemporary to **5n**, binding pattern of compound **5l** was found to be quite different, moreover, compound **5l** adopted U-shaped confirmation inside the NNIBP of 3MEE (Fig. **7.4**). Further, THIQ entity of **5l** along with connecting linker showed hydrophobic interactions with non-aromatic residues like Val-179 and Val-106. Trifluoromethyl phenyl component of **5l** adopted the position in parallel with indole ring of Trp-229, both shared prominent hydrophobic as well as *pi-pi* interactions. Trifluoromethyl phenyl moiety also showed weak hydrophobic interactions with residues like Tyr-181, Tyr-188, Leu-234 and Phe-227. Further, bound confirmation of **5l** possessed extra strain due to more bending around the linker, although bending helps in optimization of interactions with the surrounding residues, but in parallel overstrain due to bending can also hamper the stability of the ligand-receptor complex [4].

So, overall quite variability in the binding pattern of compounds **5n** and **5l** inside the NNIBP of 3MEE may be responsible for the difference in their *in-vitro* activity (58.12 and 27.64% inhibition, respectively) against HIV- RT.

7.1.2 Docked pose analysis of best (9h) and least active (9a) compounds from series 9a-o

Docked pose view of compound **9h** (Fig. **7.5**) revealed that its 6,7-dimethoxy-THIQ moiety displayed hydrophobic interactions of weak intensity with Val-179, Leu-100 and Val-106, while methyl of glycinamide linker showed similar interactions with Tyr-318. Further, methoxy group at the 7^{th} position of THIQ ring displayed hydrogen bonding interactions with the backbone of Lys-101 as well as the side chain of Lys-103. However, chlorophenyl entity of **9h** appeared in the vicinity of hydrophobic pocket surrounded by the residues Phe-227, Tyr-188, Trp-229, Leu-234. Among these, two former residues (Phe-227 and Tyr-188) displayed prominent hydrophobic as well as *pi-pi* stacking interactions with chlorophenyl entity, while Tyr-229 and Leu-234 showed hydrophobic interactions.

Further, putative binding mode of compound **9a** was found to be quite distinct, for example 6,7-dimethoxy-THIQ entity of **9a** was observed in close proximity with Tyr-181, Trp-229, Tyr-188, Phe-227, Leu-234 and showed hydrophobic interaction with aforementioned amino acids (Fig. **7.6**). Further, it was worthy to note that aromatic components of residues Tyr-181, Trp-229, Tyr-188 and Phe-227 did not possess co-planarity with THIQ ring system, consequently *pi-pi* stacking interactions were not observed. Further, phenyl ring of **9a** showed hydrophobic

interactions with aliphatic residues like Val-179 and Leu-100, while methyl group present at the linker showed similar interactions with Val-106. Further, amidic NH of **9a** showed hydrogen binding interactions with Lys-101 residue.

Overall, putative binding mode of compounds **9n** and **9a** was found fairly distinct from each other. Moreover, former displayed more prominent interactions especially *pi-pi* stacking interactions which may be responsible for the difference in their *in vitro* HIV-1 RT inhibitory (61.42 and 28.24 % inhibition, respectively) activity.

7.1.3 Docked pose analysis of best (14j) and least active (14b) compounds from series 14a-k

The best docked pose view of compound **14j** shown in Fig. **7.7**, demonstrated that its THIQ as well as central carboxyl hydrazide linker showed very weak hydrophobic interactions with Val-173. However, methoxy group located at the 7^{th} position of THIQ showed dual hydrogen bonding interactions (with the side chain of Arg-172 and backbone of Ile-180) and supported the one terminal of **14j** inside the NNIBP. The second terminal of **14j** (benzonitrile moiety) showed hydrophobic interactions with Leu-100, Tyr-181, Leu-234 and Tyr-188. Moreover, residue Tyr-181 and benzonitrile moiety positioned in the parallel plane and shared *pi-pi* stacking interactions.

In docked view of compound **14b**, THIQ ring and methylene entity of linker showed hydrophobic interactions of weak intensity with Tyr-181, Val-179 and Leu-100 residues (Fig. **7.8**). Further, 2-methoxyphenyl component showed hydrophobic interactions with Phe-227, Tyr-188 and Leu-100. Apart from the above interactions, C=O functionality of carboxyl hydrazide linker showed hydrogen bonding interactions with NH of the Lys-101 residue.

Overall, although compounds **14j** and **14b** displayed difference in their putative binding mode with HIV-1 RT, however, common thing observed was less involvement of THIQ entity in binding interactions. This might be the probable reason that neither of the compounds showed significant activity, instead compounds **14j** and **14b** showed moderate and weak *in-vitro* HIV-1 RT inhibition activity (32.82 and 17.24% inhibition), respectively.

7.1.4 Docked pose analysis of best (17h) and least active (17a) compounds from series 17a-o

Docked pose view of best active compound **17h** revealed that its 6,7-dimethoxy-THIQ nucleus exhibited hydrophobic interaction with amino acids like Tyr-188, Tyr-181 and Trp-229, while it's

another hydrophobic wing (*p*-chlorophenyl) showed similar interactions with Val-106 and Tyr-318 residues (Fig. **7.9**). Further, NH of **17h** exhibited hydrogen bonding interaction with Lys-101, which additionally enhanced its binding affinity with HIV-1 RT. Substitution with chloro at *para* position of phenyl enhanced the hydrophobic area of contact between the ligand-receptor complex and may be responsible for the significant *in-vitro* activity of **17h**.

In the best docked pose view of compound **17a**, its 6,7-dimethoxy-THIQ component displayed hydrophobic interactions mainly with residues like Trp-229, Tyr-188, Tyr-181, Val-108, Leu-234, Phe-227 and Leu-100 (Fig. **7.10**). Further, 2-methoxyphenyl component of **17a** showed similar interactions predominantly with Val-179 and weakly with Val-106, Tyr-181 and Leu-100.

Overall, the binding pattern of both the compounds **17h** and **17a** shared somewhat similarity and both adopted horse shoe type or "U" confirmation inside the NNIBP, but unlike compound 1**7h,** compound **17a** appeared slightly more strained in the best scoring pose, moreover NH entity of **17a** also lack hydrogen bonding interaction with Lys-101. So, these factors may be responsible for the difference in *in-silico* binding affinity of **17h** and **17a,** consequently also in *in-vitro* HIV-1 RT activity (74.82 and 45.31% inhibition), respectively.

7.1.5 Docked pose analysis of best (23o) and least active (23i) compounds from series 23a-o

In the docked pose view of compound **23o**, THQ moiety along with central linker displayed hydrophobic interactions with residues like Tyr-181, Tyr-188, Phe-227, Leu-234, Val-106 and Val-179 (Fig. **7.11**). Further, carbonyl group present at central linker showed hydrogen bonding interaction with Lys-101 and Lys-103, while *meta* nitrostyrene moiety remained outside the NNIBP in the exposure of medium, may be due to its long distance from THQ moiety and nitro substitution (polar group).

Further, **23i** shared some common hydrophobic interactions as appeared in **23o,** and its THQ moiety displayed hydrophobic interaction with residues like Tyr-181, Tyr-188, Phe-227, Trp-229, Leu-234, Pro-95, Leu-234 and Leu-100 (Fig. **7.12**). Further, in spite the presence of long hydrophilic linker compound **23i** not exhibited hydrogen bonding interaction, although linker showed weak hydrophobic interactions with residues like Leu-234, Leu-100 and Val-179. Further, nitrophenyl moiety of **23i** showed weak hydrophobic interactions with Val-106 and Val-179.

Overall, nitrostyrene moiety of **23o** remained devoid of interactions, which demonstrated it's weak to moderate binding affinity with HIV-1 RT and subsequently which may be accounted for

its moderate *in-vitro* activity against HIV-1 RT (41.76% inhibition). However, in compound **23i,** although nitrophenyl as well as the connecting linker engaged via weak hydrophobic interactions, but THQ nucleus exhibited very prominent hydrophobic interactions and overall binding affinity of the compound can be estimated of moderate to good level, but in contemporary **23i** showed weak *in-vitro* RT inhibitory activity (16.52% inhibition).

7.1.6 Docked pose analysis of best (28j) and least active (28e) compounds from series 28a-l

The analysis of best docked pose view of compound **28j** (Fig. **7.13**) revealed that it's one hydrophobic wing (contains THQ and chlorophenyl ring) displayed hydrophobic interaction with Pro-95, Trp-229, Tyr-181, Leu-100, Val-106, Tyr-318, while second aromatic wing (*p*-nitrophenyl) exhibited hydrophobic interactions with Val-179. The carbonyl group of the central carbamate linker showed dual hydrogen bonding interactions with Lys-101 and Lys-103.

While in docked pose of **28e**, THQ entity showed prominent hydrophobic interactions with residues like Tyr-181, Tyr-188, Trp-229, Pro-95, Leu-234 and Phe-227 (Fig. **7.14**), and chlorophenyl exhibited similar interactions of weak intensity with Val-179. Furthermore, fluorophenyl entity showed weak hydrophobic interactions with Tyr-318, Val-106 and Leu-234. NH of carbamate linker in **28e** displayed Hydrogen bonding interaction with Lys-101.
Based upon the docking studies, overall compound **28e** exhibited less prominent hydrophobic as well as hydrogen bonding interactions compared to the **28j**, which may be the probable reason that compound **28j** showed better potency (IC_{50} 5.42) compared to compound **28e** (IC_{50} 90.30) during the *in-vitro* HIV-1 RT assay.

7.1.7 Docked pose analysis of best (32m) and least active (32g) compounds from series 32a-n

In best docked pose view of compound **32m**, THQ and chlorophenyl entity displayed hydrophobic interactions with residues Tyr-181, Tyr-188, Trp-229, Pro-95, Leu-100, Tyr-318, Leu-234 and Val-106 (Fig. **7.15**). Nitrophenyl wing of **32m** positioned almost outside of the NNIBP pocket showed weak hydrophobic interactions with Val-179, while C=O functionality of amide linker showed Hydrogen bonding interaction with the side chain of Lys-103.

Further, the best docked pose view of compound **32g** demonstrated that it shared several common hydrophobic interactions as displayed by **32m**. For example, THQ and chlorophenyl entity of compound **32g** exhibited hydrophobic interactions with residues like Tyr-181, Tyr-188,

Leu-100, Tyr-318, Leu-234 and Val-119, while its methoxyphenyl wing showed similar interactions with Val-179 (Fig. **7.16**).

Overall, compound **32g** showed less intense hydrophobic interactions compared to compound **32m**; moreover compound **32g** also lack hydrogen bonding interaction with Lys-103. So, distinct interaction pattern may be accounted for the difference in the *in-silico* binding affinity of both compounds and consequently better *in-vitro* activity of **32m** (57.34% inhibition) compared to compound **32g** (17.86% inhibition) against HIV-1 RT.

7.1.8 Docked pose analysis of best (38b) and least active (38m) compounds from series 38a-o

The best docked pose view of compound **38b** (Fig. **7.17**) revealed that its 2-methylphenyl moiety showed prominent hydrophobic interaction with residues like Tyr-181, Tyr-188, Trp-229 and Pro-95, while its piperazine moiety exhibited similar interactions with Leu-100 and Val-179 residues. Furthermore, its THQ entity showed hydrophobic interaction with Val-179 and carbonyl group adjacent to the piperazine ring exhibited dual hydrogen bonding interaction with the hydrophilic residues Lys-101 and Lys-103, which additionally enhanced its binding affinity with the target protein.

Compound **38m** displayed overall prominent hydrophobic interactions inside the NNIBP, but its binding mode was found to be fairly distinct from **38b** (Fig. **7.18**). 6-methoxy-THQ entity of **38m** showed hydrophobic interaction with residues like Tyr-181, Trp-229, Tyr-188, Phe-227 and Leu-234 while linker along with piperazine moiety showed similar interactions with Leu-234, Val-106 and Leu-100. Benzyl moiety of compound **38m** showed hydrophobic interactions with Leu-100, Val-179 and Tyr-181.

Although, overall the intensity of hydrophobic interaction appeared more prominent in compound **38m** compared to compound **38b,** however amidic C=O of compound **38b** actively participated in hydrogen bonding interactions (with Lys-101 and Lys-103), while no such interactions were observed in **38m**. Moreover, ligand **38m** appeared more strained inside the NNIBP compared to **38b**, so these factors may be accounted as probable reason for better *in-vitro* HIV-1 RT activity of compound **38b**, (IC_{50} 12.48 µM) compared to compound **38m** (IC_{50} >100 µM).

7.1.9 Docked pose analysis of best (43m) and least active (43f) compounds from series 43a-p

Best scoring docked pose view of compound **43m** revealed that its *p*-nitrophenyl moiety displayed strong hydrophobic interactions with Tyr-188, Tyr-181 and Trp-229 residues (Fig.**7.19**), moreover it also showed *pi-pi* stacking interaction with Trp-229. Quinoline moiety of compound **43m** showed hydrophobic interactions with Phe-106, Val-106, Leu-100 and Tyr-318 residues. Further, it was noteworthy that in spite the prominent hydrophobic interactions, the central linker of compound **43m** lacks hydrogen bonding interaction with Lys-101.

In the docked pose view of compound **43f,** *p*-fluorophenyl exhibited weak hydrophobic interactions (with residues Tyr-181, Val-179 and Leu-100)**,** while connecting linker along with the quinoline moiety showed similar interactions of moderate intensity with residues Tyr-188, Trp-229, Leu-234, Phe-227 and Tyr-318 (Fig. **7.20**).

Overall, unlike compound **43m**, compound **43f** lacks *pi-pi* stacking interaction and showed less binding affinity compared to compound **43m**, consequently which may be responsible for the weak *in-vitro* HIV-1 RT inhibitory potential of compound **43f** (18.26% inhibition) compared to compound **43m** (64.74% inhibition).

7.1.10 Docked pose analysis of best (51m) and least active (51n) compounds from series 51a-n

Best scoring docked pose view of compound **51m** (Fig. **7.21**) revealed that its chlorophenyl moiety exhibited prominent *pi-pi* stacking interaction with residues Tyr-188; it also interacted with residues Phe-227 and Trp-229 *via* hydrophobic interaction, while second aromatic moiety (benzyl) exhibited similar interactions with Val-106 and Trp-318. Further, central axis of compound **51m** consisting of carbonyl phenylpiperazine moiety showed hydrophobic interactions with Tyr-181 and Val-179 residues. So, the presence of prominent *pi-pi* stacking and hydrophobic interactions may be responsible for strong binding of compound **51m** inside the NNIBP and subsequently for considerable anti-HIV-1 RT activity (IC_{50} 12.26 µM).

In contemporary, docked pose view of compound **51n** showed quite distinct binding mode compared to compound **51m**. Compound **51n** constituted two bulky wings at the both terminals (Fig. **7.22**), at one terminal it possessed benzhydryl moiety which showed hydrophobic interaction of good intensity with residues like Tyr-181, Tyr-188, Trp-229, Val-106, Tyr-318 and Leu-234. Further, piperazine moiety along with the connecting linker displayed hydrophobic interaction of weak intensity with Val-179 and Leu-100 residues. Unfortunately, the other distal

wing of molecule constituted *p*-chlorophenyl and benzyl moiety lied outside the NNIBP and not participated in interactions.

So, overall compound **51n** interacted with the target receptor in the less favoured way compared to **51m**, which may be responsible for the weak *iv-vitro* potency (IC_{50} >100 µM) of compound **51n**.

7.1.11 Docked pose analysis of best (54b) and least active (54i) compounds from series 54a-k

Compound **54b** was found to be the best inhibitor of HIV-1 RT during the *in-vitro* assay, among all series of compounds with submicromolar potency. Putative binding mode of this compound (Fig. **7.23**) was found somewhat similar to approved drug efavirenz, for example, cyclopropyl moiety of efavirenz exhibited prominent hydrophobic interactions with residues like Tyr-181, Tyr-188, Trp-229 and Leu-237 (Fig. **7.1**). In the similar fashion, 2-methoxyphenyl entity of compound **54b** showed similar prominent interactions with aforementioned residues and also with residue Phe-227 additionally. Further, C=O and N-H functionalities of oxazinone ring in efavirenz showed hydrogen bonding interaction with Lys-101, in the same way -NH group of oxindole ring in compound **54b** also exhibited similar interaction with Lys-101. Further, phenyl ring of efavirenz showed hydrophobic interaction with residues like Val-106 and Tyr-318, corresponding to this, chlorophenyl entity of compound **54b** showed similar interaction with same residues. Overall, compound **54b** shared pharmacophoric similarity with efavirenz and also exhibited similar binding pattern with HIV-1 RT and subsequently exhibited potent RT inhibitory activity (IC_{50} 0.27 µM) during the *in-vitro* assay.

However, in docked pose, compound **54i** occupied reverse orientation in contemporary to compound **54b,** for example, its chlorophenyl moiety showed hydrophobic interaction of moderate intensity with residues like Phe-227, Val-106 and Tyr-188, while its dimethoxyphenyl entity along with central linker showed similar interaction with Leu-100, Val-179 and Tyr-181 (Fig. **7.24**). Further, -NH functionality of oxindole in compound **54i** lacks hydrogen bonding interaction with residue Lys-101, instead of this Lys-101 showed hydrogen bonding interaction with 4-methoxy group of phenyl ring.

Overall, striking difference in the binding pattern of both compounds and poor *in-silico* binding affinity of compound **54i** may justify its weak *in-vitro* HIV-1 RT potency (IC_{50} 73.08 µM).

7.2 Key findings from docked pose analysis

Overall, docked pose analysis of docking results were performed for the best and least active compounds from each of the series in order to predict their putative binding mode inside the NNIBP of HIV- RT. Further, studies revealed that compounds of different series showed quite a variance in their binding mode. Moreover, in several cases, compounds of same series having the difference of single substitution on the phenyl ring also showed surprising difference in the binding pattern, which may be attributed due to the extra flexibility of NNIBP [5]. Although, preliminary selection of core nucleus of all scaffolds was done based on the extensive docking studies against the three strains of HIV-1 RT (Chapter **4**), and selection criteria were docking score and types of residues interacting with the tested ligands. However, comparative binding studies of the best and least compounds provided more detailed information regarding the putative binding mode of tested compounds.

Furthermore, to a considerable extent, this information can also help in predicting probable reason for the variance in the *in-vitro* potencies of compounds against HIV-1 RT. This elaborate study emphasized on several factors which contributed in the effective binding of the ligand with HIV-1 RT, like hydrogen bonding interaction, *pi-pi* stacking interaction and hydrophobic interactions. In overall study, we found that although the nature of residues interacting with the ligand play a vital role while estimating the stability of the receptor-ligand complex, but the way they interacted play even a better significant role. For example, aromatic residues like Tyr-181, Tyr-188, Phe-227 and Trp-229 showed hydrophobic interactions with majority of ligands, but in some ligands (like **5l**, **9h**, **14j, 43m** and **51m**) aromatic component of such residues lie in co-planner with aromatic part of ligands, in such cases apart from the hydrophobic interactions, *pi-pi* stacking interaction came into role and enhanced the stability of receptor-ligand complex. In cases, where the size of both hydrophobic wings is very large with a lengthy connecting linker (like **51n**), or the ligand having strained conformation in the binding state (like **38m**), both conditions may also hamper their stability with HIV-1 RT. So, for the future perspective, molecular dynamics study on the ligand-receptor complex can be performed in order to better predict the stability of complex and subsequently for the prediction of *in-vitro* activity.

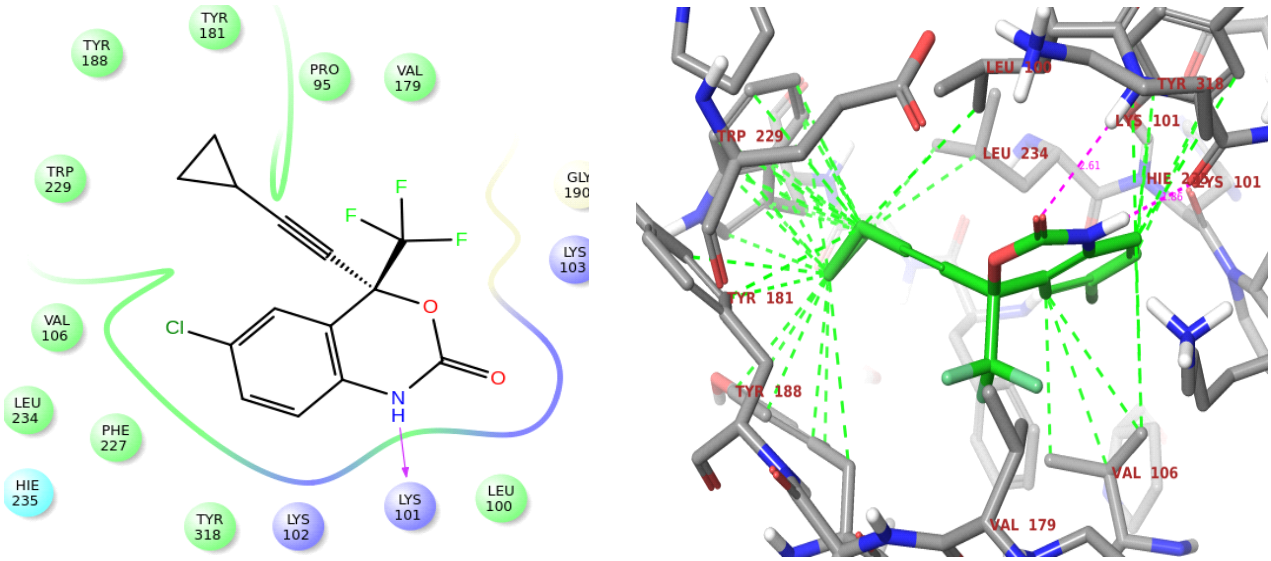

7.1a **7.1b**

Fig. 7.1 Docked pose of efavirenz inside the NNIBP of RT enzyme, showing two dimensional interactive diagram (**7.1a)** and three dimensional docked view (**7.1b**) showing hydrophobic and hydrogen bonding interactions represented by green and pink dotted lines, respectively

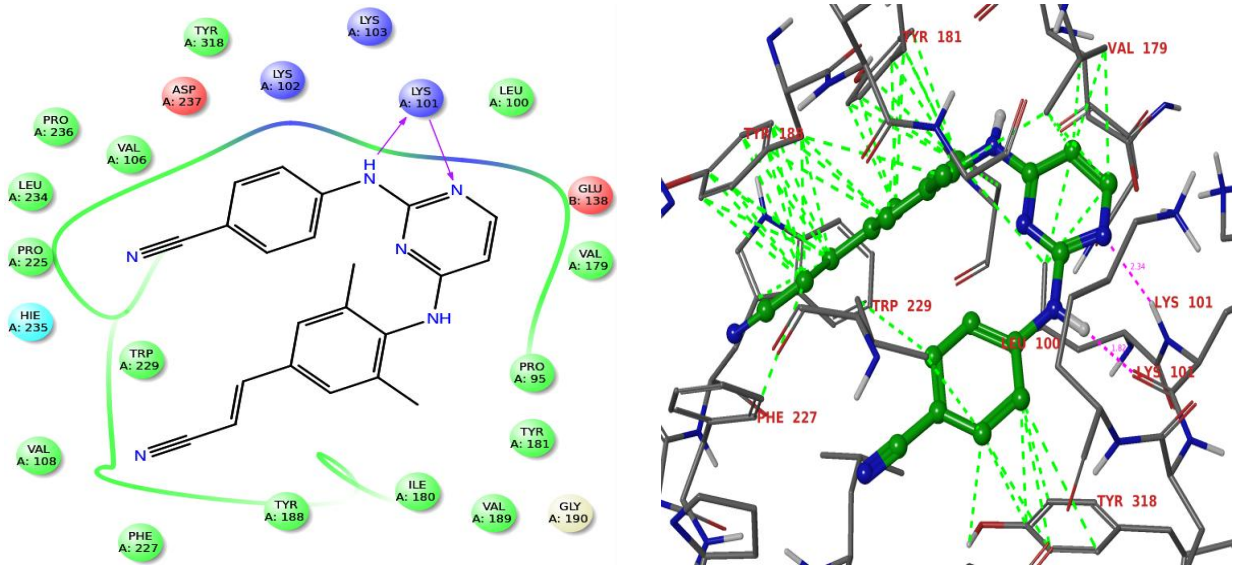

7.2a **7.2b**

Fig. 7.2 Docked pose of rilpivirine inside the NNIBP of RT enzyme, showing two dimensional interactive diagram (**7.2a)** and three dimensional docked view (**7.2b**) showing hydrophobic and hydrogen bonding interactions represented by green and pink dotted lines, respectively

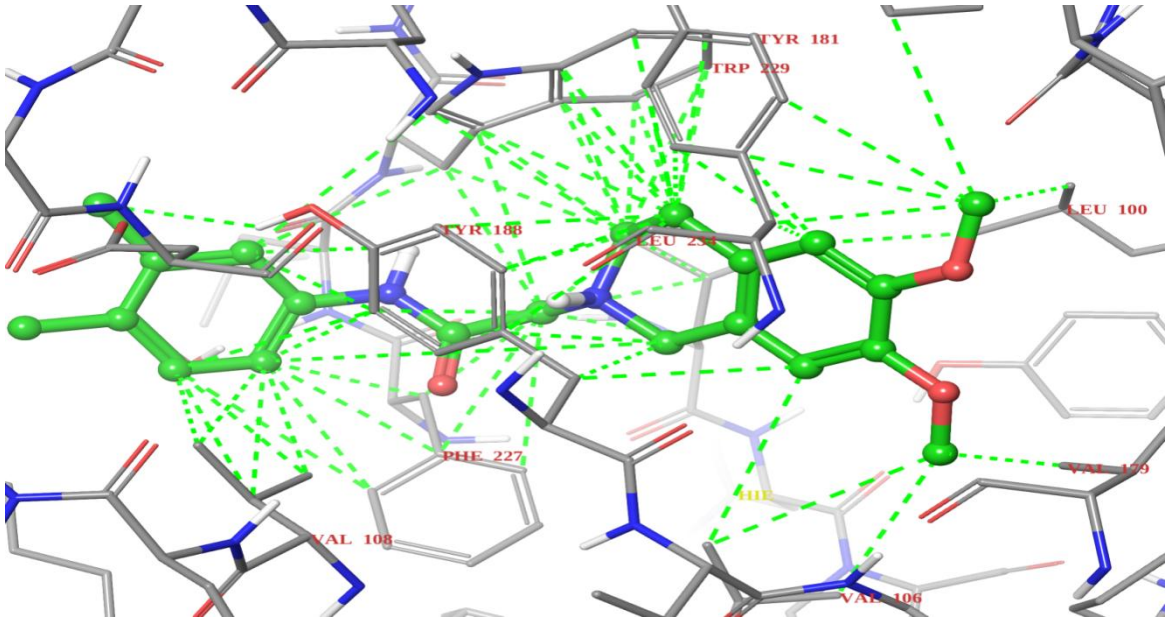

Fig. 7.3 Docked pose of compound **5n** inside the NNIBP of 3MEE enzyme, showing hydrophobic interactions represented by green dotted lines

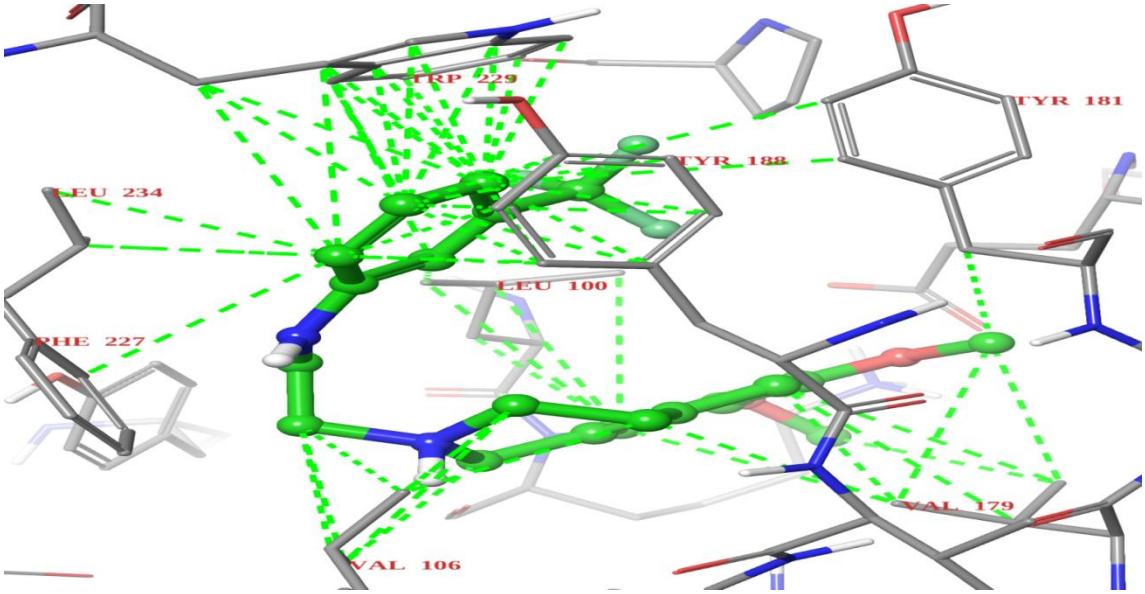

Fig. 7.4 Docked pose of compound **5l** inside the NNIBP of 3MEE enzyme, showing hydrophobic interactions represented by green dotted lines

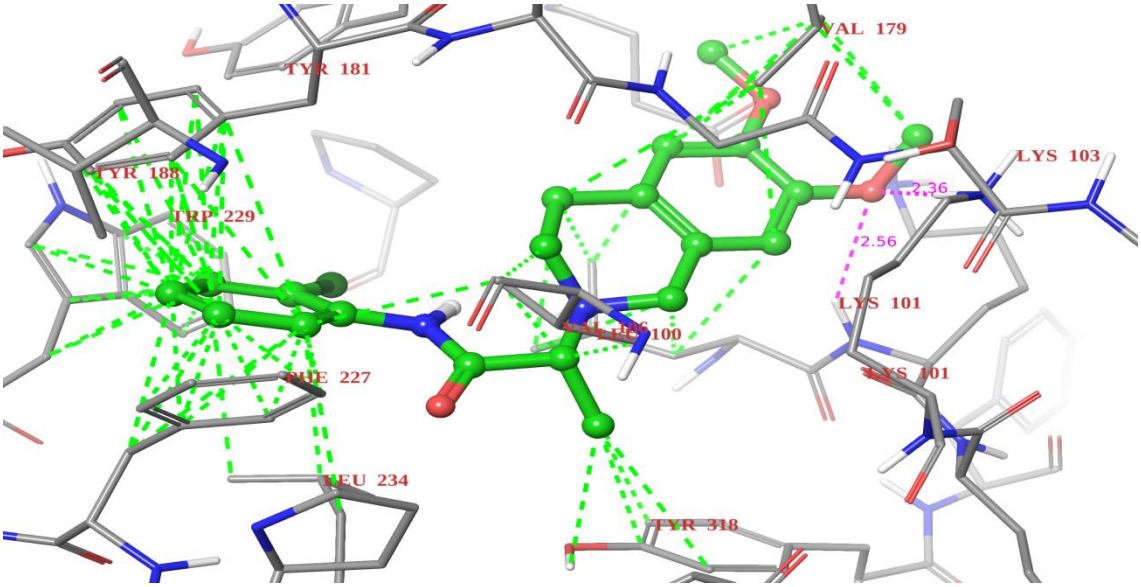

Fig. 7.5 Docked pose of compound **9h** inside the NNIBP of 3MEE enzyme, showing hydrophobic and hydrogen bonding interactions represented by green and pink dotted lines, respectively

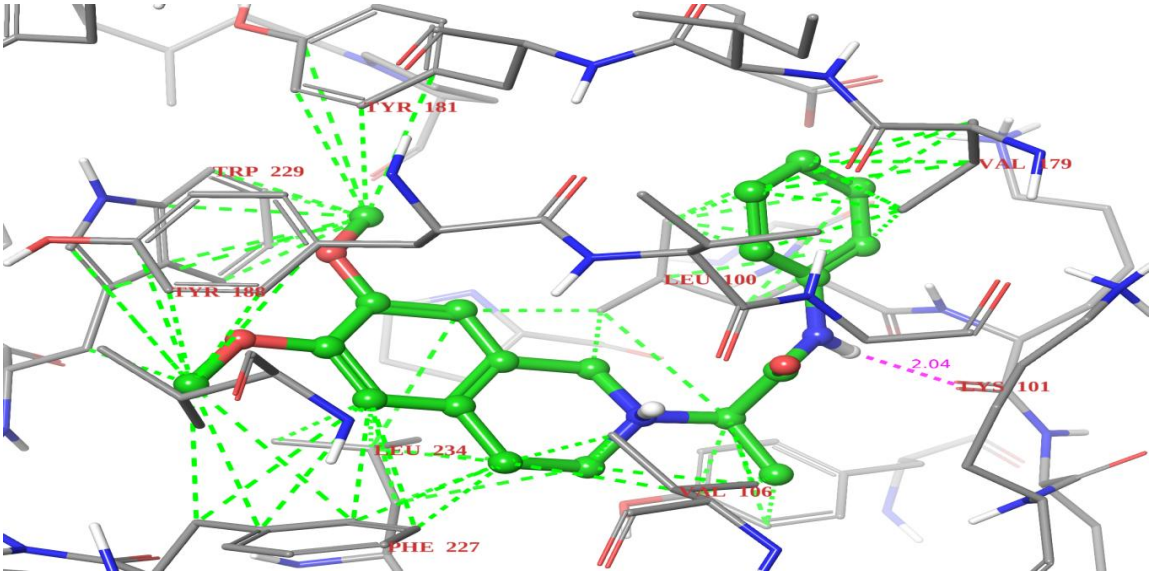

Fig. 7.6 Docked pose of compound **9a** inside the NNIBP of 3MEE enzyme, showing hydrophobic and hydrogen bonding interaction represented by green and pink dotted lines, respectively

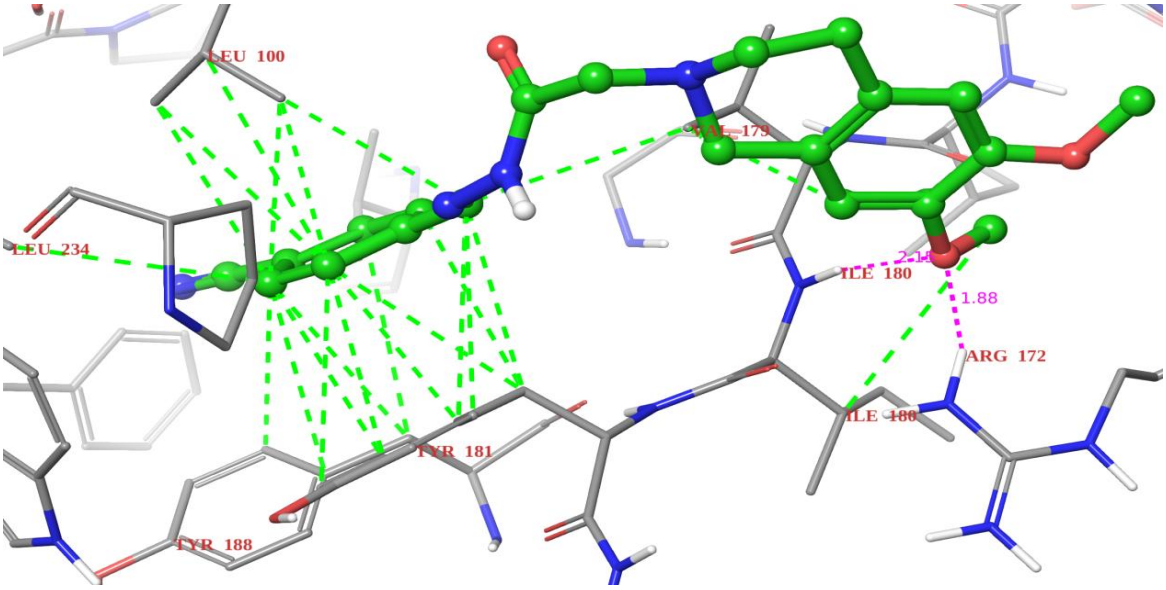

Fig. 7.7 Docked pose of compound **14j** inside the NNIBP of 3MEE enzyme, showing hydrophobic and hydrogen bonding interactions represented by green and pink dotted lines, respectively

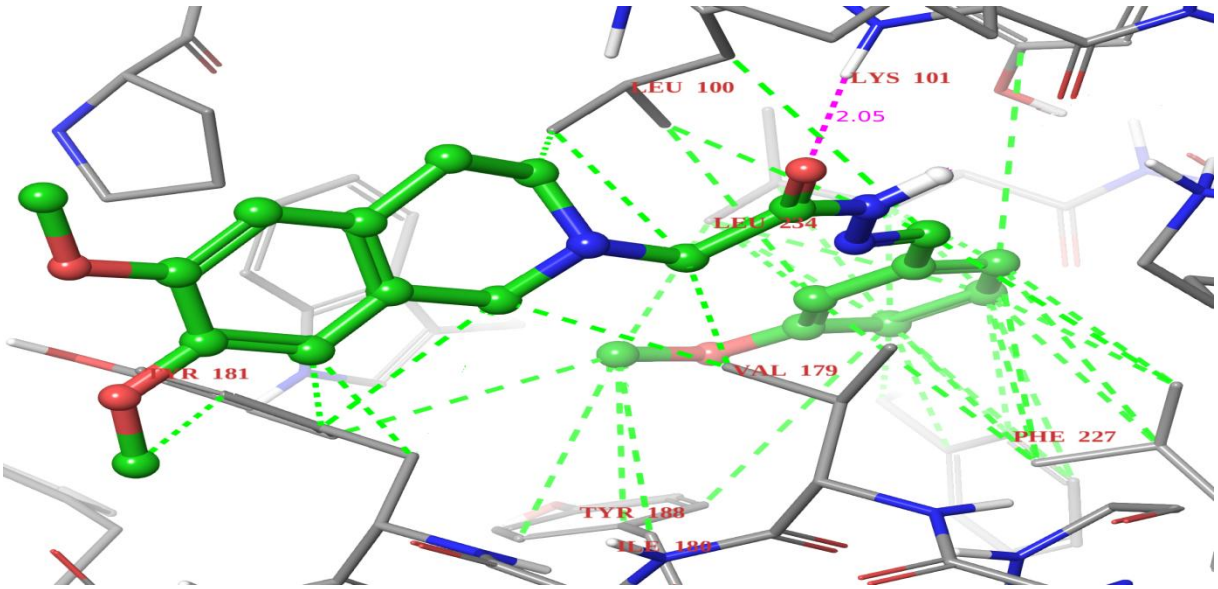

Fig. 7.8 Docked pose of compound **14b** inside the NNIBP of 3MEE enzyme, showing hydrophobic and hydrogen bonding interactions represented by green and pink dotted lines, respectively

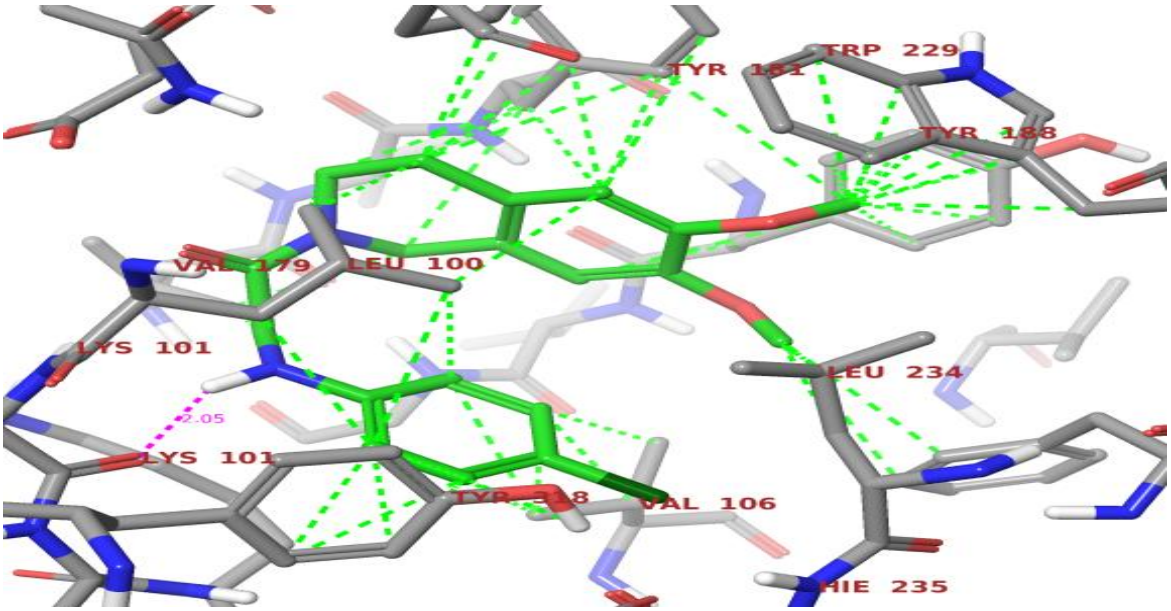

Fig. 7.9 Docked pose of compound **17h** inside the NNIBP of 3MEE enzyme, showing hydrophobic and hydrogen bonding interactions represented by green and pink dotted lines, respectively

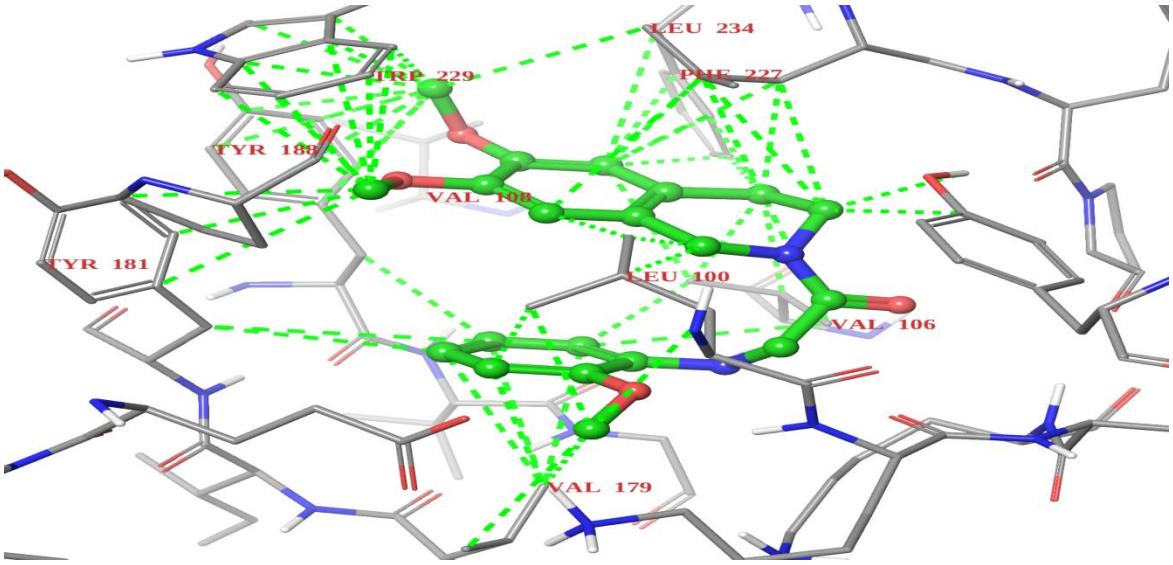

Fig. 7.10 Docked pose of compound **17a** inside the NNIBP of 3MEE enzyme, showing hydrophobic interactions represented by green dotted lines

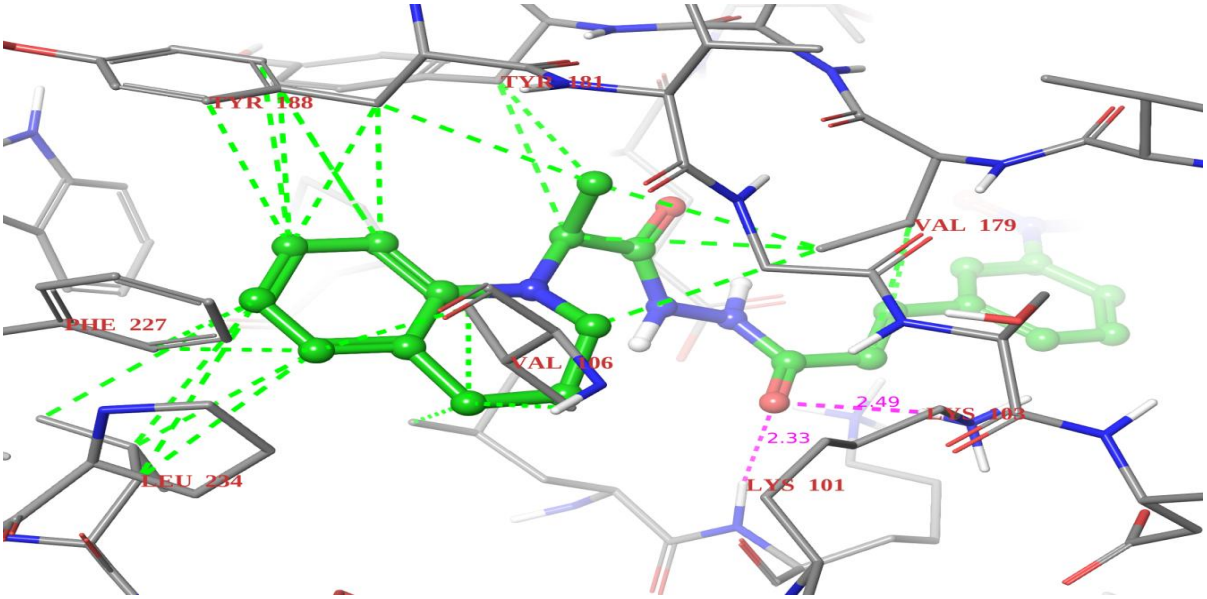

Fig. 7.11 Docked pose of compound **23o** inside the NNIBP of 3MEE enzyme, showing hydrophobic and hydrogen bonding interactions represented by green and pink dotted lines, respectively

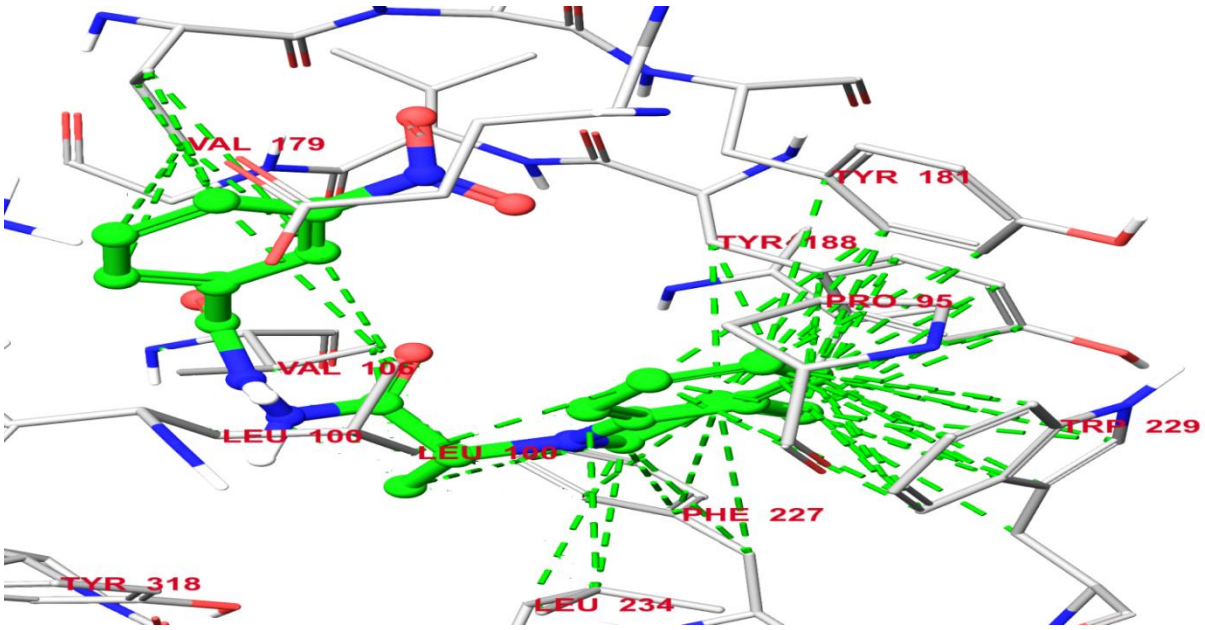

Fig. 7.12 Docked pose of compound **23i** inside the NNIBP of 3MEE enzyme, showing hydrophobic interactions represented by green dotted lines

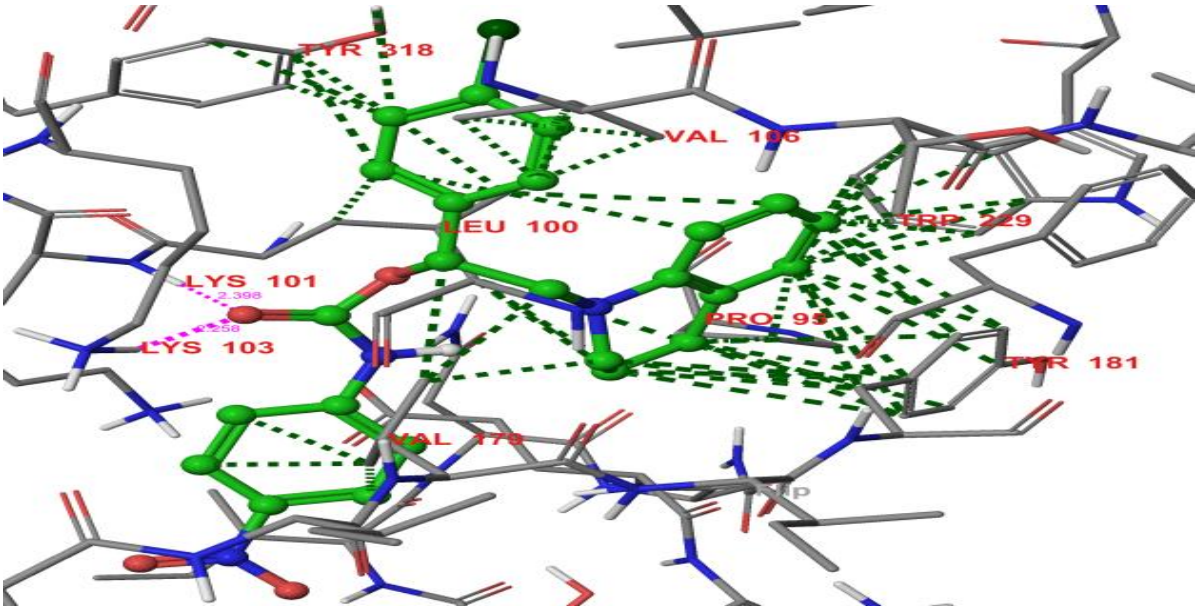

Fig. 7.13 Docked pose of compound **28j** inside the NNIBP of 3MEE enzyme, showing hydrophobic and hydrogen bonding interactions represented by green and pink dotted lines, respectively

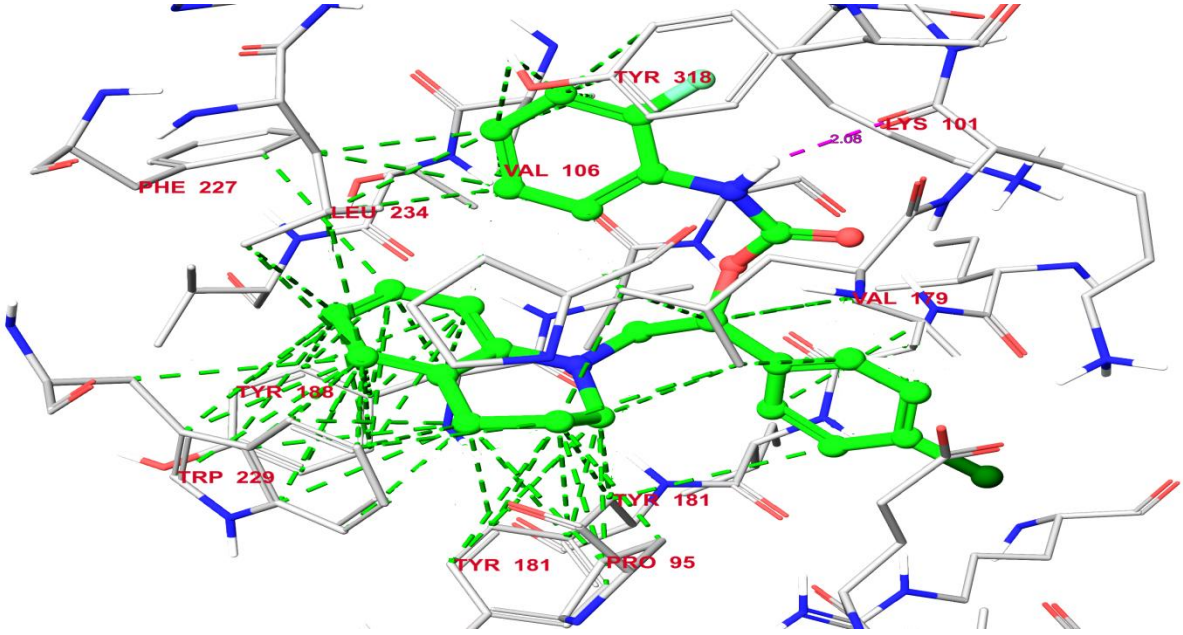

Fig. 7.14 Docked pose of compound **28e** inside the NNIBP of 3MEE enzyme, showing hydrophobic and hydrogen bonding interactions represented by green and pink dotted lines, respectively

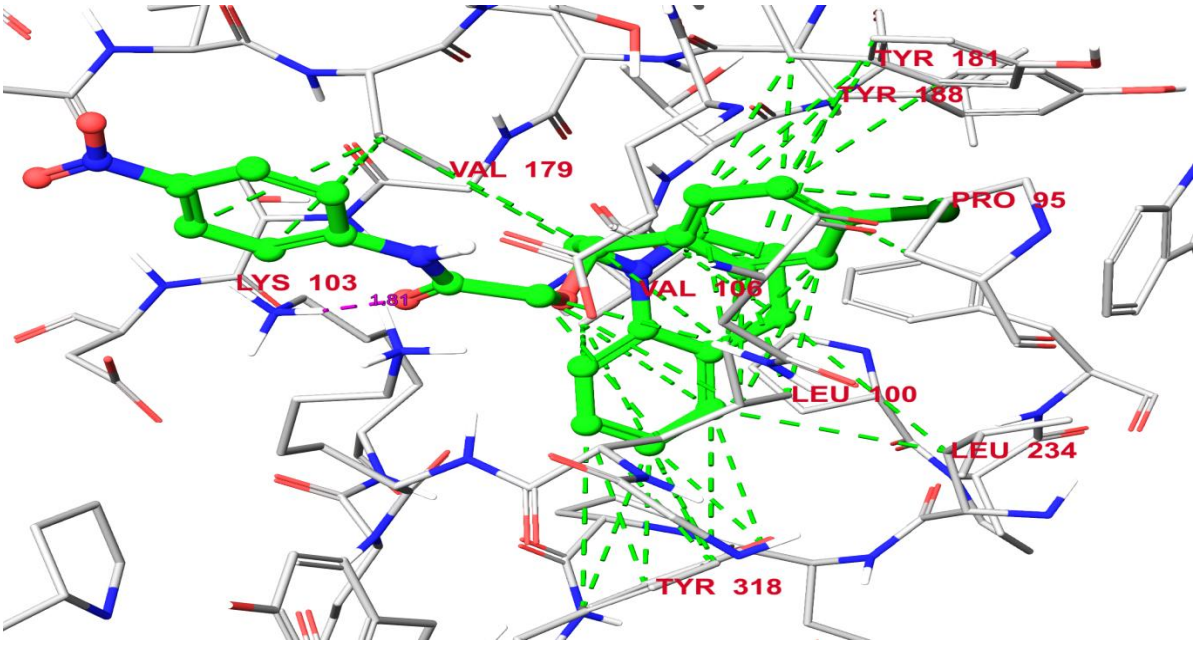

Fig. 7.15 Docked pose of compound **32m** inside the NNIBP of 3MEE enzyme, showing hydrophobic and hydrogen bonding interactions represented by green and pink dotted lines, respectively

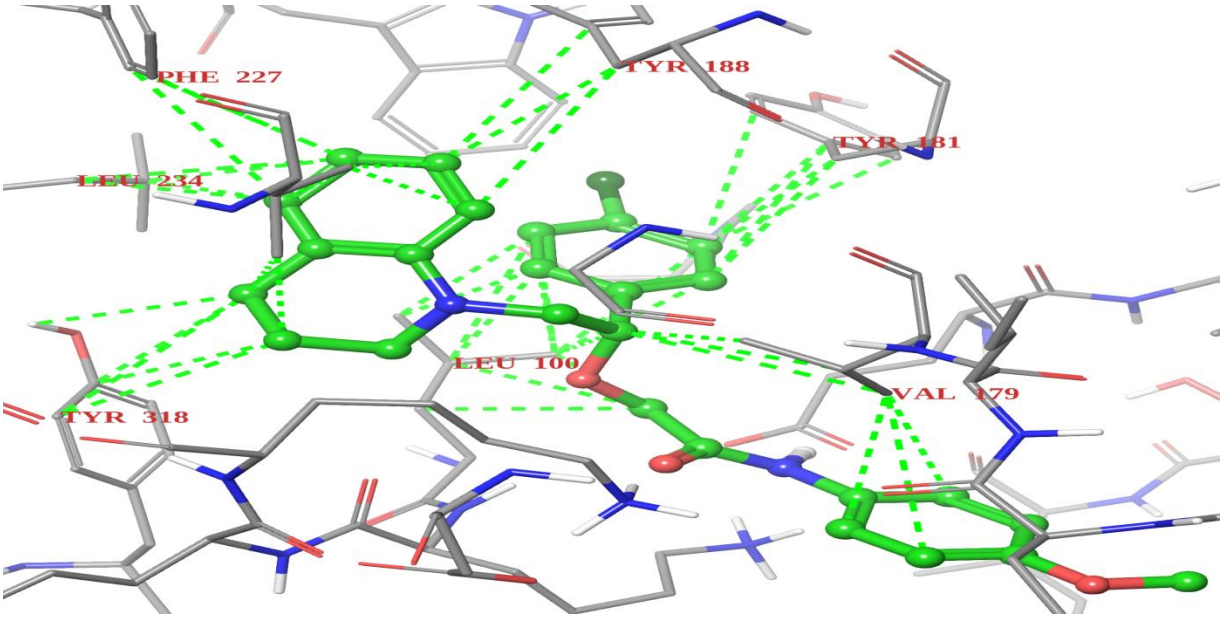

Fig. 7.16 Docked pose of compound **32g** inside the NNIBP of 3MEE enzyme, showing hydrophobic interactions represented by green dotted lines

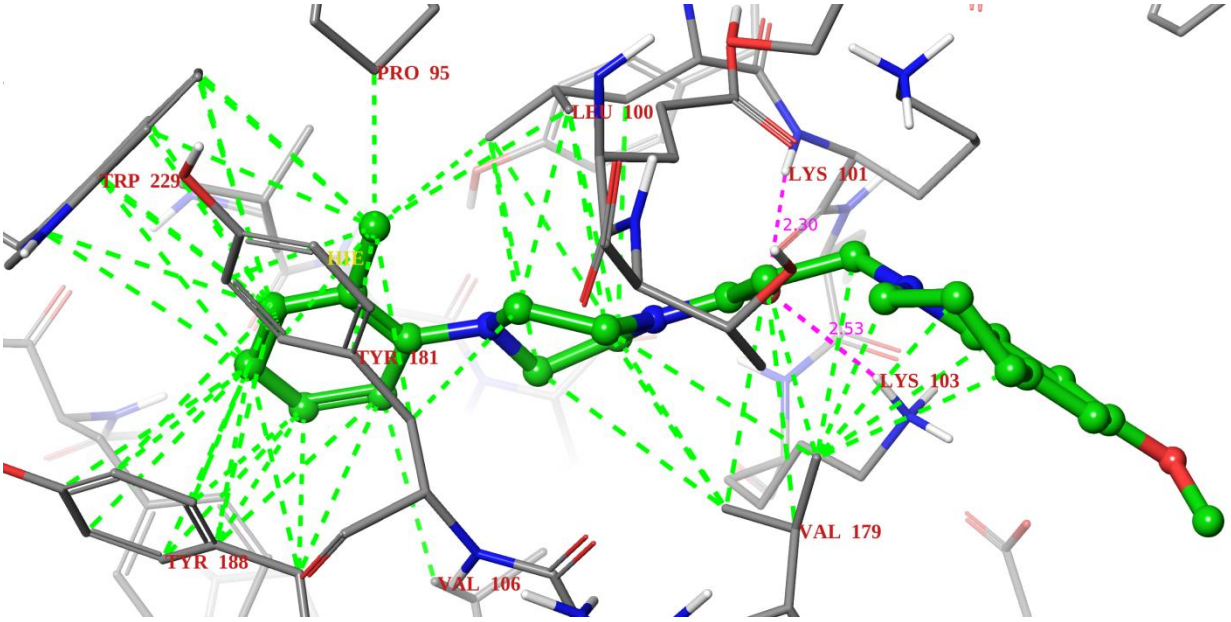

Fig. 7.17 Docked pose of compound **38b** inside the NNIBP of 3MEE enzyme, showing hydrophobic and hydrogen bonding interactions represented by green and pink dotted lines, respectively

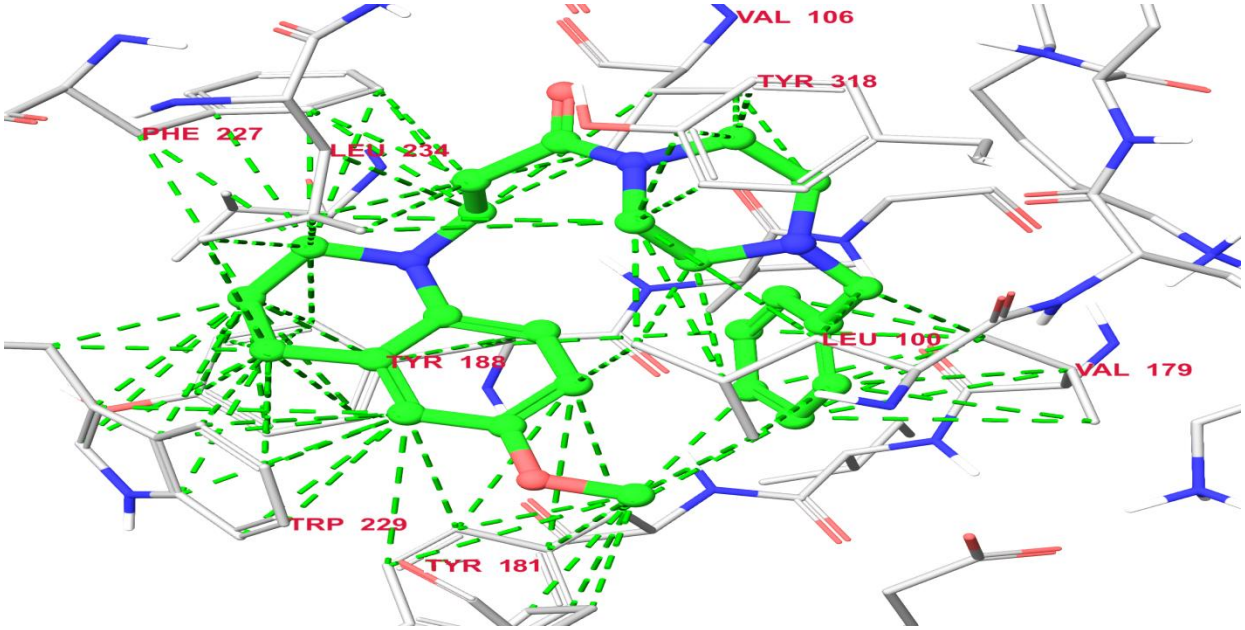

Fig. 7.18 Docked pose of compound **38m** inside the NNIBP of 3MEE enzyme, showing hydrophobic interactions represented by green dotted lines

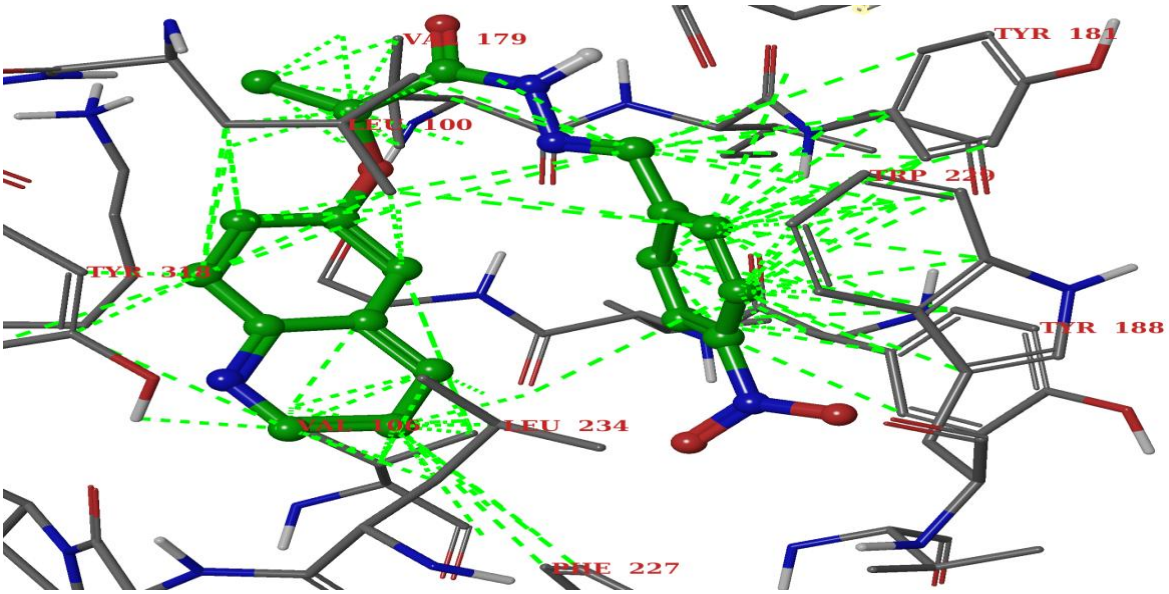

Fig. 7.19 Docked pose of compound **43m** inside the NNIBP of 3MEE enzyme showing hydrophobic interactions represented by green dotted lines

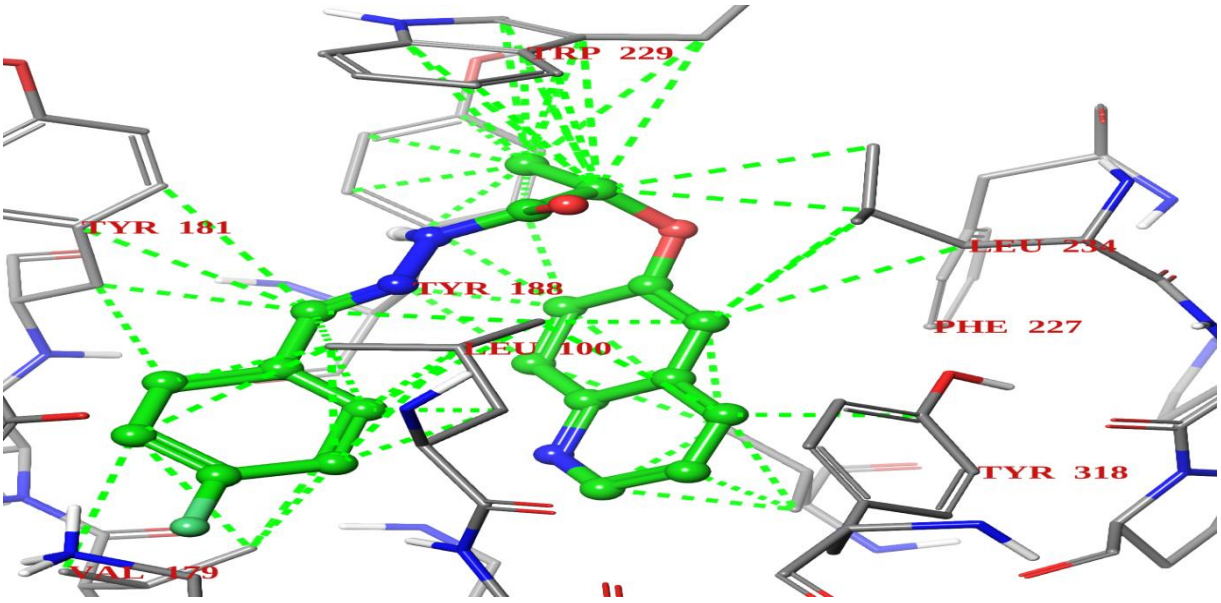

Fig. 7.20 Docked pose of compound **43f** inside the NNIBP of 3MEE enzyme showing hydrophobic interactions represented by green dotted lines

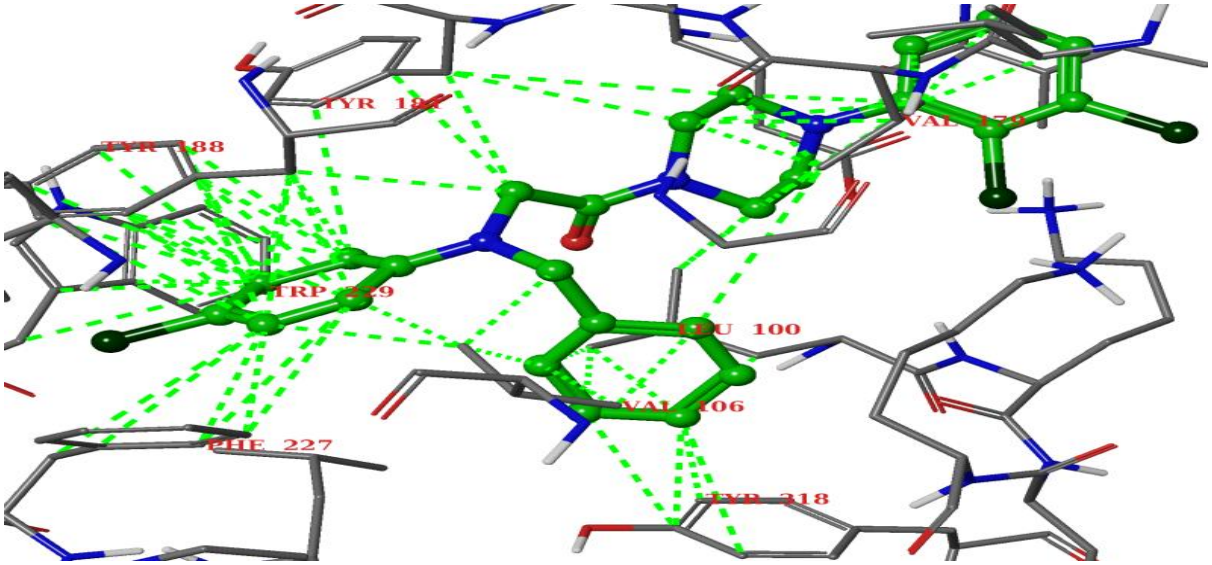

Fig. 7.21 Docked pose of compound **51m** inside the NNIBP of 3MEE enzyme showing hydrophobic interactions represented by green dotted lines

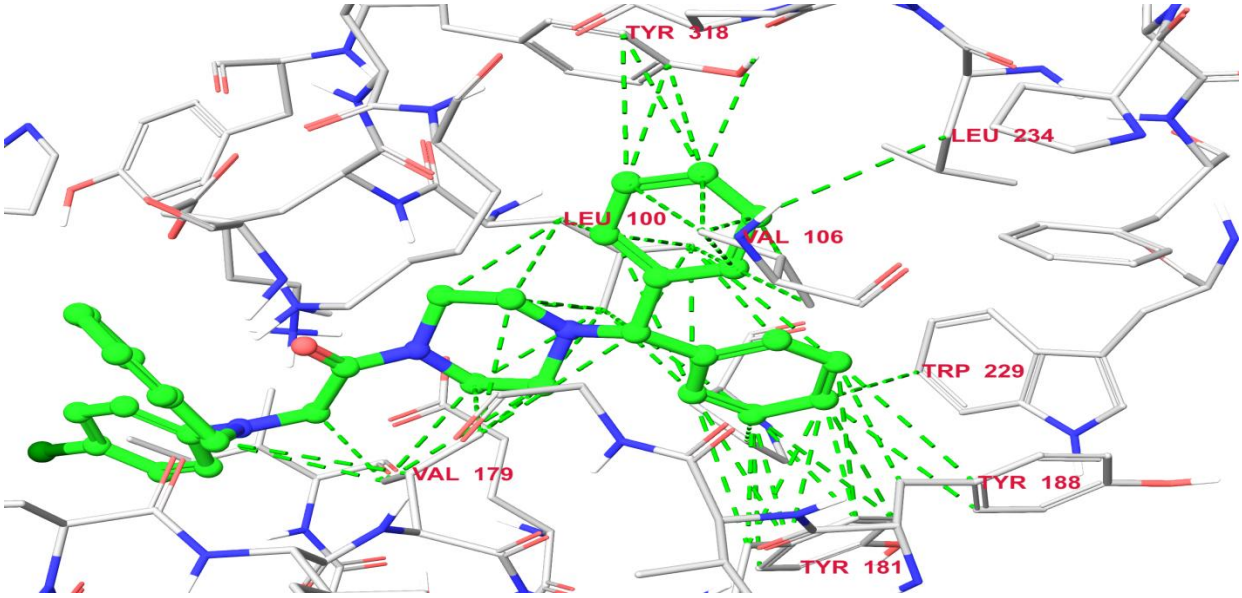

Fig. 7.22 Docked pose of compound **51n** inside the NNIBP of 3MEE enzyme showing hydrophobic interactions represented by green dotted lines

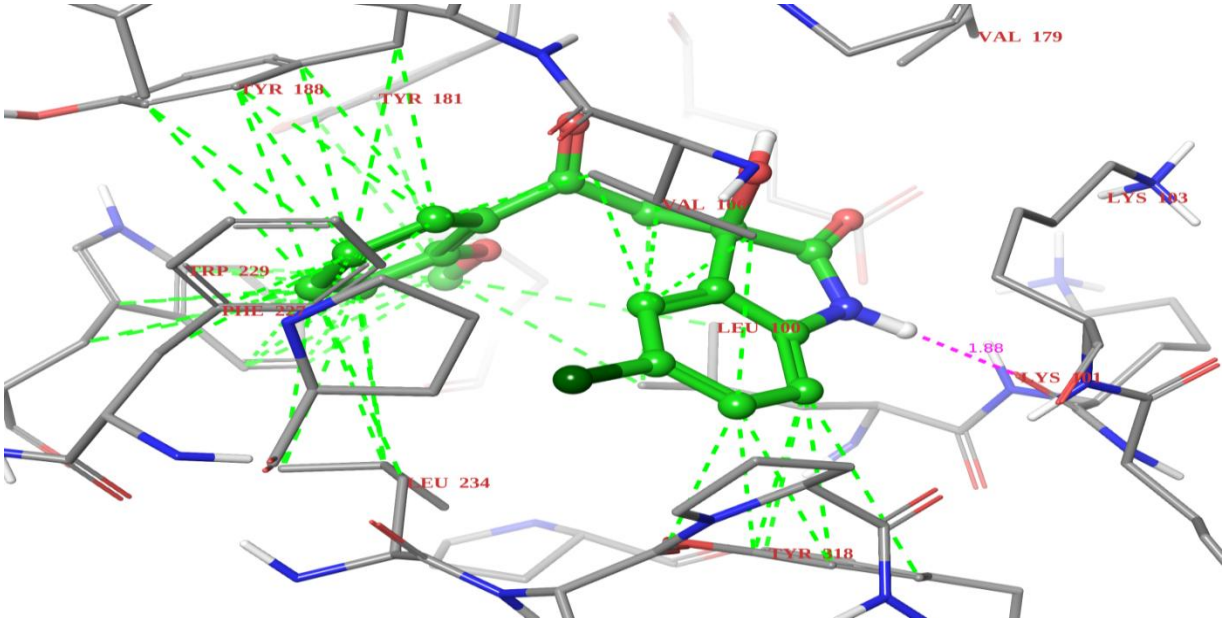

Fig. 7.23 Docked pose of compound **54b** inside the NNIBP of 3MEE enzyme, showing hydrophobic and hydrogen bonding interactions represented by green and pink dotted lines, respectively

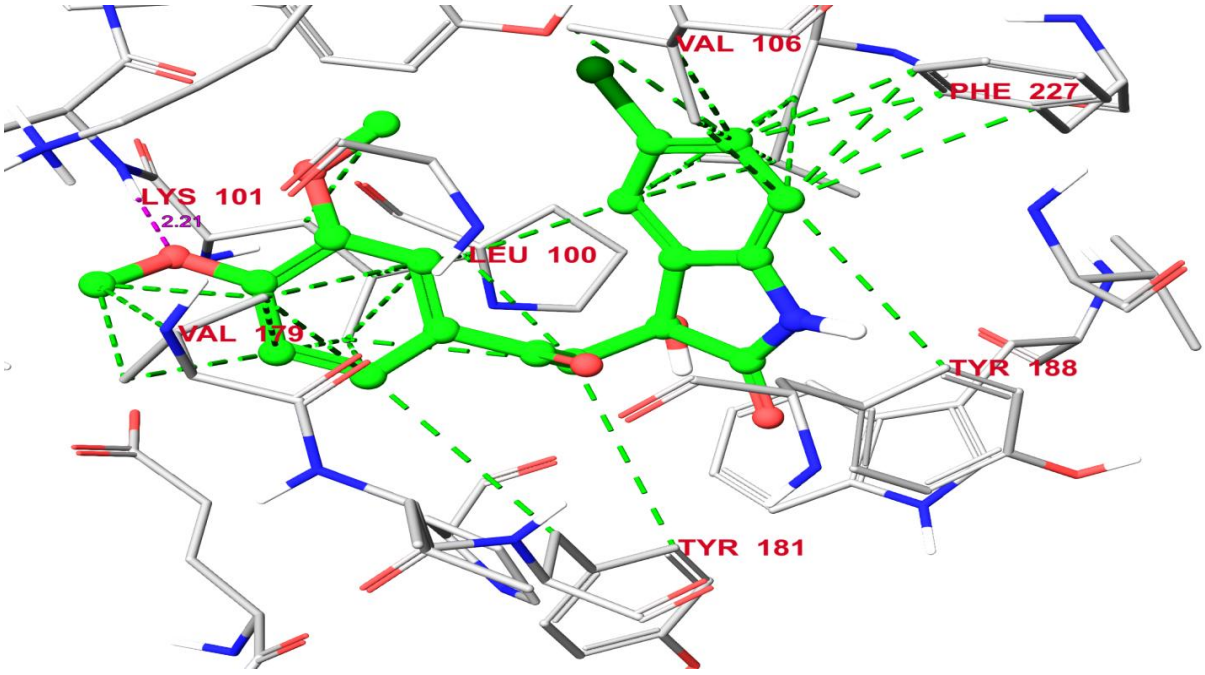

Fig. 7.24 Docked pose of compound **54i** inside the NNIBP of 3MEE enzyme, showing hydrophobic and hydrogen bonding interactions represented by green and pink dotted lines, respectively

7.3 References

1. Glide, Schrödinger, LLC, New York, Version 5.9, (2013).
2. E.B Lansdon, K.M. Brendza, M. Hung, R. Wang, S. Mukund, D. Jin, G. Birkus, Crystal structures of HIV-1 Reverse Transcriptase with Etravirine (TMC125) and Rilpivirine (TMC278): Implications for drug design. Journal of Medicinal Chemistry 53 (2010) 4295-4299.
3. http://www.rcsb.org/pdb/explore/explore.do?structureId=3mee, accessed on 14 May, 2013.
4. D.L. Mobley, K.A. Dill, Binding of small-molecule ligands to proteins: "what you see" is not always "what you get". Structure. 17 (2009) 489-498.
5. K.A. Paris, O. Haq, A.K. Felts, K. Das, E. Arnold, R.M. Levy, Conformational landscape of the human immunodeficiency virus type 1 reverse transcriptase non-nucleoside inhibitor binding pocket: Lessons for inhibitor design from a cluster analysis of many crystal structures. Journal of Medicinal Chemistry, 52 (2009) 6413-6420.

CHAPTER 8

Summary and Conclusions

In the present dissertation work, attempts were made for the design, synthesis and biological evaluation of nitrogen containing heterocyclic compounds as novel HIV-1 RT inhibitors. Furthermore, few selected compounds were tested for anti-HIV-1 activity and cytotoxicity, while all compounds were screened against some opportunistic infective microbes which are associated with AIDS. The microbial strains used for the study were; *Mycobacterium tuberculosis*, four bacterial strains (*S. aureus*, *B. cereus*, *E. coli* and *P. putida*) and two fungal strains (*C. albicans* and *A. niger*). Overall dissertation work can be summarized as:

- Total thirty one nitrogen containing heterocyclic scaffolds containing tetrahydroisoquinoline, tetrahydroquinoline, quinoline, piperazine and oxindole were designed as NNRTIs and *in-silico* screened against three strains of HIV-1 RT (one wild and two mutant strains).
- Eleven scaffolds from the above mentioned thirty one were selected based upon the *in-silico* activity against three selected strains and series of compounds (**5a-o, 9a-o, 14a-k, 17a-o, 23a-o, 28a-l, 32a-n, 38a-o, 43a-p, 51a-n** and **54a-k**) were generated.
- Drug-likeness behavior of the designed compounds was accessed based upon *in-silico* predicted physico-chemical and pharmacokinetic parameters.
- Target compounds were synthesized, characterized and screened for HIV-1 RT inhibitory activity using ELISA based *in-vitro* assay.
- Preliminary screening studies against HIV-1 RT (at 100 µM concentration), revealed that none of the compounds of series **14a-k** and **23a-o** displayed significant activity (% inhibition of RT remained <50)**,** while only one compound of series **32a-n** was found to be significantly active.
- Compounds of series **5a-o, 9a-o, 17a-o,** and **43a-p** showed better activity compared to the above mentioned series in which five, five, thirteen and nine compounds, respectively displayed significant inhibition of RT activity but none of the compounds exhibited much encouraging results, moreover their RT inhibitory ability remained <75 % at the tested concentration.
- Compounds of series **28a-l, 38a-o, 51a-n** and **54a-k** displayed overall superior inhibition among the all tested series, moreover several compounds displayed >75% inhibition of HIV-1 RT, therefore, IC_{50} was determined for all the compounds of above four series. The result of the assay revealed that twenty compounds (**28b, 28h, 28i, 28j, 28l, 38a, 38b, 38j, 38k 38o, 51a, 51b, 51d, 51k, 51l**, **51m, 54b, 54d, 54e** and **54k**) collectively from the above four series displayed encouraging potency against RT with IC_{50} ≤25 µM.

- Further, two compounds (**28b** and **28j**) of series **28a-l** and four compounds (**54b, 54d, 54e** and **54k**) of series **54a-k** displayed good potency against RT with IC_{50} ≤10 µM. Moreover, pair of compounds (**54b** and **54e**) of series **54a-k,** showed sub-micromolar potency (IC_{50} 0.27 and 0.76 µM, respectively) against HIV-1 RT and can be considered potent searched hit against the selected target.
- SAR studies on the HIV-1 RT inhibition activity revealed that inhibitory potential of compounds varied markedly with change in the core nucleus; moreover compounds within the same series also displayed significant variability in activity with change in substitution pattern around the phenyl ring.
- Among the four series containing dimethoxy tetrahdyroisoquinoline ring, compounds of series **17a-o** exhibited better inhibition as compared to other series, overall potency against the RT changed in the order **17a-o> 5a-o ≅ 9a-o> 14a-k**.
- Compounds of series **28a-l** showed superior inhibition of RT among the scaffolds containing tetrahydroquinoline ring, followed by series **38a-o**, while two other series (**23a-o** and **32a-n**) possessed moderate to weak inhibition potential.
- Compounds possessed oxindole nucleus (series **54a-k)** exhibited best RT inhibitory potential among the scaffolds based upon quinoline, piperazine and oxindole (**43a-p, 51a-n** and **54a-k,** respectively). RT inhibitory potency of these three series changed in the order **54a-k**> **51a-n**> **43a-p.**
- Overall, HIV-1 RT inhibition potential of the best active four series (**28a-l, 38a-o, 51a-n** and **54a-k**,) out of all tested eleven series varied in the order **54a-k**> **28a-l**> **51a-n**> **38a-o.** Further, pictorial summarization of SAR studies against HIV-1 RT for all series is shown in the figures **8.1** and **8.2.**

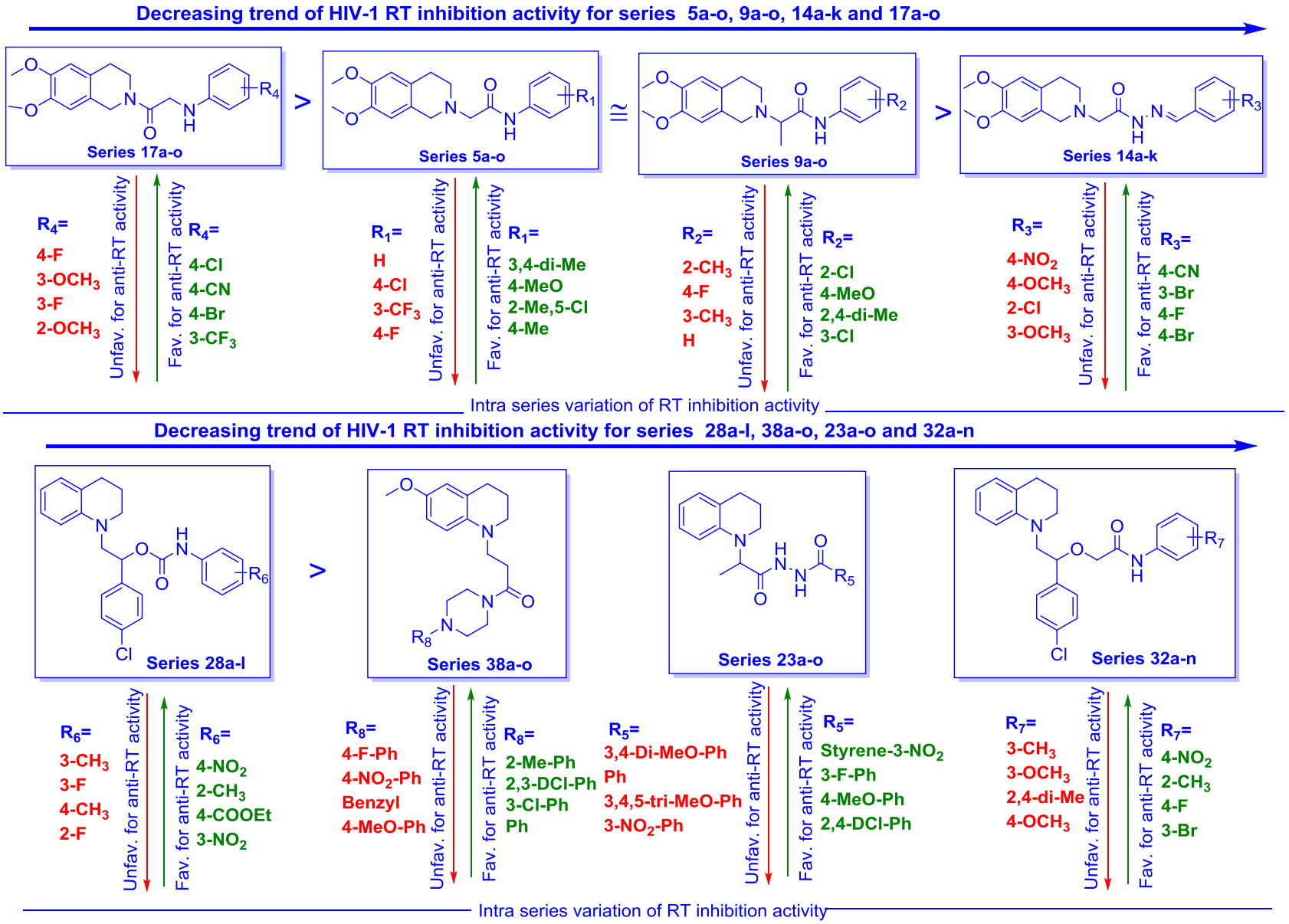

Figure 8.1 Pictorial representation of SAR studies for RT inhibition activity of compounds based on THIQ and THQ

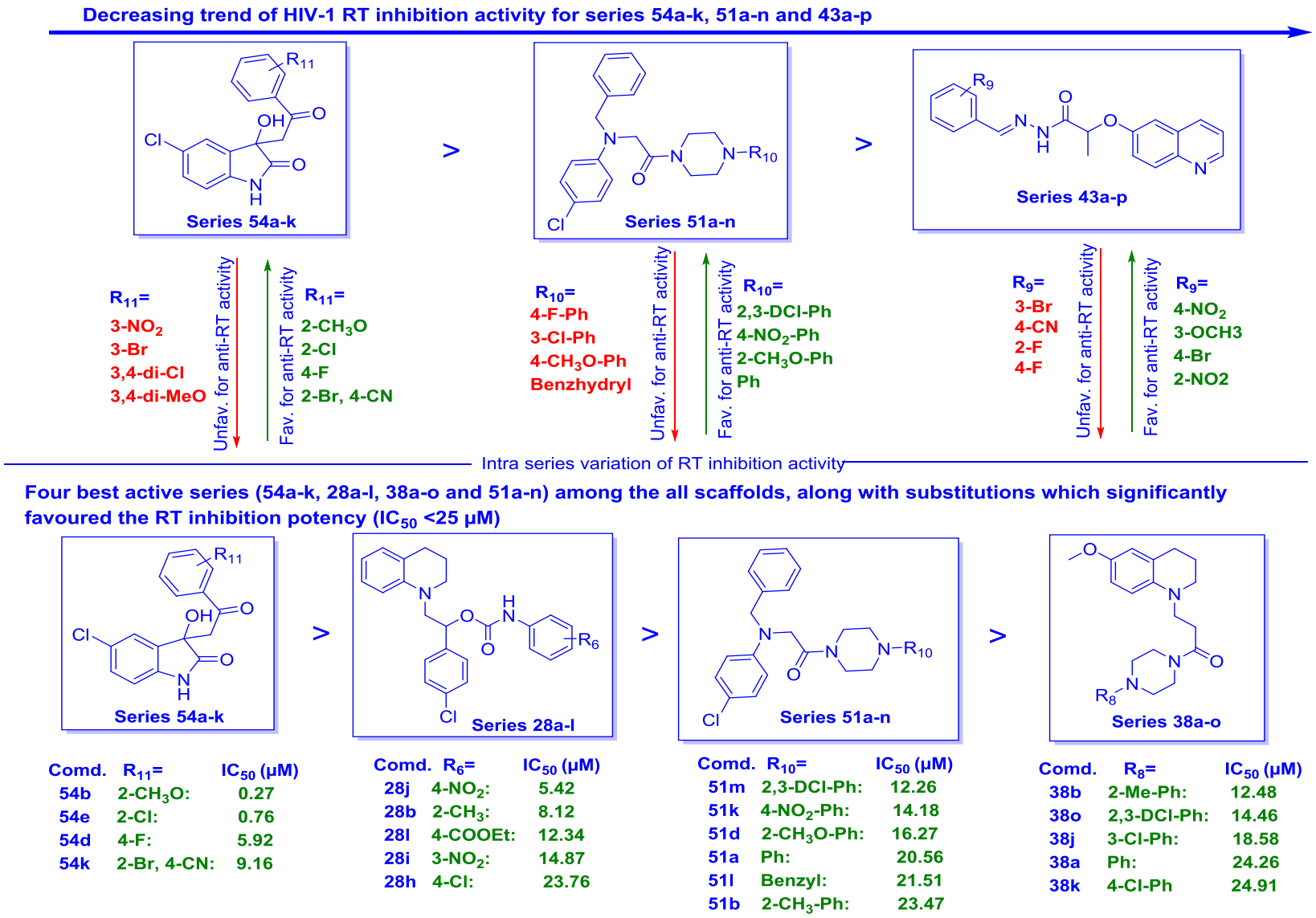

Figure 8.2 Pictorial representation of SAR studies for RT inhibition activity of compounds based on oxindole, piperazine and quinoline, along with four best active scaffolds

- Preliminary selection of core scaffolds (without any substitution) was done based upon the docking studies against the three strains of HIV-1 RT, including one wild strain (Chapter **4**). The selection criteria for the designed scaffolds were docking score and types of residues interacting with the tested ligands.
- Comparative docking studies of the best and least active compounds were performed against wild HIV-1 RT, which provided more detailed information regarding the putative binding mode of tested compounds. Moreover, this information revealed certain other factors like role of *pi-pi* stacking interaction, planarity of the aromatic rings, size of the hydrophobic moiety, strain of the binding ligand etc., which were found to play an important role to establish the overall binding affinity between receptor-ligand complexes. Furthermore, to a considerable extent, this information helped in predicting probable reason for the variance in the *in-vitro* potencies of compounds against HIV-1 RT.
- Fifteen compounds (**28b, 28j, 28l, 38a, 38b, 38j, 38o, 51a, 51d, 51k, 51m, 54b, 54d, 54e** and **54k**) which possessed good/excellent inhibition potency against HIV-1 RT were evaluated for anti-HIV-1 activity and cytotoxicity. The result of the study revealed that eight compounds (**28j, 38b, 51a, 51k, 51m, 54b, 54e** and **54k**) displayed good to excellent potency against HIV-1 (EC_{50} <10 µg/mL), six compounds (**28b**, **28l**, **38a**, **38j**, **38o** and **54d**) showed moderate potency (EC_{50} ≥10 to <20 µg/mL), while one compound (**51d**) exhibited weak potency against HIV-1. Structure of the eight best active compounds along with their RT inhibition potency (IC_{50} in µg/mL), anti-HIV potency (EC_{50} in µg/mL) and safety index (CC_{50}/ EC_{50}) are shown in figure **8.3**.
- Compounds **54b** and **54e** displayed potent activity against RT (IC_{50} 0.089 and 0.25 µg/mL, respectively) as well as HIV-1 (EC_{50} 0.030 µg/mL and 0.59 µg/mL, respectively). Furthermore, both the compounds **54b** and **54e** displayed admirable safety index (6200 and >338.9, respectively). So, overall RT inhibition, anti-HIV-1 and cytotoxicity studies afforded two potential hit (**54b** and **54e**) which possessed potent RT inhibition as well as anti-HIV-1 activity with good safety index.

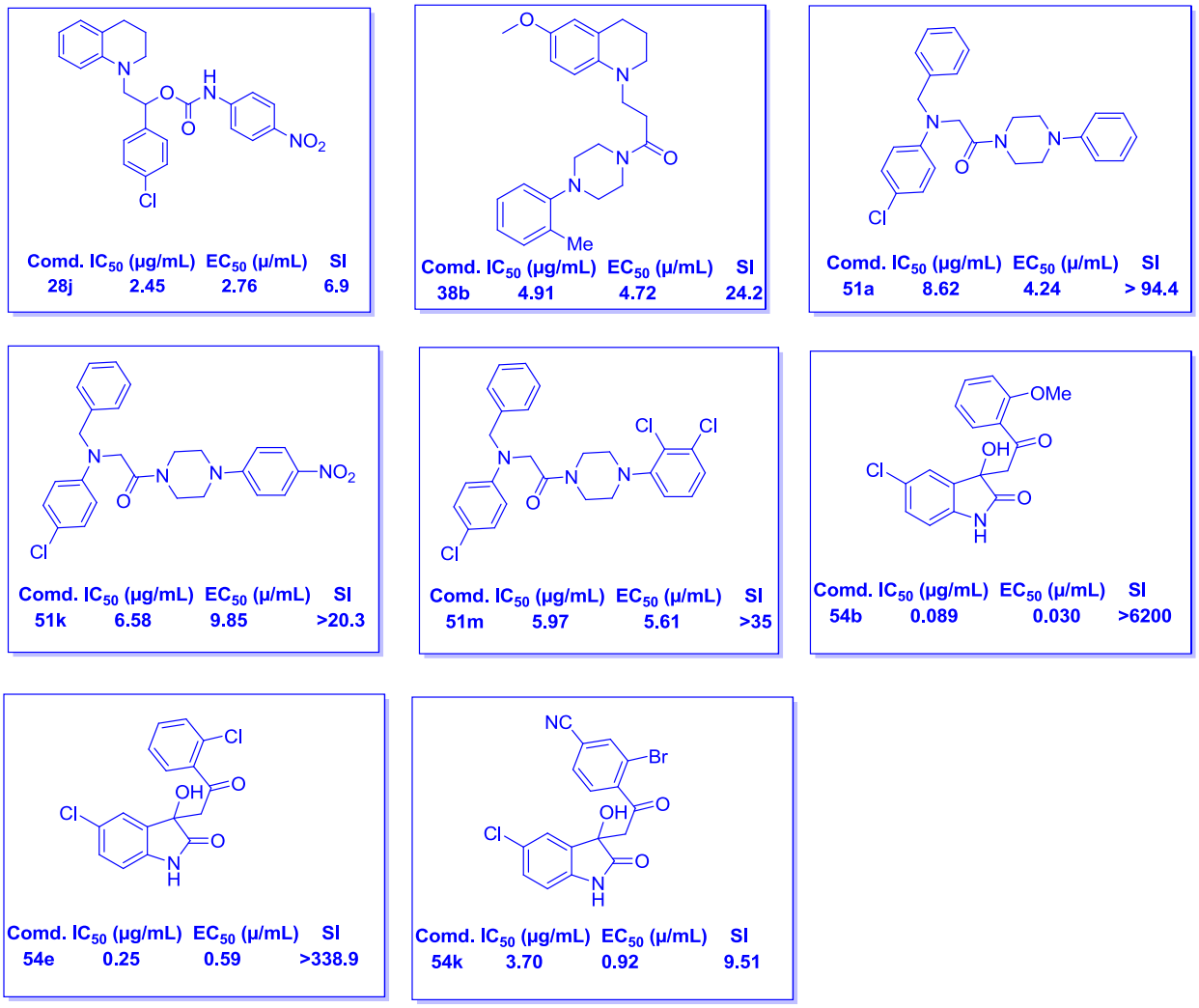

Fig. 8.3 Structure of good to excellent active compounds against HIV-1 RT as well as HIV-1

- *In-vitro* screening of compounds against four bacterial strains (*S. aureus*, *B. cereus*, *E. coli* and *P. putida*) revealed that out of all tested compounds, forty, thirty five, thirty seven and twenty five compounds possessed significant anti-bacterial activity (ZOI ≥15) against the *E. coli, S. aureus, P. putida,* and *B. cereus,* respectively.
- Out of all four tested bacterial strains, G (-)ve strain *E. coli* was found to be most sensitive towards the tested compounds, while G (+)ve strain *B. cereus* exhibited least susceptibility. Compounds of series **17a-o**, followed by **5a-o** showed overall better activity against the tested four bacterial strains, while majority of compounds of series **32a-n** and **23a-o** possessed weak to least activity against the tested strains.
- Twelve compounds (**5f, 5j, 5k**, **9f, 17d, 17f, 17j**, **28j, 28k, 28l, 38n** and **54j**) showed significant anti-bacterial activity with ZOI ≥15 mm against the all four tested bacterial

strains, in which nine compounds (**5f, 5j, 5k**, **17d, 17f, 17j, 28j, 28k** and **28l**) belonged to three series **5a-o, 17a-o** and **28a-l**.

- Structurally, scaffolds **5a-o** and **17a-o** are based on 6,7-dimethoxy tetrahydroisoquinoline connected via glycinamide linker to substituted phenyl ring, while series **28a-l** is basically tetrahydroquinoline based scaffold containing carbamate linker. Overall, all three scaffolds (Fig. **8.4**) can be considered of interest regarding their anti-bacterial activity.

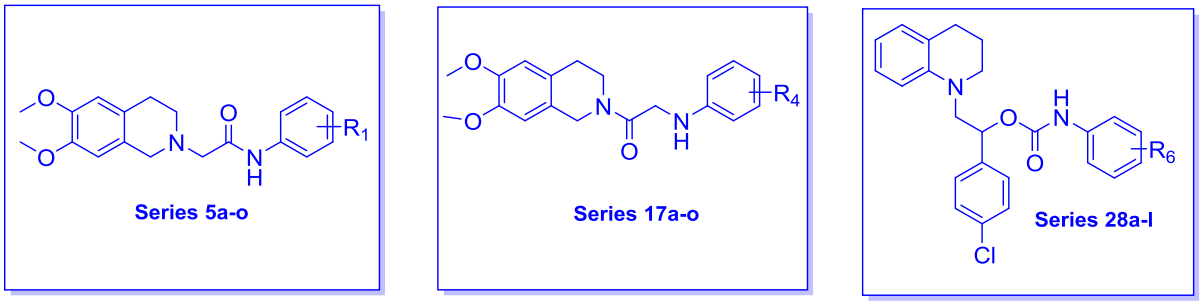

Fig. 8.4 Structure of superior active scaffolds against the all four tested bacterial strains

- *In-vitro* screening result of the synthesized compounds against two fungal strains revealed that out of all tested compounds, thirty and thirty nine compounds significantly inhibited (ZOI ≥15 mm) the growth of *C. albicans* and *A. niger,* respectively. So, fungal strain *A. niger* was found more sensitive towards the tested compounds compared to *C. albicans*.
- Collectively, fifteen compounds (**9m, 17j, 17k, 23i, 23j, 28e, 28f, 28g, 28h, 28l, 38f, 38l, 38n, 54g** and **54h**) exhibited significant growth inhibition (ZOI ≥15 mm) of both the tested fungal strains. Moreover, compounds of series **28a-l** and **38a-o** (Fig. **8.5**) possessed better anti-fungal activity compared to other series of compounds, so scaffolds containing tetrahydroquinoline moiety with carbamate linker **(28a-l)** and tetrahydroquinoline based compounds attached with phenylpiperazine entity (**38a-o**) possessed potential anti-fungal activity.
- Moreover, among the tested compounds, few compounds possessed potent fungal inhibitory activity, for example, compounds **9m**, **17k**, **38n** exhibited ZOI 18-20 mm and MIC 16 µg/mL against *A. niger*. Whereas, against *C. albicans* compounds **28g, 28h, 28l, 54g, 54h** showed potent anti-fungal activity with ZOI 17-20 mm and MIC 8-16 µg/mL.

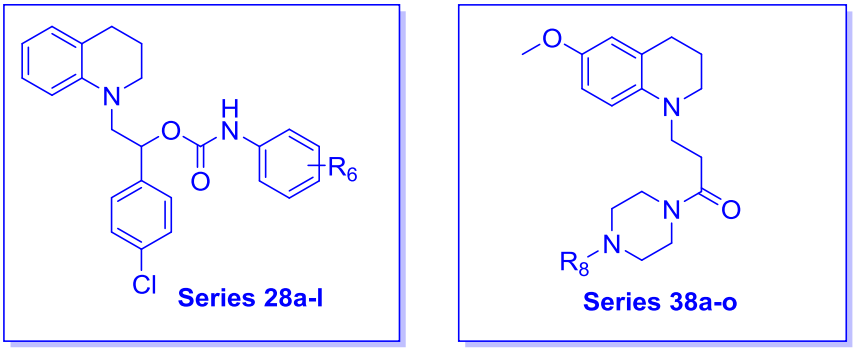

Fig. 8.5 Structure of superior active scaffolds against the both tested fungal strains

- *Anti-Mtb* evaluation of compounds revealed that majority of tested compounds not showed encouraging potency. Among the all tested compounds, around seven compounds (**14j, 23h**, **23o, 43h**, **43j**, **43l** and **43m**) exhibited significant potency (MIC ≤25 µg/mL), also seven compounds (**14i, 23a, 23l**, **28j, 43d, 43k** and **43n**) showed moderate potency (MIC between >25 to ≤50 µg/mL), while rest of the compounds possessed weak or no activity against *Mtb*.
- Majority of the compounds found to be active against *Mtb* belongs to three series **14a-k, 23a-o** and **43a-p** (Fig. **8.6**). Interestingly, all these series possessed carboxylic hydrazide as common entity which is very well known for anti-tubercular activity also present in the blockbuster drug isoniazid.
- Overall, compounds of series **43a-p** exhibited relatively better anti-*Mtb* activity compared to all other tested series. Four compounds (**43h**, **43j**, **43l** and **43m**) showed significant potency (MIC ≤25 µg/mL), in which compounds **43j** and **43m** showed MIC <10 µg/mL with safety index of more than twenty six.

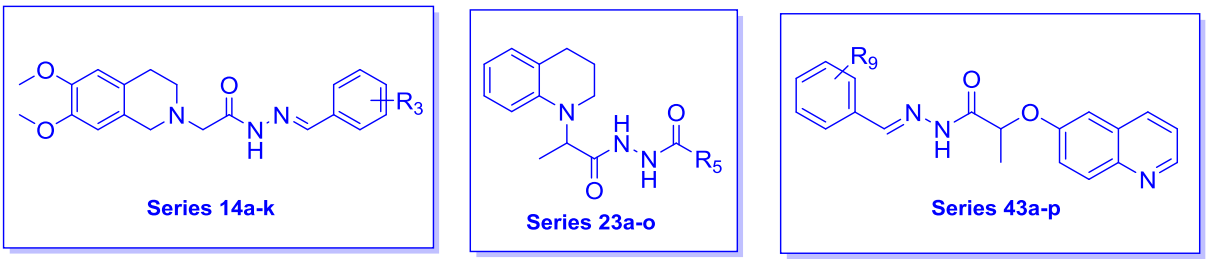

Fig. 8.6 Structure of scaffolds of interest for anti-*Mtb* activity

Chapter 9

Future Perspectives

- Compounds of series **28a-l, 38a-o, 51a-n** and **54a-k** displayed overall superior inhibition among the all tested series. So, further hit optimization studies can be performed over these scaffolds in order to find more potent hit against HIV-1 RT.
- Six compounds **28b, 28j**, **54b, 54d, 54e** and **54k** displayed good to excellent potency (IC_{50} ≤10 µM) against *in-vitro* HIV-1 RT, so all these compounds can be screened against drug resistance strains (K103N, K103N/Y181C) of HIV-1 reverse transcriptase.
- Eight compounds (**28j, 38b, 51a, 51k, 51m, 54b, 54e** and **54k**) displayed encouraging potency (EC_{50} <10 µg/mL) against HIV-1 during cellular assay with moderate to excellent safety index. Further, optimization studies can be performed in order to get more potent HIV-1 agent with better safety index.
- Two compounds (**54b** and **54e**) displayed potent activity against HIV-1 RT as well as HIV-1, with admirable safety index (6200 and >338.9, respectively). So, these compounds can be preceded for preliminary pharmacokinetic study.
- Nine compounds (**5f, 5j, 5k**, **17d, 17f, 17j, 28j, 28k** and **28l**) belonged to three series **5a-o, 17a-o** and **28a-l** showed significant anti-bacterial activity (with ZOI ≥15 mm) against the all four bacterial strains, hit optimization studies can be performed over these three scaffolds in order to get more potent anti-bacterial agent.
- Three compounds (**9m**, **17k** and **38n)** exhibited potent anti-fungal activity against *A. niger* with ZOI 18-20 mm and MIC 16 µg/mL, whereas five compounds (**28g, 28h, 28l, 54g** and **54h**) showed potent anti-fungal activity against *C. albicans* with ZOI 17-20 mm and MIC 8-16 µg/mL. Further, mechanistic studies are required on these compounds to reveal their exact mode of action.
- Two compounds (**43j** and **43m)** displayed significant activity against *Mtb* with MIC <10 µg/mL, both compounds can be used for further hit optimization studies or in designing of novel anti-*Mtb* agents.

Biographies

Dr. S. Murugesan completed his graduation in Pharmacy from Dr. M.G.R Medical University, Tamilnadu, India in the year 1999. He obtained his Master degree in Pharmacy from Birla Institute of Technology and Science, Pilani, India in the year 2002. Later, in the year 2006, he got enrolled in Ph. D. under the guidance of Dr. Swastika Ganguly and acquired his doctorate degree in the year 2009 from Birla Institute of Technology, Mesra, Ranchi, India. During the doctoral study, his working area was design, synthesis and biological evaluation of novel benzopiperidine analogs as anti-HIV agents, in addition he also studies the anti-infective activity of synthesized compounds against various bacterial and fungal strains. Then he joined in the department of Pharmacy, BITS, Pilani as assistant professor in the year 2010 and pursuing his teaching activity for B. Pharmacy and M. Pharmacy programmes. In parallel, Dr. Murugesan is actively involved in research in the area of computer aided drug design along with drug synthesis against HIV and allied opportunistic infections. He had more than 10 years of teaching and research experience. He has guided more than 10 B. Pharm, 7 M. Pharm students in the fulfillment of their dissertation work. In addition, one scholar has already completed his full time doctorate degree while one is pursuing under his guidance. He has successfully completed 2 research projects, including one as major project from DST-SERB. Dr. Murugesan has published more than 60 research papers in various peer reviewed journals of international and national reputes and also presented more than 47 papers/posters in the various international and national conferences.

Subhash Chander graduated in Pharmacy from Guru Jambheshwar University of Science & Technology, Hisar-Haryana, India in the year 2009. He received his MS degree in Medicinal Chemistry from NIPER Rae-bareli, India in 2011. He worked at CSIR-Central Drug Research Institute, Lucknow as a project trainee during the project of MS Pharm. After the completion of Master degree, he joined Jubilant Chemsys as research associate and worked for 1.5 years in the synthetic research division. In Nov. 2012, he joined the group of Dr. Murugesan, BITS Pilani, Pilani Campus as Junior Research Fellow under a project funded by DST-SERB and worked in the same project as Junior and Senior Research Fellow till its completion in the year July 2015. In parallel, he got enrolled in Ph. D under Dr. Murugesan in the year 2013 after qualifying the BITS Ph. D entrance examination. His area of interest is computer-aided drug design and development of novel nitrogen containing heterocyclic agents as anti-infective agents. He has published 10 research articles in the peer-reviewed journals and presented 8 research papers/posters in the various international and national conferences.

List of Publications (International Journals)

From Thesis Work

1. **S. Chander**, P.Wang, P. Ashok, L.M Yang, Y.T. Zheng, S. Murugesan. Design, synthesis and anti-HIV-1 RT evaluation of 2-(benzyl(4-chlorophenyl)amino)-1-(piperazin-1-yl)ethanone derivatives, **Bioorganic & Medicinal Chemistry Letters**. 27 (2017) 61-65.
2. **S. Chander**, P. Ashok, B.M. Maira, C. Davie and S. Murugesan. Design, synthesis and biological evaluation of novel tetrahydroquinoline based propanehydrazides as antitubercular agents, **Letters in Drug Design and Discovery**. 14 (2017) 293-300.
3. **S. Chander**, P. Ashok, D. Cappoen, P. Cos, S. Murugesan. Design, synthesis and biological evaluation of novel quinoline-based carboxylic hydrazides as anti-tubercular agents, **Chemical Biology & Drug Design**. 88 (2016) 585-591.
4. **S. Chander**, P. Wang, P. Ashok, L.M. Yang, Y.T. Zheng, S. Murugesan. Rational design, synthesis, anti-HIV-1 RT and antimicrobial activity of novel 3-(6-methoxy-3,4-dihydroquinolin-1(2H)-yl)-1-(piperazin-1-yl)propan-1-one derivatives, **Bioorganic Chemistry**. 67 (2016) 75-83.
5. **S. Chander**, P. Ashok, Y.T. Zheng, P. Wang, K.S. Raja, A. Taneja, S. Murugesan. Design, synthesis and in-vitro evaluation of novel tetrahydroquinolinecarbamates as HIV-1 RT inhibitor and their antifungal activity, **Bioorganic Chemistry.** 64 (2016) 66-73.
6. **S. Chander**, P. Ashok, R.P. Singh, P.N. Jha, Y.T. Zheng, P. Wang and S. Murugesan.Rational Design, Synthesis, Anti-HIV-1 RT and Anti-microbial Activity of Novel 2-(6,7-dimethoxy-3,4-dihydroisoquinolin-2(*1H*)-yl)-*N*-phenylpropanamide Derivatives. **Anti-Infective Agents,** 14 (2016) 63-73.
7. **S. Chander**, A. Penta, A. Singh, S. Murugesan. De-novo design, synthesis and evaluation of novel 6,7-dimethoxy-1,2,3,4-tetrahydroisoquinoline derivatives as HIV-1 reverse transcriptase inhibitors, **Chemistry Central Journal**. 9 (2015) DOI: 10.1186/s13065-015-0111-6.
8. **S. Chander**, A. Penta, S. Murugesan.Structure-based virtual screening and docking studies for the identification of novel inhibitors against wild and drug resistance strains of HIV-1 RT, **Medicinal Chemistry Research**. 24 (2015) 1869-1883.

9. **S. Chander**, P. Ashok, R. Singh, P.N. Jha, S. Murugesan. A Rapid, Green, Efficient Microwave-Assisted Synthesis and Antimicrobial Activity of Novel Glycinamide of 6,7 Dimethoxy-1, 2, 3, 4-Tetrahydroisoquinolines, **Current Microwave Chemistry**. 2 (2015) 44-52.

Apart from Thesis Work

1. P. Ashok, **S. Chander**, L.M.C. Chow, I. Wong, R.P. Singh, P.N. Jha, M. Sankaranarayanan. Synthesis and in-vitro anti-leishmanial activity of (4-arylpiperazin-1-yl)(1-(thiophen-2-yl)-9H-pyrido[3,4-b]indol-3-yl)methanone derivatives, **Bioorganic chemistry**. 70 (2017) 100-106.
2. S. Amaroju, M.N. Kalaga, S. Srinivasarao, A. Napiorkowska, E. Augustynowicz-Kopec, S. Murugesan, **S. Chander**, R. Krishnan, K.V.G.Chandrasekhar. Identification and development of 1-((1-(substituted)-1H-1,2,3-triazol-4-pyrazolo[4,3-c]pyridine-5(4H)-carboxamides as Mycobacterium tuberculosis Pantothenatesynthetase inhibitors, **New Journal of Chemistry**. 41 (2017) 347-357.
3. H.M. Al-Maqtari, J. Jamalis, T.B. Hadda, M. Sankaranarayanan, **S. Chander**, N.A. Ahmad, H.M. Sirat, I.I. Althagafi, Y.N. Mabkhot. Synthesis, characterization, POM analysis and antifungal activity of novel heterocyclic chalcone derivatives containing acylatedpyrazole, **Research on Chemical Intermediates**. 43 (2017) 1893-1907.
4. P. Ashok, **S. Chander**, A. Tejeria, L.G. Calvo, R.B. Fouce, S. Murugesan. Synthesis and anti-leishmanial evaluation of 1-phenyl-2,3,4,9-tetrahydro-1*H*-β-carboline derivatives against *Leishmaniainfantum,* **European Journal of Medicinal Chemistry**.123 (2016) 814-821.
5. N. Baig, R.P. Singh, **S. Chander**, P.N. Jha, S. Murugesan, A.K. Sah, Synthesis, evaluation and molecular docking studies of amino acid derived N-glycoconjugates as antibacterial agents, **Bioorganic Chemistry**. 63 (2015) 110-115.
6. **S. Chander**,A. Penta, S. Murugesan, In-silico design and docking study of novel Tetrahydroquinoline derivatives, **Journal of Pharmacy Research**. 8 (2014) 552-562.
7. P. Ashok, **S. Chander**, J. Balzarini, C. Pannecouque,S. Murugesan. Design, synthesis of new β-carboline derivatives and their selective anti-HIV-2 activity, **Bio-organic & Medicinal Chemistry Letters**. 25 (2015) 1232-1235.

8. P. Ashok, C.L. Lu, **S. Chander**, Y.T. Zheng, S. Murugesan. Design, Synthesis, and biological evaluation of 1-(thiophen-2-yl)-9*H*-pyrido[3,4-*b*]indole derivatives as anti-HIV-1 agents, **Chemical Biology & Drug Discovery**. 85 (2015) 722-728.
9. Penta, **S. Chander**, S. Ganguly, S. Murugesan. De novo design and in-silico studies of novel 1-phenyl-2,3,4,9-tetrahydro-*1H*-pyrido[3,4-b]indole-3-carboxylic acid derivatives as HIV-1 reverse transcriptase inhibitors, **Medicinal Chemistry Research**. 23 (2014) 3662-3670.
10. P. Ashok, H. Sharma, H. Lathiya, **S. Chander**, S. Murugesan.In-silico design and study of novel Piperazinyl β-carbolines as inhibitor of HIV-1 reverse transcriptase, **Medicinal Chemistry Research.** 24 (2015) 513-522.
11. P. Ashok, **S. Chander**, H. Lathiya, H. Sharma, K. Goyal, S. Murugesan. De-novo design and *in-silico* studies of novel bis-arylpiperazine derivatives as non-nucleoside inhibitors of HIV-1 reverse transcriptase. **Journal of Pharmaceutical Chemistry.** 1 (2014) 22-27.
12. K.K. Roy, S. kumar, **S. Chander**, A.K. Saxena. Lead Optimization Studies towards the Discovery of Novel Carbamates as Potent AChE Inhibitors for the potential Treatment of Alzheimer's Disease, **Bioorganic & Medicinal Chemistry**. 20 (2012) 6313-6320.

Publications in National Journals

1. **S. Chander,** S. Murugesan. In-silico based drug repositioning approach for the search of potent anti-HIV-1 RT inhibitors, **Cutting Edge**. 6 (2016) 9-14.
2. **S. Chander**, A. Penta, S. Murugesan. 1,2,3,4-Tetrahydroquinoline: A Versatile Nucleus in the New Millennium, **Research & Reviews: A Journal of Drug Design & Discovery**. 3 (2016) 1-18.
3. A. Penta, **S. Chander**, S. Murugesan. In-Silico Design and Study of Novel Tetrahydro-β-Carbolines as Inhibitor of HIV-1 Reverse Transcriptase, **Research & Reviews**: **A Journal of Drug Design & Discovery**. 3 (2016) 19-30.

Conferences attended / Poster presentations

1. **SubhashChander,** Ashok Penta, Yong-Tang Zheng, Ping Wang and Sankaranarayanan Murugesan, Poster entitled "Design, synthesis and in-vitro evaluation of novel benzopiperidinecarbamates as HIV-1 RT inhibitor" presented in international conference

entitled “Current Challenges in Drug Discovery and Delivery” held at BITS Pilani, Pilani-Campus, 2nd-4th of March 2017.

2. **SubhashChander,** Ping Wang, Ashok Penta, Liu-Meng Yang, Yong-Tang Zheng and Sankaranarayanan Murugesan, Poster entitled “Rational Design, Synthesis and Anti-HIV-1 RT evaluation of 1-(4-Phenylpeperazine-1-yl) ethanone based hybrid compounds” presented in national conference entitled “Organic Chemistry in Sustainable Development: Recent Advances and Future Challenges” held at BITS Pilani, Pilani-Campus, 29th -30th of August 2016.

3. **SubhashChander,** Ashok Penta and Sankaranarayanan Murugesan, Poster entitled “*In-silico*lead optimization, synthesis and anti-HIV-1 RT evaluation of indolin-2-one derivatives” presented in 6th International Symposium entitled “Current Trends in Drug Discovery Research (CTDDR-2016)” held at CDRI Lucknow on 25th to 28th February 2016.

4. **SubhashChander,** Ashok Penta and Sankaranarayanan Murugesan, Poster entitled “Design, synthesis, in-vitro evaluation and docking studies of novel 6,7-dimethoxy 1,2,3,4-tetrahydroisoquinoline derivatives as HIV-1 reverse transcriptase inhibitors” presented in national conference “Recent Developments in Medical Biotechnology and Structure Based Drug Designing” held at IIT Guwahati 6th -7th of December 2015.

5. **SubhashChander,** Ashok Penta and Sankaranarayanan Murugesan, Poster entitled “Design, synthesis and in-vitro evaluation of novel 1-(4-chlorophenyl)-2-(3,4-dihydroquinolin-1(2H)-yl)ethyl phenylcarbamate derivatives as inhibitor of HIV-1 RT ” presented in international conference “Nascent Development in Chemical Sciences” held at BITS Pilani, Pilani-Campus, 16th -18th of October 2015.

6. **SubhashChander,** Ashok Penta and Sankaranarayanan Murugesan, Poster entitled “In-silico virtual screening and docking studies for the identification of novel inhibitors of HIV-1 Reverse Transcriptase” presented at Indo-US conference on “Molecular Modeling and Informatics in Drug Design” held at NIPER Mohali on 3rd-6th of November 2014.

7. **SubhashChander,** Ashok Penta and Sankaranarayanan Murugesan, Poster entitled “In-Silico design and study of novel benzopiperidines as HIV-1 Reverse Transcriptase Inhibitor.” presented at International conference on “Recent Advances in Computational Drug design” held at J.N. Tata Auditorium, IISc, Bangalore on 16th and 17th of September 2013.

8. Ashok Penta, **SubhashChander** and Sankaranarayanan Murugesan. Poster entitled "Design and In-Silico study of novel 2,3,4,9-tetrahydro-1-phenyl-*1H*-pyrido[3,4-*b*]indole derivatives as Inhibitor of HIV-1 Reverse Transcriptase" presented at World Conference on Infectious Diseases (WCID-2013) organized by Jayaa Charitable and Educational Trust, Tamil Nadu. December 18-22nd, 2013.
9. Ashok P, **SubhashChander**, S. Ganguly, Rafael Balana-Fouce and S. Murugesan. Paper entitled "Synthesis and Evaluation of β-carboline derivatives as Anti-Leishmanial agents" presented at 2nd UK-India Medicinal Chemistry Conference organized by IICT, Hyderabad. March 22-23rd, 2013.

Invited lecture

Delivered an invited lecture entitled “Design, synthesis and anti-HIV-1 RT evaluation of quinoline based carboxylic hydrazide derivatives” at the Sixth Euro-India International Conference on Holistic Medicine (ICHM-2016), 9th-11th Sept. 2016, held at Kottayam, Kerala.

Study of Novel NNRTIs as Potential Agents Against HIV-1 and Opportunistic Infections

THESIS

Submitted in partial fulfillment

of the requirements for the degree of

DOCTOR OF PHILOSOPHY

by

Subhash Chander

ID. No. 2012PHXF404P

Under the Supervision of

Dr. S. Murugesan

BIRLA INSTITUTE OF TECHNOLOGY AND SCIENCE, PILANI

(RAJASTHAN) INDIA

2017

Chapter 9

Future Perspectives

- Compounds of series **28a-l, 38a-o, 51a-n** and **54a-k** displayed overall superior inhibition among the all tested series. So, further hit optimization studies can be performed over these scaffolds in order to find more potent hit against HIV-1 RT.
- Six compounds **28b, 28j**, **54b, 54d, 54e** and **54k** displayed good to excellent potency (IC_{50} ≤10 µM) against *in-vitro* HIV-1 RT, so all these compounds can be screened against drug resistance strains (K103N, K103N/Y181C) of HIV-1 reverse transcriptase.
- Eight compounds (**28j, 38b, 51a, 51k, 51m, 54b, 54e** and **54k**) displayed encouraging potency (EC_{50} <10 µg/mL) against HIV-1 during cellular assay with moderate to excellent safety index. Further, optimization studies can be performed in order to get more potent HIV-1 agent with better safety index.
- Two compounds (**54b** and **54e**) displayed potent activity against HIV-1 RT as well as HIV-1, with admirable safety index (6200 and >338.9, respectively). So, these compounds can be preceded for preliminary pharmacokinetic study.
- Nine compounds (**5f, 5j, 5k**, **17d, 17f, 17j, 28j, 28k** and **28l**) belonged to three series **5a-o, 17a-o** and **28a-l** showed significant anti-bacterial activity (with ZOI ≥15 mm) against the all four bacterial strains, hit optimization studies can be performed over these three scaffolds in order to get more potent anti-bacterial agent.
- Three compounds (**9m**, **17k** and **38n)** exhibited potent anti-fungal activity against *A. niger* with ZOI 18-20 mm and MIC 16 µg/mL, whereas five compounds (**28g, 28h, 28l, 54g** and **54h**) showed potent anti-fungal activity against *C. albicans* with ZOI 17-20 mm and MIC 8-16 µg/mL. Further, mechanistic studies are required on these compounds to reveal their exact mode of action.
- Two compounds (**43j** and **43m)** displayed significant activity against *Mtb* with MIC <10 µg/mL, both compounds can be used for further hit optimization studies or in designing of novel anti-*Mtb* agents.